Natural Attenuation of Landfill Leachate

van Breukelen, B.M.

2003

document version
Publisher's PDF, also known as Version of record

Natural Attenuation of Landfill Leachate:

a Combined Biogeochemical Process Analysis and Microbial Ecology Approach

Boris M. van Breukelen

Cover: Pictures of the research area downstream of the Banisveld landfill; transmission electron micrograph of *Geobacter metallireducens* respiring insoluble Fe(III) (source: www.geobacter.org).

This study was partly funded by the Dutch Research Program In-situ Bioremediation (NOBIS/SKB) under grant no. 96-3-04 and SV-206. Research was carried out at the Departments of Hydrology and Molecular Cell Physiology, Faculty of Earth- and Life Sciences, Vrije Universiteit Amsterdam.

The full text of this thesis and additional background information are available on the internet at http://www.geo.vu.nl/users/breb/

Natural attenuation of landfill leachate: a combined biogeochemical process analysis and microbial ecology approach. Boris van Breukelen, Doctoral Thesis Vrije Universiteit Amsterdam. - With index, ref. - With summary in Dutch.

ISBN 90-9016928-8
NUR-code: 934

Subject headings: natural attenuation / degradation / landfill leachate / contaminated aquifer / biogeochemistry / bacteria / solute transport / hydrology / groundwater / isotope hydrology / modelling

Printed by: PrintPartners Ipskamp, Enschede, The Netherlands

VRIJE UNIVERSITEIT

Natural Attenuation of Landfill Leachate:

a Combined Biogeochemical Process Analysis and Microbial Ecology Approach

ACADEMISCH PROEFSCHRIFT

ter verkrijging van de graad van doctor aan
de Vrije Universiteit Amsterdam,
op gezag van de rector magnificus
prof.dr. T. Sminia,
in het openbaar te verdedigen
ten overstaan van de promotiecommissie
van de faculteit der Aard- en Levenswetenschappen
op donderdag 12 juni 2003 om 15.45 uur
in het auditorium van de universiteit,
De Boelelaan 1105

door

Boris Maurijn van Breukelen

geboren te Amsterdam

promotor:	prof.dr. J.J. de Vries
copromotoren:	dr. H.W. van Verseveld
	dr. J. Griffioen

Aan mijn ouders

CONTENTS

LIST OF FIGURES

LIST OF TABLES

Chapter 1

GENERAL INTRODUCTION

1.1 Background

Pollution of groundwater resources is a significant environmental problem throughout the world and recognized since the 1970s. Water scarcity and pollution rank equal to climate change as most urgent environmental issues for the 21^{st} century (UNEP, 1999). Groundwater serves as a principle source for drinking water, and is also used for irrigation and industrial purposes, while deterioration of its quality may also affect ecological systems. Groundwater resources become increasingly polluted by a wide variety of contaminants: e.g. mono- and polycyclic aromatic hydrocarbons, chlorinated solvents, heavy metals, nitrate, pesticides, radionuclides, and cyanide (Fetter, 1993). Principal sources are industrial activities, leaking underground petroleum tanks, dry-cleaning, use of pesticides in agriculture, exploration of oil and gas fields, military exercises, traffic, and landfill sites.

Landfill sites contribute to pollution of groundwater to a large extent. A small country like the Netherlands harbors about 3800 old municipal household-refuse landfill sites (total area of 91 km^2), while over 100,000 landfill sites are spread across the USA (Suflita et al., 1992). Landfills were constructed without taking too much care of the surrounding environment before the 1980s. Landfills were generally not capped after closure to prevent the formation of leachate by infiltration of rainwater, nor were precautions taken to prohibit spreading of leachate to underlying aquifers. Therefore, release of hazardous chemicals to the environment continues, although many landfills are closed now. As a result, leachate plumes have been formed downstream from many landfill sites with a length up to a few kilometers (Christensen et al., 2001). Old landfills are suspect, in particular in the Netherlands, as many of them could contain illegally dumped chemical waste before the 1980s. Consequently, leachate may contain a wide variety of chemicals. However, observations show that concentrations of specific contaminants in landfill leachate plumes are generally modest when compared to plumes from petroleum hydrocarbon or chlorinated solvent spills, where contamination with a select group of chemicals happens. Nevertheless, drinking water standards for several organic pollutants (e.g., benzene, toluene, ethylbenzene, xylene (BTEX), naphthalene) and ammonium are generally exceeded in landfill leachate plumes (see Table 7.1). A random check on 80 landfill sites in the Netherlands showed that also chloroben-

zene, trimethylbenzene and phenol are generally present in landfill leachate, while pesticides and chlorinated aliphatic hydrocarbons are usually absent (IPO, 2002). Polycyclic aromatic hydrocarbons (PAHs) adsorb strongly onto organic matter and were therefore barely observed in high concentrations outside the landfill body. Heavy metals (in particular barium, arsenic, zinc and nickel) exceeded intervention values (see Chapter 7) most often, but this was to less extent also the case for background groundwater (IPO, 2002).

Remedial measures to clean contaminated sites and to protect groundwater resources, like excavation of soil in combination with purification or controlled storage, pump-and-treat, or techniques to physically retain pollution, are either expensive or have usually limited effect (Swett and Rapaport, 1998). Fortunately, research performed primarily during the 1990s, showed that there is potential for biodegradation of many organic contaminants. Furthermore, contaminants decrease in concentration or retard with respect to groundwater flow by physico-chemical processes as pore water mixing and sorption. The combined effect of naturally occurring processes resulting in a reduced spreading of pollution or a decrease in concentration away from the source is called *natural attenuation* (NA). *Intrinsic-* or *passive bioremediation* refer to the microbiological component of NA, while artificial stimulation of biodegradation is called *active* or *enhanced bioremediation*. When NA is sufficiently strong it will counteract further migration of pollution and a steady-state plume develops after some time. Exhaustion of the pollution source and diminution of the flux in time may eventually lead to shrinking plumes. Section 1.2 deals in more detail with the current scientific insight in NA processes.

Protocols on NA exist (NRC, 2000), and point out that sites must be monitored in time to verify the continuity of NA processes. Consequently, implementation of NA is called monitored NA (MNA). Advantages of MNA compared to other remediation techniques include lower volumes of remediation wastes, reduced human exposure, lower remediation costs (EPA, 1999; Heath, 1999), and better allocation of remediation resources (Swett and Rapaport, 1998). Disadvantages of MNA is that time frames for remediation are long and not easy to predict; hence long-term monitoring is required (Swett and Rapaport, 1998; EPA, 1999; Heath, 1999). Moreover, the robustness of continuation of biodegradation is of serious concern (e.g. EPA, 1999; Smets et al., 2002). A strong rise in application of MNA at the Superfund program and in particular the Underground Storage Tank (UST) program occurred in the USA at the end of the 1990s (MacDonald, 2000). However, mistakes in data interpretation are often made in practice (Matson and Schuhmann, 1999; Odermatt, 1999), or the level of documentation that is being accepted is not sufficient, resulting in application of MNA at sites where its effectiveness has not been adequately demonstrated (Renner, 2000). Furthermore, opinions on whether NA is an appropriate strategy for managing groundwater contamination are highly polarized (MacDonald, 2000). Critics think that regulatory acceptance of MNA happened too quickly (Renner, 2000). A total of 14 guidelines for application of MNA from a range of organizations were recently reviewed by the USA's National Research Council's (NRC's) Committee on Intrinsic Remediation (NRC, 2000). The principle findings of this report were that 1) MNA is an established remedy for only a few types of contaminants, 2) rigorous protocols are needed to ensure that

NA potential is analyzed properly, and 3) MNA should be accepted as a formal remedy for contamination only when the processes are documented to be working and are sustainable. Furthermore, the report concluded that the key to demonstrating the effectiveness of NA at a site is establishing the cause-and-effect relationship between loss of contaminant and the natural processes responsible for the loss (Bekins et al., 2001). However, the processes controlling the subsurface fate of many contaminants are only partially understood and are still topics of active research.

The attitude and policy in the Netherlands towards soil and groundwater pollution changed during the 1990s from fear and ideology towards opportunities and pragmatism, in line with international developments. The old policy strove for the clean-up of all polluted sites or at least the isolation of pollution sources (IBC: Isoleren, Beheersen, Controleren) to prevent further spreading of contaminants. However, this goal turned out to be too expensive and technically not practicable. For example, controlling the chemical release of the 3800 old landfills in the Netherlands using conventional methods would cost about 5-7 billion € but this sum is expected to halve at least, if MNA can be selected as remediation option for many sites (Van Kasteren, 1999). The Dutch government decided in 1997 that the policy on soil and groundwater remediation needed to change profoundly because of stagnation in the remediation operation (Tweede Kamer, 1997). The new policy (BEVER: BEleidsVERnieuwing bodemsanering) will be function-oriented (a level of pollution will be allowed depending on intended land-use function), cost-effective, Monitored NA is accepted as an option to remediate contaminated sites including landfills, but the aim is still to remove most of the pollution (BEVER/UPR, 2000).

A key issue in this new policy (Doorstart-A5, 2001) is that mobile contaminants are allowed to spread if a stationary plume will be reached within a time frame of 30 years (and if the resulting situation is socially acceptable). Currently, a project is being conducted (ROSA: RObuste SAneringsvarianten) to evaluate how this new policy on mobile contaminants will work out in practice. It will be a guide on dealing with typical remediation situations, and bottlenecks, possible gaps in policy, and the information-need for authorities will be identified. Modeling of NA in order to predict the extent and stability of plumes, takes a central position in a decision-support-system used in the Netherlands on evaluation of NA as a remediation option (Sinke et al., 2001). In conclusion, the tendency to implement MNA as a solution to many cases of groundwater pollution in Western countries calls for a further investment in scientific research in order to understand NA of pollutants at contaminated sites in a proper way.

1.2 The act of natural attenuation: degradation and redox reactions

Occurrence of natural attenuation (NA) makes aquifers suitable as natural subsurface treatment systems. Degradation, sorption, dilution, volatilization, precipitation and ion-exchange are processes which attenuate pollution (Christensen et al., 2001), but only (microbial) degradation really removes the mass of organic contam-

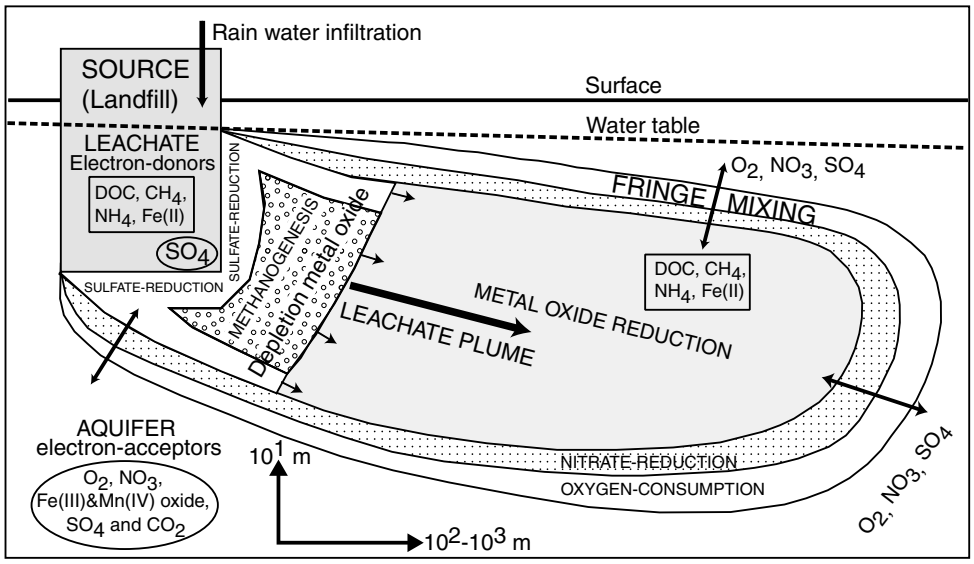

Figure 1.1: Spatial distribution of redox processes coupled to degradation of dissolved organic carbon (DOC) in a typical landfill leachate plume. Methane, Fe(II), and ammonium compete with DOC for electron-acceptors at the plume fringe.

inants, and is essential for reaching stationary plumes. Natural attenuation of landfill leachate plumes has recently been reviewed by Christensen et al. (2001). Degradation of spreading organic pollution often leads to a sequence of redox zones from the source zone to the outskirts of a plume as available electron-acceptors are used in preferential order (e.g. Christensen et al., 2000a; Christensen et al., 2001). Prediction of the development of redox zones is of utmost importance for evaluation of NA, as the potential and rate of degradation of specific organic compounds depends on the redox conditions of the subsurface, i.e., the availability of oxygen, nitrate, iron oxide, and sulfate (Krumholz et al., 1996; Christensen et al., 2000a; NRC, 2000; Christensen et al., 2001). For example, benzene is well degraded with oxygen, but rates are much slower or even zero under anaerobic conditions, and changes per location depending on the available electron-acceptor (Lovley, 2000).

Microorganisms transform organic compounds by means of electron-transfer reactions in order to extract free energy by synthesizing ATP. Usually, organic compounds act as reductor (e.g. BTEX), while inorganic compounds (e.g. O_2, SO_4^{2-}) are used as oxidant. However, some organic compounds (e.g. halogenated hydrocarbons: trichloroethylene, etc) act as oxidant via reductive dehalogenation, and require (natural) reductants in aquifers such as organic matter or pyrite (Haas and Shock, 1999). Also fermentation transforms organic compounds, but external oxidants are essential for full oxidation to CO_2. Degradation of organic contaminants determines the development of redox conditions in hydrocarbon plumes. In contrast, dissolved organic carbon (DOC) in landfill leachate consists mainly of humic-, fulvic-, and fatty acids, while specific organic contaminants contribute usually less than 1‰–1%. Therefore, degradation of DOC drives the development of redox

conditions in a leachate plume, and hence determines the spatial-temporal degradation potential of specific organic chemicals. Thermodynamics mainly determines the order in which microorganisms use electron-acceptors, as microorganisms tend to perform redox reactions close to thermodynamic equilibrium, which leads to the sequence of redox conditions observed (Fig. 1.1). The Gibbs free energy for oxidation of organic carbon decreases at neutral pH in the order: O_2, NO_3^-, Mn(IV)-oxide, Fe(III)-oxide, SO_4^{2-} and CO_2 (Fig. 1.2). Therefore, aerobic degradation followed by nitrate reduction oxidizes organic carbon at the fringes of plumes. Inside plumes, where oxygen and nitrate are absent, anaerobic degradation occurs, and reduction of metal oxides (manganese followed by iron) prevails. The large content of metal oxide in the aquifer sediments compared to the concentration of DOC, makes reductive dissolution of metal oxide an important anaerobic degradation process (Christensen et al., 2000a; Lovley and Anderson, 2000; Christensen et al., 2001). When metal oxides become depleted from the source, sulfate reduction follows and finally methanogenesis. Sulfate reduction may occur near the landfill body, as leachate is a source of sulfate, and at the fringes, where sulfate from the pristine groundwater mixes and metal oxides are depleted (Fig. 1.1).

Zones of iron reduction, sulfate reduction and methanogenesis are often observed to overlap (Christensen et al., 2000a; Christensen et al., 2001) depending on pH, redox species concentrations, and solubility of iron-oxide minerals. Postma and Jakobsen (1996) explained the simultaneous occurrence of these redox processes by a partial equilibrium approach, where fermentation of organic compounds is overall rate limiting, while microbial oxidation is considered to be close to equilibrium. Primary redox processes involve the oxidation of organic carbon and release of reduced redox species (CH_4, H_2S, Fe(II), Mn(II)). These reductants become oxidized in secondary redox processes. At the fringe of a leachate plume in particular, secondary redox processes happen and compete with organic carbon degradation processes for available electron-acceptors (Figs. 1.1, 1.2).

In conclusion, the degradation rate for organic chemicals depends largely on the availability of oxidants/reductants in the aquifer, providing that the necessary microorganisms are present. Rates will decrease in time when electron-acceptors are consumed, which leads to enlargement of the steady-state plume. Consequently, a steady-state plume can be expected to expand before shrinking if the redox buffering capacity of the aquifer depletes before the source exhausts and the flux diminishes.

1.3 Monitoring and evaluating MNA

The United States Environmental Protection Agency (U.S. EPA) proposed a three-tiered approach to evaluate the potential for MNA at a contaminated site (EPA, 1999). These three-tiers or "lines of evidence" are: 1) documentation of contaminant mass reduction, 2) data indirectly indicating the occurrence (and rate) of specific NA processes (e.g. redox processes), 3) field/lab studies directly demonstrating microbial degradation. Tier one is in principle sufficient for authorities to grant the use of MNA as remediation technique, but in most cases data requiring the

nature and rates of NA processes are required (Tier 2). Tier three is only necessary if data from tiers one or two are inconclusive. Relying solely on a positive tier one is risky, because the rate of degradation is not an intrinsic property of the concerned organic contaminant (e.g. radioactive decay), but instead the corollary of environmental conditions and microbial activity. Therefore, tier two is essential for assessing the sustainability of degradation, i.e., to be able to predict reactive transport of contaminants, and to consider the possibility that the degradation rate may deteriorate, as a result of oxidant/reductant consumption.

The distribution of redox-sensitive compounds in aquifers is used to deduce the occurrence of redox processes (Christensen et al., 2000a). However, concentrations of redox-sensitive compounds are also controlled by geochemical processes, such as cation-exchange and mineral precipitation/dissolution, which may be secondary (i.e., induced by degradation reactions) or not (Fig. 1.2). Therefore, all major geochemical processes must be considered for proper evaluation of the redox chemistry, as other reactions may mask the act of microbial processes. Hydrogeochemical data sets contain the information on governing NA processes. Modeling is essential to deduce and quantify these processes in order to demonstrate and understand NA mechanisms, to identify the factors that control kinetics, and to evaluate of the sustainability of NA. The present (low) status of quantitative models is a principle reason that US-EPA requires long-term monitoring of NA at sites where MNA is implemented as remediation technique (O'Steen, 1999). Moreover, quantitative modeling can be used to guide new data needs (Bekins et al., 2001). More quantitative information and models are needed - in particular, on the potential for NA to occur and on rate-limiting factors (Williams, 1999). Both inverse and forward geochemical transport models have been made to model the processes at landfill leachate plumes, in order to deduce and quantify the operative biogeochemical processes (see Chapter 5).

Although environmental conditions for degradation of certain organic chemicals may be suitable, presence of specific microorganisms for occurrence of degradation is a prerequisite. For example, the capacity to degrade benzene coupled to iron reduction varied among petroleum-contaminated aquifers. Here, the presence of species from the *Geobacter* genus determined the occurrence of this process, while geochemical variables were not predictive (Rooney-Varga et al., 1999). Therefore, molecular community analysis could be a powerful tool for predicting a site's potential for anaerobic benzene degradation. Culturing-independent molecular techniques rapidly advance our understanding of microbial ecology (e.g. Röling and Van Verseveld, 2002). These methods have the advantage over culturing methods that they are fast, but most importantly, they are not selective (see Von Wintzingerode et al., 1997), whereas culturing methods select culturable microorganisms, which represent in general only a small fraction of the total microbial community (Amann et al., 1995). On the other hand, the molecular genetic methods only give information on presence, which is not synonymous with activity.

In order to explain and predict changes in groundwater composition away from contaminant sources, the combined control of microbiological and physico-chemical processes should be addressed. Physico-chemical conditions confine microbial degradation processes, while microbial activity changes physico-chemical conditions

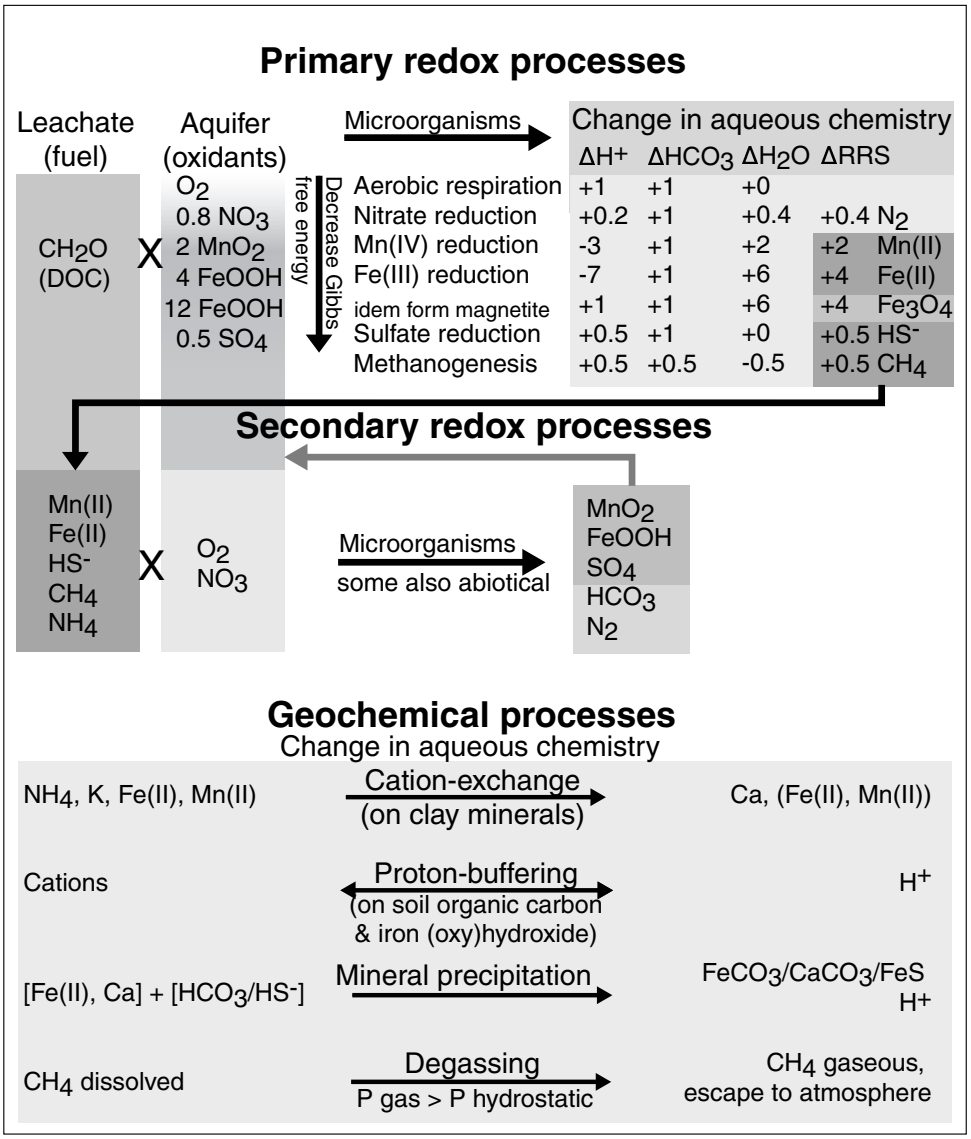

Figure 1.2: Biogeochemical reaction network in landfill leachate plumes. Primary DOC degrading redox processes change pH, dissolved inorganic carbon (DIC) and release reduced redox species (RRS). The stoichiometry per mol DOC degraded is shown for consumed oxidants, produced/consumed protons/H_2O, and produced bicarbonate and RRS. Geochemical processes buffer concentrations of RRS, pH and DIC. Secondary redox processes involve oxidation of RRS, and compete with DOC for O_2 and NO_3^- at the plume fringe.

by for example consumption of specific electron-acceptors. The combination of physico-chemical conditions and microbial community structure determine the extent of degradation, but the latter could be decisive for degradation of specific organic chemicals, and for degradation under less favorable conditions. This means that microbiology and geochemistry cannot be considered as two separate disciplines within NA research, but that they are complementary (i.e., biogeochemistry).

Evaluation of natural attenuation of organic chemicals at landfill leachate plumes is likely to be more difficult than at sites contaminated with a single type of organic contaminant such as petroleum or chlorinated hydrocarbons plumes. The reasons are: the large size of landfills, heterogeneity of waste material, and large amount of potential contaminants involved (Christensen et al., 2000b). Consequently, a dense sampling network seems essential to evaluate NA at landfill sites with sufficient confidence. Still, MNA is an attractive option at landfill sites in view of the fact that few feasible alternatives exist. Concentrations of organic contaminants are also about two to three orders of magnitude lower than in hydrocarbon spills reducing the environmental health risks of landfill sites.

1.4 Specific objectives

The objective of this study is to improve the understanding of the biogeochemical processes, the interactions among them and the changes in microbial ecology, as induced by inflow of landfill leachate into a pristine aquifer. Proper scientific knowledge about the operative processes, associated kinetics, and microbiology is needed to be able to determine whether MNA is a feasible remediation technique for landfills and other contaminated sites or not.

A field study of the biogeochemistry and microbial ecology of a landfill leachate plume is presented in this thesis. This study distinguishes itself from previous studies on NA of landfill leachate plumes with regard to the completeness of the data gathered (geochemistry, hydrochemistry, isotope geochemistry, microbiology), application of molecular microbial techniques, and insightful reactive transport modeling. The studied aquifer was anaerobic under pristine conditions, while other previously studied aquifers polluted with landfill leachate were aerobic (Christensen et al., 2001), with the exception of one (Cozzarelli et al., 2000). Processes were studied both in the flow direction and for the first time in detail across the fringe of the plume.

The site used for the research presented in this thesis is the Banisveld landfill, 5 km southwest of Boxtel, the Netherlands. This site was selected as it ranked high on a priority list of landfill sites in the Province of Noord-Brabant, potentially impairing the surrounding environment. Furthermore, spreading of leachate at this location is a potential threat for a nature reserve nearby ("de Smalbroeken"). The site is suitable as a research site, since 1) the leachate plume could be easily detected using geophysical techniques, 2) was present close to the surface, and 3) accessibility of the landfill and the surrounding area was high.

Various techniques were applied to determine which redox processes were coupled to degradation of DOC inside the plume. Both inverse geochemical modelling

and forward reactive transport modelling were performed to deduce and quantify the network of biogeochemical processes changing the leachate composition downstream of the source zone. Furthermore, factors controlling the rate of kinetic reactions (e.g., degradation of organic carbon and carbonate mineral precipitation) were identified in a comparison with other studies.

Little research has been performed on biogeochemical processes at the fringes of pollution plumes. However, for modelling/prediction of NA it is essential to know if available oxidants in pristine groundwater are consumed also by reductants other than DOC or organic chemicals. Therefore, the biogeochemistry and mixing processes at the top fringe of the plume were investigated to gain insight into which secondary redox processes (i.e., oxidation of ammonium, methane, Fe(II), etc) compete with organic carbon oxidation for available electron-acceptors.

Little is known about the role of microbial communities in biogeochemical processes. Whether or not microbial communities differ between pristine and polluted aquifers is also barely known. Microbial communities were investigated by profiling physiological (CLPP using Biolog microtiter plates) and genetic characteristics (16S rDNA-DGGE); the presence of specific species was determined via cloning and sequencing (see Section 1.5). Relations were sought between microbial communities and hydrogeochemical parameters, redox conditions, and degradation potential.

1.5 Outline and general methodology

Chapter 2 discusses the biogeochemistry and isotope geochemistry of the Banisveld landfill leachate plume (Boxtel, the Netherlands). Various geophysical methods were applied in advance to determine the spatial distribution of the pollution plume in order to limit the necessary amount of groundwater and sediment samples. Redox processes coupled to degradation of organic carbon in the plume were investigated by a combination of techniques, such as thermodynamic calculations using hydrogen gas concentrations. An inverse geochemical model of the landfill leachate plume was constructed to quantify the processes changing leachate composition in downstream direction.

The subsequent two chapters present research to the microbiology of the polluted aquifer. Chapter 3 deals with the physiological properties of the microbial communities in relation to state of pollution. Physiological information (substrate utilization) was obtained by community-level physiological profiling (CLPP) using Biolog microtiter plates (Röling et al., 2000a). Microbial community structure in relation to pollution, degradation extent, redox condition and aquifer geochemistry was investigated using denaturing gradient gel electrophoresis (DGGE) of 16S-rDNA isolated from groundwater and sediment samples, and discussed in Chapter 4. Cloned 16S rDNA was sequenced to find out which microbial species are present in the aquifer, and if their presence is related to environmental conditions.

Chapter 5 presents a reactive transport model of the leachate plume. The model was constructed using PHREEQC-2 (Parkhurst and Appelo, 1999) in order to quantify the most important biogeochemical processes changing the downstream leach-

ate composition. In addition, the carbon isotope geochemistry of the plume was simulated. The impact of individual biogeochemical reactions on the change in downstream leachate composition is shown. Rate constants for oxidation of electron-donor (dissolved organic carbon), and kinetic precipitation of carbonate minerals were obtained using the non-linear optimization program PEST by matching hydrochemical observations with the kinetic model. Factors controlling the rate of degradation via reductive dissolution of Fe-oxides are discussed for landfill leachate plumes in general.

Chapter 6 studies biogeochemical reactions at the top fringe of the Banisveld plume, where leachate mixes with pristine groundwater. A high-resolution data set on the hydrochemistry and isotope chemistry was obtained by installing densely spaced multi-level-samplers across the fringe. Reactive transport modelling was performed to identify the ongoing hydrochemical reactions, and the potential for oxidation of various reductants present (DOC, CH_4, NH_4^+, Fe(II), and Mn(II)) at the fringe was evaluated.

Finally, Chapter 7 (the synthesis) presents the summary and the conclusions of the research performed. Directions for future research to NA of landfill leachate plumes are given. Furthermore, the following aspects are discussed: the development of redox conditions in landfill leachate plumes, the availability of Fe(III)-oxides for iron reduction, current developments in molecular microbial ecology research and its use for MNA, and technical and policy issues in MNA of landfill leachate pollution.

Chapter 2

BIOGEOCHEMISTRY AND ISOTOPE GEOCHEMISTRY OF THE BANISVELD LANDFILL LEACHATE PLUME

Abstract

The biogeochemical processes were identified which improved the leachate composition in the flow direction of a landfill leachate plume (Banisveld, the Netherlands). Groundwater observation wells were placed at specific locations after delineating the leachate plume using geophysical tests to map subsurface conductivity. Redox processes were determined using the distribution of solid and soluble redox species, hydrogen concentrations, concentrations of dissolved gases (N_2, Ar, CH_4), and stable isotopes (δ^{15}N-NO_3^-, δ^{34}S-SO_4^{2-}, δ^{13}C-CH_4, δ^{2}H-CH_4 and δ^{13}C of dissolved organic and inorganic carbon (DOC, DIC)). The combined application of these techniques improved the redox interpretation considerably. Dissolved organic carbon (DOC) decreased downstream in association with increasing δ^{13}C-DOC values confirming occurrence of degradation. Degradation of DOC was coupled to iron reduction inside the plume, while denitrification could be an important redox process at the top fringe of the plume. Stable carbon and hydrogen isotope signatures of methane indicated that methane was formed inside the landfill and not in the plume. Total gas pressure exceeded hydrostatic pressure in the plume, and methane seems subject to degassing. Quantitative proof for DOC degradation under iron-reducing conditions could only be obtained if the geochemical processes cation-exchange and precipitation of carbonate minerals (siderite and calcite) were considered and incorporated in an inverse geochemical model of the plume. Simulation of δ^{13}C-DIC confirmed that precipitation of carbonate minerals happened.

Published as: Van Breukelen, B.M., Röling, W.F.M., Groen, J., Griffioen, J., Van Verseveld, H.W. Biogeochemistry and isotope geochemistry of a landfill leachate plume. *Journal of Contaminant Hydrology* (in press).

2.1 Introduction

Landfills are an important group of groundwater contaminating sites. Leachate from most household refuse landfills contains various organic contaminants, but individual concentrations are generally modest when compared to polluted sites like petroleum hydrocarbon or chlorinated solvent spills. Nevertheless, drinking water standards for several organic pollutants and ammonium in groundwater are often exceeded. Monitored natural attenuation (MNA) has received considerable attention as a remediation technique, partly because it seems a cheap alternative to techniques which actively decontaminate polluted groundwater. Aquifers have properties to act as natural subsurface treatment systems, which attenuate spreading landfill leachate (Christensen et al., 2001). Degradation, sorption, dilution, volatilization, precipitation and ion-exchange are processes which attenuate pollution. But only degradation, microbially mediated or not, really removes the mass of organic contaminants. Evaluation of natural attenuation (NA) at landfill leachate plumes is likely to be more difficult than at other contaminated sites as a consequence of the large size of landfills, heterogeneity of waste material, and the large number of potential contaminants involved (Christensen et al., 2000b).

Inflow of organic carbon to an aquifer leads to sequential use of electron-acceptors upon degradation, resulting in the development of redox zones (Christensen et al., 2000a; Christensen et al., 2001). Aerobic degradation followed by nitrate reduction oxidizes organic carbon at the fringe of a plume. Inside a plume reduction of metal oxides (manganese followed by iron) prevails and is observed to be an important anaerobic degradation process (Christensen et al., 2000a; Christensen et al., 2001; Lovley and Anderson, 2000). Where iron oxide has been depleted, sulfate reduction occurs, and finally methanogenesis serves to remove redox equivalents.

Characterization of the redox chemistry should be a main objective in natural attenuation studies, since redox conditions are a crucial factor determining the potential and rate of degradation of specific organic contaminants (Christensen et al., 2001). Recently, Christensen et al. (2000a) reviewed available methods to characterize redox conditions in groundwater. The goal of the present study was twofold: to determine which redox processes were coupled to the oxidation of dissolved organic carbon (DOC) in a landfill leachate plume (Banisveld landfill, the Netherlands), and to evaluate the various methodologies. Methods recommended in the review (distribution of solid and aqueous redox species, and hydrogen concentrations) were applied. In addition, stable isotopes (δ^{13}C of dissolved inorganic carbon, DOC, and methane, δ^{2}H of methane, δ^{34}S of sulfate, and δ^{15}N of nitrate) and dissolved gases (N_2, Ar) were measured in order to qualify the redox processes in the aquifer better. Finally, inverse geochemical modelling was performed to quantify the biogeochemical processes causing the observed improvement in leachate composition downstream.

2.2 Field site description

The Banisveld landfill site (6 ha), located 5 km southwest of Boxtel, the Netherlands, contains about 400,000 m^3 of primarily household refuse, and is not sealed by an artificial or natural liner. Landfilling occurred in a former 6-m-deep sand pit between 1965 and 1977, while chemical waste may have been dumped illegally. The lithology of the phreatic aquifer consists of a 7-9 m thick layer of fine to coarse-grained unconsolidated clayey sands. Below these relatively permeable sediments, alternations of clay, peat and sand layers are present. The fluvio-eolian sediments of Pleistocene age were deposited under periglacial conditions.

The largest part of the landfill body resides below the groundwater table, which is less than 2 m below surface. The 10-m-wide and 1.5-m-deep "Heiloop" stream to the northwest and downstream of the landfill (Fig. 2.1) drains groundwater from the area. Groundwater flow is directed NE to N towards a nature reserve beyond the Heiloop stream. The hydraulic gradient (i) downstream of the landfill (between wells W2b and W9b) varied between 0.0003 m/m and 0.007 m/m (average 0.003 m/m) in the period June 1998 to October 2001. The hydraulic permeability has not been determined, but empirical relations based on grain size distributions (Vukovic and Soro, 1992) suggest permeability to range between 0.1-5 m/day depending on clay content. Groundwater flow velocity is expected to be around 4 m per year.

2.3 Methods

2.3.1 Geophysical methods

An electromagnetic survey was performed using a Geonics EM-34 with an inter coil spacing of 10 m both in vertical (VL) and horizontal loop (HL) mode to measure the apparent conductivity of the subsurface (McNeill, 1980). Cone penetration tests (CPTs) were subsequently executed whereby the cone resistance, the sleeve friction and the electrical formation conductivity were simultaneously registered. The ratio between the cone resistance and the sleeve friction is named the friction ratio, which is indicative for the lithology according to an empirical relation (sands, 0.6–1.2; silts/loam, 1.2–4; clay, 3–5; peat, $>$5).

2.3.2 Groundwater sampling and analysis

Groundwater observation wells were installed in June 1998 in a series along the main direction of groundwater flow: upstream of the landfill (WUP), downstream above, inside and below the plume (W1–W9), and in front of the plume (WF) across the Heiloop stream (Figs. 2.1, 2.2). Observation wells were installed in bailer drillings with a diameter of 22 cm, and the lithology of the soil was described. Two or three PVC wells with 52 mm inner diameter were installed in each hole. Totally 29 wells were placed in 11 boreholes. The groundwater monitoring wells are indicated by the following notation: Wxy, where x is the code of the well site (UP, 1-9, F) and y refers to the screen depth of an individual well at well site x

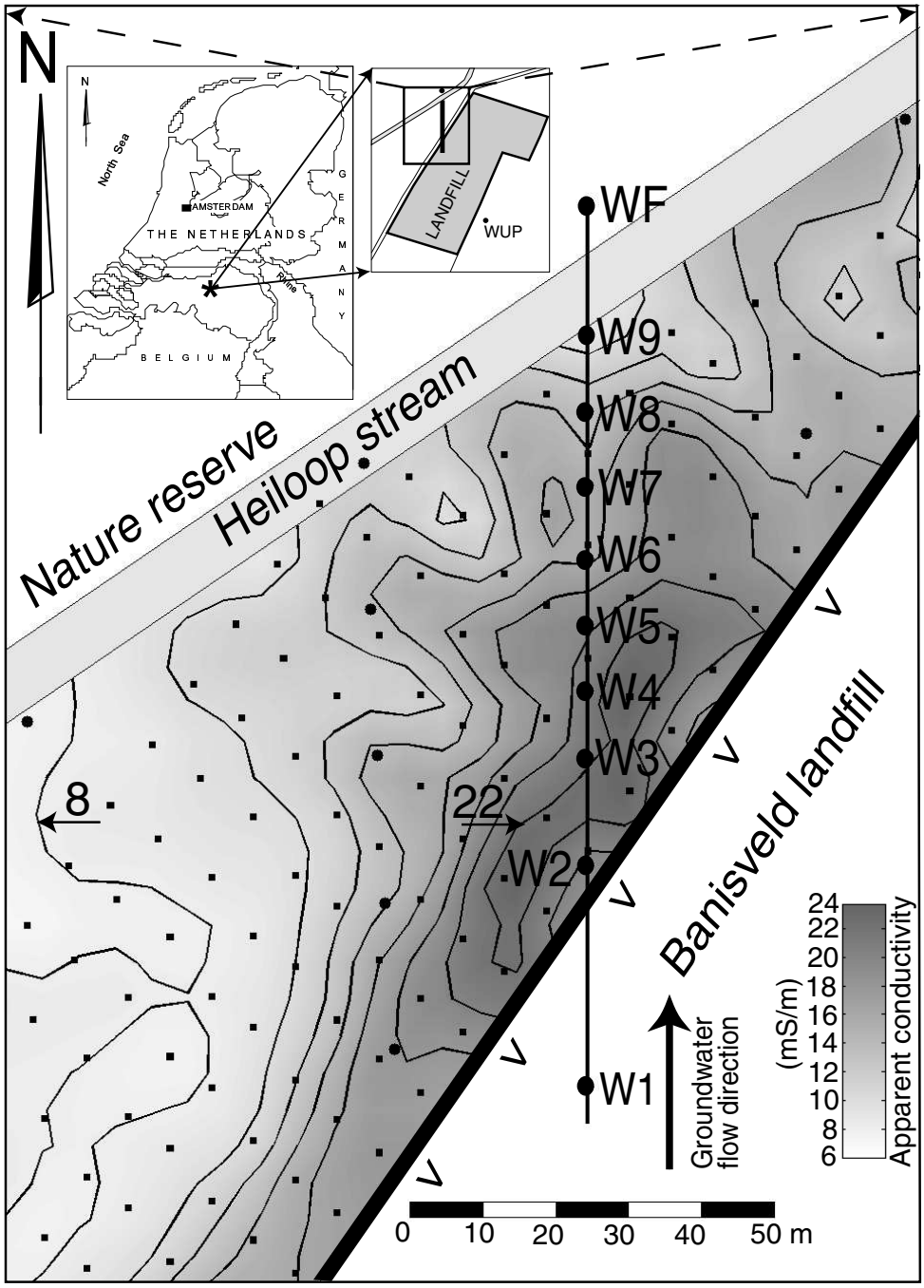

Figure 2.1: Map of the apparent conductivity (mS/m) measured by EM-34 (10-m intercoil spacing, horizontal loop) from the enlarged area between the NW border of the landfill and the Heiloop stream. The S-N transect is shown with well sites W1-W9 and WF placed in the direction of groundwater flow.

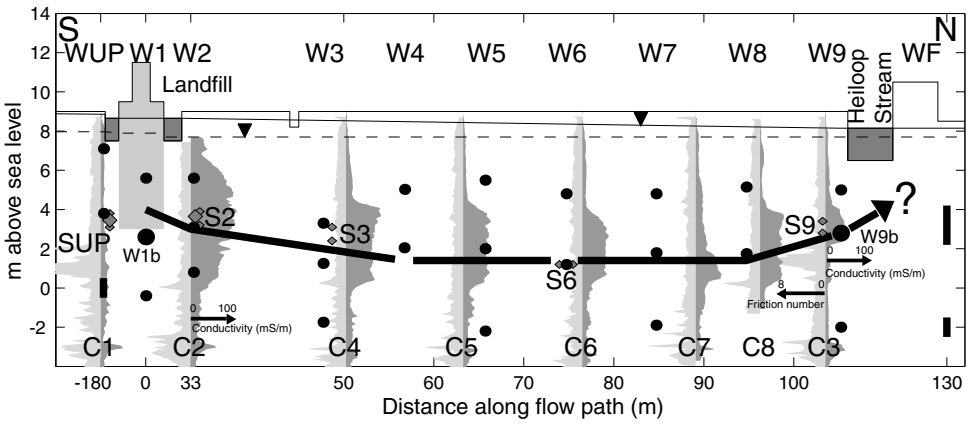

Figure 2.2: Cross section of the S-N research transect. Results of the cone penetration tests (C1–C8), the position of the observation well sites (WUP, W1–W9, WF), the locations where sediments samples have been taken (SUP, S2, S3, S6, S9), and the min and max observed hydraulic heads are shown. Screens of individual observation wells are indicated by black dots (20-cm screen length) or black vertical lines for longer screens. The formation conductivity (dark grey) is plotted from left to right (max C2 = 102 mS/m). The friction number (light grey) is plotted from right to left (max C3 = 8).

(a–upper screen (generally above plume); b–middle screen (inside plume); c–lower screen (below plume)). The length of the screens is 20 cm, but wells WUPc, WFa, and WFb have screen lengths of 1 or 2 m.

The observation wells were sampled three times using a peristaltic pump: one week after placement in June 1998, three months later in September 1998 and 16 months later in October 1999. A limited amount of samples and parameters were taken and analyzed in April 2001. pH, temperature, dissolved oxygen and electrical conductivity were determined on site using electrodes placed in flow cells. Alkalinity was determined by Gran titration in the laboratory within a few days. Samples for dissolved methane analysis were taken by putting the sampling tube on a 10 mlpolyethylene (PE) syringe and injecting 6.0-ml of groundwater into 13-ml vacuum blood sample vials (Lyngkilde and Christensen, 1992b). Analysis was performed on a gas chromatograph with flame ionization detector (GC-FID). Samples for chloride, sulfate, nitrate, nitrite and alkalinity were not filtered and kept in 50-ml PE bottles. Samples for calcium, magnesium, sodium, potassium, iron, manganese, ammonium, barium and phosphate were taken by connecting the sampling tube to a syringe while minimizing air contact. The water was filtered using 0.45-μm filters and conserved in 50-ml PE bottles containing 0.4 ml concentrated nitric acid. The anions and ammonium were analyzed by spectrophotometry. The cations were analyzed by inductively coupled plasma-atomic emission spectrometry (ICP-AES). Filtered samples for dissolved organic carbon (DOC) were conserved in 10-ml PE tubes with screw pods containing 100 μL pre-added 18% HCl. Analysis for DOC was done on a Dohrmann DC-190 TOC analyser, after removal of dissolved inorganic carbon (DIC) by adding acid and using a vortex. Samples for hydrogen sulfide were taken in 10-ml PE tubes prefilled with a 2-ml zinc acetate solution trap-

ping the sulfide. Sulfide analysis was performed by spectrophotometry in the laboratory. For analysis of BTEX, naphthalene, and chlorinated aliphatics (June 1998), two 250-ml glass bottles were filled to the top and closed after the bottle overflowed to some extent. Two drops of a $CuSO_4$ solution were added in advance for conservation. Analysis was performed using a GC-FID coupled to a mass spectrometer (GC-FID/MS). Detection limit of the method was 0.2 μg/l. All samples were kept cool after sampling till analysis.

Hydrogen was measured in the groundwater using the "bubble strip" method (Chapelle and McMahon, 1991) in September 1998 and in October 1999. A 3-month rest period after installation of the wells is supposed to be sufficiently long to reach steady-state hydrogen levels representative of the initial undisturbed situation (Bjerg et al., 1997). A bladder pump was used, and a peristaltic pump the second time. These pumps give equal results (Chapelle et al., 1997).

Samples for Ar and N_2 gas analysis were taken in October 1999 using a Grundfos MP1 submersible pump and kept under pressure inside stainless steel cylinders to prohibit degassing. Gases were extracted using He, and concentrations were determined using a Hewlett-Packard 6890 GC equipped with a thermal conductivity detector (TCD) and a 1.8 m Molsieve 5-Å column.

A sample for δ^2H-CH_4 and δ^{13}C-CH_4 analysis was taken as follows: a 1-l glass bottle was filled and allowed to overflow for some time into a bucket. The filled bottle was put upside down into the partially filled bucket. The hose was put into the bottle and pumping continued. Degassing created a gas-phase of about 10 to 100 ml in most sample bottles. A butyl rubber stopper and a screw pod with a hole were put on the bottle under water. Afterwards an I_2-KI solution (1.5 g I_2 and 3 g KI to 100 ml aqua dest.) was added (five drops per 100 ml) using a syringe in order to stop microbial activity. For δ^{34}S-SO_4^{2-} and δ^{15}N-NO_3^-, 1-l high-density polyethylene (HDPE) bottles were filled and allowed to overflow with tubing at the bottom. Samples were conserved by adding in advance 50 mg zinc acetate and 15 ml 6M HCl, respectively. Isotope analysis of methane, sulfate and nitrate was performed at the Environmental Isotope Laboratory (EIL), University of Waterloo, Canada.

For δ^{13}C-DIC and δ^{13}C-DOC sampling, 100-ml glass bottles were filled and the I_2-KI solution was added. Analysis was done at the Centre for Isotope Research (CIO), University of Groningen, the Netherlands. Samples for δ^{13}C-DOC were acidified to remove DIC and subsequently freeze dried to obtain solid organic carbon, which was analyzed in triplicate. Samples for all isotopes were taken in October 1999, with the exception of δ^{13}C-DIC (September 1998).

2.3.3 Sediment sampling and analysis

Sediment samples were taken at one upstream location (SUP) and four downstream locations inside the plume (S2, S3, S6, and S9) in October 1998 (Fig. 2.2). A core pushing device (Delft Geotechnics) was used (Appelo et al., 1990). Immediately after recovery the cores were capped and stored in an airtight container made anaerobic by flushing with nitrogen gas, kept anaerobic, and transferred the same day to an anaerobic glovebox.

The Fe and S chemistry of the locations were investigated by performing chemical extractions on triplicates of sediment samples from which the pore water was extracted. Reactive Fe(III) and Mn oxides which are assumed to be available to microorganisms, were quantified using a reductive Ti(III)-EDTA extraction (Heron et al., 1994a) on 0.6, 0.8 and 1.0 g of sediment. Iron and Mn in the extracts were quantified using ICP-AES. Acid volatile sulfides (AVS: e.g., FeS minerals) and chromium reducible sulfide (CRS: e.g., pyrite) were quantified in a sequential AVS-CRS extraction performing a distillation (Fossing and Jørgensen, 1989). $SnCl_2$, 15%, was added to the 6 M HCl solution to enhance the recovery of sulfides, since iron hydroxides were present in the sample (Chanton and Martens, 1985). Here, sulfides were trapped in a 20 ml 4 % ZnAc solution with a drop of antifoam, and analyzed using spectrophotometry. Other extractions performed were a 24-h 0.5 M HCl extraction and a 3-week 5 M HCl extraction both at room temperature, to get a rapid indication of the redox state of the aquifer iron and to determine total Fe(II) and Fe(III), respectively (Heron et al., 1994b). Cation exchangeable Fe(II) was determined using a 1M NH_4OAc extraction (Thomas, 1982).

Calcium carbonate was determined according to Scheibler by measuring the CO_2 produced after adding HCl to a sediment suspension. The grain size distribution was measured on a FRITSCH Laser Particle Sizer A22 (Fritsch, Idar Oberstein, Germany), where the clay and silt fraction were determined according to Konert and Vandenberghe (1997). Soil organic carbon was determined after acidification of the sample on a Carlo Erba 1500NA elemental analyser.

2.3.4 Geochemical calculations

PHREEQC-2 (Parkhurst and Appelo, 1999) was used for all geochemical calculations, except for inverse modelling of δ^{13}C-DIC. NETPATH (Plummer et al., 1994) was used for this purpose. Henry's law constants taken from Andrews (1992) were used to calculate Ar and N_2 partial pressure. The pe $(-log[e^-])$ adopted for speciation calculations was computed from the NO_2^- / NO_3^- redox couple (pe $\approx$ 11) for nitrate-containing samples, while the H_2/H^+ redox couple (pe $\approx$ -3.0) was used for other pristine and plume samples. Acetate concentration determines alkalinity in acid-phase leachate (Devlin, 1990), but Albrechtsen et al. (1999) measured acetate concentrations below 6 μmol/l in older methanogenic-phase leachate like present at this site. Therefore, DOC likely contributes only 1–2 % to alkalinity in the present plume: Hemond (1990) determined that each mg organic carbon per liter lowers Gran alkalinity by 4.6 μeq/l. Consequently, DIC concentration was computed assuming only bicarbonate to contribute to alkalinity at pH below 8.2.

2.4 Delineation of the leachate plume

An electromagnetic survey using EM-34 was performed to find the lateral extent of the leachate plume (Nobes et al., 2000; Woldt et al., 1998). Subsequently, a series of cone penetration tests were carried out to verify the apparent conductivity pattern, and to map the vertical extent of the plume.

Apparent conductivity measured by EM-34 for the unpolluted upstream part (SE and SW side of landfill) ranged between 4.5–6.5 mS/m and 6–8 mS/m for the vertical loop (VL) and horizontal loop (HL) orientation, respectively. Results from a 10 m spaced grid stretching from the downstream sides of the landfill, showed relatively high values of apparent conductivity (7–22 mS/m for VL, 9–24 mS/m for HL). A northward stretching high conductivity zone was found in the area at the NW side of the landfill (Fig. 2.1).

Cone penetration tests (CPTs) were performed along a S–N transect and also upstream of the landfill (Fig. 2.1, C1–C8 in Fig. 2.2). The transect was assumed to be oriented in the flow direction of the plume. The formation conductivity recorded by the CPTs shows anomalously high values up to 100 mS/m (Fig. 2.2: C2) in the upper sand layer along the S–N transect downstream from the landfill. The high conductivity zone stretching from the landfill border to the Heiloop stream must be attributed to elevated electrical conductivity of pore water as the lithology remains sandy as indicated by the friction ratio (Fig. 2.2) and later confirmed by bailer drillings. The top of the leachate plume decreased from groundwater level at the landfill to a depth of 5 m below surface further downstream, while the maximum depth of the plume was found at about 9 m below surface. Remarkably, the conductivity of the leachate decreased in the flow direction as indicated by CPTs (Fig. 2.2), EM-34 measurements (Fig. 2.1), and electrical conductivity (EC) measurements of the groundwater (results not shown). Inverse modelling of the hydrochemistry showed that the EC decrease is explained by precipitation of carbonate minerals in the plume, and not by dilution (as shown later).

2.5 Hydrogeochemistry

2.5.1 Composition of the leachate and pristine groundwater

The pristine aquifer is anaerobic at shallow depth. Nitrate has only been observed above the leachate plume, and upstream of the landfill where it decreases with depth. The pristine aquifer does not contain $CaCO_3$ (<0.5% w/w). Pristine groundwater is slightly acid (pH 4.6–6.0, but up to 6.6 below plume), has a low alkalinity, and low concentrations of methane, sulfide and moderate concentrations of Fe(II) (Table 2.1). The leachate contains high concentrations of dissolved organic carbon (DOC), alkalinity, methane, ammonium, iron, and other major ions (except SO_4^{2-} and NO_3^-), and has a pH just below neutral (Table 2.1). Sulfate concentrations are low in leachate, but somewhat higher upstream and above the plume in pristine groundwater. The hydrochemistry changed little in time for most wells, except at well W9b, and sulfate decreased in time.

2.5.2 Fate of organic carbon in the plume

Dissolved organic carbon (DOC) decreases from 9.2 to 5.4 mmol/l in downstream direction, while no dilution appears to take place as indicated by high and constant chloride concentrations along the central flow path in the plume (Table

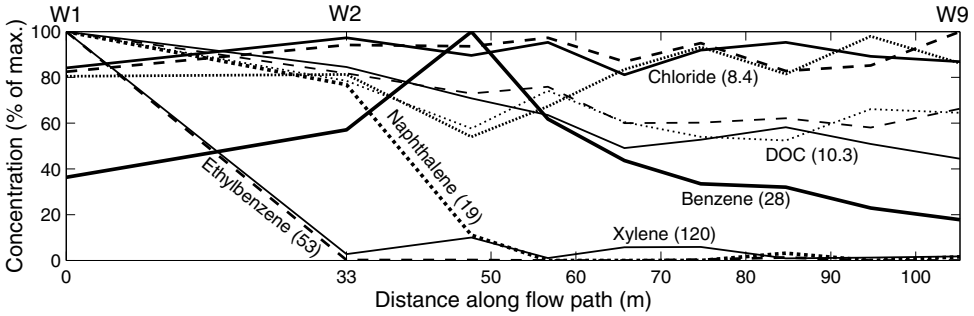

Figure 2.3: Concentrations (scaled to maximum observed concentration) of conservative chloride, organic micropollutants (benzene, ethylbenzene, xylene, naphthalene), and dissolved organic carbon (DOC) plotted along the central flow path indicated in Fig. 2.2. Maximum concentrations are shown between parentheses (chloride and DOC, mmol/l; organic micropollutants, μg/l). Chloride and DOC are shown from first (full lines), second (dashed), and third time of sampling (dotted).

2.1, Fig. 2.3). The decrease was largest in the vicinity of the landfill and more sluggish downstream. Microbial degradation must have lowered the DOC concentration downstream, since sorption of DOC to aquifer sediments having a low solid organic carbon content (Table 2.2) is not of importance (Christensen et al., 2001). Dissolved organic carbon in methanogenic-phase leachate consists mainly of humic- and fulvic acids (Christensen et al., 1998; Christensen et al., 2001), and its concentration is about 3 orders of magnitude higher than the total concentration of organic micropollutants at this site.

Concentrations of aromatic compounds (benzene, ethylbenzene, xylene and naphthalene) decrease in downstream direction as well (Fig. 2.3). Other organic contaminants measured (toluene, chlorinated aliphatics) had concentrations below 1 μg/L. However, occurrence of degradation cannot be ascertained for organic contaminants, since sorption and spatial and temporal source heterogeneity could produce the concentration profiles as well (computations not shown).

2.5.3 Distribution of redox species

Oxygen was not detected in any well, but nitrate is present in the shallow background groundwater upstream of the landfill (max 6.1 mmol/l) and above the plume (max 1.2 mmol/l). Nitrate reduction, probably coupled to oxidation of iron-sulfide minerals, causes disappearance of nitrate with depth upstream from the landfill (e.g., Postma et al., 1991). Nitrate reduction is a likely process at the mixing zone of landfill leachate and shallow nitrate containing groundwater.

High methane concentrations are observed inside the leachate plume, which tend to decrease downstream (Fig. 2.4). Methane is probably produced inside the landfill body, and subsequently transported with groundwater flow, as supported by isotope analysis and discussed later.

Several measurements and calculations were performed to evaluate the occurrence of sulfate reduction in the plume. Sulfate concentration did not decrease

downstream (Fig. 2.4), and dissolution of sulfate minerals does not occur, as groundwater is undersaturated for both gypsum and barite. Hydrogen sulfide concentrations close to the detection limit of the method, were detected throughout the plume ($H_2S \approx 3$–6 μmol/l) and may indicate equilibrium with amorphous FeS (SI ≈ -0.5 to +0.2) rather than occurrence of sulfate reduction. The content of acid volatile sulfides (AVS) and chromium reducible sulfides (CRS) was low in the polluted part of the aquifer, and not much higher than upstream, where FeS minerals could have been partially dissolved by inflow of nitrate (Table 2.2). Occurrence of sulfate reduction reflected by an elevated FeS content decreasing in downstream direction of the plume (Heron et al., 1994b) was not observed here. In conclusion, the sulfur chemistry indicated lack of sulfate reduction in the plume.

Considerable evidence for occurrence of iron reduction in the plume was found. The Fe(II) concentrations are elevated in the plume, and increase in downstream direction (Table 2.1, Fig. 2.4). Iron(III)-oxide that is considered to be bio-reducible, is present, although in low contents (Table 2.2). Remarkably, the iron oxide content is higher in the plume than for the background sample, while a decreasing gradient of iron oxide content towards the source, reflecting occurrence of iron reduction

Table 2.1: Composition of leachate leaving the landfill border (W1b), leachate at the downstream end of the plume (W9b) and pristine groundwater

Parameter	Leachate (border)		Leachate (end)		Pristine
Chloride (mmol/l)	6.74–7.05	(6.91)	7.22–8.38	(7.62)	0.34–2.17
DOC (mmol C/l)	9.0—8.2—10.3	(9.2)	4—5.4—6.7	(5.4)	0.25–1.92
Ammonium (mmol/l)	19.2–19.8	(19.4)	1.4–5.2	(3.0)	0.006–0.067
Alkalinity (mmol/l)	51.3–56.8	(54.8)	9.9–22.2	(15.4)	0.2–6.6
DIC calculated[a] (mmol/l)	73.8—90.0—87.6	(83.8)	39.3—59.6—71.8		1.3–19
pH	6.4–6.7	(6.56)	5.85–5.96	(5.90)	4.6–6.6
EC (μS/cm)	4520–5260		1790–2560	(2150)	189–754
Oxygen (mmol/l)	0		0		0
Nitrate (mmol/l)	0		0		0–1.2–6.1
Nitrite (μmol/l)	1–6.5		1.3–2.2		0–4.3
Iron (II) (mmol/l)	0.20–1.24	(0.81)	1.20–1.97	(1.52)	0.002–0.47
Manganese (II) (μmol/l)	6.4–9.1	(7.6)	18–40	(25)	0.5–13
Sulfate (mmol/l)	0.058–0.073		0.073–0.10		0.018–1.72
Sulfide (μmol/l)	3–6		6		0–9
Methane (mmol/l)	1.33–1.48		0.77–0.87		0–0.56
Sodium (mmol/l)	7.7–9.39	(8.4)	8.22–8.7	(8.4)	0.3–2.6
Potassium (mmol/l)	5.55–6.14	(5.9)	0.28–1.07	(0.61)	0.03–0.41
Calcium (mmol/l)	7.83–10.4	(9.21)	2.27–3.27	(2.87)	0.42–2.72
Magnesium (mmol/l)	3.1–4.36	(3.9)	1.3–2.1	(1.65)	0.12–0.49
Phosphate (μmol/l)	$<$0.1 (W1a: 23)		0.2		$<$0.1–2
SI Siderite	+1.05 to +1.58		+0.78 to +1.27		-5.7 to -0.7
SI Calcite	+0.67 to +0.75		-1.17 to -0.62		-5 to -1.2
SI Dolomite	+0.89 to +1.05		-2.66 to -1.51		-11 to -3.2
δ^{13}C-DIC (‰)	+13.1		+9.6 (W7b)		-19.55
δ^{13}C-CH_4 (‰)	-53.1		-52.7		-72.6
δ^{13}C-DOC (‰)	-27[b]		-27[b]		-27[b]

Range of concentrations in time and averages in parentheses (n = 3) are given. For DIC and DOC concentrations for all measurement events are given (June 1998 — September 1998 — October 1999).

[a] *Dissolved inorganic carbon (DIC) has been calculated in PHREEQC using alkalinity and pH.*

[b] *Value of δ^{13}C-DOC is average for nine plume samples (W1b–W9b). Pristine values are about equal.*

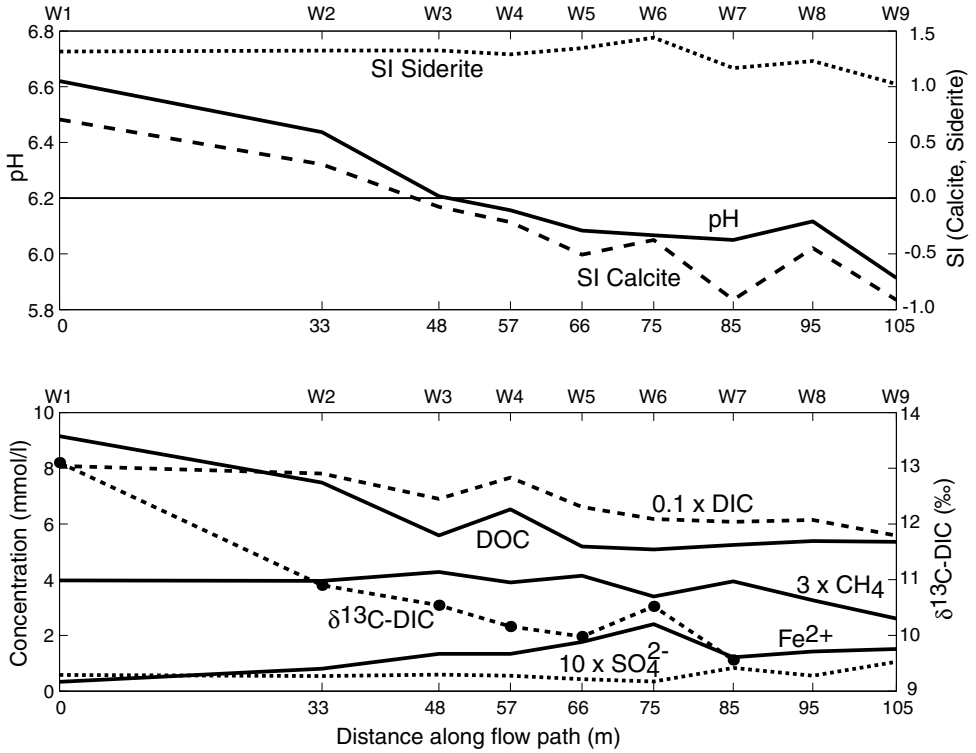

Figure 2.4: Average concentrations (n = 3) for various parameters along central flow path in leachate plume (W1b to W9b): (above) pH and saturation indices (SI) of calcite and siderite; (below) redox species, DOC, DIC and δ^{13}C-DIC. For methane and sulfate concentrations from the last measurement event are shown. δ^{13}C-DIC has been measured in September 1998. Concentrations of methane, sulfate and DIC are multiplied by a factor of 3, 10 and 0.1, respectively.

Table 2.2: Geochemistry and characteristics of sediment samples[a]

Sample	Fe(III)-r[b] (μg Fe/g)	Fe(III)-t[c] (μg Fe/g)	FeS[d] (μg S/g)	FeS_2[d] (μg S/g)	"$FeCO_3$"[e] (μg Fe/g)	org C (%)	Clay (%<2μm)
SUP, Upstream	35±2	318±44	0±0	35±6	20	0.034	1.44
S2, 33m	154±5	585±53	2.2±2.2	23±2	94	0.255	2.22
S3, 48m	155±8	652±89	2.2±2.2	82±9	72	0.069	6.11
S6, 75m	203±3	806±30	0.4±0.6	73±1	24	0.075	6.99
S9, 105 m	82±1	257±15	2.7±2.4	126±16	20	0.054	2.26

[a] *Values are the means and standard deviations of five replicates for Fe(III)-r, of three or four replicates for Fe(III)-t, and triplicates for FeS and FeS_2.*
[b] *Reactive iron-oxide: Ti(III)-EDTA extraction.*
[c] *Total Fe(III): Fe-total minus Fe(II) in 5M HCl extraction.*
[d] *Sequential AVS-CRS extraction to determine FeS and FeS_2, respectively.*
[e] *Fe(II) soluble in 0.5M HCl minus FeS and ion-exchangeable Fe(II).*

(Heron et al., 1994b), is non-existing. Apparently, natural variations in iron oxide content conceal this geochemical trace of iron reduction (Heron et al., 1998).

A strong argument in favor of iron reduction is supersaturation of siderite in the plume ($FeCO_3$; SI +0.8 to +1.8), while pristine groundwater was undersaturated. Supersaturation for siderite has been observed at other landfill leachate plumes where iron reduction occurred (Nicholson et al., 1983; Kehew and Passero, 1990; Baedecker et al., 1993; Bjerg et al., 1995; Amirbahman et al., 1998). Siderite precipitation has been observed under laboratory conditions (Jensen et al., 2002), and likely happens in the present plume as well, buffering the concentration of Fe(II) released by iron reduction. Manganese reduction was negligible, as both Mn(II) concentration (Table 2.1) and content of manganese oxide ($<$1.4 μg Mn/g) were about 2 orders of magnitude lower than Fe(II) and Fe oxide, respectively.

Siderite is difficult to measure when present in low content, and no good extraction method exists (Christensen et al., 2001). According to Heron et al. (1994b), iron(II) extracted in 0.5 M HCl during 24 hours minus iron associated with acid volatile sulfide (AVS) minus ion-exchangeable Fe(II), gives a semi-quantitative estimate for the content of siderite. However, the 0.5 M HCl extraction needs to be corrected for dissolution of Fe-silicates (cf. Griffioen and Broers, 1993), which was not performed in this study. Still, the combination of extractions used by Heron (1994b) gave higher values in the plume than upstream, and decreased in downstream direction (Table 2.2: "$FeCO_3$"). This might reflect occurrence of siderite precipitation in the plume.

2.5.4 Gibbs free energy of hydrogen-oxidizing redox reactions

The Gibbs free energy (ΔG_r) of hydrogen-oxidizing redox reactions or terminal electron-accepting processes (TEAPs) oxidizing H_2 (e.g. CO_2 reduction, sulfate reduction, iron reduction) can be calculated when the concentrations of redox species involved, the pH, temperature and the H_2 concentration is known (Hoehler et al., 1998; Jakobsen et al., 1998). Microbial communities conducting a TEAP appear to control the H_2 concentration in order to keep ΔG_r of the reaction at some (negative) threshold value necessary to synthesize ATP. A threshold value of -7 kJ/mol H_2 (Schulz and Conrad, 1996) was assumed for TEAPs to be favorable (Jakobsen et al., 1998). The general equation for H_2oxidizing reactions, where the stoichiometric coefficient for H_2 is 1, is given by:

$$1H_2 + aOx + bH^+ \longrightarrow cRed + dH_2O \tag{2.1}$$

The associated Gibbs free energy is calculated as:

$$\Delta G_r = \left(\Delta G_T + RTln\left(\frac{[Red]^c}{[Ox]^a[H^+]^b} \right) \right) - RTln[H_2] \tag{2.2}$$

where Ox and Red are the activity of the electron-acceptor and its reduced species, respectively, ΔG_r is the Gibbs free energy of the reaction, ΔG_T is the Gibbs free energy under standard conditions at temperature T (K), R is the gas constant, and T is the absolute temperature (K).

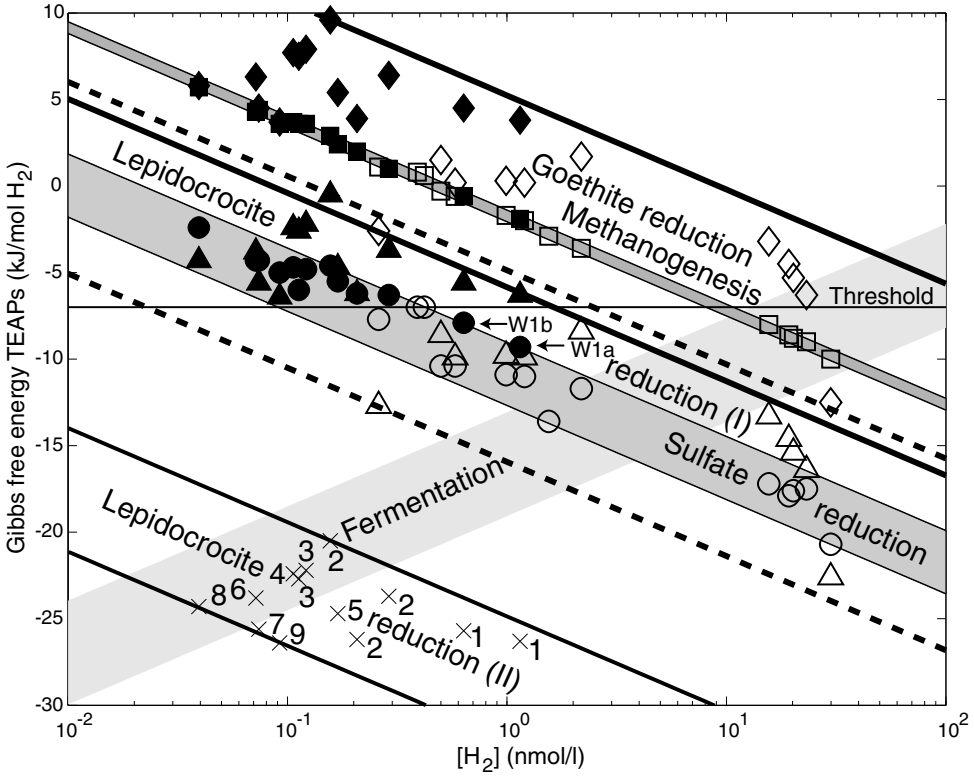

Figure 2.5: Measured hydrogen gas concentrations and calculated Gibbs free energies (ΔG_r) of terminal electron-accepting processes (TEAPs): goethite reduction (1998: ◇, 1999: ◆), methanogenesis (1998: □, 1999: ■), sulfate-reduction (1998: ○, 1999: ●), stable lepidocrocite (I) reduction (1998: △, 1999: ▲), and less-stable lepidocrocite (II) reduction (1999: x, number of observation well site W1–W9). Calculated H_2–ΔG_r areas for methanogenesis, sulfate-reduction, and possible area of fermentation are shaded, while areas for goethite-reduction, stable and less-stable lepidocrocite reduction are bound by full lines, dashed lines and full lines, respectively. A threshold of -7 kJ/mol H_2 is shown.

Equation 2.2 plots as a straight line, when temperature, pH and activities of redox species are taken constant. Therefore, for each order of magnitude of decrease in H_2 concentration, ΔG_r increases (for fermentation, which produces H_2, it decreases) with 5.4 kJ/mol H_2 at 11 °C. The minimum and maximum value of the first part of eq. 2.2 (between parentheses) were calculated from the total data set for each TEAP to determine the area wherein the measured data should fit (Fig. 2.5). A community of microorganisms is thought to lower the H_2 concentration to a minimum threshold value in order to outcompete members of the community performing less favorable TEAPs (Lovley and Goodwin, 1988). An additional explanation for maintaining low H_2 concentrations by hydrogen consuming microorganisms could be to maximize ΔG_r for fermentation (Fig. 2.5), which might increase H_2 turnover.

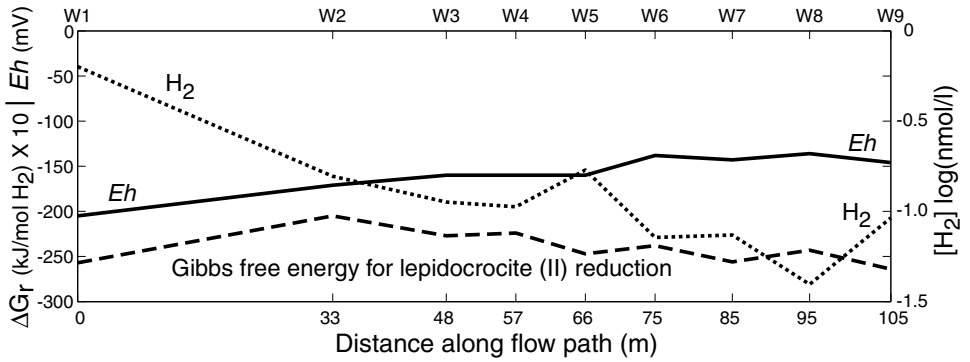

Figure 2.6: Downstream change in Gibbs free energy for lepidocrocite (II) reduction, H_2 concentration, and *Eh* calculated using the H_2/H^+ redox couple.

Hydrogen concentrations measured 3 months after installation of the observation wells were much higher (0.26–30 nM) than those measured the following year (0.04–1.15 nM, Fig. 2.5), while the concentrations of redox-species and pH did not differ much. Apparently, H_2 concentrations did not reach steady-state at this site within a three month period, which was thought to be sufficient (Bjerg et al., 1997). If unnoticed, a non-equilibrium situation for H_2 leads to an erroneous qualification of redox conditions: too reduced and overlapping (Fig. 2.5).

Methanogenesis appears not to happen (at least in the permeable parts of the aquifer) and is for most samples even thermodynamically unfeasible (up to +5.7 kJ/mol H_2). Reverse methanogenesis is not likely to occur as the threshold for this process leading to removal of methane is expected to be at +10 kJ/mol H_2 (Hoehler et al., 1994). The Gibbs free energy is at most locations also too low for sulfate reduction to happen, but sulfate reduction might be favorable inside and just below the landfill (W1a and W1b, Figs. 2.2, 2.5). It must be concluded that iron reduction is the dominant TEAP, as sulfate-reducers and methanogens are not capable of maintaining the low observed hydrogen concentrations.

The calculated ΔG_r for iron reduction depends to a large extent on the Gibbs free energy of formation of the iron oxide mineral being reduced. The iron oxides lepidocrocite and goethite were most abundant in similar Quaternary sediments in Denmark (Jakobsen et al., 1998). Lepidocrocite has a variable reactivity confined by type I and II (least and most reactive, respectively; Jakobsen et al., 1998). Figure 2.5 shows that ΔG_r for goethite and lepidocrocite (I) reduction is too high for iron reduction by H_2 to happen. Apparently, lepidocrocite with an intermediate reactivity is present and being reduced.

Hydrogen was measured for two nitrate-containing wells above the plume (W6a and W8a). Concentrations were not lower (0.09–0.10 nM) than inside the plume. Possible nitrate reduction at these locations did not result in the lowest hydrogen concentrations as would be expected (Lovley and Goodwin, 1988). Hydrogen was for two pristine locations below the plume in the same range as inside the plume (W3c: 0.13 nM, W5c: 0.16 nM). Here, ΔG_r was favorable for iron reduction.

The hydrogen concentration decreased with distance from the landfill, while ΔG_r for iron reduction kept quite constant (Fig. 2.6). The change of hydrogen seems controlled by iron-reducers responding to the decrease in pH downstream (Fig. 2.4), while being active at a fixed threshold value (Fig. 2.6). Similar effects have been observed for changing sulfate concentrations, temperature and pH in laboratory experiments (Hoehler et al., 1998). The geochemical reactions of proton-buffering and carbonate mineral precipitation cause the pH to decrease (see Chapter 5). Consequently, the geochemical provoked pH decrease, leads to a microbiological controlled H_2 decrease, and results in an increase of redox potential (*Eh*) downstream (Fig. 2.6).

2.5.5 Distribution of dissolved gases and degassing

The gas composition of the leachate plume was measured in 1999. Results are shown in Table 2.3. Partial pressure of N_2 and argon inside the plume (pN_2 = 0.51 atm, pAr = 0.0041 atm at 11 °C) are lower than for groundwater in equilibrium with the atmosphere (pN_2 = 0.78 atm, pAr = 0.0093 atm) or pristine groundwater (W8a). This is explained by production of methane and carbon dioxide inside the landfill body causing simultaneous degassing of these gases along with Ar and N_2. Argon and N_2 concentrations, 25 times lower than background, suggested methane removal by gas exsolution in a crude-oil spill (Revesz et al., 1995). Outgassing of methane from a pollution plume has been argued before (Baedecker et al., 1993), and Blicher-Mathiesen et al. (1998) calculated degassing using dissolved argon concentrations. Argon shows variable pressures in the plume but no tendency in downstream direction. So, no unequivocal data exist here to calculate potential degassing inside the plume. Remarkably, total gas pressure exceeds hydrostatic pressure for all samples with 0.1 to 0.6 atm (Table 2.3). Degassing will occur when total gas pressure exceeds hydrostatic pressure and capillary effects can be overcome (Yager and Fountain, 2001). Perhaps the fine aquifer sediments pro-

Table 2.3: Partial pressure of gases and hydrostatic pressure in leachate plume

Sample	pAr (atm)	pN_2 (atm)	pCH_4 (atm)	pCO_2 (atm)	ΣP gases (atm)	Elevation screen (m +msl)	Hydraulic head[a] (m +msl)	Hydrostatic pressure[a] (atm)
W1b	–	–	0.73	0.60	–	2.35	8.64–7.87	1.55–1.63
W2b	0.0018	0.19	0.72	0.93	1.84	3.04	8.47–7.72	1.47–1.54
W3b	0.0029	0.31	0.78	0.72	1.81	1.16	8.38–7.71	1.66–1.72
W4b	0.0036	0.51	0.71	0.94	2.16	2.01	8.32–7.70	1.57–1.63
W5b	0.0029	0.33	0.76	1.01	2.10	1.85	8.30–7.70	1.59–1.65
W6b	0.0041	0.37	0.62	1.32	2.31	1.11	8.26–7.70	1.66–1.72
W7b	0.0032	0.37	0.72	1.09	2.18	1.73	8.24–7.70	1.60–1.65
W8b	0.0025	0.27	0.60	1.23	2.10	1.68	8.21–7.68	1.60–1.65
W9b	–	–	0.48	0.96	–	2.67	8.20–7.69	1.50–1.55
W8a	0.0091	1.18	0.17	0.22	1.57	5.10	8.20-7.69	1.26–1.31

Sampling was done in October 1999. Pressures were calculated for a groundwater temperature of 11 °C.
[a] *Maximum and minimum values for hydraulic head and hydrostatic pressure are given for the period June 1998–Februari 2001 (n = 11).*

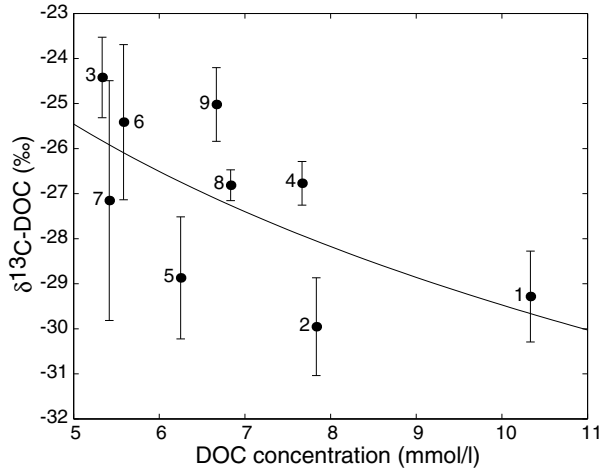

Figure 2.7: Relation between δ^{13}C-DOC and DOC concentration in leachate plume. Averages and standard deviations of triplicates and corresponding well numbers are shown.

hibit degassing and cause gas supersaturation. However, occurrence of degassing is likely and could explain the slight decrease of methane in downstream direction (Table 2.3, Fig. 2.4).

Partial pressure of nitrogen gas in nitrate-containing well W8a above the plume is 50 % higher than atmospheric nitrogen partial pressure, supplying further evidence to occurrence of denitrification above the plume. Total gas pressure above the plume exceeds hydrostatic pressure as well, but apparently not much degassing has happened, as argon is close to atmospheric partial pressure. Degassing of methane inside the plume, and subsequent dissolution above the plume explains the presence of methane in nitrate-containing sample W8a.

2.6 Isotope geochemistry

2.6.1 δ^{13}C of dissolved organic carbon

A considerable range was found for δ^{13}C-DOC in leachate (-24 ‰ to -30 ‰, n = 9), and an average of -27 ‰ was calculated. These signatures were in agreement with the values found for C3 plants (Mook, 2000). δ^{13}C-DOC showed a tendency to increase with distance from the landfill (R^2 = 0.32), and an inverse correlation with DOC concentration was found (R^2 = 0.39). Degradation of certain organic compounds favors the ^{12}C with respect to the ^{13}C isotopes, which results in an enrichment of δ^{13}C in the residual fraction (Faure, 1986). Therefore, the observed (weak) correlation between increasing δ^{13}C-DOC values and decreasing DOC concentrations supports that degradation of DOC takes place in the plume (Fig. 2.7). The calculated enrichment factor (ϵ) for DOC degradation was 5.9 ± 2.7 ‰.

2.6.2 δ^{13}C of dissolved inorganic carbon

δ^{13}C-DIC in the plume (+9.6 ‰ to +13.1 ‰) is strongly enriched with respect to background (-19.6 ‰). High δ^{13}C-DIC values are generally observed for landfill leachate and are thought to be related to production of isotopically positive CO_2 by methanogenesis (Hackley et al., 1996), and to a lesser extent by outgassing of CO_2 (Baedecker and Back, 1979; Hornibrook et al., 2000). Microbial degradation at mesophilic temperatures could be another reason (Hornibrook et al., 2000).

We pose that the pH value of leachate determines the impact of CO_2 outgassing on δ^{13}C-DIC enrichment. Hornibrook et al. (2000) suggested that a leachate pH between 7 and 8 is an important condition for causing increased δ^{13}C-DIC values due to outgassing of CO_2. However, in that pH range degassing of carbon dioxide cannot be of major importance as DIC is dominated by bicarbonate. On the contrary, leachate of many landfills, including this one, has a pH between 6 and 7. Consequently, DIC comprises dissolved CO_2 and HCO_3^- in comparable quantity. Isotopic and chemical equilibrium exists in groundwater between the two species with bicarbonate enriched by +10.7 ‰ to +8.4 ‰ with respect to aqueous carbon dioxide (and +9.6 ‰ to +7.4 ‰ with respect to CO_2(g)) at 10 °C and 30 °C, respectively (Mook, 2000). So, degassing of CO_2 can happen in a mixed bicarbonate-carbon dioxide system, while the difference between δ^{13}C-CO_2 and δ^{13}C-DIC is large, and consequently the impact of CO_2 degassing on δ^{13}C-DIC increase will be considerable. Indications of occurrence of carbon dioxide and methane degassing are the low Ar and N_2 concentrations in the plume as discussed before.

δ^{13}C-DIC in the plume decreases in downstream direction from +13.1 ‰ at the landfill border (W1b) to +9.6 ‰ further downstream at W7b (Fig. 2.4, no data for W8 and W9). Processes thought to cause this decrease are discussed in Section 2.7.

2.6.3 δ^{13}C and δ^{2}H of methane

δ^{2}H and δ^{13}C of dissolved methane were measured in 1999 for 9 samples along the central flow path in the flow direction of the plume (W1b to W9b), for one sample below (W5c), and for one sample above the plume (W8a). Methane isotopes inside the plume were characteristic of landfill gas and acetate fermentation (δ^{13}C-$CH_4 = -53.3 \pm 0.5$ ‰; δ^{2}H-$CH_4 = -304 \pm 6$ ‰), while the methane found below the plume (δ^{13}C-$CH_4 = -72.6$ ‰; δ^{2}H-$CH_4 = -241$ ‰) was apparently formed by the CO_2 reduction pathway (Hackley et al., 1996). Methane measured above the plume was lower in concentration and slightly enriched in ^{13}C (-50.3 ‰) with respect to landfill leachate methane. This confirms methane degassing in the plume (see before), followed by methane oxidation at the top fringe of the plume under nitrate-reducing or sub-oxic conditions, as δ^{15}N-NO_3^- determined from the same sample was very positive (+41.5 ‰, 0.19 mmol/l). Anaerobic methane oxidation by NO_3^- has been hypothesized to occur at the fringe of leachate plumes (Griffioen, 1999), and this field evidence indicates the act of anaerobic methane oxidation.

A weak correlation was found ($R^2 = 0.53$) between decreasing methane concentrations and slightly increasing δ^{13}C values in the flow direction of the plume. The calculated fractionation factor was low ($\alpha \approx 1.001$) and may be indicative of de-

gassing, as oxidation involves larger fractionation (Bergamaschi, 1997). However, no correlation was found for δ^2H-CH_4, which fractionates more strongly.

According to Hornibrook et al. (2000) the isotopic separation between δ^{13}C-CH_4 and δ^{13}C-DIC increases when the ratio of availability of labile organic matter to availability of oxidants decreases. The lower the ratio, the larger the contribution of the CO_2 reduction pathway (which involves larger fractionation) to methanogenesis, and the lower the contribution of acetate fermentation. Hence, we argue that methane produced inside a leachate plume might have a more negative isotopic signature than methane produced inside a landfill body, as the availability of organic substrates in the plume is less. If this holds, active methanogenesis inside a leachate plume might be established using isotopes, and absence of an observed downstream decrease in isotopic methane signature may then reflect the lack of methanogenesis in the plume.

2.6.4 δ^{34}S of sulfate

Sulfate concentrations in leachate decreased by a factor 30 from around 0.34 mmol/l down to 4–27 μmol/l in a period of nearly three years after installation of observation wells, but concentrations did not decrease in downstream direction in any of the four sampling events. Seven samples obtained in October 1999 were analysed for δ^{34}S, of which five originate from within the plume (0.03–0.1 mmol/l, wells 3, 5, 6, 7, 9), one from above the plume (W8a: 0.56 mmol/l), and the last one from below the plume (W5c: 0.018 mmol/l). The samples showed low δ^{34}S values (-3.3 ‰ to +9.1 ‰) indicating that the origin of sulfate could be meteoric (-3 ‰ to +9 ‰ for anthropogenic sulfate in rainfall (Krouse and Mayer, 2000)). Sulphur isotopes of sulfate confirm that sulfate reduction is not occurring in the plume, because the enrichment factor calculated following Strebel et al. (1990) was too low ($\epsilon \approx 4.6$ ‰, n = 5) for sulfate reduction (ϵ = 10 ‰ to 24 ‰ and higher (Krouse and Mayer, 2000)). A high correlation (R^2 = 0.87, n = 7) between δ^{34}S and the inverse of sulfate concentration suggests that a source with a δ^{34}S signature around -2.5 ‰ such as pyrite may have caused elevated sulfate concentrations. However, possible oxidation of FeS minerals during construction of observation wells can only account for a third of the sulfate concentration observed after installation. In conclusion, sulfate reduction is not occurring. Elevated sulfate concentrations seem related with the placement of observation wells, but cannot be explained in a mechanistic way.

2.7 Quantification of redox and geochemical processes in the plume

Results of qualitative methods for interpretation of redox conditions were presented in previous sections. Inverse geochemical modelling is a better and quantitative approach to interpret redox conditions using groundwater composition data (Amirbahman et al., 1998; Baedecker et al., 1993). In this section the results will be presented of an inverse geochemical model integrating the governing biogeochemical processes changing the leachate composition in downstream direction.

Previous sections showed that degradation of DOC in the plume is coupled to microbial iron reduction, but geochemical processes are expected to change the leachate composition as well. Precipitation of carbonate minerals was included in the model, since leachate is supersaturated for siderite over the full length of the plume, and for calcite and dolomite (SI up to +1.8) near the landfill (Fig. 2.4). Furthermore, concentrations considerably lower downstream than near the source indicate that cation-exchange retards ammonium and potassium (Table 2.1). Calculations on the composition of exchange sites in equilibrium with pristine and polluted groundwater (results not shown) indicated that NH_4^+ and K^+ exchange in release for mainly Ca^{2+} and also Fe(II), since the pristine aquifer is anaerobic and contains a Fe(II) concentration up to 0.5 mmol/l. Sodium and magnesium exchange is less significant. Degassing was not included because it only lowered the methane concentration.

The inverse model was constrained by the observed compositions of the first (W1b) and final well (W9b) along the flow path. Calculations were performed for each of the three sampling events and using the average composition given in Table 2.1. Values of some parameters (pH, DIC) were changed by less than 4 % in order to obtain stable solutions, with exception of the model for the last sampling occasion where DIC in the model was changed by 9 %. The model presumes that the leachate composition in the final well (W9b) has evolved from the composition in the initial well (W1b).

Table 2.4 shows the list of reactions (phases) included in the model. Nitrate reduction at the top fringe of the plume did not affect the hydrochemistry at the inner part of the plume, and was therefore irrelevant for the model. The calculated contribution of individual reactions is expressed in mmol per liter. A negative sign means the phase is consumed and a positive sign means it is produced. The inverse model confirmed that degradation of DOC was coupled to reduction of iron oxide, and explained together with cation-exchange and precipitation of carbonate minerals the observed change in leachate composition. Results for cation-exchange and carbonate mineral precipitation were comparable for various sampling events (Table 2.4). The consumption of iron oxide, however, varied considerably because

Table 2.4: Inverse geochemical model of central flow path in leachate plume (W1b to W9b)

Reaction	Phase	Reaction equation	Change[a,b]	(mmol/l)
1	DOC	$CH_2O + H_2O \rightarrow CO_2 + 4H^+ + 4e^-$	−3.8	(−5.0, −2.7, −3.4)
2	Iron-oxide	$FeOOH + 3H^+ \leftrightarrow Fe^{3+} + 2H_2O$	−15.3	(−20, −11, −13)
	Redox transfer	$Fe^{3+} + e^- \leftrightarrow Fe^{2+}$	+15.3	
3	Siderite	$Fe^{2+} + CO_3^{2-} \rightarrow FeCO_3$	+14.6 to +25.5	(+31, +21, +23)
4	Calcite	$Ca^{2+} + CO_3^{2-} \rightarrow CaCO_3$	+4.1 to +15	(+2.7, +3.5, +6.9)
5	Dolomite	$Ca^{2+} + Mg^{2+} + 2CO_3^{2-} \rightarrow CaMg(CO_3)_2$	+2.3	(+3.1, +2.9, +1.3)
$\sum$3–5		$Fe_{0.43-0.74}Ca_{0.19-0.50}Mg_{0.07}CO_3$	+34.2	
6	KX	$K^+ + X^- \rightarrow KX$	+5.3	(+5.3, +5.7, +5.2)
7	NH_4X	$NH_4^+ + X^- \rightarrow NH_4X$	+16.6	(+18, +17, +17)
8	IX_2	$I^{2+} + 2X^- \leftarrow IX_2$	−10.9	(−12, −11, −11)
		where ($I^{2+} = \sum Fe^{2+} + Ca^{2+}$)		

[a] *Results are shown for model constrained by average concentrations. Results for individual sampling events (taking Fe^{2+} for I^{2+}) are given between parentheses (June 1998, September 1998, October 1999).*

[b] *A negative value means the phase is consumed, a positive value means the phase is produced.*

it was determined by the downstream DOC decrease, which differed substantially at each sampling event.

The inverse model shows that it is essential to take (secondary) geochemical processes into account for both qualification and quantification of redox processes using groundwater composition data. This is illustrated in a batch model simulating the impacts of the individual reactions on the downstream change in leachate composition (Table 2.5). Iron reduction cannot be quantified using the Fe(II) distribution while ignoring secondary geochemical processes, since the Fe(II) concentration resulting from DOC degradation would be an order higher than observed (Table 2.5: R1–2). Precipitation of carbonate minerals must happen to buffer released Fe(II), and lower the Ca, Mg, and DIC concentration, as well as the pH downstream (Table 2.5: R1–5). The observed decrease in pH and DIC downstream can only be fully matched if cation-exchange is considered, as release of Ca and Fe(II) to leachate enhances precipitation of carbonate minerals (Table 2.5: R1–8). The model gives the total amount of divalent cations released for NH_4^+ and K^+ exchange, but cannot predict the proportion of Ca^{2+} and Fe(II). Carbonate minerals of mixed composition could precipitate in addition to or instead of pure phases (Table 2.4). Precipitation of ferroan calcite ($Fe_{0.8}Ca_{0.2}CO_3$) was observed in a crude oil polluted aquifer (Baedecker et al., 1993), and could happen in the present leachate plume as well.

The calculated total amount of carbonate minerals precipitated (34 mmol/l C) was low when expressed on a weight basis ($\approx$ 0.06 % w/w). Unfortunately, the measurement method used (having a detection limit of 0.5 % w/w) was not able to detect these low contents. Carbon isotopes were added as constraints to the inverse model to verify the occurrence of carbonate mineral precipitation. An average value of -27 ‰ was adopted for δ^{13}C-DOC, although a tendency of increasing leachate δ^{13}C-DOC values was observed during degradation (Fig. 2.7). NETPATH calculated δ^{13}C-DIC to decrease from +13.1 ‰ at the landfill to +11.1 ‰ at final well W9b when only degradation of DOC was modelled and fractionation associated with carbonate mineral precipitation was neglected. Observations were unfortunately not available for the final well (W9b), but a decreasing tendency of downstream δ^{13}C-DIC values make it plausible that δ^{13}C-DIC is lower than the value of +9.6 ‰ measured at W7b (Fig. 2.4). A δ^{13}C-DIC value of +8.2 ‰ at W9b was calculated when fractionation during precipitation of carbonate minerals was included. Consequently, the observed decrease in δ^{13}C-DIC reflects the occurrence of carbonate mineral precipitation.

Table 2.5: Leachate composition (mmol/l) used in the inverse geochemical model (W1b: initial solution, W9b: final solution) and impact of individual processes (R1–8) on the downstream change in leachate composition

	pH	DOC	DIC	Ca^{2+}	Mg^{2+}	K^+	NH_4^+	Fe^{2+}	SI $FeCO_3$
W1b	6.53	9.2	87.5	9.27	3.93	5.95	19.6	0.82	+1.51
W1b + R1–2[a]	7.22	5.4	91.4					16.1	+3.49
W1b + R1–5	6.44	5.4	68.1	2.88	1.66			1.53	+1.68
W1b + R1–8 = W9b	5.94	5.4	57.2	2.88	1.66	0.61	3.01	1.53	+1.05

[a] *R1–2 = modeling of reaction 1–2 in Table 2.4.*

Other studies also identified siderite as principal sink of Fe(II) released by reductive dissolution of iron-oxide (Baedecker et al., 1993; Kehew and Passero, 1990). Christensen et al. (2000a) pointed out that previous studies underestimated the importance of iron reduction, because accumulation of Fe(II) in solid phases was not considered. Many natural attenuation models ignore buffering geochemical reactions and do not use pH and DIC as constraints (e.g., Essaid et al., 1995), making them not capable of simulating the iron chemistry properly.

The content of reactive iron oxide still available in the plume sediments ($\approx$ 10–25 mmol/l, assuming a porosity of 0.3, and bulk density of 1.86 g/cm^3) is comparable to the content used between W1b and W9b (11–20 mmol/l, Table 2.4). Iron reduction will cease at some point in time near the landfill and progressively further downstream in the plume, since the availability of iron oxide is limited. Sulfate can only replace iron oxide as an equally good oxidant when its concentration in leachate exceeds at least 2 mmol/l. However, observed concentrations are below 0.1 mmol/l. Consequently, methanogenesis may follow soon after depletion of iron oxide.

2.8 Conclusions

Three geochemical lines of evidence indicated reductive dissolution of Fe-oxides as natural attenuation process inside the leachate plume: 1) hydrogen concentrations, 2) supersaturation for siderite, and 3) inverse geochemical modelling. The strong contribution of iron-reducing microorganisms of the family *Geobacteraceae* to the microbial communities in this plume (Chapter 4) reflects the occurrence of iron reduction. We experienced that a combination of redox characterization methods strengthened conclusions, and considerably prevented misinterpretation emanating from weaknesses of particular methods. Furthermore, only few samples were needed to evaluate NA once the plume had been delineated. Natural attenuation occurs, but is not very effective, since only half of DOC is degraded and benzene is still present in the front of the plume. The limited supply of iron oxide and the close distance to surface water may hamper its feasibility as solution for remediation.

A full sequence of redox zones, such as observed at other sites (Christensen et al., 2000a; Christensen et al., 2001) has not been identified for this plume. Iron reduction prevailed inside the plume, whereas denitrification dominated at the top fringe. Hydrogen concentrations might indicate the on-set from iron reduction to more reduced conditions below the landfill. The observation of an extensive iron-reducing zone is in agreement with observations at other contaminates sites (Christensen et al., 2000a; Christensen et al., 2001; Lovley and Anderson, 2000).

Slightly decreasing methane, nondecreasing sulfate concentrations, absence of sulfate minerals in the aquifer, as well as natural isotope signatures of these redox species indicate the lack of methane production and sulfate reduction inside the plume. Methane in the leachate plume was formed inside the landfill body, as evidenced by isotope analysis, and transported by groundwater flow. Methane may be subject to degassing as total gas pressures exceeded hydrostatic pressure of the plume. This was supported by presence of methane with a leachate signature in

pristine groundwater above the plume. Nitrate reduction is an important oxidizing process at the top fringe of the plume, as shown by both enriched δ^{15}N-NO_3^- and partial N_2 pressure exceeding atmospheric equilibrium. Furthermore, anaerobic methane oxidation by nitrate reduction above the plume was documented by isotope analysis.

Precipitation of siderite was shown to be an important sink of Fe(II) released by reductive dissolution of iron oxide, and could be deduced from changes in pH, DIC and δ^{13}C-DIC. Therefore, downstream Fe(II) gradients may not be so informative of iron reduction; the saturation state with respect to siderite needs to be considered as well.

Chapter 3

PHYSIOLOGICAL PROFILING OF MICROBIAL COMMUNITIES IN THE CONTAMINATED AQUIFER

Abstract

Previously, we observed that microbial community structure and functional diversity in aquifers might be enhanced by landfill leachate infiltration. To study this hypothesis, groundwater samples were taken near the Banisveld landfill, the Netherlands. Based on hydrochemical parameters, the samples clustered into two groups. One group corresponded to polluted samples from the plume of landfill leachate and the second group to clean samples from outside the plume. Most Probable Number-Biolog was used to select Eco Biolog plates with similar inoculum densities. Analysis of substrate utilization profiles of these plates revealed that anaerobic microbial communities in polluted samples clustered separately from those in clean samples. Especially substrates containing an aromatic nucleus were more utilized by microbial communities in the leachate plume. Both substrate richness and functional diversity were significantly enhanced in the plume of pollution. This study shows that community-level physiological profiling is a useful and simple tool to distinguish between anaerobic microbial communities in and near a landfill leachate plume.

Published as: Röling, W.F.M., Van Breukelen, B.M., Braster. M., Van Verseveld, H.W., 2000b. Linking microbial community structure to pollution: Biolog-substrate utilization in and near a landfill leachate plume. *Water Science and Technology* 41(12): 47-53.

3.1 Introduction

Several thousands of old landfills are present in the Netherlands. Landfilling at many of these locations has started in times when its impact on the surrounding environment was not yet recognized. No liners were used to prevent the leaching of landfill percolate into the underlying aquifers. In the last decennia, several scandals concerning illegal dumping of toxic waste have raised the concern about possible hazards of landfills for water management and the environment. At some landfills, this has led to the enforcement of protective measures to prevent landfill leachate polluting nearby aquifers. These prevention measures were quite expensive and could be a great financial burden to Dutch society since illegal activities are suspected to have occurred at many other landfills as well.

Research on landfill leachate plumes has shown that the spreading of pollution in aquifers is often less than expected, due to natural attenuation. Microorganisms largely contribute to the natural attenuation (Christensen et al., 2001). Information on composition of microbial communities will contribute to the understanding, prediction and enhancement of microbial processes involved in natural attenuation. Previously, we successfully developed and applied characterization methods for microbial communities in the anaerobic, landfill leachate polluted aquifer at Coupépolder, Alphen aan de Rijn, the Netherlands (Röling et al., 2000a). Anaerobic community-level physiological profiling using Biolog plates indicated that microbial communities were physiological more diverse in the anaerobic leachate plume than in the surrounding clean aquifer. However, unambiguous conclusions were hard to draw as only four locations were sampled, of which only one location was obviously contaminated. Furthermore, the samples came from different geological settings.

The subsurface at the Banisveld landfill, Boxtel, the Netherlands, has only small variations in lithography. After delineating the leachate plume, 29 groundwater observation wells were installed in and near the plume in June 1998 (Chapter 2). Groundwater samples were withdrawn from these wells in October 1999 to test the hypothesis that landfill-leachate polluted parts of the aquifer contain more physiologically diverse communities than nearby, unpolluted parts.

3.2 Methods

Groundwater observation wells were installed near the landfill in June 1998 in a series along the main direction of groundwater flow (see Chapter 2; Figs. 2.1 and 2.2). Wells were placed upstream of the landfill (WUP), above, inside, and below the plume (W1-W9; well number increases with distance from the landfill), and in front of the plume (WF). At each well site two or three PVC wells were installed, usually one well above, one in and one below the leachate plume. The following notation is used in this chapter to refer to (samples taken from) the monitoring wells: xy, where x is the code for the well site (UP, 1-9, F), and y is the code for the screen depth of an individual well at well site x (a–upper screen (generally above plume); b–middle screen (inside plume); c–lower screen (below plume)).

In October 1999, anaerobic groundwater samples were collected in sterile glass bottles by letting the bottles overflow, after first removing 3 times the volume of standing water in the wells using a peristaltic pump. Bottles were capped with as little air as possible remaining and transferred at 4 °C to the laboratory.

Sampling, conservation, and analysis methods for hydrochemical parameters (pH, electrical conductivity (EC), Cl^-, alkalinity, O_2, NO_3^-, NO_2^-, Mn^{2+}, Fe^{2+}, SO_4^{2-}, H_2S, CH_4, Ca^{2+}, Mg^{2+}, K^+, Na^+, NH_4^+, Si, Al, and dissolved organic carbon (DOC)) are given in Chapter 2.

Within a day after obtaining the groundwater samples anaerobic community-level physiological profiling (Röling et al., 2000a) was performed, using Eco-Biolog plates (Biolog Inc. Hayward, CA, USA). Each plate contains a triplicate of 31 substrates and 1 control well without substrate (blanc). Groundwater was 1:9 and 1:99 diluted in suspension-medium (Röling et al., 2000a). Dilutions and undiluted groundwater were inoculated into Biolog plates. After incubation for 28 days at 12 °C, plates were read spectrophotometrically at 596 nm (Titertek Multiskan MCC/340). Data were transported to a spreadsheet program and absorbance of the blanc was subtracted from the measured values. Data regarding D-xylose, Tween 40 and Tween 80 were not used for subsequent analysis, as wells containing these substrates colored when inoculated with suspension medium only. The net increase in absorbance was translated into a positive or negative response with the threshold absorbance value of 0.1. Richness (S) in substrate utilization was calculated as the number of positively reacting substrates in an Eco-Biolog plate. The Shannon-Weaver index or substrate diversity (H) was calculated as:

$$H = -\sum p_i (ln\, p_i) \tag{3.1}$$

where p_i is the ratio of the absorbance for a particular substrate (averaged over the triplicate) to the sum of absorbances for all substrates (Zak et al., 1994). Most probable number-Biolog (MPN-Biolog) was determined per substrate, based on the number of positive responses over three subsequent dilutions. In case no positive response was observed, the MPN was regarded to be 0.06 cell/well (Gamo and Shoji, 1999). Maximum MPN value for a sample was calculated as the average of the 5 highest MPN values observed.

The relation between hydrochemical or Biolog parameters of groundwater samples was determined by principal component analysis (PCA) in SPSS 9.0. PCA projects the original data onto new axes (principal components (PCs)) that reflect intrinsic patterns in the multidimensional data set. SPSS 9.0 was also used for correlation and student t-tests.

3.3 Results and discussion

Groundwater samples were retrieved in October 1999 and subjected to community level physiological profiling and hydrochemical characterization. All samples were anaerobic. The ordination plot derived from PCA on the hydrogeochemical parameters is shown in Fig. 3.1. It is evident that the groundwater samples clus-

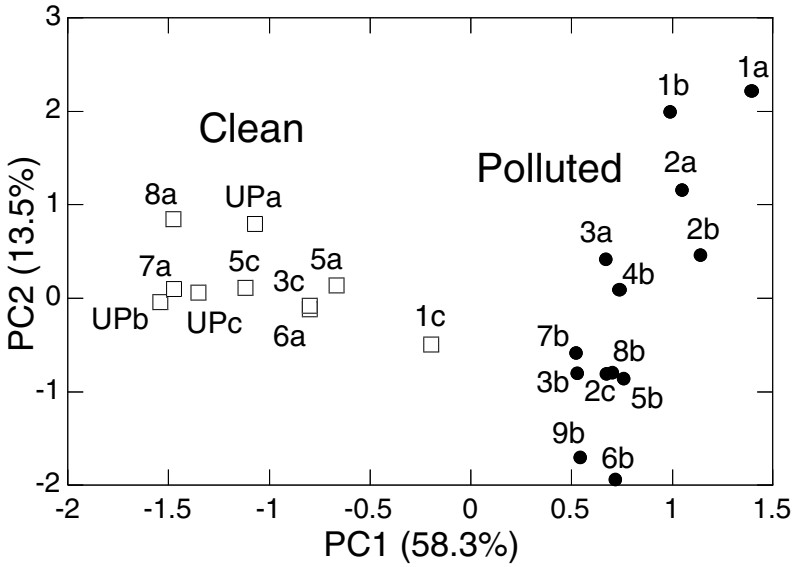

Figure 3.1: Ordination produced from PCA of hydrochemical determinations on 23 groundwater samples from the Banisveld landfill. Two clusters of clean (□) and polluted (●) groundwater samples from within the plume are shown.

tered into two groups, separated along the PC1-axis. PC1, explaining 58.5 % of the total variance, strongly correlated with parameters indicative of pollution by landfill leachate (correlation coefficients in parentheses): EC (0.967), alkalinity (0.960), magnesium (0.944), methane (0.890), calcium (0.870), ammonium (0.855), chloride (0.845), sodium (0.822), DOC (0.814) and potassium (0.810). No strong correlation of parameters with the PC2 was observed. Thus, two clusters of 'clean' locations and 'polluted' locations were determined. No major changes appear to have occurred during 1.5 year, as the members of the clusters were also in May 1998 assigned as clean and polluted, respectively, on basis of electrical conductivity measurements during cone penetration tests (Chapter 2).

For community level physiological profiling, it has been suggested to use a standardized inoculum density (Haack et al., 1995; Garland, 1997). However, determination of cell density prior to inoculation is time consuming. Also, microorganisms able to grow in the Biolog plates are not always culturable on agar plates and their numbers do not relate to total cell counts, as determined via acridine orange staining (Garland, 1997). Therefore, in general the measured absorbances are divided by the average well color development (AWCD). This approach is only useful when samples have similar numbers of positive wells (Garland, 1997), which was not the case in our study at Coupépolder landfill (Röling et al., 2000a). Furthermore, the correction via AWCD has been criticized as it assumes that a universal constant AWCD per unit biomass exists (Howard, 1997). To overcome these problems, we performed MPN-Biolog (Gamo and Shoji, 1999). This allowed us to determine the density of microorganisms culturable in Biolog plates, without measuring cell

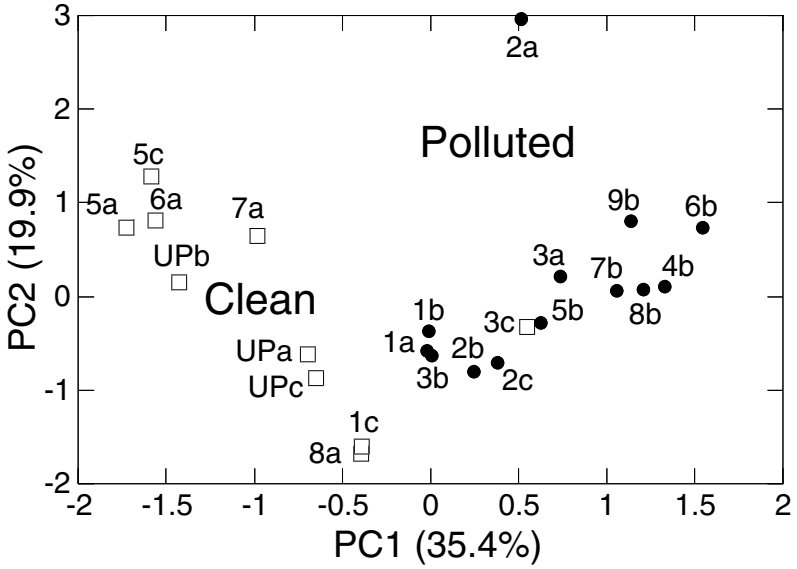

Figure 3.2: Ordination plot from PCA of Biolog profiles of clean (□) and leachate polluted (●) groundwater samples from within the plume.

density prior to Biolog plate inoculation. A disadvantage is that this approach is more resource demanding. MPN-Biolog showed that maximum MPN values for all plates fell within the same order of magnitude, with the exception of sample 6b, whose MPN value was one order of magnitude higher. The MPN values for clean groundwater samples were not significantly different from the MPN values for polluted samples ($p < 0.05$).

Based on the MPN-values, the absorbance data for undiluted samples were used in PCA, only for the 6b sample the 1:9 dilution was used. The ordination plot showed that the substrate utilization profiles of microbial communities in clean samples in general can be distinguished from those of microbial communities in polluted samples (Fig. 3.2). Only one sample, 3c, clustered differently. The screen from which this sample was taken is less then one meter below the leachate plume, according to cone penetration tests in May 1998 (Chapter 2). Separation of samples was mainly along the PC1 axis, which positively correlated with (correlation coefficients in parentheses); α-cyclodextrin (0.851), glycyl-L-glutamic acid (0.848), L-threonine (0.839), L-arginine (0.797), putrescine (0.809), i-erythritol (0.773), L-phenylalanine (0.751) and 2-hydroxy benzoic acid (0.747). These substrates, together with 4-hydroxybenzoic acid, D-glucoaminic acid and phenylethylamine were significantly better utilized by the microbial communities in the landfill leachate polluted samples ($p < 0.05$). D-mannitol, D-cellobiose and glucose-1-phosphate were significantly better utilized in the unpolluted aquifer. Remarkably, when considering all substrates available in the Eco Biolog plate, was that most amino acids and all substrates containing an aromatic nucleus were favored by the microbial communities present in the polluted aquifer. Benzene, toluene, ethylbenzene, xy-

lene and naphthalene are present in the leachate plume and decrease in concentration in downstream direction (Chapter 2, Fig. 2.3). However, occurrence of degradation cannot be ascertained. These pollutants and their degradation intermediates contain aromatic rings. Possibly, the preference for aromatic ring containing substrates in Biolog plates is indicative for the potential for pollutant degradation, but this has to be examined in more detail.

AWCD has been found to be a factor strongly contributing to PCA (Garland and Mills, 1991). However, in this study no significant correlation ($r = -0.057$) between AWCD and PC1 was found, when analyzing plates with similar maximum MPN values. This indicates the validity of our approach. When MPN values were subjected to PCA, sample 6b clustered differently from the other samples, as expected since it has a much higher maximum MPN value. Dividing the MPN value of a certain substrate with the maximum MPN value gives a measure of the relative number of microorganisms able to utilize the particular substrate for a particular sample. The ordination plot of the PCA on the corrected MPN values again showed a clear separation between clean groundwater samples and polluted samples (data not shown). Separation between microbial communities in a landfill leachate polluted aquifer and from less polluted parts was also recently shown by phospholipid fatty acid analysis (PLFA: Ludvigsen et al., 1997). However, PLFA is much more labor intensive and resource demanding.

Functional or substrate diversity can also be determined with Biolog plates (Zak et al., 1994). The simplest approach is substrate richness, the number of different substrates that are used by the microbial community. Biolog plates with similar maximal MPN values were compared, thus richness is informative per unit microorganisms. In this case one unit consists of an inoculum of about 30 cells/ml. Although not mentioned in the original paper by Zak et al. (1994), it should be realized that when an inoculum of 30000 cells/ml is used, this probably will lead to a higher number of utilized substrates and thus an apparent higher substrate richness. Fig. 3.3A clearly shows that substrate richness was much larger in the polluted part of the aquifer. A student t-test revealed that this difference is significant ($p < 0.001$). No relation between distance from the landfill and substrate richness was evident. Functional or substrate diversity, which encompasses both substrate richness and relative usage of carbon sources, can be expressed by the Shannon-Weaver Index (Zak et al., 1994). Like substrate richness, functional diversity in the plume was significantly higher ($p < 0.001$) than outside the plume. Again, no clear relation existed between distance and functional diversity (Fig. 3.3B). When Shannon-Weaver indices were calculated on basis of the MPN values, similar observations were made (data not shown). A significant, positive correlation was observed between Shannon-Weaver indexes calculated on basis of absorbance values and MPN values ($r = 0.677$; $p < 0.01$). Both substrate richness ($r = 0.893$) and diversity ($r = 0.810$) significantly correlated with the PC1 axis of the PCA on the hydrogeochemical data ($p < 0.01$). Thus, functional aspects of biodiversity differed among the clean and polluted sites. Microbial communities in polluted aquifer were physiological more diverse. The results obtained at the Banisveld landfill support our observations for Coupépolder landfill (Röling et al., 2000a). Likely, the higher substrate availability in the plume, as reflected in significantly higher dis-

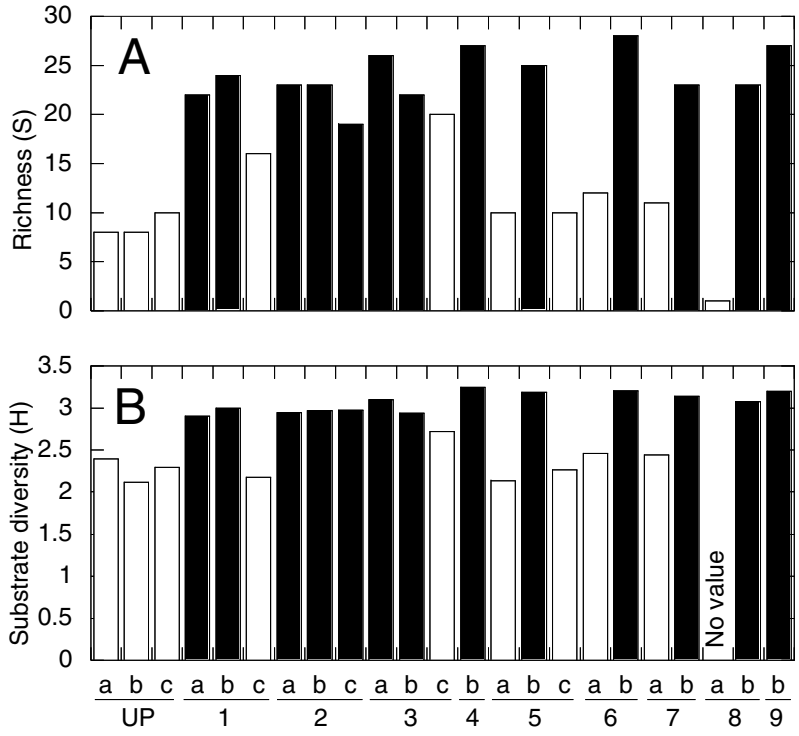

Figure 3.3: Biolog-substrate richness (A) and diversity (B) in and near the Banisveld landfill leachate plume. Clean samples are indicated by white bars, polluted samples by black bars.

solved organic carbon ($p < 0.01$), contributed to these differences in functional diversity and substrate usage. Recently, an increase in microbial diversity in a leachate polluted aquifer was also shown in a labor-intensive approach using restriction fragment length polymorphism of cloned environmental 16S rDNA fragments (Cho and Kim, 2000). This aquifer was polluted by livestock waste water.

A comparison of the experiments in October 1999 was made with experiments conducted in September 1998, 3 months after installation of the wells. At that time only 1:9 diluted groundwater samples were inoculated into Biolog plates. Results from 1998 were not in accordance with those of 1999; Biolog profiles from polluted sites could not be distinguished from those of clean sites. Substrate richness, as calculated for the 1:9 dilution, was in general much higher for both polluted and clean sites than in 1999. Also some hydrogeochemical parameters were obviously different, sulfate concentrations were a factor ten higher at some locations while at several locations high hydrogen concentrations were measured (see Chapter 2). Increased concentrations of hydrogen, an intermediate in microbial degradation of organic matter, are normal after installing monitoring wells, and several months have to be allowed before the situation will be normalized (Bjerg et al., 1997). Furthermore, disturbance is known to lead to changes in microbial communities in stored samples (Haldeman et al., 1995; Brockman et al., 1998), especially when re-

garding culturability. These disturbance-related changes possibly also occur in the field. All these factors indicate that for this research location a 3 month period is not sufficient for stabilization of the microbial communities and determination of community structure via community-level physiological profiling.

3.4 Conclusions

This research has shown that functional diversity was significantly increased in the landfill leachate plume at Banisveld landfill. Community-level physiological fingerprints were different between clean and polluted samples, when comparing plates with similar inoculation densities. Therefore, community-level physiological profiling (CLPP) is promising as a simple approach for analyzing microbial communities at landfill leachate polluted aquifers. Since CLPP is a culturing method and culturability of microorganisms is easily affected and difficult to control, attention should be focused on the time required after installation of a monitoring well before groundwater can be retrieved for reliable CLPP.

Chapter 4

RELATIONSHIPS BETWEEN MICROBIAL COMMUNITY STRUCTURE AND HYDROGEOCHEMISTRY

Abstract

Knowledge about the relationship between microbial community structure and hydrogeochemistry (e.g., pollution, redox and degradation processes) in landfill leachate polluted aquifers is required to develop tools for predicting and monitoring natural attenuation. In this study analyses of pollutant and redox chemistry were conducted in parallel with culture-independent profiling of microbial communities present in a well-defined aquifer (Banisveld, The Netherlands). Degradation of organic contaminants occurred under iron reducing conditions in the plume of pollution, while upstream of the landfill and above the plume denitrification was the dominant redox process. Beneath the plume iron reduction occurred. Numerical comparison of 16S rDNA-based denaturing gradient gel electrophoresis (DGGE) profiles of *Bacteria* and *Archaea* in 29 groundwater samples revealed a clear difference between microbial community structure inside and outside the contaminant plume. A similar relationship was not evident in sediment samples. DGGE data were supported by sequencing cloned 16S rDNA. Upstream of the landfill members of the β subclass of the class *Proteobacteria* (β-proteobacteria) dominated. This group was not encountered beneath the landfill, where Gram-positive bacteria dominated. Further downstream the contribution of Gram-positives to the clone library decreased while that of (δ-proteobacteria strongly increased and β-proteobacteria reappeared. The β-proteobacteria (*Acidovorax, Rhodoferax*) differed considerably from those found upstream (*Gallionella, Azoarcus*). Direct comparisons of cloned 16S rDNA with bands in DGGE profiles revealed that the data from each were comparable. A relationship was observed between dominant redox processes and the bacteria identified. In the iron reducing plume *Geobacteraceae* made a strong contribution to the microbial communities. Because the only known aromatic hydrocarbon degrading, iron-reducing bacteria are *Geobacter* spp., their occurrence in landfill leachate contaminated aquifers deserves more detailed consideration.

Published as: Röling, W.F.M., Van Breukelen, B.M., Braster, M., Lin, B., Van Verseveld, H.W., 2001. Relationships between microbial community structure and hydrochemistry in a landfill leachate-polluted aquifer. *Applied and Environmental Microbiology* 67(10): 4619-4629.

4.1 Introduction

Contamination of groundwater is a serious environmental problem throughout the world as it affects drinking-water resources and impacts oligotrophic environments. In the Netherlands, an important source of contamination is landfill leachate. In the past, landfilling was performed without the presence of appropriate liners to prevent percolation of leachate into underlying aquifers. Although many old landfills are closed now, the cessation of landfill operations does not stop chemical releases into the environment. Organic compounds, originating from household and industrial waste, are found in most municipal landfills. Dramatic changes in aquifer geochemistry and microbiology downstream of landfills occur as the result of the high organic load of leachate (Christensen et al., 2001). A sequence of redox zones develops in time and space, as the organic matter is microbiologically degraded and electron acceptors are depleted (Christensen et al., 2001; Lovley, 1997b).

Iron reduction and to a less extent manganese reduction are important redox processes occurring in polluted aquifers (Albrechtsen et al., 1999; Christensen et al., 2001; Heron et al., 1994a; Lovley, 1995; Lovley, 1997a). Solid iron-oxyhydroxydes and manganese-oxides are reduced, which releases soluble metal species into the groundwater. These metals, together with other reduced species such as methane, ammonium and hydrogen sulfide can pose a threat to drinking-water and oligotropic nature reserves (Christensen et al., 2001; Lovley, 1997a). Also, pathogenic bacteria might be present in the leachate (Christensen et al., 1994). However, of particular concern is contamination of groundwater by aromatic compounds (especially benzene, toluene, ethylbenzene and xylene (BTEX)). These compounds are often encountered at landfills (Christensen et al., 2001). Although accounting for at most a few percent of the organic matter in leachate, concern is related to their toxicity and relatively high solubility. BTEX components are readily degraded under aerobic conditions, but far more persistent under anaerobic conditions (Lovley, 1997b), typical within and downgradient of landfills (Christensen et al., 2001).

It is often difficult and expensive to remediate a subsurface environment. However, despite unfavourable conditions, appreciable anaerobic microbial degradation of BTEX has been observed in landfill leachate polluted aquifers (Acton and Barker, 1992; Lyngkilde and Christensen, 1992a; Schaal, 1991). Ability to predict potential for natural attenuation and to monitor on-going degradation processes will help to limit the number of landfills and aquifers that have to be actively remediated. Thorough knowledge of microbial community structure in polluted aquifers, the capabilities of the microbial populations present and how these affect their environment and vice versa, will aid in the development of tools for predicting and monitoring natural degradation. Here, we describe the relationship between hydrogeochemistry and microbial community structure in a landfill leachate polluted aquifer close to the town of Boxtel, the Netherlands. From this aquifer 29 groundwater samples and 5 sediment samples were obtained. Chemical analyses were conducted to determine the level of pollution and deduce the principal redox processes. Community structures of *Archaea* and *Bacteria* were profiled using denaturant gradient gel electrophoresis (Muyzer et al., 1993), and the profiles were

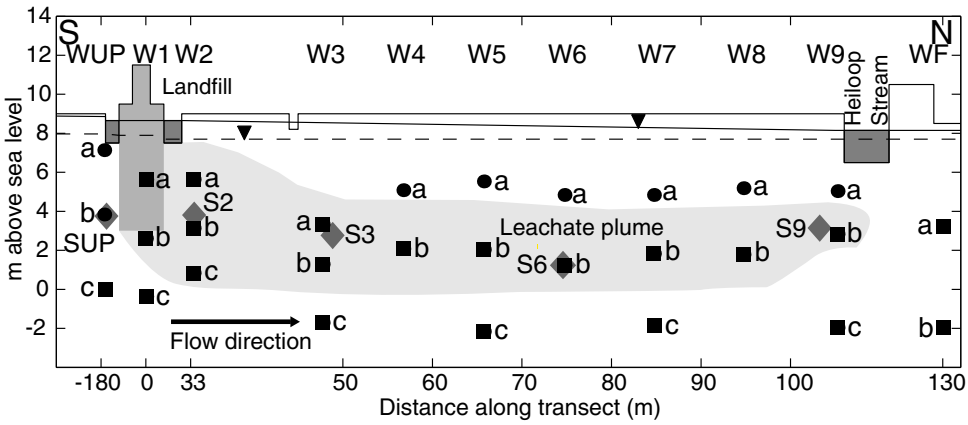

Figure 4.1: Cross section of the leachate plume downstream of the Banisveld landfill, showing the locations of the 11 well sites. Each well site has a code, which indicates its location: upstream (UP), at the plume (1–9), or in front of the plume (F). Two or three screens were placed per well site, as indicated by a, b, and c. Symbols: ●, screen from which in September 1998 a groundwater sample with a nitrate concentration > 0.5 mg/l was obtained; ■, screen from which a sample containing no nitrate was obtained; ◆, sediment (S) sampled in October 1998.

numerically compared (Röling et al., 2000a). For three groundwater samples clone libraries were made to obtain more detailed information on the composition of the microbial communities.

4.2 Materials and methods

4.2.1 Site description and installation of observation wells

The Banisveld landfill is located 5 km southwest of Boxtel, the Netherlands. Unlined landfilling of primarily household refuse occurred in a 6 m deep sand pit between 1965 and 1977. The geology of the aquifer consists of an 11 m thick layer of fine to coarse unconsolidated sands positioned upon less permeable clay and peat deposits alternating with sandy layers. Groundwater flow (estimated at 4 m/year) is directed northeast to north towards a nature reserve, which is a habitat for a rare oligotrophic ecosystem. An electromagnetic survey and cone penetration tests revealed the horizontal and vertical distribution of the leachate (Chapter 2). In June 1998, this information was used to install a transect of 11 groundwater observation well sites, along the direction of groundwater flow (Fig. 4.1). Wells were placed upstream of the landfill (WUP), above, inside, and below the plume (W1–W9; well number increases with distance from the landfill), and in front of the plume (WF). At each well site two or three PVC wells were installed, usually one well above, one in and one below the leachate plume. The following notation is used in this chapter to refer to (samples taken from) the monitoring wells: xy, where x is the code for the well site (UP, 1–9, F), and y is the code for the screen depth of an individual well

at well site x (a–upper screen (generally above plume); b–middle screen (inside plume); c–lower screen (below plume)). The screen length was 20 cm, but three wells had screen lengths of 1 to 2 m (UPc, Fa, Fb).

4.2.2 Sampling

In September 1998, anaerobic groundwater samples were collected in sterile glass bottles by letting the bottles overflow, after first removing 3 times the volume of standing water in the wells using a peristaltic pump. Bottles were capped with as small a headspace as possible. In October 1998, sediment cores were anaerobically taken with a core pushing device (Delft Geotechnics, the Netherlands; Appelo et al., 1990) at five locations (SUP, S2, S3, S6, S9; codes refer to nearby well sites), one from upstream and 4 downstream, in the plume of leachate (Fig. 4.1). After retrieving, the ends of the stainless steel cores (length 20 cm, internal diameter 30 mm) were immediately capped and cores were stored in a container which was made anaerobic by flushing with nitrogen gas. Sediment cores and groundwater were transferred to the laboratory and stored for less than 24 hours at 4 °C. Next, 100 ml groundwater was vacuum filtered over 45 mm diameter 0.2 μm filters (Sartorius). Cores were sampled under a nitrogen atmosphere in an anaerobic glovebox (Mecaplex). The outer ends of the cores (several centimeters) were not used. For molecular analysis, sediment and filters were frozen at -80 °C until DNA isolation.

4.2.3 Chemical analysis

Sampling, conservation, and analysis methods for hydrochemical parameters (pH, electrical conductivity (EC), Cl^-, alkalinity, O_2, NO_3^-, NO_2^-, Mn^{2+}, Fe^{2+}, SO_4^{2-}, H_2S, CH_4, Ca^{2+}, Mg^{2+}, K^+, Na^+, NH_4^+, Si, Al, dissolved organic carbon (DOC), benzene, toluene, ethylbenzene, xylene, and naphthalene) and sedimentological parameters (lime, humus, sand, clay, silt, carbon, and nitrogen contents) are given in Chapter 2. Samples were grouped based on chemical characteristics by using principal-component analysis and cluster analysis (Systat 7).

4.2.4 DGGE Profiling

DNA extraction was performed as described previously (Röling et al., 2000a). *Bacteria*-specific PCR was performed in a total volume of 25 μl containing 0.4 μM primer F341-GC (Muyzer et al., 1993), 0.4 μM primer R518 (Muyzer et al., 1993), 0.4 mM dNTPs, 10 μg BSA, Expand buffer (Boehringer, Mannheim, Germany), 2.6 U Expand enzyme and 1 μl undiluted DNA template. Amplification was performed in a Perkin Elmer DNA Thermo Cycler as follows: 94 °C for 4 min, after which 35 cycles of 94 °C for 0.5 min., 54 °C for 1 min and 72 °C for 1 min, with a final elongation at 72 °C of 5 min. For profiling of *Archaea*, a nested approach was applied. Primers pRA46f (Øvreås et al., 1997) and univ907r (Amann et al., 1992) were used to produce a 0.9 kb fragment, which after hundredfold dilution was used as a template in an amplification with primers pARCH340f and pARCH519r (Øvreås

et al., 1997). The amplifications were performed with the same settings as for the *Bacteria*-specific amplification.

DGGE was performed with the Bio-Rad DCode^{TM} system. PCR product was loaded on 1 mm thick 8 % (wt/vol) polyacrylamide (37.5:1 acrylamide:bisacrylamide) gels containing a 40–60 % or 40–70 % linear denaturing gradient for *Bacteria* and 45–70 % for *Archaea*. 100 % denaturant is defined as 7 M urea and 40 % (v/v) formamide. Gels were run in 1 x TAE buffer (40 mM Tris, 20 mM acetic acid, 1 mM Na-EDTA (pH 8.0)) at 70 V and 60 °C for 16h. Gels were stained in 1 x TAE buffer containing 1 μg ethidium bromide ml^{-1} and recorded with a CCD camera system (The imager, Appligen, Illkirch, France). Gel-images were converted, normalized and analyzed with the GelCompar 4.0 software package (Applied Maths, Kortrijk, Belgium), using the Pearson product-moment correlation coefficient and unweighted pair-group clustering method using arithmetic averages (UPGMA). To aid the conversion and normalization of gels, a marker consisting of 11 clones was added on the outsides of the gel as well as after every four samples. The outer two lanes of the gels were not used. In all analyses the markers clustered over 95 % similarity.

4.2.5 Cloning and sequencing of 16S rDNA

PCR primers 8f and 1512r (Felske et al., 1998) were used to amplify near complete 16S rDNA. Products (cleaned with Qiaquick Rep Purification Kit (Qiagen, Germany)) were cloned into *Escherichia coli* JM109 by using the Promega pGEM-T vector system (Promega, Madison, Wis., USA). Transformants were checked for correctly sized inserts by performing a PCR with pGEM-T specific primers T7 and Sp6. Correctly sized products were used as template in a PCR with primers F341-GC and R518 to compare the banding position in DGGE to that of the environmental sample from which the clone was derived. Sequencing PCR was carried out with the ABI PRISM^{TM} Dye Terminator Cycle Sequencing Core Kit (Perkin Elmer) and the purified products were run on a SEQUAGEL-6 sequence gel (National Diagnostics, USA) in a 373A/DNA Sequencer (Applied Biosystem, USA). At least the V3 region (*E. coli* position 341 to 518) was sequenced, a number of clones completely. Both strands of the 16S rRNA gene were sequenced. Sequences were compared to sequences deposited in the GenBank DNA database by using the BLAST algorithm (Altschul et al., 1990).

4.2.6 MPN-PCR

Serial twofold dilutions of DNA extracts were made in sterile water and used as template for PCR. Most-probable-number PCR (MPN-PCR) of members of the family *Geobacteraceae* was performed with primers 8f and Geo825 (Snoeyenbos-West et al., 2000). MPN-PCR numbers of *Bacteria* were performed using primers 8f and R518. To account for variations in efficiency of DNA extraction and recovery, numbers of *Geobacteraceae* were expressed relative to *Bacteria*.

4.2.7 Nucleotide sequence accession numbers

Nucleotide sequences have been deposited in the Genbank database under accession numbers AY013585 to AY013658 and AY013660 to AY013698.

4.3 Results

4.3.1 Hydrogeochemistry of the landfill leachate plume

Groundwater samples for hydrochemical and microbiological analysis were retrieved in September 1998 from 29 wells (see Fig. 4.1 and Section 4.2.1. for numbering of wells). An ordination plot on the basis of the measured hydrogeochemical parameters (Fig. 4.2) revealed clustering of the sampling points into three groups, two large clusters (C and P1) and one small (P2). The two large clusters were mainly separated along the PC1-axis, which explained 58.8 % of the total variance. PC1 correlated strongly with parameters indicative of pollution by landfill leachate (correlation coefficients in parentheses): electrical conductivity (0.985), alkalinity (0.978), dissolved inorganic carbon (DIC; 0.977), magnesium (0.970), dissolved organic carbon (DOC; 0.957), calcium (0.934), ammonium (0.929), potassium (0.894), chloride (0.891) and sodium (0.856). Cluster C in Fig. 4.2 contained groundwater samples having low values for these parameters (slightly polluted or clean) while clusters P1 and P2 contained samples having high values for these parameters and therefore were obviously polluted (P). The grouping of the samples (Fig. 4.2) corresponded exactly with the delineation of the plume by vertical continuous profiles of formation conductivity obtained by cone penetration tests performed in May 1998 (Chapter 2).

Clusters P1 and P2 were separated along the PC2 axis. This axis (which explains 16.3 % of the variance) positively correlated with Si (0.860), ethylbenzene (0.781), xylene (0.759) and naphthalene (0.563) and correlated negatively with reduced redox species Fe(II) (-0.733) and Mn(II) (-0.617). Only samples from cluster P2 (1a and 1b) contained obvious concentrations of ethylbenzene (53 mg/l) and xylene (120 mg/l). These aromatic compounds were not present in well W2 downstream of the landfill, while naphthalene had disappeared in well W3 (Fig. 2.3). Benzene (maximum concentration, 28 mg/l) was more persistent, and its concentration decreased along the flow path, to 6 mg/l at the front of the leachate plume (W9). The concentration of chloride (used as a conservative tracer, with a background concentration of 12–70 mg/l upstream of the landfill) was constant (mean value in the plume of pollution, 270 mg/l), indicating that the decreases in the concentrations of organic contaminants were not due to dilution. However, occurrence of degradation cannot be ascertained, because sorption and source heterogeneity can produce the profiles as well (Chapter 2).

Degradation of dissolved organic carbon (DOC) appeared to occur under iron reducing conditions in the plume. Oxygen (< 0.1 mg/l) was not detected in any of the samples. Nitrate (> 0.5 mg/l, with a maximum of 76 mg/l) was only encountered upstream of the landfill and above the plume (Fig. 4.1), indicating that denitrification is likely a dominant redox process at the top fringes of the plume. In

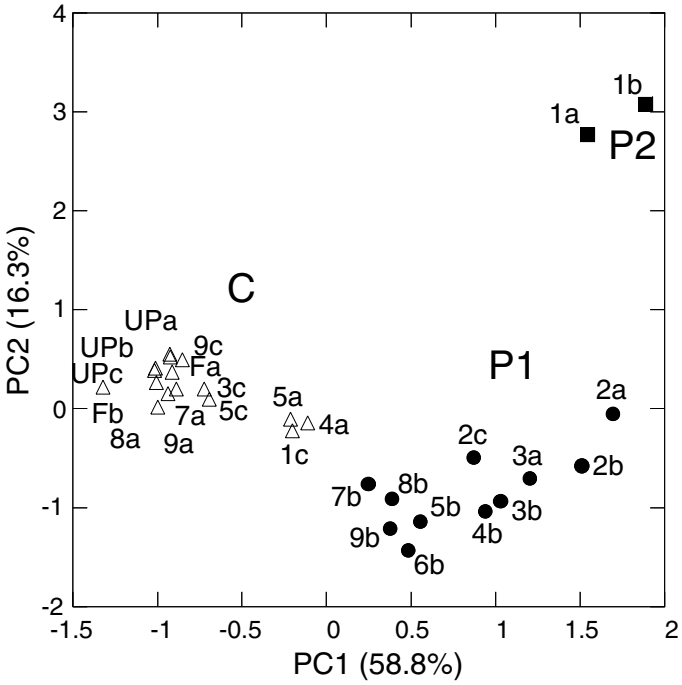

Figure 4.2: Ordination plot produced from principal component analysis on hydrochemical parameters of groundwater samples from the aquifer surrounding Banisveld landfill. Three clusters of clean (C [△]) and polluted (P1 [●] and P2 [■]) groundwater samples are shown. The code and lowercase letters indicate the samples examined (Fig. 4.1).

the plume, Fe(II) concentrations in general showed an increase along the transect while the presence of a pool of Fe(III)oxyhydroxydes and hydrogen gas measurements (Chapter 2) were also indicative of iron reduction as dominant redox process. Also below the plume the absence of nitrate and measured concentrations of hydrogen indicated iron reduction as the dominant redox process.

4.3.2 Microbial community structure within the aquifer

Microbial communities in groundwater were profiled by denaturing gradient gel electrophoresis (DGGE) of amplified 16S rDNA fragments. Profiles of bacterial communities were complex and showed a high degree of variation between samples (Fig. 4.3). To establish relationships between samples, the whole densitometric curves of the tracks were numerically compared, using Pearson product-moment correlation coefficient (Rademaker et al., 1999; Röling et al., 2000a). In general, cluster analysis with the unweighted pair-group method using arithmetic averages (UPGMA) grouped samples of polluted groundwater into one large cluster at a similarity of 35 %, while clean samples clustered separately (Fig. 4.3). Only three DGGE profiles (3c, 1c, 9b) out of 29 groundwater samples were not clustered in accordance with their degree of pollution. Differences in microbial composition and

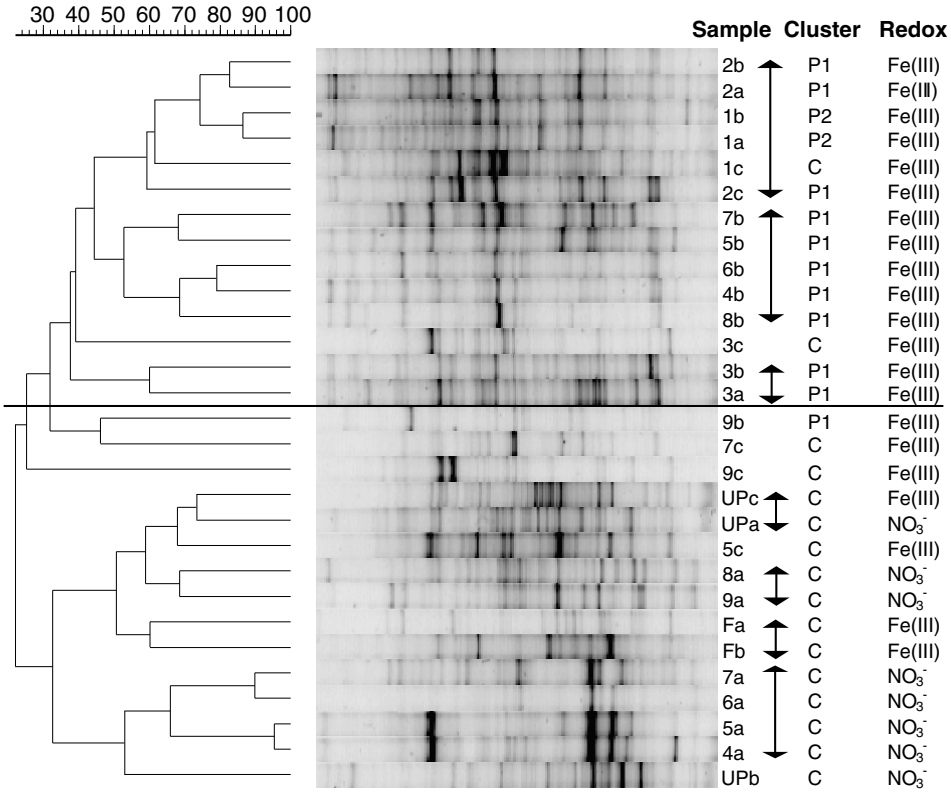

Figure 4.3: UPGMA cluster analysis of DGGE profiles of *Bacteria* (40–60% denaturant gradient) in groundwater after Pearson product moment correlation. For each lane the sample designation (Fig. 4.1), pollution level (P1, P2 and C refer to groups in Fig. 4.2), and proposed dominant redox process (NO_3^-, denitrification; Fe(III), iron reduction) are indicated.

thus community heterogeneity within the plume are clear from the fact that samples from the plume clustered only at 35 %. Samples from in and just beneath the landfill (1a, 1b; cluster P2 in Fig. 4.2) and 33 m downstream (2a, 2b, 2c; cluster P1 in Fig. 4.2) showed the most identical profiles. Bacterial communities in groundwater obtained from outside the plume showed more variation than those from within the plume. The nitrate containing groundwater samples from above the plume (4a, 5a, 6a and 7a) clustered together, while samples from further downstream but also containing nitrate (8a and 9a), clustered separately.

A more distinctive difference in community structure within and outside the plume was observed for archaeal communities (Fig. 4.4). DGGE profiles were less complex than observed for *Bacteria*. Profiles of samples from the plume showed a few strong dominant bands, causing a strong correlation at above 70 % for most of the samples from the plume. Two of the dominant bands were only clearly visible in the polluted groundwater samples, interestingly one of the bands disappeared in the samples furthest downstream of the landfill (7b, 8b, 9b). Archaeal PCR products were not obtained from any of the samples from below the plume.

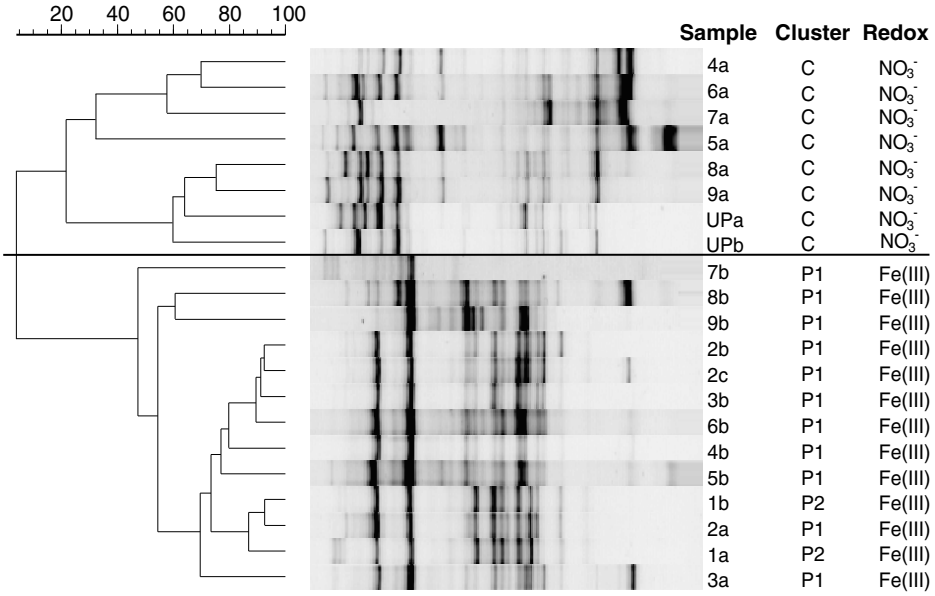

Figure 4.4: UPGMA cluster analysis of DGGE profiles of *Archaea* (45–70% denaturant gradient) in groundwater after Pearson product moment correlation. For each lane the sample designation (Fig. 4.1), pollution level (P1, P2 and C refer to groups in Fig. 4.2), and proposed dominant redox process (NO_3^-, denitrification; Fe(III), iron reduction) are indicated.

4.3.3 Composition of microbial communities in groundwater

Analysis of clone libraries was applied as a second method to characterize the microbial communities in groundwater and allowed more detailed phylogenetic information on microorganisms present in groundwater samples to be obtained. This also generated more specific data on how community structure was affected by landfill leachate. Libraries were prepared from 3 groundwater samples, each representing one of the 3 clusters as seen in Fig. 4.2 and obtained from approximately the same depth: upstream UPb (clean, cluster C), beneath the landfill 1b (polluted, cluster P2) and downstream of the landfill 2b (polluted, cluster P1).

Nearly complete 16S rDNA sequences of *Bacteria* were amplified and cloned. Between 95 to 105 clones were screened per clone library. Clones, as well as the PCR fragments used for cloning, were re-amplified with primers F341-GC and R518 and their DGGE profiles were compared to that of the original sample (Figs. 4.5 and 4.6). The similarity between directly amplified groundwater DNA samples and nested PCR (amplification with as template the 1.5 kb PCR fragment used for cloning) was more than 80 % (Fig. 4.5). This indicates that the PCR required for cloning did not lead to an obvious cloning bias. 74 % (UPb) to 85 % (2b) of the clones matched to bands in the community DGGE profiles.

Ninety-six clones were randomly selected and the part of the cloned 16S rDNA that was also profiled in DGGE (corresponding to *E. coli* position 341 to 518, including V3 region), was sequenced. Later, seventeen of the partial sequenced clones and

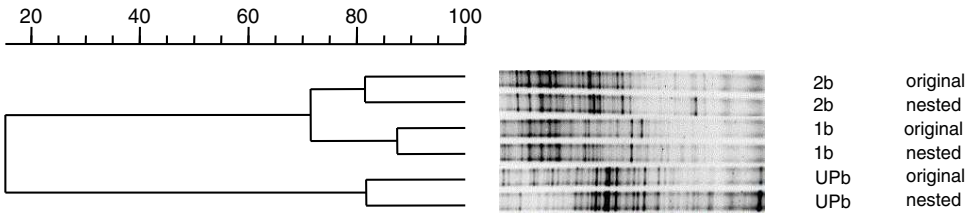

Figure 4.5: UPGMA cluster analysis of DGGE profiles (40 to 70% denaturant gradient) of groundwater samples UPb, 1b and 2b used for constructing clone libraries. For each sample, primers F341-GC and R518 were used directly with isolated groundwater DNA (original) or with the PCR-fragment obtained with primers 8f and 1512r and used for cloning (nested).

seven additional clones, mainly clones with DGGE banding corresponding to dominant bands in the original profiles, were nearly completely sequenced. Sequencing near complete 16S rDNA did not result in an assignment to a phylogenetic group that differed from that based on the V3 region. The majority of the clones resembled (facultative) anaerobic and micro-aerophilic microorganisms. Sequences relating to facultative anaerobic and micro-aerophilic microorganisms were especially observed for the upstream sample. No pathogens were encountered. The distribution of the 96 randomly sequenced clones over phylogenetic groups is shown in Table 4.1. Sixteen to 25 % of the sequences showed less than 90 % similarity to sequences deposited in GenBank and were described as unclassified. It is obvious that microbial composition differed for each groundwater sample. Upstream of the landfill a strong dominance was observed by bacteria belonging to the β-proteobacteria (48.6 %), mainly resembling *Gallionella ferruginea* (four clones, 93–95 % similarity) and *Azoarcus* BS5.8 (five clones, 93–95 % similarity).

Table 4.1: Relative levels of bacterial clones related to various phylogenetic groups in clone libraries from aquifer groundwater samples obtained upstream (sample UPb), beneath (sample 1b), and downstream (sample 2b) of the Banisveld landfill

	% in following samples:		
Phylogenetic group	UPb[a]	1b[b]	2b[c]
Low–G+C–content gram–positive group	3	38	11
High–G+C–content gram–positive group	9	13	6
α–Proteobacteria	6	0	0
β–Proteobacteria	49	0	20
γ–Proteobacteria	0	8	0
δ–Proteobacteria	9	4	26
Green nonsulfur bacteria	3	4	6
Spirochaetales	0	8	0
Cytophaga–Flexibacter–Bacteroides group	3	0	6
Holophaga	0	0	3
Verrucomicrobia	3	0	0
WS5 division	0	0	3
Unclassified ($<$ 90 % similarity)	17	25	20

[a] *Principal-component analysis cluster C (Fig. 4.2); the dominant redox process is denitrification.*
[b] *Principal-component analysis cluster P2 (Fig. 4.2); the dominant redox process is iron reduction.*
[c] *Principal-component analysis cluster P1 (Fig. 4.2); the dominant redox process is iron reduction.*

Linking of the clone identities to banding position in DGGE (Fig. 4.6, Table 4.2) indicates that these sequences also referred to dominant bands in the DGGE profile of the microbial community. Several sequences relating to genera capable of denitrification (*Azoarcus*, *Actinobacteria*) were found in this groundwater sample taken from a denitrifying environment, also in the dominant bands (band 2, 7 and 8 in Fig. 4.6). Furthermore, two sequences relating to sulfate reducers were encountered of which one corresponded to a dominant band in the DGGE profile (band 9).

None of the clones from the groundwater beneath the landfill (1b) showed affiliation to β-proteobacteria (Table 4.1). Here a strong dominance by Gram-positives was observed, 12.5 % of the clones belonged to the high G+C Gram-positives and 37.5 % to the low G+C Gram-positives, of which five clones (21 %) closely resembled *Acetobacterium* sequences (95–98 % similarity). These clones could be linked to dominant bands in the DGGE profile of the groundwater beneath the landfill (band 10 and 11 in Fig. 4.6). Another clone falling in the low G+C Gram-positive group also showed mobility similar to a dominant band in DGGE (band 13 in Fig. 4.6), further showing the apparent dominance of low G+C Gram-positives beneath the landfill. Only one sequence related to known iron reducers (*Geobacter*-like sequence) was encountered, this clone related to a subdominant band in the DGGE profile of the microbial community (band 12 in Fig. 4.6).

Downstream of the landfill the relative number of low G+C Gram-positive clones decreased, and β-proteobacteria reappeared (Table 4.1). The identities of the β-proteobacteria were quite different from those encountered upstream of the landfill. Sequences related to *Acidovorax* (2 clones, 93–96 % similarity), *Rhodoferax* and several uncultured β-proteobacteria were most frequently encountered in this clone library. Also δ-proteobacteria, especially sequences related to *Geobacteraceae* (8 clones, 93–98 % similarity), strongly contributed to the clone library (25.7 % of clones analyzed). Two clones, that based on sequencing of the V3 region were shown to relate to clone K20-06 (Genbank accession number AF145810) were also identified as *Geobacter* spp. Initially, four clones with similar migration in DGGE (band 16 in Fig. 4.6) showed this affiliation after sequencing the V3 region. Sequencing of near complete 16S rDNA for two of these clones showed that both were closely related to *Geobacter* sp. CdA2. Dominant bands in the DGGE profile from groundwater samples downstream of the plume also appeared to be contributed by members of the δ-proteobacteria (*Geobacteraceae*; bands 16 and 19) and β-proteobacteria (bands 18 and 21 in Fig. 4.6). The strong dominance by iron reducing *Geobacteraceae* is in agreement with iron reduction being the major redox process. One sequence related to a potential denitrifier (*Azoarcus* related) and another sequence related to a sulfate reducer were also encountered. The potential denitrifier showed co-migration with five *Geobacter* clones (band 16) and corresponded to a dominant component of the DGGE profiles. As can be seen in Fig. 4.6 and Table 4.2 clones with different phylogenetic associations often exhibited similar migration in DGGE gels.

Confirmation that members of the *Geobacteraceae* were an important group of bacteria in the iron reducing aquifer was obtained by an MPN-PCR using *Geobacteraceae* specific primers and expressing the number relative to the MPN number obtained using general bacterial primers. Upstream the number was less then 0.5 %, underneath the landfill 6 % and downstream 25 %. Performing DGGE after a

Table 4.2: Identities of clones related to numbered bands in Fig 4.6, as determined by partial or near complete 16S rDNA sequencing

Band	Accession no.	Closest relative in GenBank database (accession no.)	% Sim.	Phylogenetic group
1	AY013676[a]	*Desulfosporosinus* sp. strain S10 (AF07527)	96	Low-G+C gram-pos
2	AY013696[a,b]	*Gallionella ferruginea* (L07897)	94	β-Proteobacteria
	AY013693[b]	Uncultured *Duganella* sp. strain CTHB-18 (AF067655)	93	β-Proteobacteria
3	AY013670	Unidentified β-proteobacterium cda-1 (Y17060)	96	β-Proteobacteria
	AY013688	Unidentified β-proteobacterium cda-1 (Y17060)	96	β-Proteobacteria
	AY013694[a,b]	*Gallionella ferruginea* (L07897)	95	β-Proteobacteria
	AY013698[a,b]	*Gallionella ferruginea* (L07897)	93	β-Proteobacteria
	AY013691[b]	*Actinomyces* sp. (X92701)	96	High-G+C gram-pos
	AY013663	Uncultured bacterium RB25 (Z95718)	88	Unclassified
4	AY013697[a,b]	*Gallionella ferruginea* (L07897)	92	β-Proteobacteria
	AY013695[b]	Unidentified bacterium BD4-9 (AB015559)	88	Unclassified
5	AY013690[a]	*Azoarcus* sp. strain BS5-8 (AF011350)	93	β-Proteobacteria
6	AY013666[a]	*Azoarcus* sp. strain BS5-8 (AF011350)	93	β-Proteobacteria
7	AY013669[a]	*Azoarcus* sp. strain BS5-8 (AF011350)	94	β-Proteobacteria
	AY013681[a]	*Azoarcus* sp. strain BS5-8 (AF011350)	94	β-Proteobacteria
8	AY013674	Unidentified bacterium DGGE band 10 (AJ009652)	98	High-G+C gram-pos
	AY013684[a]	*Azoarcus* sp. strain BS5-8 (AF011350)	98	High-G+C gram-pos
	AY013664[a]	Denitrifying bacterium 72Chol (Y09967)	95	β-Proteobacteria
	AY013675[a]	*Azoarcus* sp. strain BS5-8 (AF011350)	93	β-Proteobacteria
	AY013689	Uncultured bacterium t0.6.f (AF005745)	91	Green nonsulfur bact
	AY013682	Candidate division OP11 clone OPd29 (AF047561)	90	Unclassified
9	AY013665[a]	*Desulfovibrio aminophilus* (AF067964)	93	δ-Proteobacteria
10	AY013593	*Acetobacterium carbonolicum* (X96956)	98	Low-G+C gram-pos
	AY013613	*Acetobacterium wieringae* (X96955)	97	Low-G+C gram-pos
	AY013610[b]	*Acetobacterium malicum* (X96957)	97	Low-G+C gram-pos
	AY013607[b]	*Acetobacterium malicum* (X96957)	95	Low-G+C gram-pos
11	AY013591	*Acetobacterium wieringae* (X96955)	98	Low-G+C gram-pos
12	AY013609[a,b]	*Geobacter akaganeitreducens* (U96918)	94	δ-Proteobacteria
13	AF013603	Uncultured eubacterium WCHB1-21 (AF505080)	96	Low-G+C gram-pos
14	AY013658	Uncultured freshwater bacterium (AF109142)	98	Unclassified
15	AY013644[a,b]	*Geobacter* sp. strain CdA-2 (Y19190)	96	δ-Proteobacteria
16	AY013634[a]	Metal-contaminated soil clone K20-06 (AF145810)	98	δ-Proteobacteria
	AY013642[a]	Metal-contaminated soil clone K20-06 (AF145810)	95	δ-Proteobacteria
	AY013647[a,b]	*Geobacter* sp. strain CdA-2 (Y19190)	96	δ-Proteobacteria
	AY013648[a,b]	*Geobacter* sp. strain CdA-2 (Y19190)	94	δ-Proteobacteria
	AY013651[a]	*Geobacter* sp. strain CdA-3 (Y13131)	93	δ-Proteobacteria
	AY013641[a]	*Azoarcus* sp. PCR strain (X85434)	93	δ-Proteobacteria
	AY013649[b]	Uncultured bacterium WCHB1-60 (AF050598)	91	Candidate div WS5
17	AY013652/3[a,c]	*Geobacter* sp. strain (GSPY19190)	96	δ-Proteobacteria
18	AY013646[b]	*Acidovorax* sp. strain UFZ-B517 (AF235010)	96	δ-Proteobacteria
	AY013643[b]	*Rhodoferax fermentas* (D16211)	96	δ-Proteobacteria
	AY013650[b]	*Acidovorax devluvii* (Y18616)	91	δ-Proteobacteria
19	AY013645[a,b]	*Geobacter* sp. strain CdA-2 (Y19190)	95	δ-Proteobacteria
	AY013633	*Eubacterium limosum* (M59120)	94	Low-G+C gram-pos
	AY013638	Uncultured bacterium clone H1.4.f (AF005748)	93	Green nonsulfur bact
20	AY013620[a]	Uncultured sulfate-reducing bacterium 368 (AJ389629)	91	δ-Proteobacteria
21	AY013625	Uncultured clone CRE-FL35 (AF141457)	97	β-Proteobacteria

[a] *The identity of the closest relative in the GenBank database gives an indication of the ability to perform redox reactions (microaerophilic, denitrification, iron reduction, or sulfate reduction).*

[b] *The 16S rDNA was almost completely sequenced.*

[c] *E. coli positions 8 to 518 and 1002 to 1512 were sequenced.*

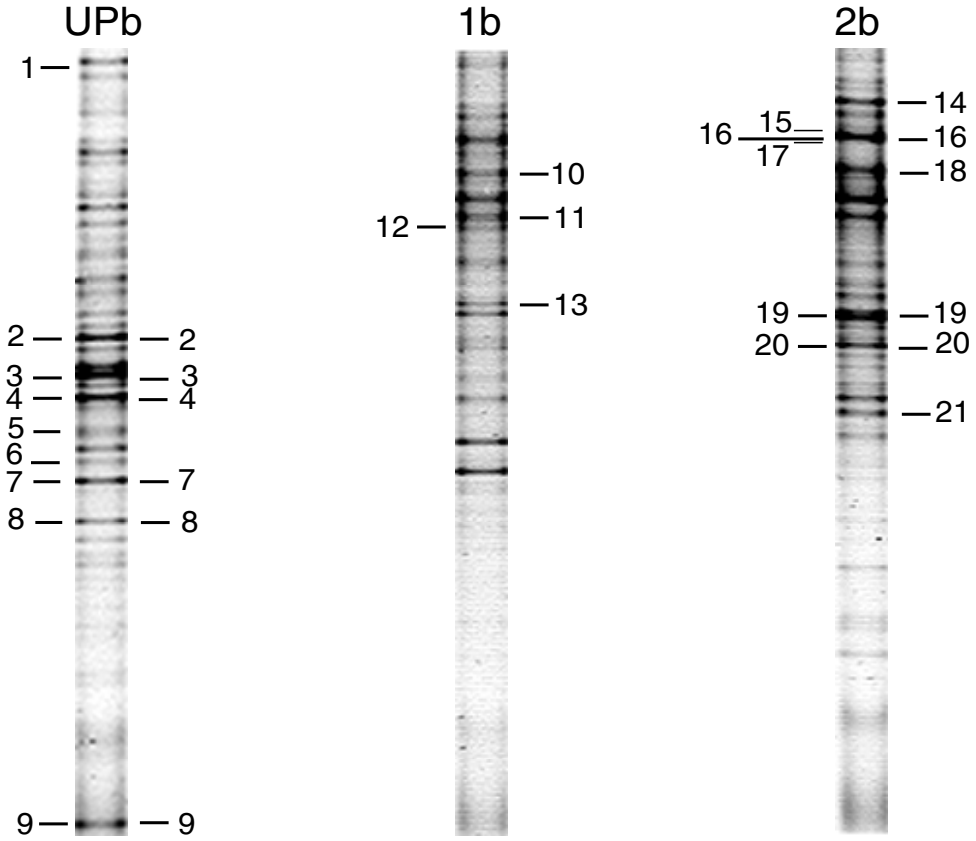

Figure 4.6: Linking of bacterial clone identities to DGGE profiles (40 to 70% denaturant gradient) of groundwater samples taken upstream (sample UPb), beneath (sample 1b), and downstream (sample 2b) of the Banisveld landfill. The band positions of clones that showed DGGE migration similar to that of a dominant band in the groundwater community DGGE profile are indicated on the right site of the track. The band positions for clones with identities indicating an ability to perform redox reactions are shown on the left of each track. The identities of the numbered bands are given in Table 4.2.

nested PCR with primers F341-GC and R518 on the *Geobacter* specific PCR product revealed a dominant band corresponding to band 16 in Fig. 4.6 for all iron reducing samples (groundwater from the plume and below the plume). This band was not present in any of the denitrifying samples (data not shown).

As the clustering of *Archaea* DGGE profiles appears to be due to the presence or absence of two dominant bands (Fig. 4.4), only these bands were sequenced after excision from the gel. The upper band was 100 % similar to methanogenic endosymbionts of the anaerobic protozoa *Trimyema compressa* (Emb Z16412) and *Metopus contortus* (Emb Z13957), the lower dominant band was 96 % similar to an unidentified archeaon (AF050617).

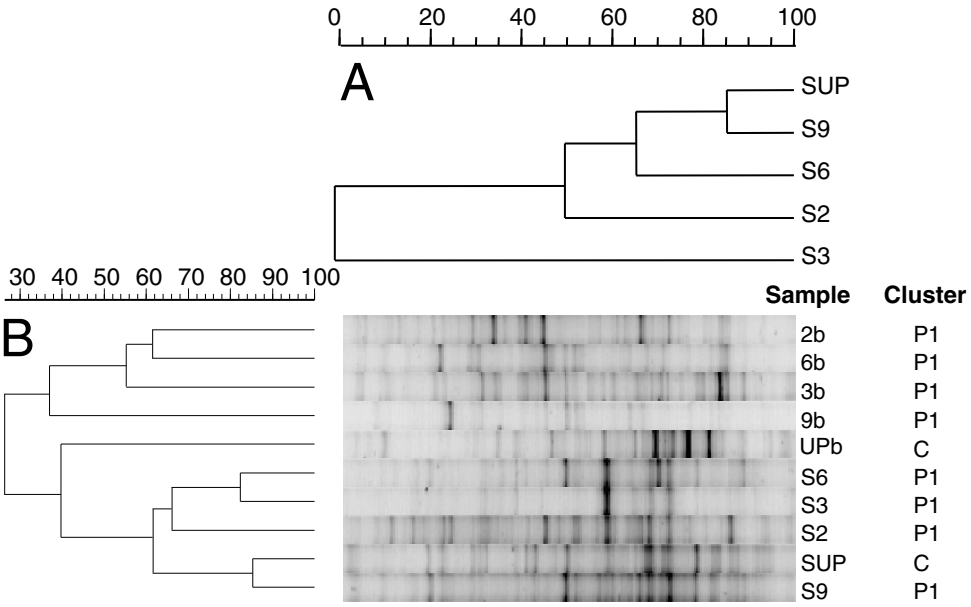

Figure 4.7: UPGMA cluster analysis of pollution-independent sediment parameters (A) and *Bacteria* DGGE profiles for sediment and corresponding groundwater samples (40 to 60% denaturant gradient) (B). For each lane the sample designation (Fig. 4.1; SUP, S2, S3, S6, and S9 refer to sediment samples) and level of pollution (Fig. 4.2) are indicated.

4.3.4 Geochemistry and microbial community structure of sediment

Sediment samples were retrieved from 5 locations, one upstream and 4 in the plume of leachate in October 1998 (Fig. 4.1). Analysis of the chemical composition of sediment pore water and subsequent cluster analysis clearly revealed that the sediment samples from the plume were polluted and that the upstream sample was clean and did not cluster with the four sediment samples (data not shown). When parameters not affected by pollution (percentages of lime, humus, clay, silt, carbon and nitrogen in sediment) were used for cluster analysis, a low relationship was observed (Fig. 4.7A), indicating the aquifer had a heterogeneous sediment composition. Samples SUP and S9 showed the highest similarity in chemistry.

After numerical comparison of DGGE profiles of *Bacteria* the five sediment samples clustered together, at 60 %, with SUP and S9 most similar to each other (Fig. 4.7B). Groundwater samples showed much less similarity. The profiles of sediment were quite different from groundwater extracted from the same position and depth.

4.4 Discussion

In this study we attempted to relate microbial community structure to hydrochemistry in a landfill leachate polluted aquifer. Microbial community structures

were determined using cultivation-independent, molecular methods. The different steps (DNA extraction, PCR and profiling) in such a molecular approach have their pitfalls (Von Wintzingerode et al., 1997). However, since all samples were treated similarly, these pitfalls can be considered to be equal for all samples, allowing between-sample comparison. The comparison between samples was achieved by numerical analysis of DGGE profiles, using the Pearson product moment correlation coefficient. This coefficient is robust and objective, since whole curves are compared and subjective band-scoring is omitted (Rademaker et al., 1999). Difficulties with band assignment are especially likely to occur with highly complex and varying profiles, as in our study. Furthermore, the Pearson coefficient does not suffer from mismatches between peaks and shoulders as often found when using band-scoring (Rademaker et al., 1999) and is much less laborious.

4.4.1 Comparison between microbial community structures from groundwater and sediment

In contrast to groundwater, no relation to pollution was apparent from the analysis of microbial community structure of sediment. The number of particle-bound microorganisms per gram sediment is usually an order of magnitude higher than the number of free-living microorganisms per milliliter in landfill leachate polluted aquifers (Albrechtsen and Windig, 1992; Holm et al., 1992). Since 1 cm^3 of sediment weights about 2.65 g and contains about 30 % water (valid for quartz sands with a porosity of 0.3), the number of sediment-associated microorganisms will be about two orders of magnitude higher than that present in water. Given that, on a geological scale, a relatively short time has elapsed since landfilling started (1965), leachate may have had little impact on microorganisms closely associated with the 10,000 to 100,000 year old sediments. A large part of the sediment-bound microorganisms could be physically (e.g., in pores) or biologically (e.g., in biofilms) protected from the influence of leachate. Furthermore, the pollutant-independent heterogeneity in sediment composition (Fig. 4.7A) may have contributed to variability in microbial community structure (Ludvigsen et al., 1999) and hampers the observation of changes related to pollution. The differences in community structure between sediment and nearby groundwater is in agreement with previous observations at landfill leachate polluted aquifers (Röling et al., 2000a) and other environments for which communities of particle-bound and free-living bacteria were determined (Crump et al., 1999; Kilb et al., 1998).

4.4.2 Groundwater community structure in relation to pollution and redox processes

In the leachate plume, iron reduction is a dominant redox process and in the zone of iron reduction BTEX compounds may get degraded. These observations have also been made for other landfill leachate affected aquifers (Albrechtsen et al., 1999; Heron et al., 1994a; Lyngkilde and Christensen, 1992a; Rügge et al., 1995). Both DGGE and clone library data indicate that the microbial community structure of the iron reducing leachate plume differed considerable from the unpolluted

groundwater upstream, above and below the plume of pollution. Clustering of DGGE profiles of *Bacteria* showed that 90 % of the samples were correctly separated based on level of pollution. Two clean samples (1c, 3c) were assigned as polluted and one polluted sample as clean (9b). The latter is from the well in the plume that was furthest located from the landfill and thus influenced by landfill leachate for the shortest time. Some hydrochemical parameters of sample 1c, such as chloride concentration were remarkably high for a clean sample (data not shown). Sample 3c was also the only sample wrongly assigned when culture-dependent anaerobic community-level physiological profiling was used (Chapter 3). All *Archaea* DGGE profiles were assigned to the correct cluster, based on the level of pollution. Thus, groundwater sampling was shown to be suitable for determining differences in microbial community structure associated with pollution. Microbial degradation can also be determined using only groundwater samples, although degradation rates are lower and groundwater sometimes exhibits lower degradation potential than aquifer sediment (Albrechtsen et al., 1996; Holm et al., 1992).

Analysis of DGGE profiles showed that while communities of *Archaea* and *Bacteria* in the plume clustered together, more variation was observed outside the plume. Outside the plume more variation in dominant redox processes was found, denitrification occurred upstream and above the plume and iron reduction below the plume. Clustering of *Bacteria* DGGE profiles correlated partially with these differences in redox processes. Communities of *Archaea* were clearly different, in the sense that all samples from iron reducing, non-plume locations failed to yield a PCR product in the *Archaea*-specific PCR, while samples from locations characterized by denitrification did give rise to a PCR product. Cluster analysis on DGGE profiles of the latter showed that these profiles grouped together, and were different from the *Archaea* communities in the leachate plume.

The results from the clone libraries linking particular organisms to bands in DGGE profiles were consistent with the observed redox conditions. Upstream, where denitrifiying conditions prevailed, sequences related to potential denitrifiers (*Azoarcus* (Zhou et al., 1995), *Actinobacteria* (Schaal, 1991)), as well as microaerophilic iron-oxidizing *Gallionella ferruginea* (Hanert, 1991) were encountered. Sequences related to aerobic and denitrifying bacteria were seldom encountered beneath and downstream of the landfill. Beneath the landfill strictly anaerobic, fermentative microorganisms, especially members of the *Clostridiaceae*, dominated. Also one sequence related to *Geobacteraceae* was encountered. Downstream, where iron-reducing conditions dominated, a high percentage of the sequences (22 %) was closely related to this family. Iron reduction is a general trait of cultivated members of the *Geobacteraceae* (Lonergan et al., 1996). Downstream one sequence related to a potential denitrifier (*Azoarcus*) and one related to a sulphate reducer were obtained, while upstream two sequences relating to sulphate reducers were also obtained. Culture dependent studies on a Danish landfill leachate plume also showed that usually several types of redox reaction performing microorganisms are present at the same location, even when redox conditions are unfavourable (Ludvigsen et al., 1999). Specific phospholipid fatty acid biomarkers paralleled the occurrence of sulfate- and iron reduction in the Danish aquifer (Ludvigsen et al., 1999).

4.4.3 Community structure and degradation in the leachate plume

While cluster analysis of DGGE profiles obtained with general bacterial and archaeal primers was able to separate communities from polluted and clean groundwater, it was not clearly able to distinguish between samples from within the plume and relate them to hydrochemistry or processes. In part, this might be due to the fact that iron reduction is the dominant redox process throughout the plume. Clustering of the DGGE profiles of members of the *Bacteria* revealed separation of samples close to the landfill (sampling wells 1 and 2) from samples farther away, but based on hydrochemistry the samples obtained near the landfill were members of cluster P1 (hardly any BTEX compounds) and P2 (containing BTEX compounds) (Fig. 4.2) and thus could not be clearly related to degradation. The lack of a relationship between microbial community structure and degradation is not surprising since (i) xenobiotic compounds (primarily BTEX [$<$ 204 mg/l]) contribute less then 1 % of the dissolved organic carbon (57-98 mg/l) in the plume and thus microorganisms metabolizing BTEX make only a minor contribution to the total microbial community and (ii) in addition to organic carbon, microorganisms leach from the landfill and strongly contribute to the rDNA-based microbial community structure, although they may not be active. Leaching of *Bacteria* is indicated by the fact that the groundwater sample from just below the landfill (1b) is very similar in DGGE profile to that taken from in the landfill (1a). Also, the clone libraries from groundwater beneath and downstream of the landfill revealed a large number of sequences related to complex compound degrading fermentative bacteria and acetogens (genera *Acetobacterium*, *Clostridium*, *Cytophaga*, *Spirochaeta* and *Bacteroides*). In landfills, high numbers ($> 10^7$ cells per dry gram) of acetogenic, xylanolytic and cellulolytic bacteria are present, while only simple organic compounds leach out (Barlaz et al., 1989). A large number of *Clostridium*- and *Cytophaga*-like sequences were also detected in a molecular study on a Canadian landfill (Lloyd-Jones and Lau, 1998). Microorganisms can persist in groundwater over long distances, anaerobic microorganisms from livestock waste water constituted a major part of the microbial community at an aerobic sampling well 400 m from the point of pollution (Cho and Kim, 2000). Although the molecular analysis of rRNA instead of rDNA is advocated to be more useful as it would favor the detection of the active microbial community (e.g., Felske et al., 1998), it is unlikely to be of much benefit for studying environments as addressed here. Starved bacteria can maintain high numbers of ribosomes, up to 30 % of their maximum (Fukui et al., 1996). Furthermore, if one assumes that indeed an universal relation between RNA/DNA ratio and growth rate (μ) exists and that this relation can be described with RNA/DNA = 1.65 + 6.01 $\mu^{0.73}$ (Kemp, 1995), then even if microorganisms were growing in their natural environment at the unrealistically high rate of 0.5 h^{-1} (generation time of 80 minutes), their RNA/DNA ratio (with RNA mainly being rRNA) will only be 3 times higher than under zero growth conditions. In the subsurface, growth-rates can be assumed to be much lower (Whitman et al., 1998). Therefore, like rDNA based analysis, rRNA based analysis will merely indicate presence and not activity.

High methane concentrations in groundwater indicated methanogenic conditions in the landfill, thus leaching of archaeal cells from the landfill might be ex-

pected. Remarkably one of the dominant bands in the archaeal profiles was clearly related to a methanogenic endosymbiont of an anaerobic protozoan. This suggests the presence of anaerobic protozoa. Pollution usually increases protozoal numbers (Novarino et al., 1997), although no protozoa could be detected in a Danish landfill leachate polluted aquifer (Ludvigsen et al., 1999). Predation by protozoa and variations in hydrochemical composition in the plume, could explain why despite clustering together, considerable variation (profiles clustering only at 35 %) was found in microbial community structure in the leachate plume.

Multivariate analysis on the relation between phospholipid fatty acid (PLFA) profiles and microbial redox processes revealed that PLFA profiles also had limited value for identifying more specific microbial communities in a landfill leachate plume (Ludvigsen et al., 1997). It is well known that some numerically minor groups of microorganisms are essential for major environmental processes, e.g. nitrifiers in the N-cycle (Phillips et al., 2000). In contrast to PLFA, specific functional groups of microorganisms can be more adequately investigated by molecular methods, as used in this study. The knowledge on genes involved in anaerobic BTEX degradation is still limited (Heider et al., 1998), but expands steadily. Hydrocarbon-degrading bacteria were recently quantified using a real-time PCR method targeting a catabolic gene associated with anaerobic toluene and xylene degradation (Beller et al., 2002). Molecular techniques linking community structure to function have also recently been developed. Application of stable-isotope probing (Radajewski et al., 2000) or bromodeoxyuridine labelling (Urbach et al., 1999) in carefully designed microcosm assays that mimic the natural situation as closely as possible, will help to establish a clearer relation between microbial community structure and degradation processes. Also, for this aquifer, with iron reduction as major redox process and degradation under these redox conditions, a logical choice for future research would be to focus on iron reducing bacteria. While iron reducing bacteria are phylogenetically diverse (Amann et al., 1992; Coates et al., 1999; Cummings et al., 1999; Lonergan et al., 1996; Lovley, 1997a), only sequences related to *Geobacteraceae* were encountered. Clone libraries, linking identities to DGGE profiles of whole microbial communities and MPN-PCR revealed a considerable contribution of *Geobacteraceae* to the microbial community. The results presented here underline that *Geobacteraceae* are widely and dominantly distributed in a diversity of iron reducing environments (Coates et al., 1996; Snoeyenbos-West et al., 2000). Interestingly, up to now only members of this genus have been found to be capable of toluene oxidation under iron reducing conditions (Coates et al., 1996; Lovley et al., 1989), while there are strong indications that *Geobacteraceae* are also involved in anaerobic benzene degradation (Rooney-Varga et al., 1999). Members of the *Geobacteraceae* are also important humic acid reducers (Coates et al., 1998) and capable of using humic acids as electron shuttles to facilitate iron reduction (Lovley et al., 1998). Humic acids make up about 10 % of dissolved organic carbon in landfill leachate (Christensen et al., 1998). Consequently, members of the *Geobacteraceae* are a good first choice for more detailed community studies in relation to natural attenuation in landfill leachate-polluted aquifers.

Chapter 5

REACTIVE TRANSPORT MODELLING OF BIOGEOCHEMICAL PROCESSES WITHIN THE LEACHATE PLUME

Abstract

The biogeochemical processes governing leachate attenuation inside a landfill leachate plume (Banisveld, the Netherlands) were revealed and quantified using the 1D reactive transport model PHREEQC-2. Biodegradation of dissolved organic carbon (DOC) was simulated assuming first-order oxidation of two DOC fractions with different reactivity, and was coupled to reductive dissolution of iron oxide. Implicit simulation of a growing population of iron-reducing microorganisms was not incorporated in the model as this was found to have only a minor effect on the results obtained. The following secondary geochemical processes were required in the model to match observations: kinetic precipitation of calcite and siderite, cation-exchange, proton-buffering and degassing. Rate constants for DOC oxidation and carbonate mineral precipitation were determined, and other model parameters were optimised using the non-linear optimization program PEST by means of matching hydrochemical observations closely (pH, DIC, DOC, Na^+, K^+, Ca^{2+}, Mg^{2+}, NH_4^+, Fe(II), SO_4^{2-}, Cl^-, CH_4, saturation index of calcite and siderite). Rate of precipitation of carbonate minerals was low with respect to other studies, and is expected to be caused by absence of these minerals in the pristine aquifer, inhibitory effects of fulvic acids, and the low groundwater temperature. Rate of iron reduction was compared to rates observed at other landfill leachate plumes: a positive relation between the rate of iron reduction and the content of reactive iron oxide in a particular aquifer was found. The modelling demonstrated the relevance and impact of various secondary geochemical processes on leachate plume evolution. Concomitant precipitation of siderite masked the act of iron reduction. Cation-exchange resulted in release of Fe(II) from the pristine anaerobic aquifer to the leachate. Degassing, triggered by elevated CO_2 pressures caused by carbonate precipitation and proton-buffering at the front of the plume, explained the observed downstream decrease in methane concentration. Simulation of the carbon isotope geochemistry independently confirmed the proposed reaction network.

Parts of this chapter have been submitted to *Journal of Contaminant Hydrology*, with J. Griffioen, W.F.M. Röling and H.W. Van Verseveld as co-authors

5.1 Introduction

Natural attenuation (NA) processes are able to restrict the spreading of organic pollution in aquifers (e.g., Christensen et al., 2001). However, uncertainty about the continuation of NA necessitates a continuous monitoring. Monitored natural attenuation (MNA) is therefore an emerging remediation technique. Predictive models on plume evolution may reveal important processes and factors that control NA and can thereby guide and optimise the monitoring. Modelling and data gathering should therefore be considered as an iterative process. Besides the occurrence, also the type, the kinetics and sustainability of the governing degradation reactions should be determined. The type of degradation process (e.g., aerobic, nitrate reduction, iron reduction, etc) changes in time and space as reflected by a sequence of redox zones observed from the source zone to the outskirts of an organic pollution plume (e.g. Christensen et al., 2000; Christensen et al., 2001). Prediction of the redox chemistry is essential, since the extent of degradation of specific organic pollutants depends on the associated redox process (Krumholz et al., 1996; Christensen et al., 2000; Christensen et al., 2001).

Constraining a reactive transport model to site-specific observations enables quantification of redox processes and prediction of plume evolution. Various reactive transport model codes have been developed in the last decade (Essaid et al., 1995; Clement et al., 1998; Abrams and Loague, 2000a; Murphy and Ginn, 2000; Islam et al., 2001; Van der Lee and De Windt, 2001; Brun and Engesgaard, 2002). A reactive transport model should include in addition to the primary degradation reactions (e.g., degradation of organic carbon coupled to iron reduction) also secondary redox (e.g., Fe(II) oxidation) and other geochemical reactions (e.g., cation-exchange, siderite precipitation) in order to constrain the redox equations, since these reactions affect concentrations of redox species and pH as well (Hunter et al., 1998). This intrinsic capability makes multicomponent geochemical transport models superior to multiple solute transport models.

Several studies exist where reactive transport models were used to model field observations in aquifers contaminated by point sources of organic pollution (Essaid et al., 1995; Prommer et al., 1999; Abrams and Loague, 2000b; Mayer et al., 2001; Brun et al., 2002). Modelling the biogeochemical reactions in a landfill leachate plume seems especially complicated because of the diversity of solutes and processes involved, and has been performed only recently (Brun et al., 2002). Brun et al. (2002) incorporated Monod kinetics with biomass growth for five bacterial populations equal to the number of redox zones to simulate the degradation of dissolved organic carbon (DOC), but were less ambitious with respect to simulating the complexity of the geochemical system. The discrepancy between the model and observations (e.g., pH, bicarbonate, Fe(II)) was attributed to uncertainty on initial conditions (DOC concentration, iron oxide content), a high yield factor for microbial growth, and omission of siderite precipitation.

The present study illustrates that simulation of various secondary geochemical processes (cation-exchange, proton-buffering, kinetic precipitation of carbonate minerals, and degassing) is required to explain the observed downstream improve-

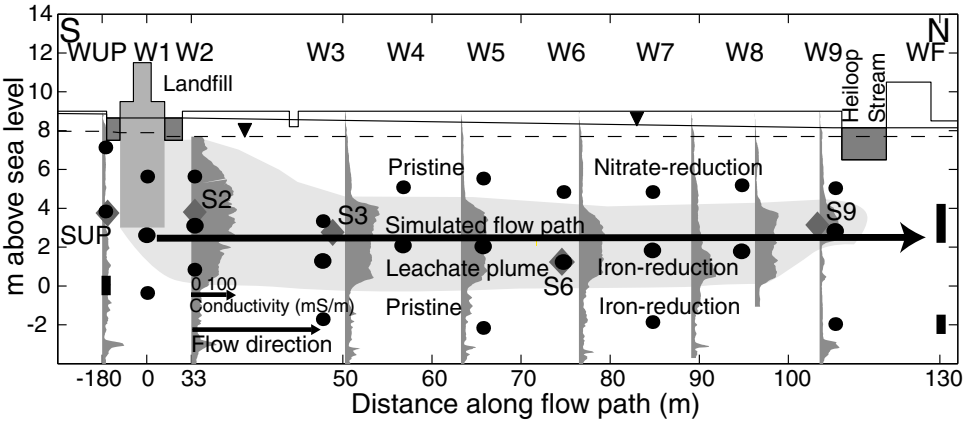

Figure 5.1: Cross section of the research transect downstream of the landfill site. The leachate plume is depicted in light gray and delineated using the formation conductivity, which is plotted from left to right (dark gray). The position of the groundwater observation wells (WUP, W1–W9, WF: black dots or vertical lines), sediment samples (SUP, S2, S3, S6, S9: ◆), the minimum and maximum observed hydraulic head (▼), and the simulated flow path are shown.

ment in leachate composition along a central flow path in an iron-reducing landfill leachate plume (Banisveld landfill, the Netherlands). The model includes simulation of the carbon-13 isotope geochemistry of the plume in order to verify model results. First-order DOC degradation was applied instead of Monod kinetics with biomass growth, in order to reduce the number of sensitive and unknown parameters (Essaid et al., 1995; Keating and Bahr, 1998). Rate constants for DOC oxidation, and calcite/siderite precipitation were calibrated, while other model parameters were optimised using the non-linear optimization program PEST (Watermark Computing, http://www.sspa.com/pest).

5.2 Construction of the reactive transport model

5.2.1 Banisveld landfill research site

The Banisveld landfill (6 ha) is situated 5 km southwest of Boxtel, the Netherlands. Disposal of primarily household refuse occurred in a former 6-m-deep sand pit between 1965–1977. Artificial or natural liners are absent, while most of the waste is present below the groundwater table, which lies less than 2 m below surface. The hydrogeochemistry of the site is described in Chapter 2. Here, only a brief summary will be given. A leachate plume was detected using cone penetration tests at a depth of about 4 to 9 m below surface to a distance of about 70 m from the landfill border (Fig. 5.1). The plume migrates through a heterogeneous phreatic aquifer, which consists of fine- to coarse-grained unconsolidated clayey sands. Groundwater observation wells (WUP, W1–W9, WF) were placed in the direction of groundwater flow within and around the plume (Fig. 5.1). At each well

site two or three wells were placed with 20-cm length screens at different depths. Wells are indicated by the following notation: Wxy, where x is the code of the observation well site (UP, 1–9, F), and y refers to the screen depth of a well at well site x (a–upper screen (generally above plume); b–middle screen (inside plume); c–lower screen (below plume)). Sampling and analysis of groundwater were performed in June 1998, September 1998 and October 1999. Sediment samples were taken at five locations (SUP, S2, S3, S6, and S9; see Fig. 5.1) at plume depth for geochemical analysis in October 1998.

5.2.2 Model code

The 1D PHREEQC-2 model code (Parkhurst and Appelo, 1999) was used to simulate the evolution of groundwater quality along the central flow path in the leachate plume (Fig. 5.1). The PHREEQC database provided equilibrium constants for acid-base reactions, complexation of inorganic species, and the solubility of minerals and gases (CH_4, CO_2). Solubility of Ar and N_2 were taken from Andrews (1992). The possible contribution of dissolved organic carbon (DOC) to alkalinity was neglected (< 2 %, Chapter 2).

Simulation of 1D transport was appropriate, because no dilution of leachate occurred along the flow path (Chapter 2): chloride concentrations in leachate were much higher than in pristine groundwater (Table 5.1) and remained constant in the flow direction (Fig. 5.5). The model assumes that the leachate composition in downstream wells W2 to W9 has evolved from the leachate composition in well W1.

5.2.3 Simulation of transport

A groundwater flow velocity of 4 m/year was assumed as best estimate (Chapter 2) and used in the model. A time-step of 0.5 years was taken and the cell-length was set at 2 m. The flow path was simulated by a series of 80 'cells' with a total length of 160 m (Fig. 5.1). Since landfilling occurred between 1965–1977, and groundwater sampling was performed in the period 1998–1999, duration of advective transport is 34 years at most. Total transport time was optimised using PEST as 30.5 years (see Section 5.2.6). A flux in the start- and end-cell was taken as boundary condition. The diffusion coefficient was set at 3×10^{-10} m^2/s, while a low value for longitudinal dispersivity of 0.1 m was specified. As the plume length was about 100 m (Fig. 5.1), a longitudinal dispersivity of 10 m (one tenth of the flow length) could be expected at most (Gelhar, 1986). A longitudinal dispersivity of 10 m could not match constant observed chloride concentrations in the plume, while a value of 1.0 m did not affect results much in comparison with the adopted value of 0.1 m.

5.2.4 Composition of leachate and pristine groundwater

Table 5.1 shows the observed compositions of inflowing leachate and pristine groundwater and the compositions adopted in the model. The composition of pristine groundwater used in the model was calibrated using PEST (see section

5.2.6). The model composition for inflowing leachate was taken equal to the average composition of well W1b, located just below the landfill (Fig. 5.1). However, for Cl^-, SO_4^{2-}, N_2 and Ar, the average concentration observed in the whole plume was adopted, because (near) conservative behaviour is observed. Leachate contains high concentrations of the following species with respect to pristine groundwater: Cl^-, alkalinity, DOC, Fe(II), CH_4, NH_4^+, Ca^{2+}, Mg^{2+}, K^+ and Na^+. Leachate leaving the landfill body is supersaturated with respect to siderite and calcite. Concentrations of SO_4^{2-}, N_2 and Ar are lower in the plume than in pristine groundwater.

The pristine aquifer is anaerobic. Nitrate was observed only in shallow groundwater upstream and above the plume, and was assumed to be absent at plume depth before landfilling started. Nitrate reduction is likely to be an important redox process at the top fringe of the plume. DOC degradation inside the leachate plume was coupled to iron reduction, while sulfate reduction and methanogene-

Table 5.1: Composition of inflowing leachate and pristine groundwater (observed and adopted in model)

Parameter	Unit	Leachate observed[a]	model	Pristine observed[a]	model
Chloride	(mmol/l)	4.03–8.74	7.36	0.34–2.17	1
EC[b]	(μS/cm)	4520–5260	–	189–754	–
Alkalinity[c]	(mmol/l)	51.3–56.8	56	0.2–6.6	0.5
pH		6.4–6.7	6.6	4.6–6.7	5
pe[d]		-3.6	-3.6	-2.7 to -3.4	-3.0
Temperature	(°C)	10–13	11.0	–	11.0
DOC[e]	(mmol C/L)	8.2–10.3	9.2 (2 fractions)	0.25–1.92	0
Oxygen	(mmol/l)	0	0	0	0
Nitrate[f]	(mmol/l)	0	0	0/1.2/6.1	0
Mn(II)	(μmol/L)	6.4–9.1	–	0.5–13	–
Fe(II)	(mmol/l)	0.20–1.24	0.81	0.002–0.47	0.11
Sulfate[a]	(mmol/l)	0.03–0.11	0.06	0.018–1.72	1
Sulfide	(μmol/l)	3–6	–	0–9	–
Methane	(mmol/l)	1.33–1.48	1.33	0–0.56	0.1
Nitrogen gas[a]	(mmol/l)	0.16–0.42	0.28	0.98	0.98
Argon[a]	(μmol/l)	3.3–7.5	5	16.5	16.5
Ammonium	(mmol/l)	19.2–19.8	19.8	0.006–0.067	0.067
Calcium	(mmol/l)	7.83–10.4	10.4	0.42–2.72	0.42
Magnesium	(mmol/l)	3.1–4.36	3.70	0.12–0.49	0.12
Potassium	(mmol/l)	5.55–6.14	6.01	0.026–0.41	0.41
Sodium	(mmol/l)	7.7–9.39	8.22	0.3–2.6	2.6
δ^{13}C-DIC	(‰)	+13.1	+13.1	-19.55	-19.55
δ^{13}C-CH_4	(‰)	-53.1	-53.1	-72.6	-72.6
δ^{13}C-DOC	(‰)	-24 to -30	-27	≈ -27	–

[a] *Observation well W1b was taken as representative for leachate. For conservative Cl, SO_4^{2-}, Ar and N_2 observed ranges for the total plume are given. Pristine groundwater was characterized by 13 wells. (For Ar and N_2: W8a).*

[b] *EC = Electrical conductivity.*

[c] *Alkalinity comprises acid buffering of dissolved organic carbon.*

[d] *pe was calculated from the H_2/H^+ redox couple.*

[e] *Dissolved organic carbon from the leachate was assumed to be reactive, while pristine DOC was not. In the model two DOC fractions differing in reactivity were used (see Table 5.2).*

[f] *Observed nitrate concentrations in pristine groundwater are given as maximum concentrations for below the plume, above the plume and upstream of the landfill, respectively.*

sis were restricted to the landfill body (Chapter 2). This is reflected by the strong contribution of iron-reducing bacteria of the family *Geobacteraceae* to the microbial communities in this plume (see Chapter 4). Iron reduction is expected to be the dominant redox process in the pristine aquifer at plume depth as well. Undersaturation with respect to calcite ($CaCO_3$) and siderite ($FeCO_3$) indicates that the pristine aquifer does not contain these minerals. Supersaturation with respect to siderite and calcite indicates that precipitation of these carbonate minerals probably happens within the leachate plume (Fig. 5.7).

5.2.5 Simulation of the biogeochemical processes

Degradation of dissolved organic carbon coupled to reduction of iron oxide

Dissolved organic carbon (DOC) degradation was simulated using first-order kinetics, assuming two DOC fractions differing in reactivity (see Table 5.2 and Section 5.3.2). Individual DOC components were not simulated: the total concentration of mono-aromatic hydrocarbons was three orders of magnitude lower than the DOC concentration, while Albrechtsen et al. (1999) measured equally low concentrations of volatile fatty acids in methanogenic-phase leachate under iron-reducing conditions. Dissolved organic carbon in methanogenic-phase leachate consists mainly of humic- and fulvic acids (Christensen et al., 1998). Oxidation of soil organic matter was not included because its reactivity was expected to be much lower than the leachate DOC reactivity. Sorption of DOC to sandy aquifer sediments is low (Christensen et al., 2001) and therefore neglected in the model.

Kinetic degradation of DOC was simulated following the two-step partial equilibrium approach (e.g., Brun and Engesgaard, 2002) by transforming conservative (to the model) DOC species into "reactive" CH_2O, which is instantaneously oxidized in the PHREEQC model while maintaining thermodynamic equilibrium. The adopted FeOOH solubility (Table 5.2) falls in the solubility range for lepidocrocite and was calculated from hydrogen gas concentrations assuming that iron-reducers need a minimum threshold of -7 kJ/mol H_2 to oxidize H_2 (Chapter 2). The hydrogeochemical conditions (absence of oxygen and nitrate, solubility FeOOH, pH) determine that Fe(III) is the preferential electron-acceptor and has a higher affinity to accept electrons than sulfate or carbon dioxide. The initial content of FeOOH in the aquifer was taken constant and sufficiently high in order to prohibit depletion of iron oxide close to the landfill.

Precipitation of carbonate minerals

Precipitation of siderite and calcite were modelled as kinetic reactions, because the leachate was supersaturated and far from thermodynamic equilibrium with these mineral phases. Rate of precipitation (R) was modelled as the product of the observed or effective rate constant (k_{obs}) times the saturation state minus 1 (e.g., Nancollas, 1979):

$$R = k_{obs}(\Omega - 1) \tag{5.1}$$

$$\Omega = \frac{IAP}{K} \tag{5.2}$$

where Ω is the saturation state, IAP is the ion activity product, and K is the thermodynamic equilibrium constant. The saturation state is 1 at thermodynamic equilibrium, and the water is supersaturated with respect to a particular mineral when Ω exceeds 1. The observed rate constants were determined (Table 5.2) by matching the observed saturation indices of the minerals using PEST (see Section 5.2.6). The equilibrium constants of calcite and siderite (Table 5.2) were taken from the PHREEQC database.

Cation-exchange and proton-buffering

Proton buffering was included in the model because pH changed from slightly acidic in the pristine aquifer to close to neutral in the landfill (Table 5.1). Proton buffering on soil organic matter (SOM) was modelled according to the approach of Appelo et al. (1998), with exchange coefficients for proton exchange taken from Tipping and Hurley (1992). Proton buffering on iron oxide was neglected because PHREEQC calculations on surface complexation (results not presented) showed that proton desorption from iron oxide was much less than from SOM. However, it will be of more importance in aquifers having lower SOM to FeOOH ratios.

Following Appelo et al. (1998), cation exchange capacity (CEC) was estimated using the average clay content of the sediments (3.8 $\pm$ 2.3 %; n = 5), while the

Table 5.2: Biogeochemical reactions modelled

Reaction	log (K)[a]	Rate (mol/l/yr)	Amount (mmol/l)
Biodegradation of dissolved organic carbon			
$DOC \rightarrow\ CH_2O$		1.03 x 10^{-2} x [DOCp][b]	6.14 (DOCp)
		1.06 x 10^{-1} x [DOCr][b]	3.06 (DOCr)
			9.2 (total DOC)
$CH_2O + H_2O \rightarrow\ CO_2 + 4e^- + 4H^+$		instantaneous	
Iron reduction			
$FeOOH + 3H^+ \leftrightarrow\ Fe^{3+} + 2H_2O$	-0.15		50
$Fe^{2+} \leftrightarrow\ Fe^{3+} + e^-$	-13.02		
Carbonate precipitation			
$CaCO_3 \leftrightarrow\ Ca^{2+} + CO_3^{2-}$	-8.48	7.3 x 10^{-4} x $(\Omega - 1)$[c]	0
$FeCO_3 \leftrightarrow\ Fe^{2+} + CO_3^{2-}$	-10.89	3.3 x 10^{-5} x $(\Omega - 1)$[c]	0
Cation-exchange & proton-buffering			
Cation exchange capacity (CEC)			113 (142 ± 85)[d]
Proton buffer (Y_{tot})			30 (30 ± 24)[d]
Degassing[e]			
$\Sigma\, p(CO_2, CH_4, Ar, N_2) \leq\ P - hydro$		instantaneous	

[a] *log (K) is given for 25 °C.*
[b] *DOCr = reactive fraction of dissolved organic carbon; DOCp = persistent (less reactive) DOC fraction.*
[c] *Ω = saturation state for specific mineral in groundwater.*
[d] *CEC (meq/l) = 0.6 x [% $< 2\mu m$] x 10 x (ρ_b/ϵ); Y_{tot} (meq/l) = 4.8 x [% OC] x 10 x (ρ_b/ϵ), (Appelo et al., 1998). For porosity (ϵ) a value of 0.3 was adopted, while for calculation of the bulk density (ρ_b) the specific weight of quartz (2.65 g/cm^3) was taken for the sediment grains. Model values are given, while observed averages and standard deviations are shown in parentheses.*
[e] *P-hydro = hydrostatic pressure = 1.68 atm.*

amount of proton exchangeable sites (Y_{tot}) was estimated using the average organic carbon content of the aquifer (0.10 $\pm$ 0.08 %; n = 5; Table 5.2). Exchange coefficients on clay and organic matter were taken from the PHREEQC database and Appelo et al. (1998), respectively. Exchange coefficients of Fe^{2+} and NH_4^+ to organic matter are not known, but were assumed to be equal to Mg^{2+} (Griffioen, 1992) and K^+ (Bruggenwert and Kamphorst, 1982), respectively. The exchange coefficient of Fe^{2+} to clay (X^-) was taken equal to Mg^{2+}.

Degassing

The landfill leachate plume contains high concentrations of CH_4 and CO_2, and the total gas pressure exceeds hydrostatic pressure (Chapter 2). Gas bubbles may therefore form (Blicher-Mathiesen et al., 1998), and volatilization from the plume may occur. In particular volatile methane can be expected to decrease in concentration as result of degassing (Baedecker et al., 1993).

PHREEQC calculates, given the hydrostatic pressure, whether or not a gas phase forms including the moles of gas and its composition in equilibrium with groundwater. Gases included in the model were: CO_2, CH_4, N_2 and Ar. The hydrostatic pressure was fixed at 1.68 atm along the flow path, which was in the range of hydrostatic pressure along the flow path (1.5 to 1.7 atm), and equal to the total gas pressure of the leachate source composition. A developing gas phase was modelled to be instantaneously lost from the leachate.

Modelling of ^{13}C isotope geochemistry

The carbon isotope geochemistry was simulated in PHREEQC by adding "C12" and "C13" as separate imaginary solutes to the model. The exact concentration of ^{12}C and ^{13}C was calculated from the DIC isotope signature in leachate and pristine groundwater (Table 5.1). Degradation of DOC was simulated without isotope fractionation, and C12 and C13 were added to the model cells in absolute amounts calculated from the average observed δ^{13}C-DOC value of -27 ‰ (Chapter 2).

Potential anaerobic methane oxidation was simulated as a first-order process, and fractionation as a result of oxidation was included:

$$R^{13}C = k \bullet [CH_4] \bullet \left(\frac{[^{13}C]}{[^{13}C] + [^{12}C]} \right) \bullet \alpha \tag{5.3}$$

$$R^{12}C = k \bullet [CH_4] \bullet \left(\frac{[^{12}C]}{[^{13}C] + [^{12}C]} \right) \tag{5.4}$$

where $R^{13}C$ and $R^{12}C$ are the oxidation rates of ^{13}C-CH_4 and ^{12}C-CH_4, respectively, k is rate constant for methane oxidation fitted to the observed downstream methane decrease, [i] is concentration of species i, and α is the fractionation factor (α = 1.014). This value has been calculated for anaerobic methane oxidation observed within another landfill leachate plume (Grossman et al., 2002). The δ^{13}C-CH_4 of inflowing leachate and pristine groundwater was taken at -53.1 ‰ and -72.6 ‰, respectively (Table 5.2).

The δ^{13}C of precipitating carbonate minerals (siderite and calcite) was determined at each time step and distance by calculating the δ^{13}C of bicarbonate (using [HCO_3^-], [CO_2], δ^{13}C-DIC and a fractionation factor ${}^{13}\epsilon_{bicarbonate-CO_2(aq)}$ of +10.6 ‰ (Mook, 2000)) and adopting a fractionation factor (${}^{13}\epsilon_{carbonate\ mineral-bicarbonate}$) relative to bicarbonate. Two sets of fractionation factors (${}^{13}\epsilon_{carbonate\ min-bicarbonate}$) were tested (see results).

Finally, the effect of carbon dioxide degassing on δ^{13}C-DIC was simulated. Following the approach of carbonate mineral precipitation, δ^{13}C-CO_2 (g) was calculated using δ^{13}C-CO_2 (aq) and taking a fractionation factor ${}^{13}\epsilon_{CO_2(g)-CO_2(aq)}$ of +1.13 ‰ at 11 °C (Mook, 2000).

5.2.6 Calibration of the reactive transport model using PEST

Calibration of the model was done using the parameter estimation software PEST (Watermark Computing, http://www.sspa.com/pest). PEST optimises the sum of weighted least squares between the model outputs and the field observations by changing assigned model parameters within given ranges of uncertainty. The program uses a nonlinear estimation technique known as the Gauss-Marquardt-Levenberg method.

The following model parameters were optimised: Fe(II), Ca^{2+}, Mg^{2+}, K^+, Na^+ and NH_4^+ of pristine groundwater (within observed concentration range), observed rate constant (k_{obs}) for siderite and calcite precipitation, oxidation rate of the two DOC fractions (rate of reactive fraction was set 10 times faster than less reactive fraction), proportion of the two DOC fractions, total transport time, and cation-exchange capacity (CEC). Cation-exchange capacity was optimised because the standard deviation of the estimates was high. The optimum found was 20 % less than the calculated average (Table 5.2). Other parameters were kept constant.

The following groundwater hydrochemical variables were used as constraints and taken to calculate the weighted sum of square differences with model results: pH, DIC, DOC, Na^+, K^+, Ca^{2+}, Mg^{2+}, NH_4^+, Fe(II), together with the saturation indices of siderite and calcite (for SI calcite only well W2b was used because SI $>$ 0 at that point). Eight screens were used (W2b-W9b), and for each screen average values over time (n = 3) were taken. Consequently, the total sum consisted of 81 square differences.

The weight factor for each variable was taken as the reciprocal of its average observed concentration in the plume. High sum of residuals for cations (NH_4^+ $>$ Ca $>$ K $>$ Mg $\approx$ Fe(II)) resulted in a sub-optimal fit for variables having a low sum of residuals. Therefore, weight factors of some key variables were multiplied to enhance the fit: pH (x10), DOC (x10), SI siderite and SI calcite (x$\sqrt{10}$).

5.3 Results of reactive transport modelling

Several reactive transport simulations (S1–S8) will be discussed (see Table 5.3) to show the effects of the various processes on the downstream change in leachate composition.

5.3.1 Cation-exchange and proton-buffering

Cation-exchange and proton-buffering change the composition of the leachate flowing through the aquifer. Figure 5.2 shows the composition of the total exchanger (T =ΣX+Y_{tot}) along the flow path for the final model (S7). Exchangeable (i.e., sorbed on the exchanger) ammonium and potassium increased, while exchangeable calcium and Fe(II) decreased in the first 60 m of the flow path with respect to pristine groundwater further downstream. Potassium and ammonium retard due to cation-exchange at clay minerals with mainly Ca^{2+} and Fe(II). Exchangeable Fe(II) is thus released to the leachate. Figure 5.2 shows that proton-buffering causes desorption of protons from sedimentary organic carbon, in response to an increase in pH by inflow of leachate. Proton-buffering causes about a unit of decrease in pH at the front of the plume (compare simulation S7 with S8 in Fig. 5.8), and subsequently triggers degassing (see Section 5.3.4) as bicarbonate shifts to carbon dioxide (Fig. 5.9).

The fit of sodium observations is fair, and for potassium and magnesium reasonable (Figs. 5.3, 5.4). However, simulated calcium and ammonium concentrations further than 50 m downstream were higher and much lower, respectively, than observed (Figs. 5.3, 5.4). PEST used the maximum observed pristine concentrations of K^+, Na^+, and NH_4^+, and the minimum observed concentration of Ca^{2+} in order to suppress simulated concentrations of calcium and improve the overall fit of the model. Varying the exchange selectivity coefficients of Ca^{2+} and NH_4^+ within reported ranges (Bruggenwert and Kamphorst, 1982) did not significantly improve the fit of Ca^{2+} (results not shown). Excluding proton-buffering from the model slightly decreased the match with Fe(II) and Ca^{2+} observations (results not shown). Retardation factors for potassium and ammonium were calculated as respectively 3.4 and 2.9 using model concentrations, but for ammonium observed retardation seems less than 2.

Table 5.3: Simulations performed

Sim	Processes included	Remarks
S1	No reactions (only conservative transport)	
S2	Cation-exchange and proton-buffering	
S3	S2 + DOC degradation coupled to iron reduction	
S4	S3 + methane oxidation coupled to iron reduction	
S5	S3 + precipitation of siderite and calcite	[Fe(II)] prist. = min observed
S6	idem	[Fe(II)] prist. = calibrated
S6a	$^{13}\epsilon_{calcite-bicarbonate}$, $^{13}\epsilon_{siderite-bicarbonate}$ = 0.21 ‰	
S6b	$^{13}\epsilon_{calcite-bicarbonate}$ = 1 ‰, $^{13}\epsilon_{siderite-bicarbonate}$ = 2.7 ‰	
S7	S6 + degassing	Final calibrated model
S8	S7, but without proton-buffering	

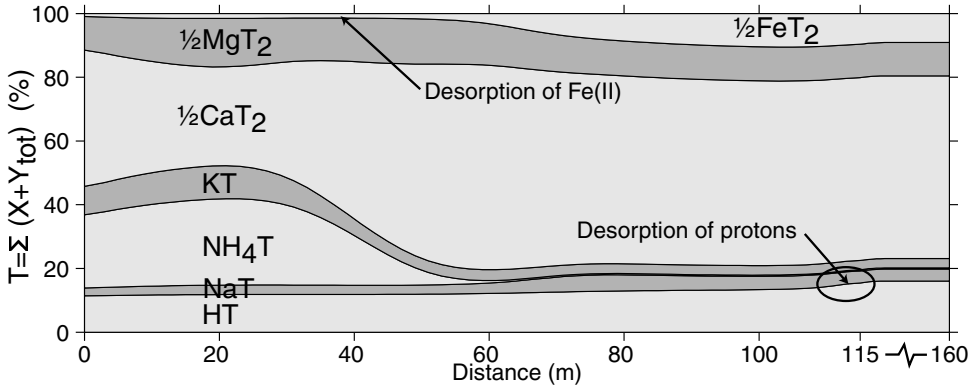

Figure 5.2: Simulation of exchange site composition (T = Σ(X+Y_{tot})) along the flow path.

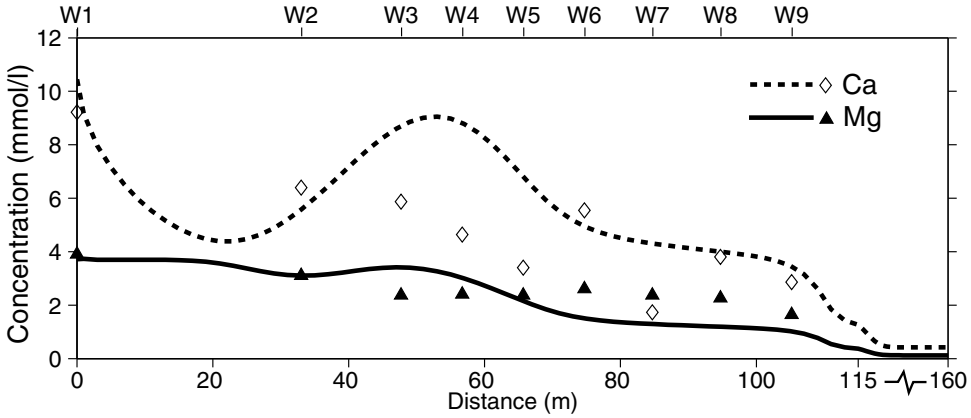

Figure 5.3: Observations and simulation of calcium (◇) and magnesium (▲).

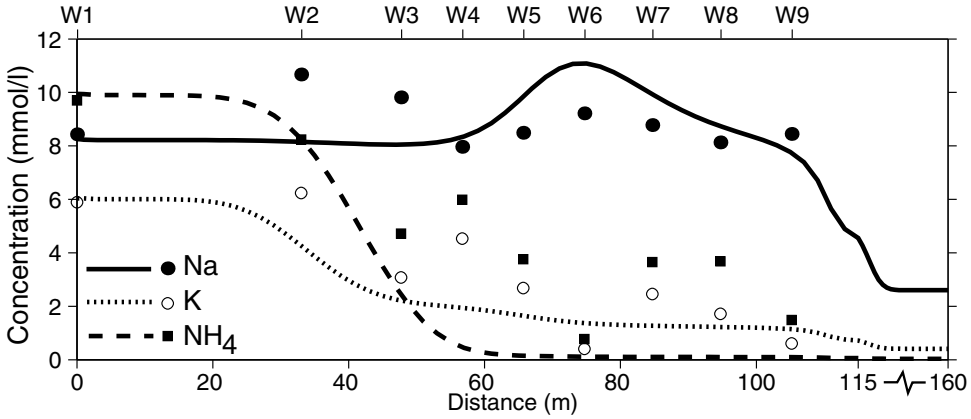

Figure 5.4: Observations and simulation of sodium (●), potassium (○), and ammonium (■).

5.3.2 Degradation of DOC coupled to iron reduction

Degradation of DOC is coupled to reduction of iron oxide in the leachate plume (Chapter 2). Zero- or first-order DOC degradation kinetics did not result in a reasonable match with observations (results not shown), as a consequence of a very sluggish decrease of observed DOC concentration in the downstream part of the plume (Fig. 5.5). Monod kinetics may be a suitable rate formulation but describes biodegradation of specific substrates and consequently does not apply for leachate DOC. Biodegradation of complex organic matter like DOC is usually simulated considering an infinite number of reactive fractions (Bosatta and Ågren, 1995). Here, a simpler model considering first-order degradation of only two DOC fractions with different reactivity simulated observations well (Table 5.2, Fig. 5.5). The decrease in overall DOC reactivity downstream is caused by depletion of the reactive DOC fraction according to this degradation model. PEST optimised the proportion of the most reactive fraction as a third of total DOC.

The content of iron oxide was almost completely consumed close to the landfill after 30.5 years (Fig. 5.6). However, the few measurements do not show a decrease in iron oxide content towards the landfill. Depletion of iron oxide downstream from the landfill is however expected in the near future as degradation proceeds. Taking a lower solubility for FeOOH equal to goethite (log (K) = -1.0) causes iron reduction to be energetically less favorable and results in a short sulfate-reducing zone at the landfill border succeeded by simultaneous methanogenesis and iron reduction downstream (Fig. 5.11). FeS was allowed to precipitate in this model. Note that, once methanogenesis is active, degassing strongly impedes the methane concentration to increase downstream. This illustrates that occurrence of methanogenesis is difficult to determine from methane concentrations in contaminant plumes, once the sum of partial gas pressures starts to exceed the hydrostatic pressure.

Simulation S3 predicts that, if only cation-exchange and iron reduction would occur, pH, DIC and Fe(II) should increase downstream (Figs. 5.8–5.10). However, decreases in pH and DIC were observed, while the observed dissolved Fe(II) concentrations were much lower than the calculated Fe(II) concentrations (up to 14 mmol/l), resulting in simulated saturation indices of siderite (up to 3.5) and calcite (up to 2.0) which are much higher than observations (results not shown).

5.3.3 Precipitation of calcite and siderite

The discrepancy between field observations and model S3, which excludes precipitation of carbonate minerals, indicates that precipitation of siderite ($FeCO_3$) and calcite ($CaCO_3$) takes place. Kinetic precipitation was simulated because observed saturation indices for these minerals were substantially above zero (siderite: 0.8–1.8, calcite up to 0.8 near the landfill).

Rate constants for calcite and siderite precipitation were obtained by calibration using PEST and are shown in Table 5.2. One should note that the rate constant depends on the solubility constant of siderite, because the saturation state depends on this constant. The reported range of the thermodynamic equilibrium constant for siderite varies from -10.45 to -11.20 (Jensen et al., 2002) and our adopted value

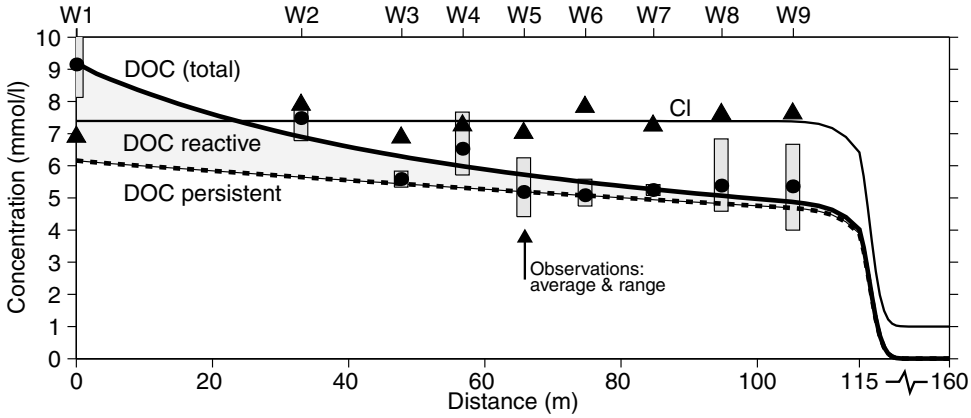

Figure 5.5: Observations and simulation of dissolved organic carbon (●) and chloride (▲).

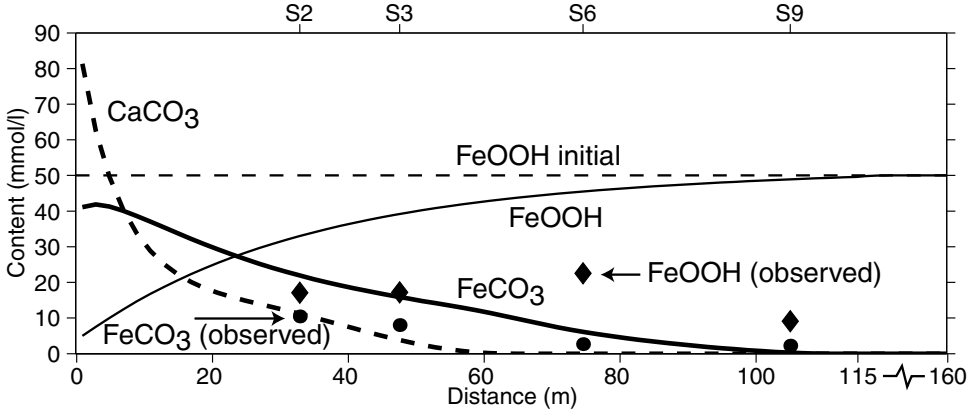

Figure 5.6: Observations and simulation of iron oxide, siderite, and calcite content.

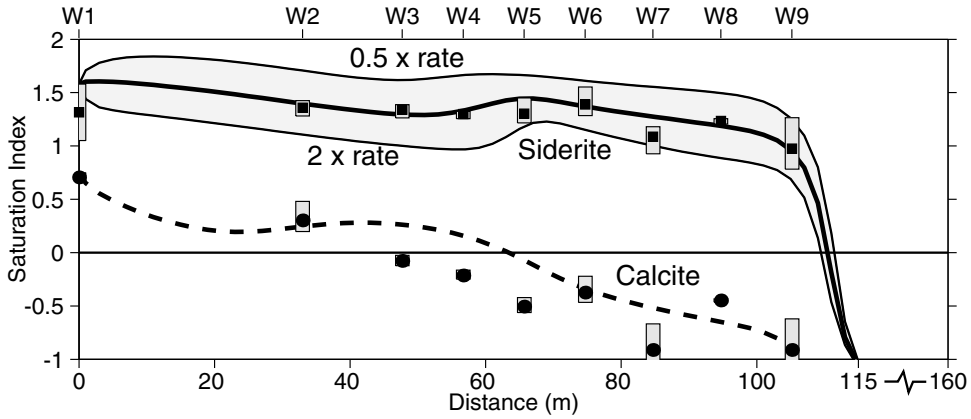

Figure 5.7: Observations and simulation of SIs with respect to siderite (■) and calcite (●).

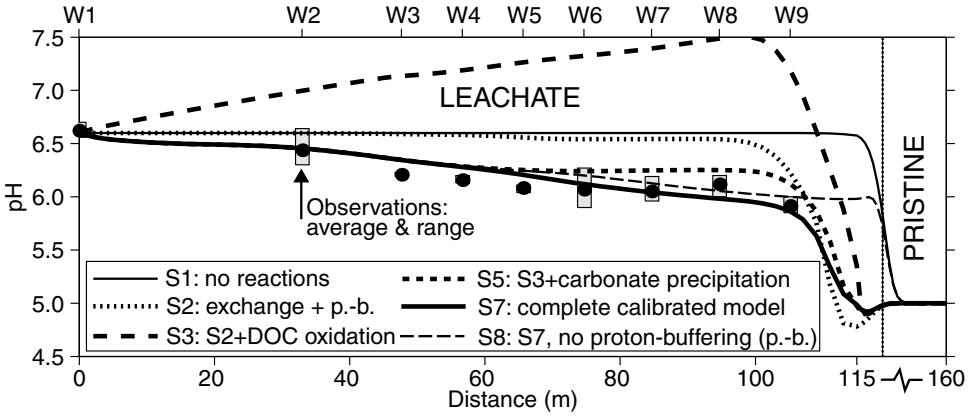

Figure 5.8: Observations and simulations of pH.

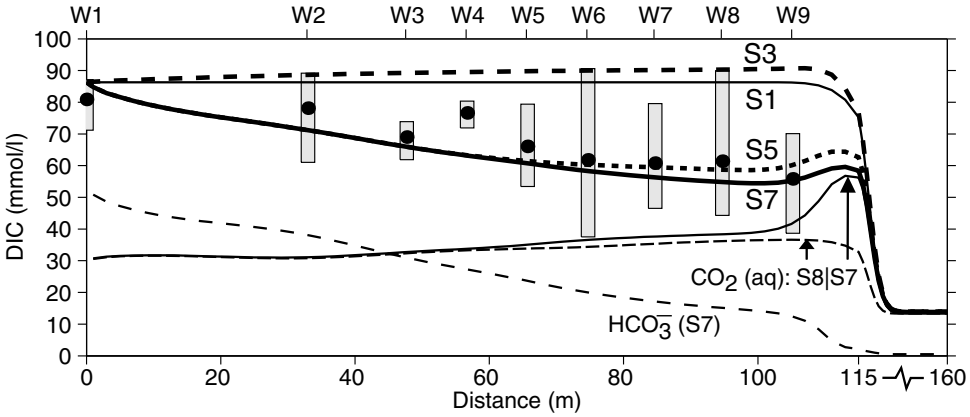

Figure 5.9: Observations and simulations of dissolved inorganic carbon (DIC).

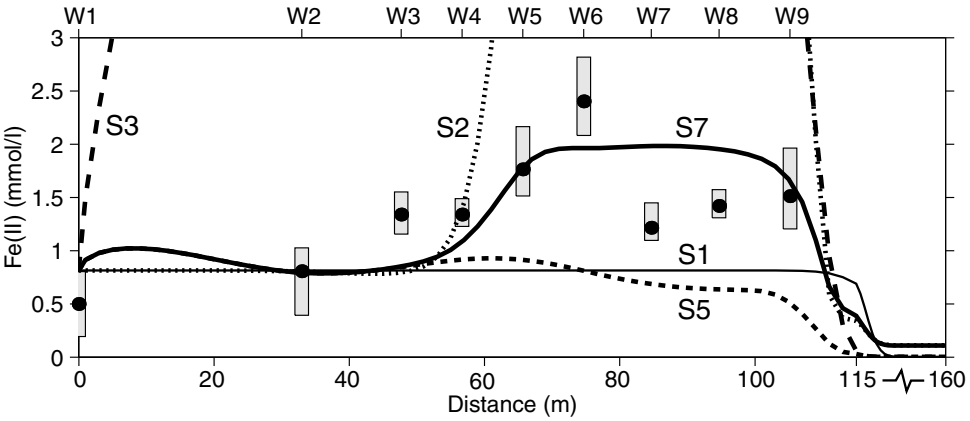

Figure 5.10: Observations and simulations of Fe(II).

(-10.89) fits in this range. Calibrated rate constant for siderite precipitation (3.3 x 10^{-5} mol/l/yr) is about 20 times lower than for calcite (7.3 x 10^{-4} mol/l/yr). However, absolute amounts of precipitated calcite and siderite are about equal (Fig. 5.6), as the lower rate constant is compensated by the higher saturation state of siderite. Lower rate constants for iron carbonate with respect to calcium carbonate precipitation, have generally been observed (Wajon et al., 1985; Jensen et al., 2002). Halving or doubling of the calibrated rate constant resulted in upper and lower limits of observed SIs for siderite (Fig. 5.7).

The final model (S7) predicts a maximum of 120 mmol/l of carbonate minerals precipitated at the landfill border (Fig. 5.6), which corresponds to a carbonate fraction of 0.023 % C at a porosity of 0.3. This amount is much smaller than the detection limit of the measurement method used (0.5 % C). Therefore, direct observational proof for precipitation of carbonate minerals was not acquired. Observations for siderite plotted in Fig. 5.6 are semi-quantitative measurements based on chemical extractions and are indicative of the total amount of siderite present (Chapter 2).

Precipitation of siderite and calcite decreases pH and DIC in downstream direction in agreement with observations (Figs. 5.8, 5.9). The SIs for siderite and calcite were also well matched by the model (Fig. 5.7). An important model variable was the adopted concentration of Fe(II) in pristine groundwater. PEST optimised the Fe(II) concentration (0.11 mmol/l) close to the observed average in pristine groundwater (0.12 $\pm$ 0.12 mmol/l, n = 26). A higher Fe(II) concentration at pristine conditions leads to a higher Fe-occupancy of the exchanger at pristine conditions. This implies a larger amount of Fe(II) expelled due to cation-exchange, when NH_4^+-rich leachate enters the aquifer, and siderite precipitation is initiated upon pH-increase. Therefore, Fe(II) at pristine conditions together with the rate constant for DOC degradation mainly control the amount of siderite precipitated, and consequently the DIC concentration. For example, if the minimum observed Fe(II) concentration was adopted ($\approx$ 2 μmol/l), Fe(II) released due to cation-exchange was substantially lower (simulation S5). Consequently, simulated Fe(II) was lower than observed (Fig. 5.10), less siderite was precipitated (result not shown) and pH simulated in the front part of the plume was too high (Fig. 5.8).

5.3.4 Degassing

Figure 5.12 shows the simulated partial gas pressures of CO_2, CH_4, N_2 and Ar for the final model, as well as the total gas pressure for the simulation excluding degassing (S5). The gas pressure in the leachate is high due to production of CO_2 and CH_4 inside the landfill body. The total gas pressure starts to exceed the hydrostatic pressure from about 40 m downstream in case degassing is not simulated (S5). It reaches a maximum pressure (2.2 atm) at the front of the plume. Carbon dioxide and methane are lost in about equal molar amounts when degassing is modelled (i.e., total gas pressure is not allowed to exceed hydrostatic pressure). However, the relative loss of methane is much higher, due to its lower solubility. The simulated decrease in methane by degassing at the most downstream well W9b was 14 %, while a decrease of 34 % was observed (Fig. 5.11). Mono-aromatic pollutants

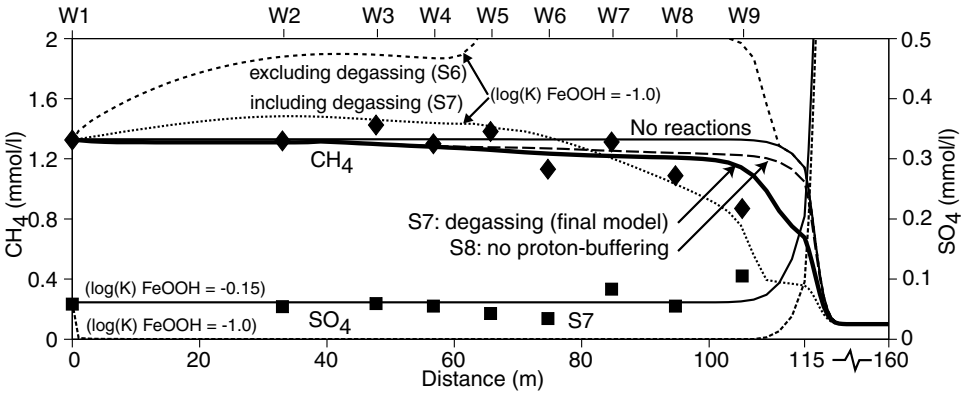

Figure 5.11: Observations and simulations of dissolved methane (◆) and sulfate (■).

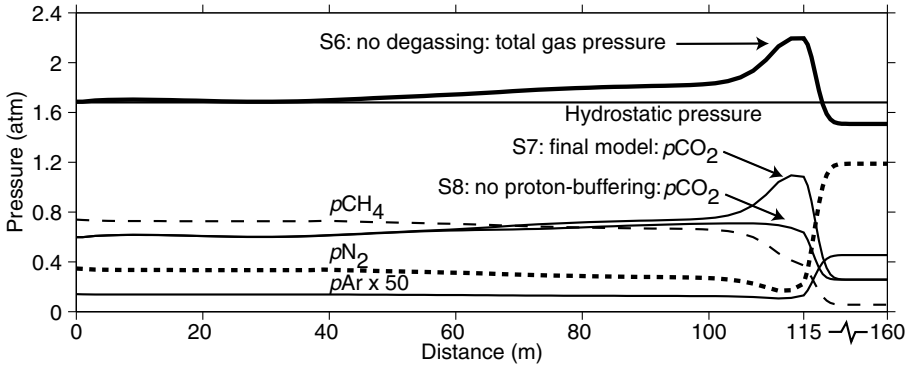

Figure 5.12: Simulation of degassing of dissolved gases in leachate plume.

will not be attenuated by degassing as these compounds are much less volatile than methane.

Degassing is not caused by in-situ production of gases in this aquifer (DIC production due to DOC oxidation is less than DIC removal by precipitation of carbonate minerals), but triggered by both proton-buffering and precipitation of carbonate minerals. Both geochemical processes cause a decrease in leachate pH (Fig. 5.8), which shifts bicarbonate to carbon dioxide (Fig. 5.9) and consequently increases $p\mathrm{CO}_2$ and total gas pressure (Fig. 5.12). Carbonate mineral precipitation induces degassing between 40-100 m downstream, while proton-buffering is the main trigger at the front part of the plume (Fig. 5.11).

5.3.5 Modelling of the carbon isotope geochemistry

Simulation of δ^{13}C-DIC was performed to verify the model. Figure 5.13 presents the contribution of various processes to the δ^{13}C-DIC evolution. Oxidation of DOC contributes inorganic carbon depleted in δ^{13}C (-27 ‰) and consequently lowers

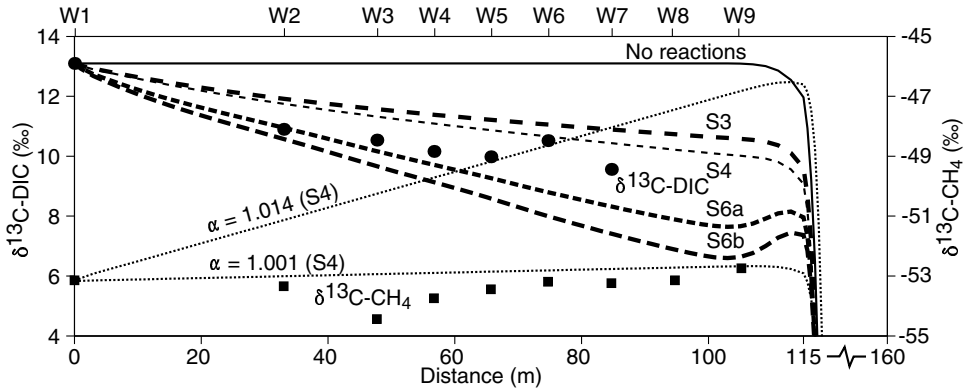

Figure 5.13: Observations and simulations of δ^{13}C-DIC (●) and δ^{13}C-CH_4 (■): DOC oxidation (S3) in combination with anaerobic methane oxidation (S4) or precipitation of carbonate minerals (S6a & S6b).

δ^{13}C-DIC in the direction of flow (Fig. 5.13: S3). The observed δ^{13}C-DIC decrease however is larger and supports occurrence of carbonate mineral precipitation (Fig. 5.13: S6a, S6b). Carbonate mineral precipitation and DOC oxidation have a comparable impact on the δ^{13}C-DIC decrease.

The fractionation factor for calcite precipitation differs somewhat in literature, and has not been determined for siderite precipitation at low temperature. Simulations were therefore run with two sets of fractionation factors (Table 5.3: S6a and S6b). For simulation S6a, the fractionation factor for $CaCO_3$ at a temperature of 11 °C (+0.21 ‰) was taken from Mook (2000) and was assumed to apply for $FeCO_3$ as well. Romanek et al. (1992) observed higher fractionation factors for calcite and aragonite: +1.0 ‰ and +2.7 ‰ respectively. Fractionation of aragonite conducted in experiments between 10–40 °C (Romanek et al., 1992) appeared similar to carbon-13 fractionation of siderite measured recently in precipitation experiments between 45–75 °C (Zhang et al., 2001). The fractionation factor for siderite can therefore be taken from aragonite for this low-temperature aquifer (Horita and Zhang, 2001). Simulation S6b adopted the higher fractionation factors observed by Romanek et al. (1992) and therefore resulted in a stronger δ^{13}C-DIC decrease. Simulation S6a simulated observations closer than simulation S6b (Fig. 5.13).

The effect of carbonate mineral precipitation on the downstream δ^{13}C-DIC decrease is considerable because of the slightly acidic conditions in this aquifer. The positive equilibrium fractionation factors between DIC species and carbonate minerals results in a preferential removal of ^{13}C from the leachate. However, the equilibrium fractionation factor with respect to carbonate minerals is much higher for dissolved carbon dioxide than for bicarbonate ($^{13}\epsilon_{bicarbonate-CO_2(aq)} \approx$ +9.5 ‰ at 20 °C and +11.4 ‰ at 5 °C (Mook, 2000). Therefore, fractionation due to carbonate mineral precipitation is relatively large under the slightly acidic conditions in this aquifer, where CO_2(aq) makes up a large part of DIC, compared to fractionation at neutral and alkaline pH, where bicarbonate or carbonate dominate DIC.

Degassing of carbon dioxide from the plume had a negligible effect on δ^{13}C-DIC because the amount of degassed CO_2 was low with respect to total DIC (results of simulation not shown). The potential effect of anaerobic methane oxidation on δ^{13}C-DIC was little compared to DOC oxidation or carbonate mineral precipitation (Fig. 5.13). The model predicts in disagreement with observations a strong increase in δ^{13}C-CH_4 values downstream (Fig. 5.13). A much lower fractionation factor (α = 1.001) below the reported range for oxidation (α = 1.003–1.037) but indicative for degassing (Bergamaschi, 1997), explained observations better. Consequently, occurrence of anaerobic methane oxidation inside this plume is unlikely, which confirms earlier interpretation (Chapter 2). Simulation of the carbon isotope geochemistry supports the probability of the hydrogeochemical model, and indicates that carbonate mineral precipitation occurs, although δ^{13}C-DIC observations were not perfectly matched.

5.4 Discussion

5.4.1 Model improvement by simulating microbial growth?

Simulation of microbial degradation kinetics including microbial growth using a multiple Monod formulation, is often incorporated in reactive transport models (e.g. Brun and Engesgaard, 2002; Essaid et al., 1995; Murphy and Ginn, 2000; Rittmann and Van Briesen, 1996). However, microbial reactions were simulated as kinetically controlled chemical reactions by us and others (Keating and Bahr, 1998), without modelling growth of microbial populations themselves. The inclusion of growth of iron-reducers will not likely improve the performance of the model, as discussed below.

The two approaches of simulating microbial reactions in reactive transport models differ on two main aspects: firstly, degradation kinetics in microbial growth models is not only controlled by environmental factors but also by the (growing) size of microbial populations. Secondly, when heterotrophic microbial growth occurs, a fraction of organic carbon degraded is transformed into biomass. Consequently, less electron-acceptor will be used per amount of DOC degraded, compared to a situation without growth.

Theoretically, a steady-state will be reached some time after inflow of organic carbon, where all consumed DOC will be utilized to extract free energy for maintaining an increased but stable population size (Stouthamer et al., 1990). The effective biochemical redox reaction is then equal to the chemical reaction equation. Therefore, the length of the growth period and the increase in biomass are important constraints for microbial models. Knowledge on these aspects is limited (e.g. Ludvigsen et al., 1999) and these aspects have not been considered in mathematical leachate-modelling approaches.

The microbial yield for iron reduction can be estimated using data from lab studies on the amount of cells produced per mmol FeOOH reduced (2.0–6.4 x 10^9; Liu et al., 2001a; Roden and Zachara, 1996), cell weight estimates (0.45–6.4 x 10^{-10} mg/cell; Essaid et al., 1995, Liu et al., 2001a), and a stoichiometry of $C_5H_7O_2N$ for

biomass, and results in microbial yields between 0.005 to 0.18 C/C (mol carbon-biomass produced per mol carbon-substrate consumed). In the culturing studies a high-energy organic substrate (lactate) was used. The microbial yield can be expected to be lower when low-energy leachate DOC serves as substrate. Additionally, we estimated the microbial yield for iron reduction between 0.02 and 0.1 C/C following the theoretical method of McCarty (1971), assuming a threshold of -20 kJ/mol H_2 for iron reduction and an acetate concentration of 5 μmol/l as carbon source. The above mentioned measurements and theoretical estimates indicate that the microbial growth yield of iron reduction is less than 0.1 C/C. Therefore, total amount of iron oxide reduced in the leachate plume could be at most 10 % less if growth of iron-reducers is simulated, which is comparable to the uncertainty in DOC concentration taken as model constraint.

Yields for iron reduction assumed in other models constrained by observations were either high (0.5 C/C; Brun et al., 2002), or rather low (0.003 C/C; Schäfer et al. (1998)). The observed iron oxide depletion was not captured by a reactive transport model of the Vejen landfill leachate plume, which was attributed to an initial large DOC flux not considered in the model, and overestimation of the initial iron oxide content in the polluted part of the aquifer (Brun et al., 2002). The unrealistic high microbial yield adopted (taken equal for all redox processes) may be another explanation for the discrepancy observed, as only 50 % of DOC degraded became oxidized by reduction of iron-oxide, while the other half was transformed into biomass.

Microbial growth models involve addition of many unknown parameters, and hence the problem might be underconstrained (Keating and Bahr, 1998). Essaid et al. (1995) found that microbial growth parameters were very sensitive. Although a hydrochemical pattern can be matched using these models, caution should be taken when making predictions. For example, degradation rates could increase in time as populations are still simulated to grow and increase in size. To suppress unstable effects of exponential microbial growth on degradation kinetics, biomass inhibition factors were used (Essaid et al., 1995), or initial biomass size chosen was very large (Brun et al., 2002). Following Keating and Bahr (1998), we consider simple kinetic formulations more reliable than the sophisticated Monod formulations, as the former reduce the degrees of freedom in the model and result in tighter constrained process parameters. Furthermore, the fraction of organic carbon transformed to biomass is little for iron-reducing conditions and therefore neglecting microbial growth is reasonable. Increase of the microbial population size is also likely to be a temporary process instead of a permanent one.

5.4.2 Kinetics of carbonate mineral precipitation

Solid solutions of Fe, Ca and Mg carbonates may form instead of pure phases supposed in this study, as leachate was supersaturated for several carbonate minerals (siderite, calcite and dolomite). Precipitation of ferroan calcite (assigned as $Fe_{0.8}Ca_{0.2}CO_3$) was observed in a crude oil-polluted aquifer, where siderite was supersaturated, but calcite was in equilibrium (Baedecker et al., 1993). Supersaturation for siderite together with saturation for calcite may indicate equilibrium

with a calcium siderite, as this solid solution is more soluble than pure siderite (Wajon et al., 1985). However, precipitation of pure calcite and siderite was modelled, since equilibrium constants for mixed Fe/Ca/Mg carbonates were not found in literature.

Observed rate constants for siderite precipitation vary over six orders of magnitude (Table 5.4). The observed rate constants (k_{obs}) are simple empirical constants, which incorporate the intrinsic rate constant (K_{int}) and the specific surface area of the mineral (s) (Kazmierczak et al., 1982). The observed rate constant is often used, as the mineral surface area in natural sediments is difficult to determine or not known. Rate constants observed in this study for both siderite and calcite precipitation, were low when compared to other observations (Table 5.4), but for siderite close to the rate experimentally determined in a recent study (Liu et al., 2001b). Besides the mineral surface area, inhibitory compounds and temperature determine the observed rate constant. Magnesium, organic acids and phosphate are known inhibitors of calcite precipitation (Appelo and Postma, 1993; Griffioen, 1992), but magnesium and phosphate concentrations in the Banisveld leachate plume were too low to inhibit precipitation. A fulvic acid concentration of only 0.028 mmol/l completely inhibited precipitation of calcite (Inskeep and Bloom, 1986). Fulvic acids made up $\approx$ 60 % of leachate of the Vejen landfill (Christensen et al., 1998), while the DOC concentration in the Banisveld leachate plume ranged between 4 and 10 mmol/l, offering an explanation for the low precipitation rates. Next, temperature has a large control on siderite precipitation rate. We calculated that the rate increased an order of magnitude per 16 °C (R^2 = 0.98, n = 5, 15–40 °C, Wajon et al., 1985) to 20 °C (R^2 = 0.99, n = 4, 27–76 °C, Greenberg and Tomson, 1992) rise in temperature, using data from these studies. However, this temperature effect is not sufficient to explain the orders of magnitude lower precipitation rate observed in this aquifer with respect to other studies involving some higher temperatures (Table 5.4).

The specific surface area of calcite and siderite is zero in the pristine aquifer at Banisveld as carbonate minerals are absent. When minerals start to precipitate out

Table 5.4: Reported observed rate constants for siderite and calcite precipitation

Study	Environment	Initial content minerals	Precipitation rate $FeCO_3$ (M/yr)	$CaCO_3$ (M/yr)	Temp. (°C)
Van Cappellen and Wang, 1995	Lake, coastal		$1x10^{-6}$		
Hunter et al., 1998	Model		$5x10^{-5}$	$6x10^{-5}$	
Liu et al., 2001b	Batch experiment	none	$5.3x10^{-5}$		25
Jensen et al., 2002[a]	Batch experiment	none	$3x10^{-4}$	$2x10^{-2}$	15
Wajon et al., 1985	Batch experiment	seed crystals	$3x10^{-3}$		15
			$2x10^{-2}$		30
Matsunaga et al., 1993	Riverbed infiltration	present	$1.3x10^{-2}$		22
Schfer et al., 1998	Riverbed infiltration	present	$1.2x10^{0}$		ambient
Inskeep and Bloom, 1985	Lab experiment	seed crystals		$3.2x10^{0}$	25
Plummer et al., 1978	Theoretical rate			$3.7x10^{0}$	25
Greenberg and Tomson, 1992[b]	Batch experiment	seed crystals	$1x10^{0}$		27
This study	Landfill leachate plume	absent	$3.3x10^{-5}$	$7.3x10^{-4}$	11

[a] *Rate constants were determined by modeling the data with a PHREEQC model (results not shown).*
[b] *Rate constant was calculated independently of total seed surface area per volume: 391.8* $L^2/mol/m^2/s$ *at 27 °C.*

of solution but no seed crystals are present, spontaneous precipitation must occur and nucleation is the first step. When some seed crystals are formed heterogeneous precipitation can follow. However, the total surface area is then still limited, and consequently the associated observed rate constant is very low. On the contrary, rate constants were much higher in experiments where seed crystals were used (Greenberg and Tomson, 1992; Inskeep and Bloom, 1985; Wajon et al., 1985), or in environments where carbonate precipitation took place for a longer period and total surface area of the minerals was probably considerable (Matsunaga et al., 1993; Schäfer et al., 1998).

In conclusion, low observed rate constants for both siderite and calcite precipitation in the Banisveld landfill leachate plume, are probably due to the initial absence of these minerals and the presence of fulvic acids in leachate, while the low temperature of groundwater had a minor contribution to sluggish rates.

5.4.3 Determination of redox rates by geochemical modelling

Iron reduction rates were obtained in this study by constraining a hydrogeochemical transport model to hydrochemical observations. Another often-applied approach to determine in-situ redox rates is via incubation of small soil samples (e.g., Cozzarelli et al., 2000). However, these redox assays have several disadvantages. Redox assays often overestimate rates established using geochemical field observations, which is probably caused by stimulation of microbial activity as a consequence of physical disruption during drilling (e.g. Röling and Van Verseveld, 2002). Furthermore, absence of advective flow in assays could affect rates (Roden and Urrutia, 1999) and might stimulate less favorable redox processes. The high detection limit of the iron reduction assay (Ludvigsen et al., 1998) impedes determination of the iron reduction rate in many aquifer systems. Finally, redox assays are representative for a much smaller scale (10^{-2} m) than the scale of a pollution plume (10^{1}–10^{2} m), and show considerable variation in response to small-scale chemical heterogeneity. Up-scaling is therefore necessary. The advantage of hydrochemical observations (representative for a scale of 10^{-1}–10^{0} m) is that groundwater samples tend to homogenize spatial chemical heterogeneity and reflect the hydrogeochemical evolution upstream of the observation point in case of advection-dominated transport (Murphy and Schramke, 1998). Hydrogeochemical modelling is therefore a better method than the redox assay to determine redox rates on the scale of a pollution plume.

5.4.4 Factors controlling iron reduction kinetics in leachate plumes

Degradation of organic contaminants is observed to be dependent on the governing terminal electron-accepting processes (TEAPs) (Christensen et al., 2000a; Christensen et al., 2001; Krumholz et al., 1996). Therefore, knowledge on the factors, which control the kinetics of the TEAPs is essential to predict the overall development and sustainability of natural attenuation at contaminated sites. Iron reduction represents an extensive redox zone with good degradation potential in the center of this and many other plumes, where the soluble electron-acceptors

oxygen and nitrate cannot penetrate (Christensen et al., 2000a; Christensen et al., 2001; Lovley and Anderson, 2000). When iron oxides deplete, degradation of organic compounds can continue under sulfate-reducing or methane-producing conditions. However, sulfate concentrations in this and other plumes are too low to maintain equal degradation potential. Consequently, a large zone of methanogenesis will eventually develop in the core of a leachate plume. This zone will be present downstream of, or shows overlap with, a small sulfate-reducing zone surrounding the landfill, while the iron-reducing zone moves downstream in time. Degradation of hydrocarbons was observed to deteriorate when microbial degradation shifted from iron reduction to methanogenesis (Chapelle et al., 2000; Cozzarelli et al., 2001; Lovley and Anderson, 2000). Therefore, prediction of iron reduction kinetics is of utmost importance for assessing long-term natural attenuation potential, as sulfate reduction and methanogenesis generally show less potential for degradation.

Iron reduction was simulated in this study by first-order kinetics assuming two DOC fractions with different reactivity. At the Vejen landfill, lack of available iron oxide close to the landfill and lack of available DOC further downstream inside the leachate plume, were observed to be controlling factors of microbial iron reduction in laboratory experiments (Albrechtsen et al., 1995). Besides reactivity (Albrechtsen et al., 1995) and concentration (Liu et al., 2001b) of the electron-donor, kinetics of iron reduction is controlled by content and form of iron oxide (Albrechtsen et al., 1995; Lovley and Anderson, 2000; Roden and Zachara, 1996), presence of humics (Lovley and Anderson, 2000), and probably availability of nutrients.

Little quantitative information is known on the reactivity of DOC in leachate. Humics are present in leachate (Christensen et al., 1998), and increase the rate of iron reduction, as these act as electron shuttle between insoluble Fe oxide and iron-reducing microorganisms (Lovley and Anderson, 2000). In particular shortage of nitrogen and phosphorous may limit microbial growth. In landfill leachate plumes nitrogen in the form of ammonium is present in abundance. On the contrary, phosphorous was measured in concentrations below the detection limit (< 0.1 μmol/l) in this leachate plume. Potential phosphorous limitation in other landfill leachate plumes could not be established, as concentrations are usually not reported in literature. Microorganisms colonized feldspars containing trace phosphorous in a petroleum-contaminated aquifer, where phosphorous concentrations in groundwater were low (Bennett et al., 2000). Shortage of phosphorous could hamper the rate of iron reduction if there is potential for growth.

Rate of iron reduction was linearly proportional with iron oxide surface area (Roden and Zachara, 1996), but the laboratory experiments were performed with easily degradable organic substances (lactate). In the field, more recalcitrant organic compounds may provide reduction capacity. However, a correlation between DOC degradation rate under iron-reducing conditions and content of iron oxide (cf. Graf-Pannatier et al., 1999) may be found in landfill leachate plumes as well. Only four landfill leachate plumes were described in literature (Vejen, Grindsted, Norman, Banisveld) where we could estimate DOC degradation and iron reduction rates, and furthermore the occurrence of other redox processes was established and quantitative information on iron oxide content was available (Table 5.5).

Table 5.5 shows that a positive relation exists between the rate of DOC degradation/iron reduction and the content of iron oxide in a particular aquifer, while landfill age or DOC concentration show no relation with rate of iron reduction. The impact of iron oxide content is apparent. While the Vejen aquifer contained abundant iron oxide and showed highest rates for iron reduction, the Norman landfill leachate plume lacked bio-available iron oxide and degradation kinetics was extremely slow. The Grindsted and Banisveld landfill leachate plumes take an intermediate position. Persistence of DOC was attributed to the age of organic matter in the Norman landfill (Cozzarelli et al., 2000), but absence of reactive iron oxide may be a better explanation. Iron-reducing rates at these landfill sites were one to several orders of magnitude higher than calculated for pristine aquifers (Murphy and Schramke, 1998). This probably reflects the availability of reactive organic matter in leachate. Degradation rate of BTEX (Σ benzene, toluene, ethylbenzene, xylene) also showed a positive relation with DOC degradation rate, and content of iron oxide (Table 5.5). Consequently BTEX degradability may decrease as iron reduction proceeds and iron oxide depletes. More insight is needed on the redox-reactivity of DOC versus the redox-reactivity of natural Fe-oxides. Under field conditions, one of these two seems to be rate controlling.

5.5 Conclusion

Multicomponent geochemical transport modelling was used to obtain quantitative insight into the reactions contributing to the changes in leachate composition downstream of the Banisveld landfill, the Netherlands. A combination of reactions needed to be incorporated in the model to explain observations: degradation of DOC coupled to reduction of iron oxide, cation-exchange, proton-buffering, and kinetic precipitation of siderite and calcite. Degassing provides an explanation for downstream decreasing methane concentrations and was triggered by carbonate mineral precipitation and proton-buffering both increasing pCO_2 by decreasing the pH. Remarkably, it was sufficient to adopt a constant leachate composition, while in other studies spatial heterogeneity (Brun et al., 2002) or temporal variability of the

Table 5.5: Estimated zero-order rates for DOC degradation coupled to iron reduction in landfill leachate plumes in relation to content of reactive iron-oxide

Landfill	DOC (mM C)	BTEX (μg/l)	Rate DOC (mol/l/yr)	Rate BTEX (μg/l/yr)	Redox process	FeOOH (mgFe/g dw)
Vejen[a]	5–42	120–400	5x10^{-3}–2x10^{-2}	230–600	Fe/SO_4^{2-}/CH_4	0.03–4
Banisveld[b]	8–10	180	max 3x10^{-4}	1-7	Fe	0.1–0.2
Grindsted[c]	2.5–9	150	0 – max 6x10^{-4}	13–35	Fe/SO_4^{2-}	0.02–0.03
Norman[d]	8–13	10	≈ 0	≈ 0 to < 0.6	Fe/SO_4^{2-}/CH_4	≈ 0

[a] *Vejen landfill (1962–1981): Lyngkilde and Christensen (1992a+b), Heron et al. (1994), Brun and Engesgaard (2002).*

[b] *Banisveld landfill (1965–1977): Chapter 2 and 5.*

[c] *Grindsted landfill (1930–1977; tertiary part aquifer): Bjerg et al. (1995), Rügge et al. (1995), Jakobsen et al. (1998), Heron et al. (1998).*

[d] *Norman landfill (1922–1985): Cozzarelli et al. (2000), Eganhouse et al. (2001).*

source (Van Breukelen et al., 1998) had to be accounted for. Simulation of the carbon isotope geochemistry confirmed the proposed reaction network independently. The study demonstrated the relevance and impact of various secondary geochemical processes on leachate plume evolution. However, the approach of modelling the processes is non-unique. For example, proton-buffering on iron oxide was omitted, a different rate law for degradation could have been adopted (e.g., taking the content of iron oxide as additional parameter (Liu et al., 2001b), Monod kinetics with microbial growth), precipitation of solid solutions may have happened, and the surface area could have been incorporated in the rate formulation for mineral precipitation.

This and other studies (Baedecker et al., 1993; Revesz et al., 1995) show that degassing is an essential secondary process to consider in solving the reaction network controlling methane. Methanogenesis will be underestimated for gas-saturated plumes if the occurrence of gas exsolution is not accounted for (see Fig. 5.11). The significance of secondary methane-oxidizing redox reactions at the fringe of pollution plumes, as demonstrated by Hunter et al. (1998) using the reactive transport modelling, will increase substantially if degassing is considered. Furthermore, degassing can lead to formation of a separate gas phase in aquifer pores and may reduce the permeability of an aquifer. The flow direction and/or velocity may change as a result (Ronen et al., 1989; Yager and Fountain, 2001). This might also be an explanation for local water table mounds observed at landfill sites (Christensen et al., 2001).

The various secondary geochemical processes identified in this specific plume should be considered as being of general importance for landfill leachate plume evolution. Cation-exchange will manifest since leachate generally contains a different salt composition and higher salt concentration than fresh groundwater in pristine aquifers (Bjerg et al., 1993; Griffioen, 1999). Cation-exchange buffers Fe(II) and retards K^+ and NH_4^+. Proton-buffering should be considered because pH changes in these systems can be considerable (Griffioen, 1999). Cation-exchange and iron reduction contribute to the supersaturation of leachate with respect to Ca- and Fe-carbonates, respectively, and this shows that precipitation is kinetically controlled. Finally, high production of CH_4 and CO_2 in the landfill body and plume makes the necessity to consider degassing evident.

Simulations show that the rate of siderite precipitation equals or exceeds the rate of iron reduction. Cation-exchange buffers released Fe(II) as well. Using the aqueous Fe(II) concentration to quantify iron reduction (Wiedemeier et al., 1995) will therefore result in underestimating the extent of reductive dissolution of Fe-oxides, and associated extent of organic species degradation. A multiple solute model is not able to simulate siderite precipitation or other geochemical reactions, and could therefore only match dissolved Fe(II) in an aromatic hydrocarbon plume when the stoichiometry ratio of Fe(II) released per amount of Fe(III) reduced was adjusted from 1 to 1 down to 0.18 to 1 (Essaid et al., 1995). Geochemical-based reactive transport models can account for secondary geochemical reactions and hold therefore more promise for simulating the evolution of pollution plumes.

Chapter 6

BIOGEOCHEMICAL PROCESSES AT THE FRINGE OF THE PLUME

Abstract

Various redox reactions may occur at the fringe of a landfill leachate plume, involving oxidation of dissolved organic carbon (DOC), CH_4, Fe(II), Mn(II), and NH_4^+ from leachate and reduction of O_2, NO_3^- and SO_4^{2-} admixing from pristine groundwater. Knowledge on the relevance of these processes is essential for the simulation and evaluation of natural attenuation (NA) of pollution plumes. The occurrence of such biogeochemical processes was investigated at the top fringe of a landfill leachate plume (Banisveld, the Netherlands). Hydrochemical depth-profiles of the top fringe were captured via installation of a series of multi-level samplers at 18, 39 and 58 m downstream from the landfill. Ten-cm vertical resolution was necessary to study NA within a fringe as thin as 0.5 m. Bromide and its ratio to chloride can be used as alternative for chloride as conservative tracer to calculate dilution of landfill leachate. The plume fringe rose towards the surface from a depth of around 5 m over a vertical distance of about 1–3 m in the course of three years, possibly as a result of soil excavation in the area. This rise invoked cation-exchange including proton-buffering, and triggered degassing of methane. The hydrochemical depth-profile was simulated well in a 1D vertical reactive transport model using PHREEQC-2. Optimization using the non-linear optimization program PEST showed that solid organic carbon and not clay minerals controlled retardation of cations. Cation-exchange resulted in spatial separation of Fe(II), Mn(II) and NH_4^+ fronts from the fringe, and thereby prevented possible oxidation of these secondary redox species. Degradation of conservative DOC seemed to happen in the fringe zone. Re-dissolution of methane escaped from the plume and subsequent oxidation could be an explanation for absence of previously present nitrate and anaerobic conditions in pristine groundwater above the plume. Stable carbon isotope ($\delta^{13}C$) values of methane suggested that anaerobic methane oxidation occurred. Methane was the principle reductant consuming soluble electron-acceptors in pristine groundwater, thereby limiting NA for other solutes including organic micro pollutants at the fringe of this landfill leachate plume.

This chapter has been submitted as "Biogeochemical processes at the fringe of a landfill leachate pollution plume: Potential for dissolved organic carbon, Fe(II), Mn(II), NH_4^+, and CH_4 oxidation" to *Journal of Contaminant Hydrology*, with J. Griffioen as co-author

6.1 Introduction

Processes occurring at the fringe of a pollution plume are in potential of considerable importance for natural attenuation (NA) of the entire plume. Diffusive and dispersive mixing of anoxic polluted groundwater with (sub)oxic pristine groundwater at the plume fringe results in dilution and may enhance degradation: degradation potential for various electron-donors like aromatic hydrocarbons is absent or limited inside plumes, but excellent in the plume fringe, due to mixing with the soluble electron-acceptors oxygen, nitrate and sulfate. Transversal mixing between oxic and anoxic groundwater therefore enables faster biodegradation for many compounds. For example, oxidation by nitrate reduction in a 2 m thick fringe took the main share of total degradation in a 20 m thick plume consisting of phenolic compounds (Mayer et al., 2001).

High quality field data are however limitedly present and this hampers progress in understanding NA processes at the fringe of pollution plumes. The hydrochemical gradient perpendicular to a plume fringe is often badly captured in pollution plume studies, because the vertical sampling point spacing is too large with respect to the fringe thickness. Consequently, the fringe of a pollution plume is poorly constrained in reactive transport models. Conventional numerical models based on rectangular grids often overpredict mixing, resulting in associated overestimation of degradation of contaminants in the plume and, consequently, underestimation of the actual plume expansion happens (Cirpka et al., 1999). However, occurrence of transient flow, which is usually not simulated, enhances dispersive mixing and hence biodegradation (Schirmer et al., 2001).

Although understanding of mixing processes is improving, knowledge on the biogeochemistry of the plume fringe lags behind. Hunter et al. (1998) made a distinction between primary redox reactions, where organic matter is degraded, and secondary redox reactions (SRR), which involve the oxidation of reduced redox species formed by the primary redox reactions. Besides dissolved organic carbon (DOC) and aromatic hydrocarbons, several reduced redox species can be subject to oxidation at the plume fringe, and compete for available oxidants, especially in landfill leachate plumes: Fe(II), Mn(II), NH_4^+, and CH_4. Secondary redox reactions can be beneficial when the electron-donor is considered as a pollutant (ammonium), but can also be regarded as unwanted (methane) because the availability of soluble oxidants then diminishes for more harmful pollutants. The potential for the various SRRs is under debate (Griffioen, 1999; Hunter and Van Cappellen, 2000), but the occurrence and extent of SRRs and geochemical processes at the plume fringe have barely been studied in the field (Christensen et al., 2000a). This knowledge needs to be developed in order to validate model simulations on degradation and dilution at the plume fringe.

Landfill leachate contains a high ammonium concentration, where nitrification of ammonium under aerobic conditions is a possible attenuation process. Recently, occurrence of anaerobic ammonium oxidation (anammox) by reduction of nitrite was proved (Jetten et al., 1998), and occurrence of anammox coupled to nitrate reduction providing nitrite for ammonium oxidation, has been observed as well

(Thamdrup and Dalsgaard, 2002). Anammox may be an important process in nature at oxic/anoxic interfaces including the fringe of landfill leachate plumes as well (Schmidt et al., 2002).

Ferrous iron is another competitor for both nitrate and oxygen. Anaerobic nitrate-dependent Fe(II)-oxidation is a microbiological process and needs the presence of an organic cosubstrate such as acetate (Straub et al., 2001). Aerobic oxidation of Fe(II) and Mn(II) occur both microbially mediated and chemically (Stumm and Morgan, 1996). Re-oxidation of ferrous iron that is mobilized upon reductive dissolution of iron oxide in association with organic matter oxidation can be beneficial as for example benzene seems more often degraded with Fe(III) than with NO_3^- as electron-acceptor (Lovley, 2000).

Finally, methane in leachate is prone to oxidation at the plume fringe, at least with oxygen (Hanson and Hanson, 1996), but in potential with other electron-acceptors too. Anaerobic methane oxidation (AMO) has been observed with sulfate as electron-acceptor, but the process is still poorly understood (Valentine and Reeburgh, 2000). Hoehler et al. (1994) and Schink (1997) proposed the mechanism of methanogens conducting reverse methanogenesis in syntrophy with sulfate-reducers oxidizing and maintaining low levels of hydrogen in order to make the reaction thermodynamically feasible. In theory, hydrogen-oxidizing microorganisms could also use electron-acceptors other than sulfate (e.g., NO_3^-, Fe(III), Mn(IV)) to keep hydrogen levels sufficiently low for reverse methanogenesis to be favorable (Hoehler et al., 1994). However, the concept of hydrogen as electron-shuttle during AMO is questioned. Hydrogen in combination with acetic acid (Valentine and Reeburgh, 2000), formate (Sorensen et al., 2001), and transfer of an electron carrier rather than a methane-derived carbon compound (Nauhaus et al., 2002), were proposed as alternatives. Anaerobic methane oxidation coupled to nitrate reduction has been suggested (Bjerg et al., 1995; Chapter 2) and observed to occur at field conditions (Smith et al., 1991), and in a reactor (Costa et al., 2000).

The biogeochemistry and microbial ecology of the Banisveld landfill leachate plume has been studied in the previous chapters 2–5. The pristine aquifer was anaerobic at about 3 m below the water table, but nitrate was present in 1998–1999 (Chapter 2). Degradation of DOC inside the plume was coupled to iron reduction. A very positive δ^{15}N-NO_3^- and an elevated N_2 partial gas pressure indicated occurrence of nitrate reduction above the plume. Some stable isotope analyses of methane indicated that methane degassed from the plume, re-dissolved in pristine groundwater above, and subsequently became oxidized in association with nitrate reduction (Chapter 2). The present study was initiated to study the biogeochemistry of the plume fringe, and in particular the relevance of several possible SRRs at the fringe. For this purpose, the (isotope) hydrochemistry was determined across the fringe, at three distances downstream from the landfill, via sampling multi-level samplers (MLS) placed in a series in order to obtain a vertical sampling interval of only 10 cm. Reactive transport modelling was performed using PHREEQC-2 (Parkhurst and Appelo, 1999) in order to deduce the governing biogeochemical processes. A series of additional simulations were performed to evaluate the relative importance of the various possible SRRs at the fringe of a landfill leachate plume more generally.

6.2 Material, methods and field work

6.2.1 Overview of multi-level-sampler (MLS) systems

A permanent multi-level sampler (MLS) was designed for the present study in order to obtain repeatedly small groundwater samples of flexible volume at small vertical spacing, with a minimum of flushing, with minimal disturbance of the biogeochemistry, and cost-effective. The variety in developed MLS systems is large. Here, an overview is presented. Nested PVC wells set at different depths in a single borehole (e.g. Cozzarelli et al., 2000) has several disadvantages: high costs, limitation to 4 or 5 piezometers per borehole to ensure reliable seals in between each sampling level (Jones et al., 1999), and large vertical spacing. A more cost-effective and reliable method is a low-density polyethylene multiport sock sampler with stainless steel inlet ports for permanent installation in an open borehole after filling the sock with bentonite (Jones et al., 1999). Bladder or gas-drive pumps are used for sampling. However, proper installation in poorly consolidated aquifers may be problematic. Advantage of the sock sampler to commercially available multilevel devices such as the Waterloo^{TM} Multilevel System (Solinst, Canada Ltd., Georgetown, Ontario) and the Westbay MP^{TM} System (Westbay Instruments Ltd., Vancouver, British Columbia) is that the sock samplers seal the entire length of the borehole.

The diffusion multi-layer sampler (DMLS^{TM}) is a series of closely spaced dialysis cells and placed in fully screened wells (Puls and Paul, 1997). However, for the present study the flexibility to purge screens is more attractive to obtain a sample volume up to three liters to enable analysis of some isotopes. Furthermore, the disadvantage of plastics is that it sorbs organic micro pollutants. Another set-up is installation of a PVC casing in a borehole with tubing at the inside and screens at the outside (Delin and Landon, 1996; Pickens et al., 1978). Polypropylene (3 mm) or stainless steel (6 mm) was used as tubing material, respectively. Stainless steel screens or glass wool, wrapped with a fibreglass cloth, was used as a screen (Pickens et al., 1978).

Installation of a MLS without expensive and disturbing drilling of boreholes is attractive. A drive-point profiler allows collection of samples from multiple points in a single drive at discrete zones (Bjerg et al., 1995; Pitkin et al., 1999), but is not a permanent monitoring system and drilling disturbs hydrogen concentrations. Dean et al. (1999) installed polyethylene tubing connected to a stainless steel screen individually to various depths in a sample array by driving probe rods into the ground using an electric hammer an retrieving them using a manual jack. Jakobsen et al. (1998) installed a MLS in the same way, but used bundles of seven 4-mm Teflon tubes wrapped around a solid PVC core, and perforated at the end to form 5-cm long screens. None of these studies used a screen spacing less than 0.5 m for obtaining hydrochemistry depth profiles.

Studies used screens made of various materials. Borosilicate glass was found to show distinctly lower sorption of metals (Koch and Grupe, 1993) and DOC (Wessel-Bothe et al., 2000) with respect to conventional ceramic cups. Nylon membranes showed low adsorption of metals (Wenzel et al., 1997), but we could not find ad-

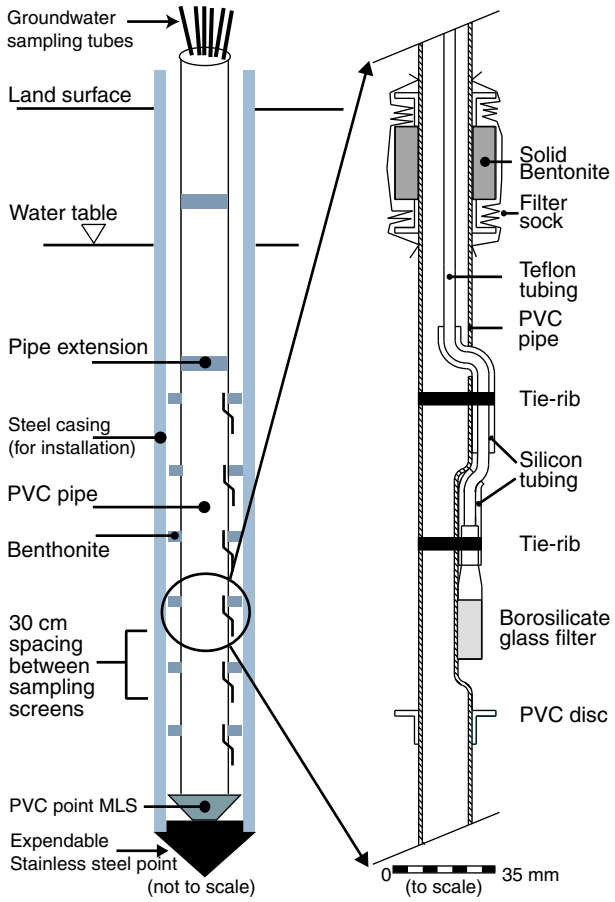

Figure 6.1: Schematic diagram of the multi-level-sampler (MLS).

sorption characteristics with respect to DOC. Stainless steel filters are often used, but (slow) corrosive reactions by e.g. H_2S or Cl^- will disturb local redox chemistry, incl. H_2 concentrations. Steady-state hydrogen gas concentrations are reached faster using plastics such as Teflon or PVC than using stainless steel casing (Bjerg et al., 1997), while iron or steel casings produce H_2 (Chapelle et al., 1997).

6.2.2 MLS designed for the present study

Figure 6.1 shows the MLS constructed for the present study. Teflon sampling tubing (inner diameter (ID) is 2 mm, outer diameter (OD) is 4 mm) and porous borosilicate glass filters (pore size is 100–160 μm, screen length is 2 cm, O.D. is 8 mm, manufacturer is Schott) were chosen to minimize alteration of hydrogeochemical conditions. Sounding was preferred above drilling the MLS into the ground as disturbance and costs are less and installation is easier. The cone resistance of this aquifer limited the maximum diameter of the probe rods and, consequently, the

diameter of the MLS system to about 36 mm. A maximum of six screens were attached using tie-ribs at a 30 cm vertical spacing interval in an indentation made at the outside of a 2 m length PVC pipe (I.D. is 16.5 mm, O.D. is 19 mm). Silicon tubing was used to seal the holes connecting the inner tubing with the outer sampling screens. In order to prohibit short-circuit flow, screens were separated by 2.5 cm thick solid cylinders (O.D. is 35 mm) of bentonite (Eijkelkamp, Giesbeek, the Netherlands), wrapped in polypropylene filter sock (Eijkelkamp, Giesbeek, the Netherlands) and confined by PVC discs (O.D. is 36 mm). PVC glue (Bizon International, Goes, the Netherlands) was used to connect all parts of the system. The MLS was extended in the field using PVC pipes of 1–2 m length and 5 cm long PVC connectors.

6.2.3 Installation of the MLS

Three locations (M1, M2, M3) were selected in the flow direction at 18, 39 and 58 m from the landfill border (well W2) along an existing research transect (Fig. 6.2). Cone penetration tests (CPTs) including measurement of aquifer formation conductivity provided the depth of the plume fringe (Chapter 2). In advance of placing the MLSs, additional CPTs were performed to verify the current depth of the fringe. MLSs were installed in January 2001.

Steel pipes (I.D./O.D. are 39/55 mm) with a stainless steel expendable point in front were pushed hydraulically to the target depth using the weight of a sounding truck. Next, the empty casing was flushed from the bottom with nitrogen gas to remove oxygen (checked with an oxygen electrode), before putting the MLS in the casing. Additional PVC extension pipe was glued to the MLS using PVC glue, connectors, and tape. After finishing the MLS construction, water was added to the casing (under a continuous flow of nitrogen gas) in order to prohibit inflow of aquifer material while the casing was retrieved. The water was a solution of 1.0 mM $CaCl_2$, 1.0 mM $NaHCO_3$ and 0.25 mM KBr with pH = 7.9, and was made anaerobic by flushing it with nitrogen gas just before adding it to the casing.

A cluster of 4 MLSs was installed at each location (coded from deep to shallow: A, B, C, and D) within a horizontal distance of 0.5 m from each other (Fig. 6.2). MLSs, having 30 cm vertical spacing intervals, were placed with a depth difference of 10 or 15 cm in order to obtain a vertical sample depth spacing of 10 cm around the plume fringe at location M1 and M3 by forming a group of three MLSs (A-C), and 15 cm at location M2 by pairing two MLSs. A single MLS (D) was placed in pristine groundwater above the group of three at locations M1 and M3, while in total two MLS pairs were placed one above each other (A with B below and C with D above) at location M2, as cone penetration tests indicated a thick fringe there. Screens were placed between about 2-5 m below surface (surface is at 9 m above mean sea level (msl)). Excavation of soil for nature development in the area, taking place end of 1999–2000, lowered the surface with 0.3 m at M1 and 0.8 m at M2 and M3. From here on, depths will be given with respect to the original surface elevation of 9 m msl.

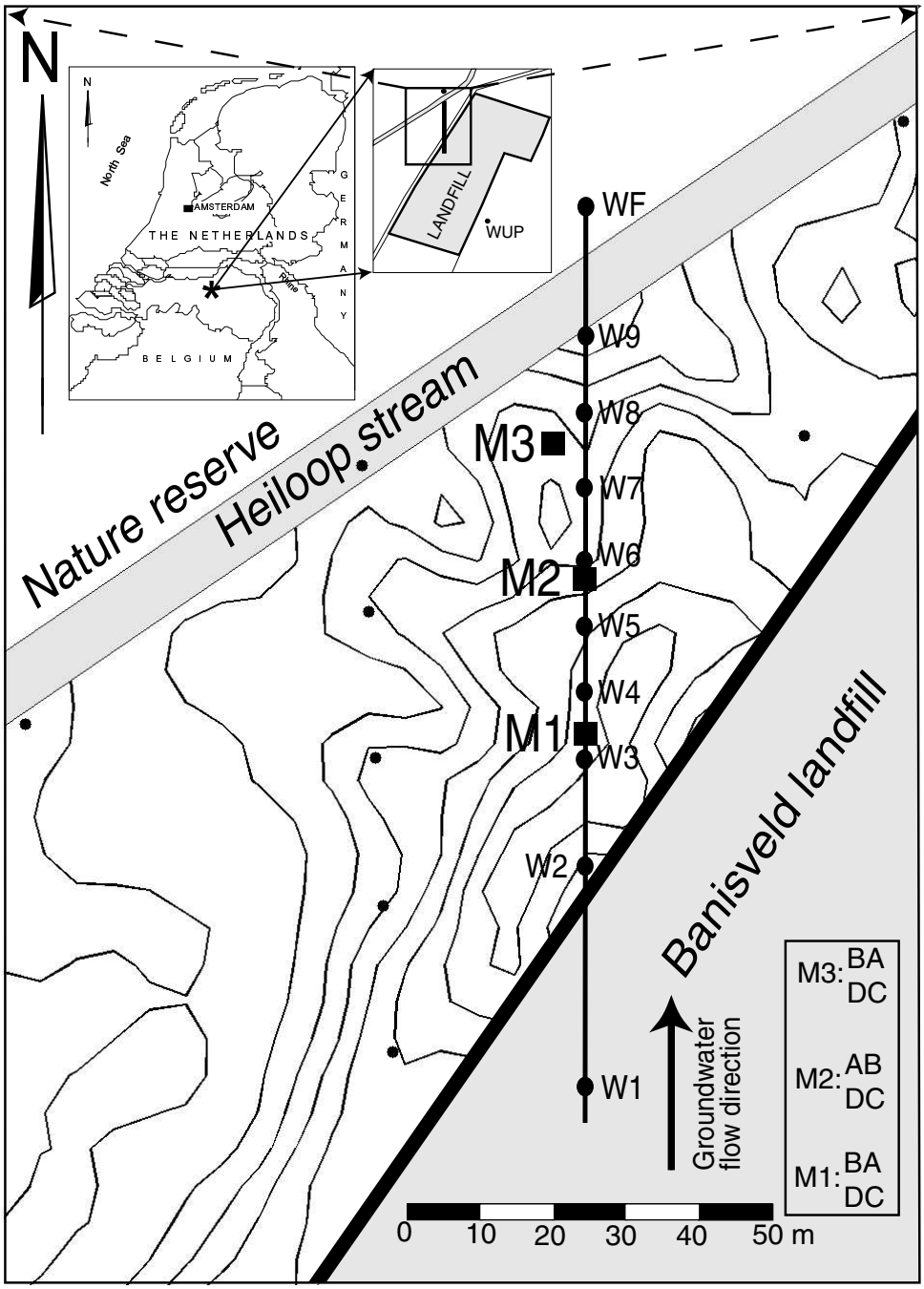

Figure 6.2: Position of locations M1-M3 with respect to research transect downstream of Banisveld landfill. Orientation of MLSs (A-D) at each location is indicated.

6.2.4 Groundwater sampling and analysis

All filters were sampled for a complete analysis of the hydrochemistry nine months later in October 2001. A selection of filters was sampled once more for both hydrochemistry and stable isotope analysis in February (M1) and March 2002 (M2, M3). Samples were taken using a peristaltic pump, and the amount of water sampled was minimized in order to obtain a sample representative for a small vertical aquifer section. Only 15–50 ml of water was needed to pump in order to flush the sampling tubing three times. Electrical conductivity (GMH 3410, Greisinger electronic, Germany), O_2 (DO-166FT, Lazar Research Laboratories, Inc., LA, USA) and pH (Model 1001, Sentron, Roden, the Netherlands) were measured by electrodes placed in flow cells (Lazar Research Laboratories, Inc., LA, USA). Sampling, conservation and analysis of alkalinity, Cl^-, NO_3^-, NO_2^-, SO_4^{2-}, Na^+, K^+, Mg^{2+}, Ca^{2+}, Fe(II), Mn(II), NH_4^+, PO_4^{3-}, CH_4, and DOC was performed, and described in Chapter 2. In addition, Br^-, Si, and Al were measured using ion chromatography (Br^-) and inductively coupled plasma-atomic emission spectrometry (Si, Al). Five-ml Venoject blood sample vials (3.0 ml groundwater, in duplicate) were used for methane analysis in 2001, while 10 ml vials (7.0 ml groundwater, in duplicate) were used during sampling in 2002.

Samples were taken for measuring the following stable isotopes: δ^2H-H_2O, δ^{18}O-H_2O and δ^{13}C-DIC (dissolved organic carbon) at the Centre for Isotope Research (CIO, University of Groningen, the Netherlands), and δ^{13}C-CH_4 and δ^{34}S-SO_4^{2-} at the Environmental Isotope Laboratory (University of Waterloo, Canada).

Ten-ml polyethylene (PE) bottles were filled for δ^2H-H_2O and δ^{18}O-H_2O analysis. For δ^{13}C-DIC analysis, 3 ml 2M NaOH CO_3-free (Fisher Chemicals) was added in a glovebox with nitrogen atmosphere to 60 ml glass vials in order to transform all dissolved CO_2 in groundwater to bicarbonate/carbonate at pH > 10. Three drops of a I_2-KI solution (1.5 g I_2 and 3 g KI to 100 ml aqua dest.) were added to inhibit further microbial activity. Vials were capped with butyl rubber stoppers, which are resistant to NaOH and prohibit gas diffusion. Afterwards, vials were evacuated outside the glovebox. Groundwater was pumped in 60 ml PE syringes and subsequently injected in the evacuated glass vials in the field.

Samples for δ^{13}C-CH_4 were taken in 150 ml glass vials capped with airtight stoppers. Eight drops of the I_2-KI solution were added before capping. Next, vials were flushed three times with helium gas and subsequently evacuated. Three aliquots of ca. 50 ml groundwater were injected in the evacuated vials using a PE syringe. High-density polyethylene (HDPE) bottles (1l) were filled with tubing at the bottom for stable isotope analysis of sulfate. Samples were conserved by adding in advance 50 mg zinc acetate.

6.3 Results

6.3.1 Mixing between leachate and pristine groundwater

Leachate showed higher concentrations than pristine groundwater (present at location M1 between 1.9-3.1 m below surface) for the following compounds: Cl^-,

Br^-, alkalinity, Na^+, K^+, Mg^{2+}, Ca^{2+}, Fe(II), Mn(II), NH_4^+, and CH_4 (Figs. 6.3 and 6.4). Pristine groundwater showed higher concentrations for SO_4^{2-}, Si and Al (results not shown for Si and Al). Its pH is slightly acidic, while leachate pH is around 6.4. Leachate is supersaturated for siderite, in equilibrium with calcite at M1, but undersaturated further downstream (locations M2, M3). Siderite and calcite are not present in the pristine aquifer (Chapter 2). The concentration of PO_4^{3-} was below 0.3 μmol/l in all samples. Hydrochemical results were comparable for both sampling events.

Mixing between leachate and pristine groundwater is determined best using conservative tracers. Chloride is used preferably as conservative tracer in landfill leachate studies (e.g., Christensen et al., 2001), but alternatives exist: deuterium (Cozzarelli et al., 2000), boron (Hofer et al., 1997) and strontium isotopes (Vilomet et al., 2001). Leachate is often enriched in deuterium with 30–60 ‰ (Hackley et al., 1996), which enabled Cozzarelli et al. (2000) to use deuterium as a conservative tracer. However, no deuterium enrichment was observed at the present landfill, which disqualified deuterium as tracer here. Remarkably, most leachate samples were depleted up to -4 ‰ in deuterium with respect to the local meteoric water line (results not shown).

Besides chloride, bromide and fluoride were measured to determine their potential as conservative tracer of landfill leachate. Chloride is not useable in some cases, for example, near landfills where road salts are applied (Bjerg et al., 1995). Chloride and bromide concentrations were an order of magnitude higher in leachate than in pristine groundwater. The correlation between chloride and bromide was high (R^2 = 0.91, n = 71). Fluoride (0–6 μmol/l) was not correlated with Cl^- or Br^-, and consequently disqualified as tracer. The Cl^- to Br^- molar ratio was 362 $\pm$ 13 in leachate, which is about half the seawater Cl^- to Br^- ratio of 639. The Cl^- to Br^- molar ratio could therefore be a useful tracer to discriminate between leachate and (dilute) salt water. The low bromide concentrations measured (1.6–18 μmol/l) and its molar ratio to chloride prove that water used for placement of the MLSs (Br^- = 0.25 mmol/l and Cl^- to Br^- molar ratio of 8) has been flushed away. No correlation between Cl^- and Br^- was observed for pristine groundwater (location M1), where the Cl^- to Br^- ratio differed considerably (160–1900).

Three positions in the hydrochemical depth-profiles (see Figs. 6.3 and 6.4) are of importance for later discussion and defined here: the pristine-end of the fringe (F1, 100 % pristine groundwater), the leachate-end of the fringe (F2, Br^- concentration is 100 % leachate), and the divalent-cation front (F3, concentrations of divalent cations are 100 % leachate). Note that Ca^{2+}, Mg^{2+}, Fe(II) and Mn(II) show a concentration decrease in upward direction. The thickness of the fringe (the distance between F1 and F2) is 0.5 m at M1 and estimated as 1 m at M2, since position F1 is absent there. The fringe is not captured at M3.

6.3.2 Upward movement of leachate plume

A comparison between formation conductivity depth-profiles measured using CPTs in May 1998 and January 2001 (results not shown), and concentration fronts of conservative species (Cl^-, Br^-) measured in October 2001, show that the top of

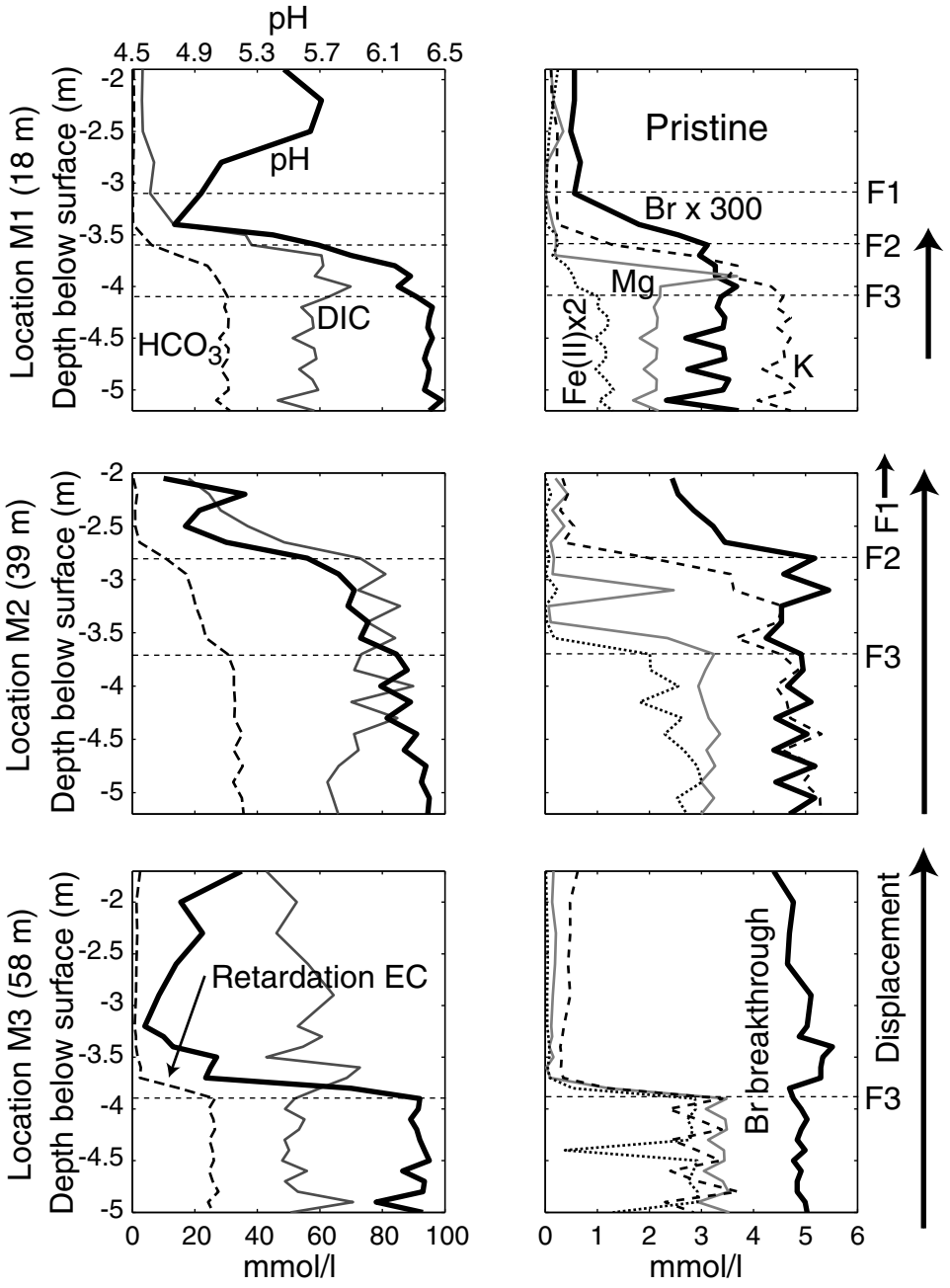

Figure 6.3: Hydrochemical depth-profiles (October 2001) at locations M1-M3. Positions F1-F3 are indicated. Arrows show the total upward displacement of the fringe since 1998. Results for pH, DIC, HCO_3^-, Br^-, K^+, Fe^{2+} and Mg^{2+} are shown.

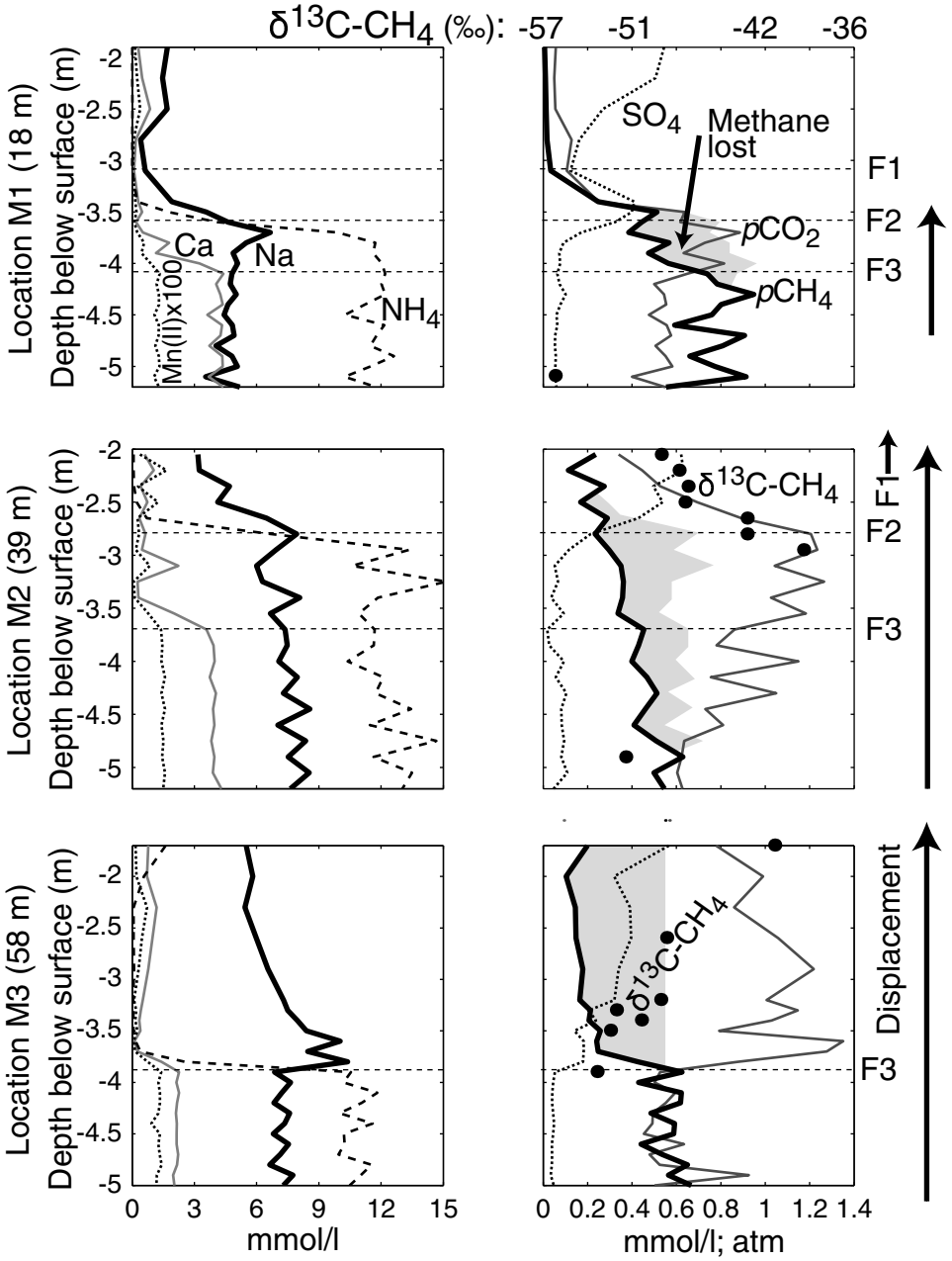

Figure 6.4: Hydrochemical depth-profiles (October 2001) at locations M1-M3. Positions F1-F3 are indicated. Arrows show the total upward displacement of the fringe since 1998. Results for Na^+, Mn^{2+}, Ca^{2+}, NH_4^+, SO_4^{2-}, pCO_2, pCH_4 and δ^{13}C-CH_4 are shown. Shaded area represents the methane lost corrected for dilution. Samples for δ^{13}C-CH_4 were taken in 2002 (methane concentration comparable).

the leachate plume moved progressively in upward direction. The electrical conductivity (EC) front detected using CPTs was present at around 5 m depth in May 1998 (Chapter 2), but about 0.6–1 m less deep in January 2001. Bromide concentrations measured in October 2001 show the plume fringe has risen even more since then (Fig. 6.3). Upward-directed advective transport in combination with geochemical processes retarding the EC (see Section 6.3.4) must have occurred to explain the considerable shift between the bromide and the EC front particularly at M3 (Fig. 6.3; EC not shown but follows bicarbonate front). Its non-conservative behavior makes EC clearly unsuitable as a mixing tracer. Since the transitions in EC were assumed to represent the fringe position, MLSs were installed somewhat too deep. Consequently, the transition to pristine groundwater (position F1) was not captured at M2 and M3. The total upward displacement of the fringe over three years increases from 1.3 m at M1 to 3.3 m at M2 and beyond at M3.

The cause for the rise of the plume is not clear, but might be related to man-made changes in the drainage system in the region, and excavation of nutrient-rich soil (unsaturated zone) for nature development in the research area in the winter of 1999–2000. Removal of soil lowered the surface level near the Heiloop stream to an altitude around or just below the observed seasonally maximum groundwater level, which could promote exfiltration by drainage of groundwater and increased evaporation. The vertical hydraulic pressure gradient, which was monitored between 1998–2001, changed with distance from the landfill: from negative at M1 (downward flow), to about neutral at M2, and positive at M3 (upward flow). It reached a maximum (about 0.06 m/m) at well W9 near the Heiloop stream. The hydraulic pressure gradient at M1 must have changed after February 2001 to explain the occurrence of upward flow. Nevertheless, rise of the plume at M2 and M3 together with its increased fringe level in downstream direction (Fig. 6.3) is in line with observations on hydraulic pressure.

6.3.3 Distribution of redox species and occurrence of redox processes across the fringe

Electron-acceptors

Oxygen was not present in leachate (detection limit estimated at 0.5 mg/l), but a concentration of 0.5–1 mg/l seems present in pristine groundwater at M1 (solubility O_2 in water $\approx$ 11 mg/l at 10 °C). Methane, present in low concentration above the plume (0.2–1 mg/l), could have consumed most of the oxygen. Data were not available to determine if the upper meter of the saturated zone was aerobic. Nitrate was measured up to 1.2 mmol/l (mean $\approx$ 0.5 mmol/1) in observation wells above the leachate plume at about 4 m below surface, during three plume snapshots taken between June 1998 and October 1999 (Chapter 2). However, nitrate was absent in the MLSs up to 2 m below surface in 2001–2002, with the exception of three samples taken in 2001 from the fringe at M2. These samples showed decreasing nitrate concentrations with depth (0.26 down to 0.16 mmol/l, MLS D). So, nitrate had disappeared recently as electron-acceptor, while it was present at an earlier stage; nitrate reduction likely occurred in the period 1998–1999 (Chapter 2).

Alternative electron-acceptors at the fringe could be metal oxides and sulfate. Low Fe(II) concentration and undersaturation for siderite indicate that iron reduction is not important at the fringe and in pristine groundwater above. The logarithm of the Mn(II) to Fe(II) mole ratio in leachate ranges between -2 and -1.6. Remarkably, it increases from the Fe(II) and Mn(II) fronts towards the surface at M2 and M3, while Mn(II) even exceeds the Fe(II) concentration for two fringe samples at M2. This indicates presence of manganese oxide in the upper part of the aquifer and that reductive dissolution probably happens upon inflow of rising leachate.

The sulfate to bromide ratio decreases with depth indicating occurrence of sulfate reduction in pristine groundwater at M1 (Figs. 6.3 and 6.4). The sulfate concentration and its decrease at M1 were less in 2002 than in 2001 (results not shown). Remarkably, sulfate has a peak concentration in the fringe zone at M1. Sulfate seems to mix conservatively in the fringe zone at M2. Bromide shows that leachate is present over the full depth-profile at M3. Oddly, sulfate exceeds typical leachate concentrations and decreases with depth there.

Sulfur isotopes of sulfate were measured to verify occurrence of sulfate reduction. Results were available for M2 and M3. Negative δ^{34}S-SO_4^{2-} values (-0.7 to -1.6 ‰) at M3, and positive but low values (+2.8 to +7.5 ‰) at M2, indicate that the origin of sulfate could be meteoric (-3 to +9 ‰ for anthropogenic sulfate in rainfall (Krouse and Mayer, 2000)). High correlation was observed between δ^{34}S and both the inverse of sulfate concentration and the natural logarithm of the remaining sulfate fraction at M2 (R^2 = 0.96, n = 5). This means that observations might be explained by either contribution of a source (signature: +1.6 ‰) or sulfate reduction ($\epsilon \approx 3.3$ ‰). Oxidation of FeS minerals, a possible source of sulfate, which could have a δ^{34}S signature of +1.6 ‰, can be ruled out, as oxygen and nitrate were absent. Furthermore, sulfate reduction is unlikely to happen at M2 or M3, as the fractionation factor associated with this process is much higher (ϵ = 10–24 ‰ and up (Krouse and Mayer, 2000)). The variation in δ^{34}S is therefore attributed to a small variation in origin. However, the downward decreasing SO_4^{2-} to Br^- ratio indicates that sulfate reduction happens in pristine groundwater at location M1.

Electron-donors

Possible electron-donors susceptible to oxidation at the fringe are divided into three groups: 1) non-sorbing organic solutes (conservative with respect to physical transport): DOC (humic- and fulvic acids) and CH_4, 2) adsorbing (non-conservative) organic contaminants (e.g., benzene), and 3) cation-exchangeable inorganic cations (non-conservative): Fe(II), Mn(II), and NH_4^+. Soluble electron-acceptors such as O_2 and NO_3^- capable of oxidizing these electron-donors mix conservatively with leachate. The concentration of an electron-acceptor admixing from pristine groundwater is per definition 100 % at the pristine end of the conservative tracer front (Figs. 6.3–6.4: F1), and zero at the leachate end of the conservative tracer front (Figs. 6.3–6.4: F2). Consequently, oxidation of Fe(II), Mn(II) and NH_4^+ will be of little importance (even if O_2 and NO_3^- were present in pristine groundwater), because retardation of cations due to cation-exchange leads to separation from the dissolved oxidants (if O_2 and NO_3^- will be present), as will be explained in more detail later.

Dissolved organic carbon (measured for M1 and M3 in 2001) showed high concentrations both for leachate (6.1–10.7 mmol/l) and pristine groundwater (6.7–9.7 mmol/l) at M1 (results not shown). However, low DOC concentrations were measured for two fringe samples at M1 (1.7 and 3.2 mmol/l) suggesting that oxidation of DOC happens at the fringe. High bromide concentrations showed that leachate was present in the complete depth-profile at M3. Five out of the upper eleven samples (above 3.9 m below surface) at M3 showed low DOC concentrations (4.8–5.1 mmol/l), while DOC concentration at larger depth was comparable to the DOC concentration measured at M1. This indicates that DOC became partly degraded after the plume rose at M3. The other organic and non-sorbing (conservative) electron-donor in leachate is methane and is present at high concentration. Processes governing the fate of methane are discussed in Section 6.3.5.

6.3.4 Impact of cation-exchange reactions and proton-buffering

The fronts of cations are clearly separated in space (Figs. 6.3–6.4). After the conservative tracer front (F1-F2), the following cation fronts follow with depth: 1) Na^+, 2) NH_4^+ and K^+ (NH_4^+ slightly before K^+), and 3) Ca^{2+}, Mg^{2+}, Fe^{2+} and Mn^{2+}. Front-spacing is as little as 10 cm at M1. The front spacing is larger at M2, while all cations except sodium are strongly retarded with respect to bromide at M3. These chromatographic patterns proof that advective instead of dispersive transport has occurred (Appelo and Willemsen, 1987), i.e., the leachate plume has risen towards the surface.

The observed chromatographic pattern is particular in the way that the K^+ and NH_4^+ fronts are present closer to the fringe (i.e., are less retarded) than the divalent cation fronts (Ca^{2+}, Mg^{2+}, Fe(II), and Mn(II); see Figs. 6.3–6.4). This order implies that solid organic carbon (SOM) rather than clay minerals control the sorption of cations, because monovalent K^+ and NH_4^+ have a lower affinity than divalent cations for SOM (Chung and Zasoski, 1994), while this is vice versa for clay minerals (Bruggenwert and Kamphorst, 1982). Measurements on clay and SOM content at a depth of 5–7 m, where the plume axis is situated, could not support this. However, the heterogeneity is large with respect to both clay (1.4–7 %) and organic carbon content (0.03–0.26 %; n = 5). Sediments possibly contain a relatively high SOM and low clay content at lower depth, and thereby invoke this specific chromatographic pattern.

The results bring forward occurrence of cation-sorption and proton-buffering on SOM at the fringe zone. Flow of pH-neutral leachate through this slightly acidic aquifer was shown to trigger release of protons from SOM as a result of proton-buffering (Chapter 5). All divalent cations become lowered in concentration from the divalent cation-front (F3; monovalent cations at somewhat higher elevation) towards the leachate end of the fringe (F2), while the pH decreases (proton concentration increases) simultaneously over the interval F3–F2. So, release of protons from SOM in exchange for cations in leachate happens in response to a rise of the leachate plume. In addition, desorption of Al from SOM and subsequent precipitation of Al-hydroxide could happen and would lower the pH and enhance pH retardation.

6.3.5 Fate of methane: degassing and anaerobic methane oxidation

Proton-buffering causes retardation of the pH front. Consequently, pH decreases between F3 and F2, while DIC behaves conservatively and remains constant until it dilutes due to mixing with pristine groundwater between F2 and F1 (Fig. 6.3). This pH change results in a decrease of bicarbonate and an associated increase in dissolved carbon dioxide and partial CO_2 pressure. The pH decrease and pCO_2 increase at location M2 set in from the bottom of the profile in upward direction, indicating that proton-buffering also occurs below F3 at M2. Remarkably, pCH_4 decreases, while pCO_2 increases. The CH_4 partial pressure was calculated for the situation that only conservative mixing would happen, where mixing is calculated from Br^- concentrations. The area is indicated where observed pCH_4 is below the partial methane pressure according to conservative mixing (Fig. 6.4). Apparently, degassing of methane compensates for an increase in total gas pressure, caused by an increase in partial CO_2 pressure as a consequence of proton-buffering. Redissolution of methane in pristine groundwater, escaped from leachate as result of a rising plume, followed by oxidation, could be an explanation for the absence of oxygen and nitrate.

Carbon-13 isotopes of methane were measured to determine if oxidation of methane occurred at the plume fringe. Previous measurements in 1999 showed that δ^{13}C-CH_4 ranged between -54.4 to -52.7 ‰ (n = 9) along the plume axis (6–8 m below surface), while a value of -50.3 ‰ (n = 1) was observed for pristine, methane-containing groundwater (CH_4 = 0.3 mmol/l, Cl^- = 0.8 mmol/l) above the plume (Chapter 2). Current measurements showed most negative values at the bottom of the MLS profiles, while lower methane concentrations and enriched δ^{13}C-CH_4 values up to -39 ‰ were observed closer to the surface (Fig. 6.4). Recently, Grossman et al. (2002) observed a correlation between decreasing methane concentrations and increasing δ^{13}C-CH_4 values downstream in the Norman landfill leachate plume, and attributed this to anaerobic methane oxidation (AMO), presumably coupled to sulfate reduction. Such a correlation is also found at location M3 (R^2 = 0.66), but absent at location M2 (Fig. 6.4). The calculated enrichment factor of -9.7 ± 3.1 ‰ for location M3, was somewhat lower than observed at the Norman site (about -13 ‰), but indicative for (anaerobic) methane oxidation (Bergamaschi, 1997; Grossman et al., 2002). Carbon-13 of DIC was not useful to verify occurrence of methane oxidation as the DIC concentration was much higher than the potential concentration of oxidized methane. Depleted δ^{13}C-DIC values indicative of methane oxidation, were neither observed in pristine groundwater at M1 (around -21 ‰, n = 2).

The fractionation factor for diffusion of methane through the water-air interface, which seems to apply for degassing, is much lower ($\epsilon \approx 1$ ‰) than for methane oxidation (Bergamaschi, 1997). Consequently, degassing alone cannot explain the observed upward δ^{13}C-CH_4 enrichment, and therefore degassing seems to happen in combination with AMO.

6.4 Reactive transport modelling of the rising plume fringe

6.4.1 Model set-up and calibration

A reactive transport model was constructed in PHREEQC (Parkhurst and Appelo, 1999) to simulate the hydrochemistry of the plume fringe at location M1, in order to verify quantitatively if proton-buffering and degassing triggered by a rising plume determine the hydrochemical patterns across the fringe. Cone penetration tests from June 1998 (assuming the conductivity front to coincide with the bromide front) and bromide data from October 2001 (Fig. 6.3) show that the fringe has risen to the surface across a vertical distance of 1.3 m in this period at M1. The model made consisted of 100 cells each having a length of 0.05 m. Leachate was present in the lower forty cells, pristine groundwater in the upper sixty cells. Advective upward transport of leachate, displacing pristine groundwater, was simulated across the observed vertical distance of 1.3 m (26 shifts). A dispersivity of 0.005 m was determined from a best fit for bromide.

The leachate and pristine groundwater composition were assumed constant. For leachate, the average observed concentration was taken between 3.8–4.9 meters below surface (n = 9; excluding screens at 4.2, 4.4, 4.8 m below surface for all species except methane). The model composition for pristine groundwater (pH, Na^+, K^+, Ca^{2+}, Mg^{2+}, NH_4^+) was optimized (see later) within the concentration range as observed for screens between 1.6 to 2.8 m below surface (n = 5). The average of observed concentrations was taken for alkalinity, Cl^-, and Br^-. Pristine concentrations for Fe^{2+} and Mn^{2+} were allowed to optimize below the observed minimum for pristine groundwater in order to improve the fit of the model. A temperature of 11 °C and a pe of -1.6 were taken for both leachate and pristine groundwater.

The proton-buffer (Y_{tot}) and the cation exchange capacity (CEC) were optimized between zero and maximum values, which were estimated from soil organic carbon and clay content measurements in the aquifer, respectively (Chapter 2), following Appelo et al. (1998). Exchange coefficients for cations on CEC were equal to those used in the reactive transport model of the central flow path in this plume (Chapter 5). Exchange coefficients for cations on the proton-buffer (Y_{tot}) were taken from the previous study as well, but were allowed to change during optimization to values 1 log unit lower than the CEC exchange coefficients.

The model was calibrated using the non-linear optimization program PEST (Watermark Computing: http://www.sspa.com/pest). Observations between 3.1–3.7 m below surface (n = 7) for pH, alkalinity, Na^+, K^+, Ca^{2+}, Mg^{2+}, NH_4^+, Fe^{2+}, Mn^{2+}, and Br^- were used to constrain the model. The reciprocal of observed values was taken as weight factor. Weights for alkalinity and ammonium at 2.8 m below surface were set to zero, because of the large discrepancy between the model and observations. Weight for pH was multiplied with a factor 10.

Degassing was simulated as described in Chapter 5. Degassing of CH_4, CO_2, and N_2 was modelled. A partial N_2 pressure of 0.8 atm was adopted for pristine

groundwater, while for leachate the average observed pN_2 of 0.34 atm (Chapter 2) was taken. For each cell a specific hydrostatic pressure was imposed, calculated using the minimum observed water table level (1.3 m below surface) in the period 1998–2001 (12 measurements) at M1. The total gas pressure exceeded the hydrostatic pressure up to some tenths of an atmosphere in the present plume (Chapter 2). Therefore, bubble formation and subsequent degassing from the groundwater to the atmosphere was only allowed if the sum of the CH_4, CO_2, and N_2 partial gas pressures exceeded the sum of the hydrostatic pressure and an adopted threshold pressure of 0.32 atm at a particular depth.

6.4.2 Model results

Results of the modelling are presented in Fig. 6.5. The model reproduces observations well. Note that the model did not aim to capture the pH variation in pristine groundwater. A realistic value was optimized for the proton-buffer, while the cation exchange capacity (CEC) was required to be very low (Table 6.1). This is explained by geochemical heterogeneity of the aquifer (see before). A larger CEC to proton-buffer ratio gives an overall higher selectivity for K^+ and NH_4^+ and could therefore not reproduce the chromatographic pattern at the site. Precipitation and dissolution of Al-hydroxide could have an additional impact on the buffering of protons, but was not included in the model. Test simulations produced a non-observed Al peak at the fringe, as a result of desorption of Al from SOM (result not shown). Absence of this Al peak indicates that Al desorption and subsequent precipitation of amorphous Al-hydroxide, are not significant. The neglect of Al yields more proton-buffering, because the occupancy of SOM with H^+ becomes higher at lower pH.

Table 6.1: Optimized model parameters and measured values (minimum, mean, maximum)

Pristine groundwater (mmol/l, M1: 1.9 to 3.1 m below surface, n = 5)									
	pH	HCO_3^-	Ca^{2+}	Mg^{2+}	Na^+	K^+	NH_4^+	Fe^{2+}	Mn^{2+}
minimum	4.94	0.18	0.09	0.005	0.41	0.11	0.005	0.009	$3x10^{-4}$
mean	5.37	0.38	0.38	0.13	1.18	0.18	0.007	0.054	0.017
maximum	5.71	0.55	0.86	0.34	1.7	0.24	0.011	0.12	0.004
optimum	5.48		0.09	0.06	1.47	0.15	0.011	0.002	$8x10^{-5}$
	Sediment[a]		*Exchange coefficients on proton-buffer*[b]						
	CEC	Y_{tot}	CaY_2	MgY_2	NaY	KY	NH_4Y	FeY_2	MnY_2
minimum	9	1.6	−0.20	−0.40				−0.40	−0.40
mean, initial	23	4.7	0.10	−0.20	−1.00	−0.75	−0.75	−0.20	−0.20
maximum	42	12.3				−0.30	−0.40		
optimum	0.2	8.3	−0.20	−0.40		−0.57	−0.75	−0.20	−0.20
	Model set-up								
	Cells	Cell-length		Shifts	Diffusion coefficient			Dispersivity	
	100	0.05 m		26	0.3 x 10^{-9} m/s^2			0.005 m	

[a] *Contents for the cation exchange capacity (CEC) and the proton-buffer (Y_{tot}) are given in meq/kg soil. Conversion to meq/l was done for the model by multiplying with 6.2 (using a porosity of 0.3 and the specific weight of quartz (2.65 g/cm^3)).*

[b] *Values are expressed as log(K) for $I^{i+} + iY^- = IY_i$.*

The minimal measured Ca^{2+}, Mg^{2+}, Fe^{2+} and Mn^{2+} concentrations, and the maximal measured Na^{+} and NH_4^{+} concentrations were optimums found for pristine groundwater. The best model fits for in particular Fe^{2+} and Mn^{2+} were attained if the selectivity of Ca^{2+} and Mg^{2+} for the proton-buffer was reduced, while the Fe^{2+} and Mn^{2+} concentration for pristine groundwater was taken below the observed minimum (Table 6.1). Decreasing the potassium selectivity for the proton-buffer resulted in a slightly better fit too. The model mimicked observations still satisfactorily, when standard values for selectivity coefficients and the minimum observed pristine Fe^{2+} and Mn^{2+} concentrations were adopted. Only the Fe^{2+} and Mn^{2+} fronts were then not captured well, and small peaks were simulated (results not shown).

Identical chromatographic patterns were observed at locations M2 and M3 (Figs. 6.3–6.4). The proton-buffering zone (the distance between F3 and F1) doubled at M2 (estimated as 2.5 m) with respect to M1 ($\approx$ 1.0 m), and is explained by the double vertical distance ($\approx$ 3.3 m at M2 versus $\approx$ 1.3 m at M1) across which the plume rose at that location. The proton-buffering zone was largest at M3 and extended from front F3 to beyond the top of the MLS profile. Cation concentrations except for sodium changed dramatically within a 20-cm vertical distance at 3.8 m below surface. Apparently, a thin layer must be present there with a high exchange capacity, prohibiting breakthrough of pH and all cations except sodium, which has the lowest affinity for exchange sites (Table 6.1).

The simulated methane concentration overshoots observations at the proton-buffering zone when degassing is not included in the model (Fig. 6.5: dashed line). The model predicts methane observations better at this zone, when simulation of degassing is included (Fig. 6.5: solid line). Proton-buffering causes a pH decrease, which results in a peak of the pCO_2 pressure at 3.5 to 4 m below surface. The total gas pressure exceeds the sum of the hydrostatic and threshold pressure then (Fig. 6.5: dashed line), and gas bubbles will form, which escape towards the atmosphere. The model reproduces the increase in pCO_2 compensated by a decrease in pCH_4 as observed in the field quite well (Fig. 6.4). The observed methane loss seems somewhat larger than simulated. This could be due to uncertainty in the threshold pressure or AMO not included in the model.

6.4.3 General model for secondary redox reactions at the fringe of a landfill leachate plume

A series of additional 1D PHREEQC simulations were performed to evaluate the potential of Fe(II), Mn(II), NH_4^{+} and CH_4 oxidation at the top fringe of landfill leachate plumes in general. Oxidation can occur if the front of an electron-donor overlaps with the opposite-oriented front of a soluble electron-acceptor admixing from pristine groundwater (i.e., the electron-donor is in physical contact with the electron-acceptor). The control of aquifer geochemistry (CEC, proton-buffering) on the potential for occurrence of secondary redox reactions was addressed. Furthermore, effects of both a stationary fringe and a transient fringe (seasonally upward and downward moving) were evaluated. In the case of a stationary fringe only diffusion was simulated in order to mimic transversal dispersion.

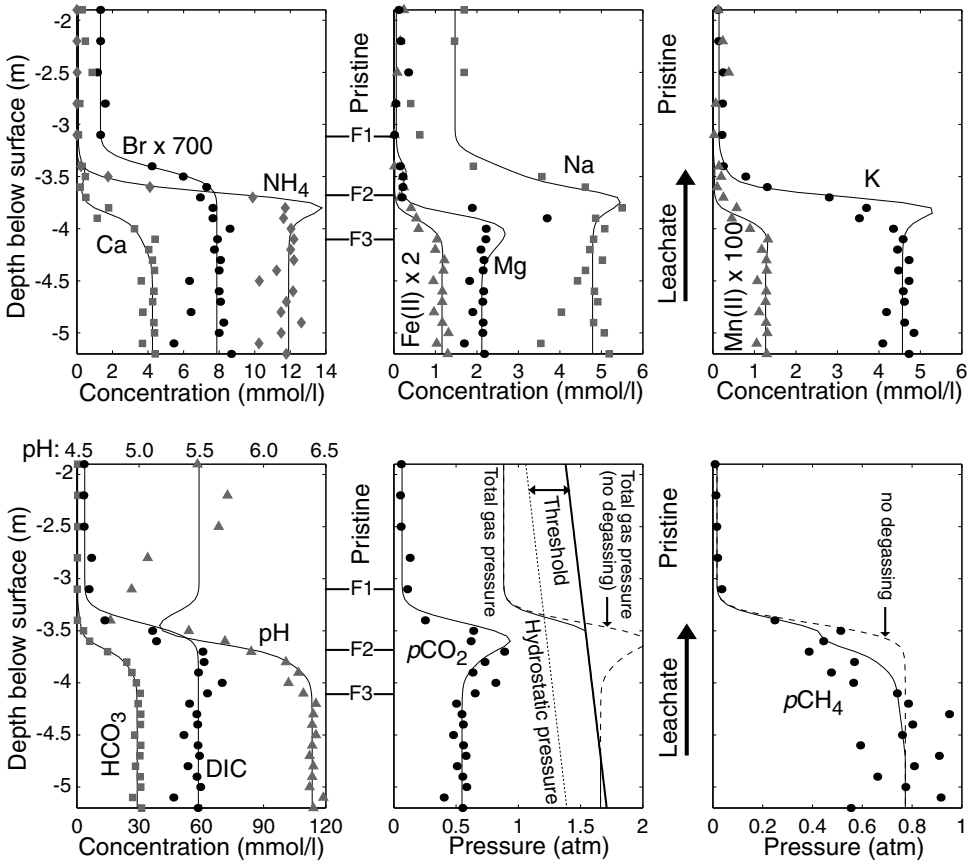

Figure 6.5: Results of reactive transport model of plume fringe at location M1. Dashed lines show partial methane pressure and total gas pressure for simulations without degassing.

Simulations (results not presented) showed that methane has best contact with electron-acceptors in pristine groundwater, and is consequently most reactive at the top fringe of a plume, in particular when a plume moves (seasonally) upwards like observed in the present study. In that case cation-exchange reactions involving NH_4^+, Fe(II) and Mn(II) result in a spatial separation with available dissolved electron-acceptors outside the plume, where the extent of separation depends on CEC and impact of proton-buffering (i.e., SOM content and pH difference across fringe). This situation is comparable to the downstream edge (front) of a plume where advective transport moves the plume downstream. In contrast, sorption-induced retardation could result in contact of NH_4^+, Fe(II) and Mn(II) with conservative electron-acceptors, if a plume moves (seasonally) downwards with sufficient amplitude. Ammonium will then be most susceptible to oxidation as it sorbs better than Fe(II) or Mn(II). Fe(II) or Mn(II) will only be the electron-donors in best contact with oxidants if the CEC is limited and the proton-buffer, preferentially sorbing Fe(II) and Mn(II) over NH_4^+, is large. Contact for all these electron-donors with dis-

solved electron-acceptors in pristine groundwater is good, but decreases slightly in the order: CH_4, NH_4^+, Fe(II) or Mn(II), for both a transient (top/bottom) fringe at average elevation and a transversal dispersion controlled stationary fringe.

6.5 Discussion and conclusion

The present study shows that NA at the fringe of this landfill leachate plume was limited, while 40 % of DOC degraded along the plume axis (Chapter 2). Limited reactivity was primarily due to absence of oxygen and nitrate in pristine groundwater. This finding contrasts with a study on NA of a plume with phenolic compounds, where redox reactions at the fringe were primarily responsible for degradation (Mayer et al., 2001). There, toxic contaminant levels probably impeded degradation in the core, while dilution and presence of O_2 and NO_3^- in pristine groundwater resulted in degradation at the fringe. Detailed vertical sampling on 0.1 m scale was necessary to capture the hydrochemical gradients across the plume fringe, which is typically tenths of meters to a few meters thick. The limited length of the plume restricted the thickness of the fringe and consequently the contribution of the fringe to total NA as well. However, the fringe dimension seems comparable to other plumes described in literature considering its short plume length (e.g., Brun et al., 2002; Frind and Hokkanen, 1987; Mayer et al., 2001).

Summarizing, the plume rose to the surface over a vertical distance of 1 to beyond 3 meters in the course of three years. This might be related to excavation of a large part of the unsaturated zone above the plume. Rising of the plume triggered proton-buffering including cation sorption, and induced degassing of methane. Sorption reactions resulted in spatial separation of NH_4^+ and in particular Fe(II) and Mn(II) from potential electron-acceptors outside the plume. Consequently, methane oxidation is in potential the most important secondary redox process at the site, and competes with primary DOC oxidation for available oxidants. Furthermore, methane can disperse further into pristine groundwater than conservative DOC, because of its volatility. This study shows that degassing of methane happens and could result in subsequent re-dissolution in above-flowing pristine groundwater, and thereby increases the importance of methane oxidation as a process scavenging available electron-acceptors. Methane concentrations between 0.2–1 mg/l in pristine groundwater, decreasing towards the surface, indicate that this occurs, while oxidation of the methane is an explanation for the absence of previously observed nitrate. Degassing may also lead to entrapment of gas bubbles in the aquifer, resulting in presence of a stationary gas phase. This reduces the hydraulic permeability at the fringe and, hence, transversal mixing or further migration of the plume towards the surface.

Cation-exchange reactions were not incorporated in a model study by Hunter et al. (1998) who addressed the importance of secondary redox reactions at the downstream front of a hypothetical landfill leachate plume. Oxidation of methane, Fe(II) and Mn(II) was included but oxidation of ammonium was not considered. Anaerobic methane oxidation was allowed to happen with sulfate but neither with NO_3^- nor iron-oxide as electron-acceptor. Oxidation of metal species and methane con-

sumed a comparable quantity of oxidants at the fringe. However, Griffioen (1999) argued that ignoring cation-exchange reactions overestimated the importance of Fe(II) and also Mn(II) oxidation at the front of the plume. Cation-exchange reactions result in separation of Fe(II) and Mn(II) from oxidants especially when transport is advection instead of dispersion controlled. Results of the present study show that this indeed occurs, and is the case for ammonium as well. Note that the type of cation-exchanger present determines the extent of retardation of NH_4^+ versus Fe(II) and Mn(II), where illite-type of clay minerals yield high retardation for NH_4^+, while SOM yields high retardation factors for divalent and trivalent metals (together with H^+).

Re-oxidation of dissolved Fe(II) at the outskirts of a plume was proposed by Christensen et al. (2001) and Heron (1994) as an important secondary redox process leading to regeneration of the aquifer oxidation capacity (OXC). This statement seems in contradiction with the theoretical considerations pointed out by Griffioen (1999). Furthermore, even if this process happens, it is in essential OXC-neutral. It would indeed regenerate the contribution of Fe(III)-oxide to the OXC, but at the expense of oxygen. This must be regarded unfavorable for the degradation of aromatic hydrocarbons, which degrade better under aerobic conditions. The idea for this process was speculated on a few outliers of high Fe(III)-oxide content (about triple background content) at the outskirts of the Vejen landfill leachate plume in the study of Heron and Christensen (1995). However, most measurements were not higher than background. The authors noted that these data could not reveal whether increased iron oxide content was due to re-precipitation of mobilized Fe(II) or sediment heterogeneity. A reactive transport model of the Vejen landfill leachate plume incorporating cation-exchange did not predict re-precipitation of dissolved Fe(II) at the downstream plume front (Brun et al., 2002).

Reductive dissolution of manganese-oxide by Fe(II) within the plume is another mechanism which prohibits re-oxidation of Fe(II) at the fringe, and is observed at the Grindsted landfill (Bjerg et al., 1995). The redox chemistry at the fringe of that plume was exclusively determined by secondary redox reactions, since DOC was completely degraded within the plume. Indications for ammonium and methane oxidation at the plume fringe were found. The observation that the methane front was enclosed by the ammonium front, suggests that oxidation of methane was preferred. Manganese concentration was elevated with respect to background in the plume including the fringe. This points out that Mn-oxide can be regarded as a fringe-oxidant next to O_2 and NO_3^-. Elevated Mn^{2+} to Fe^{2+} ratio at the fringe of the present site supports this. In conclusion, current evidence and theory shows that the process of re-oxidation of Fe(II) at the fringe of a landfill leachate plume is less significant than hypothesized by Heron (1994). However, the process could be general for hydrocarbon pollution plumes, which lack ammonium, contain usually less or no methane, and where DOC (hydrocarbons) is not conservative and retards likely more than the Fe(II) formed by iron reduction. Transient flow conditions promote occurrence of this process, especially when Fe(II) is the only available electron-donor (see Section 6.4.3).

Occurrence of anaerobic methane oxidation (AMO) inside a leachate plume would lessen the relevance of methane oxidation at the fringe (Griffioen, 1999).

Anaerobic methane oxidation coupled to sulfate reduction has been observed in marine environments (Valentine and Reeburgh, 2000), but could thermodynamically be coupled to reduction of iron oxide as well (Hoehler et al., 1994). Stable isotope analysis (SIA) of methane indicated occurrence of AMO presumably coupled to sulfate reduction inside and at the fringe of a landfill leachate plume (Grossman et al., 2002). However, the conditions for AMO seem puzzling, as the only available oxidant, sulfate, was present in very low concentration. In contrast, methane stable isotope analysis indicated absence of AMO inside the present landfill leachate plume having a higher availability of electron-acceptors (Chapter 2), and inside a hydrocarbon plume (Revesz et al., 1995). Degassing attenuated methane slightly in downstream direction in the present plume (Chapter 5). Degassing may allow methane oxidation from the top fringe upward to become relevant, where methane likely re-dissolves from gas bubbles migrating towards the surface.

The relevance of AMO or not is illustrated as follows. A typical landfill leachate methane concentration of 1 mmol/l is capable of consuming 0.35 mmol/l O_2 (groundwater in equilibrium with atmosphere at 10 °C) together with a considerable nitrate concentration of 1.3 mmol/l. The Fe(II) concentration should be much higher (8 mmol/l) than generally observed for leachate (up to 1–3 mmol/l) to have a reduction potential equal to methane. Methane oxidation can be the most important redox process at the fringe of a leachate plume, if AMO inside the plume not considerably attenuates methane, sorption-reactions retard dissolved metals/ammonium, and depth-fluctuation of the fringe is small. Then, methane can consume all available oxygen and nitrate in pristine groundwater, and thereby reduces NA at the fringe for other solutes to dilution only.

Chapter 7

SYNTHESIS

In the final chapter of this thesis first a summary and conclusions will be given of the performed research with special emphasis on the relations between the microbiology and the hydrogeochemistry. The implications for natural attenuation at the present site will be evaluated in a subsequent section. The next two sections discuss the development of redox conditions in landfill leachate plumes, and the availability of Fe(III) for iron reduction. Subsequently, the perspectives of molecular microbial ecology research for MNA are discussed. Future research directions to NA of landfill leachate are presented in Section 7.6. Technical and policy issues in MNA of landfill leachate pollution are addressed in the final section.

7.1 Biogeochemistry and microbial ecology of the Banisveld landfill leachate plume: summary and conclusions

7.1.1 Determination of redox conditions in the aquifer

Redox conditions were determined using several methods: distribution of gaseous, soluble and solid redox species, hydrogen gas measurements, and stable isotopes (Chapter 2). Hydrogen gas concentrations, supersaturation for siderite and geochemical modelling (see later) showed that degradation of dissolved organic carbon inside the plume was coupled to reductive dissolution of iron oxides. This was mirrored in the strong dominance of iron-reducing members of the family *Geobacteraceae* in the plume microbial community (Chapter 4).

No concomitant sulfate reduction or methanogenesis occurred in the plume. High methane concentrations in the plume have not been produced in the aquifer but inside the landfill body, as evidenced by stable isotope analysis of ^{13}C and ^{2}H of methane. Redox conditions are often assigned assuming subjective criteria about concentration ranges of redox-sensitive species (Christensen et al., 2000a). This could easily lead to qualifying the methane-rich zone close to landfills as methanogenic, while actually it could still be iron-reducing, such as is the case for the Banisveld landfill. Stable-isotope analysis of sulfur and oxygen isotopes

in sulfate would be a good method to determine occurrence of sulfate reduction in landfill leachate plumes.

Calculation of in-situ energies of hydrogen-oxidizing redox reactions has proven to be a good method for qualifying redox conditions. However, caution should be taken as the present study shows that it can take more than three months time, before hydrogen concentrations reach steady-state levels, after installation of wells. This time delay is substantially larger than indicated by Bjerg et al. (1997) for the Grindsted landfill. If this remains unnoticed, redox conditions will be erroneously qualified as too reduced and diverse. The non steady-state situation for the first three months after well installation apparently affected results of community-level physiological profiling (CLPP) as well (Chapter 3): substrate richness was generally much higher at that time than one year later. Consequently, differences in CLPP between pristine and polluted samples were initially not evident, but emerged only after a longer time interval.

7.1.2 Modelling the downstream change in leachate composition

Geochemical models were constrained to observations in order to determine quantitatively the full reaction network causing the downstream change in leachate composition. Both inverse geochemical and forward reactive transport modelling were performed using PHREEQC-2 (Parkhurst and Appelo, 1999). A simple inverse geochemical model, constrained to a few hydrochemical parameters from one leachate sample in the source and one downstream at the front of the plume, made plausible which biogeochemical processes occurred inside the plume (Chapter 2). The more sophisticated forward reactive transport model presented in Chapter 5, explained the change in leachate composition for all eight monitoring wells installed along the longitudinal plume axis. The latter type of model enables prediction of plume evolution.

Modelling showed that secondary geochemical processes were required in the model to match the observations in addition to simulation of the primary degradation reaction (DOC degradation coupled to reductive dissolution of Fe-oxides). Secondary reactions were: kinetically controlled precipitation of calcite and siderite, cation-exchange including proton-buffering, and degassing of methane. The present inverse and forward model show that iron reduction cannot be quantitatively solved if the secondary processes of siderite precipitation and cation-exchange are discarded. By contrast, most other models use only dissolved Fe(II) to quantify the process of iron reduction. Underestimation of the extent of reductive dissolution of Fe-oxides is the suspected consequence.

The developed reactive transport model is the first that includes a simulation of the carbon isotope geochemistry in order to verify the biogeochemical reaction network with stable carbon isotope data. Direct quantification of siderite precipitation would be best to constrain iron reduction, but the simulated amounts of precipitated carbonate minerals were too low to measure. However, simulation of the hydrochemistry and carbon isotope geochemistry supported occurrence of this process.

Rate constants for degradation of DOC coupled to iron reduction and carbonate mineral precipitation were obtained, together with the determination of other model parameters using the non-linear optimization program PEST. The empirical rate constant of precipitation of carbonate minerals was low in comparison with other studies, and is probably caused by absence of these minerals in the pristine aquifer (i.e., small or negligible carbonate surface area), inhibitory effects of fulvic acids, and the low temperature compared to other studies. The observed downstream decrease in methane concentration is explained by degassing triggered by elevated CO_2 pressures, caused by carbonate precipitation and proton-buffering at the front of the plume. Gas exsolution is presumably an important NA process, but has been little addressed so far. Finally, implicit simulation of a growing population of (iron-reducing) microorganisms, which has been included in other modelling studies, would not improve performance of the present model; rather it would make model predictions less reliable because a larger degree of freedom is obtained when a larger number of process parameters are fitted.

7.1.3 Biogeochemical processes at the top fringe of the plume

Hydrochemical depth-profiles from multi-level-samplers (MLSs) as presented in Chapter 6, showed that the plume fringe rose about 1 to more than 3 m towards the surface in the course of three years (1998-2001). The rise of the leachate plume seems related to excavation of the upper soil layer, whereby a substantial part of the unsaturated zone was removed, which could have resulted in increased seepage of groundwater and upward flow. Rise of the plume invoked cation-sorption including proton-buffering on solid organic carbon, which triggered degassing of methane. Potential oxidation of Fe(II), Mn(II), and NH_4^+ at the fringe was prohibited by sorption processes, which resulted in spatial separation of these electron-donors with potential electron-acceptors in pristine groundwater. Degradation of conservative DOC seemed to take place. However, methane oxidation after degassing from leachate and subsequent dissolution in pristine groundwater probably consumed most oxidants, and could be the cause for absence of previously (1998-1999) observed nitrate. Stable isotope analysis of δ^{13}C-CH_4 suggests that methane oxidation occurred at the fringe zone (Chapters 2 and 6).

Archaea communities inside the plume were clearly different from those in pristine groundwater above the plume, while *Archaea* DNA was not present in sufficient concentration below the plume to obtain a PCR product (Chapter 4). Presence of a large *Archaea* community in pristine groundwater above the plume, while it is lacking below the plume, suggests that these *Archaea* are involved in the oxidation of methane escaped from the underlying leachate plume.

7.1.4 Development of redox conditions in the plume

A full sequence of redox zones (e.g., from aerobic to methanogenic) has been observed at many sites polluted with organic compounds (Christensen et al., 2000a; Christensen et al., 2001), however, not at this site. Oxygen gets consumed close to the water table without being of use for NA of the plume. Nitrate was observed in

pristine groundwater above the plume in 1998–1999, while the partial nitrogen gas pressure and $\delta^{15}N$ from NO_3^- indicated that denitrification occurred there (Chapter 2). However, the rise of the plume led to methane degassing, while subsequent dissolution above the plume and oxidation could have been the cause for the later absence of nitrate in 2001–2002 (Chapter 6). Iron reduction prevailed inside the plume in agreement with observations at other organic pollution plumes (Christensen et al., 2000a; Christensen et al., 2001; Lovley and Anderson, 2000).

Sulfate reduction and methanogenesis did not yet happen in the plume. However, the low content of iron oxide in the sediment is prone to depletion within the coming decades. This would favor occurrence of sulfate reduction and methanogenesis near the landfill body. High hydrogen concentrations in and just below the landfill (Chapter 2) together with a relatively low contribution of *Geobacteraceae* to the microbial community close to the source zone (Chapter 4), indicate that the transition to more reduced conditions could at present take place. In addition, reduced conditions beneath the landfill are indicated by dominance of strictly anaerobic, fermentative microorganisms, especially members of the *Clostridiaceae*.

7.1.5 Microbial ecology of the aquifer

Substrate utilization profiling or CLPP using Eco-Biolog plates (Chapter 3) showed that anaerobic microbial communities in the leachate plume clustered separately from those in pristine groundwater. Both substrate richness and functional diversity were significantly enhanced for polluted samples, in agreement with a previous study at the Coupépolder landfill in the Netherlands (Röling et al., 2000a). Dobler et al. (2000) observed in another Biolog study under aerobic conditions that hydrocarbon-contamination increased metabolic potential, while heavy metals showed an inhibitory effect on both activity and richness of soil microbial communities. Both substrate richness and functional diversity did not show a relation with distance from the landfill, but were quite constant. Higher organic substrate availability likely contributed to increase in substrate richness and functional diversity in the plume. Microbial communities in the leachate plume degraded in particular substrates containing an aromatic nucleus better, and also favored most amino acids. Better degradation of substrates containing an aromatic ring in the leachate plume suggests that there could be potential to degrade BTEX and naphthalene at the site.

Consistent with CLPP, denaturing gradient gel electrophoresis (DGGE) profiles of *Bacteria* and *Archaea* in groundwater samples revealed a clear difference between microbial community compositions inside and outside the plume (Chapter 4). The sediment-associated microbial community was different from the community present in pore water, and its composition appeared less affected by inflow of leachate. Bacterial community heterogeneity in the plume was large, but a change with distance from the landfill was apparent, as samples from the first, middle and front part of the plume clustered together. So, not only presence of leachate, but also leachate composition and/or duration of pollution seem to affect the microbial community structure. Bacterial community structure in non-polluted groundwater was related to redox condition: iron-reducing or nitrate-reducing.

Presence of microbial species was established by sequencing cloned 16S rDNA (Chapter 4). Other classes of bacteria dominated the microbial community in the leachate plume than pristine groundwater. Metabolic capabilities of identified bacteria complied with redox conditions at the site: potential denitrifiers were observed upstream where nitrate reduction happened, while iron-reducing microorganisms dominated inside the iron-reducing plume. Members of the family of *Geobacteraceae* made up a large part of the plume microbial community. *Geobacter* spp. are the only known iron-reducing, aromatic hydrocarbon-degrading bacteria (Lovley, 2000), and their presence in this plume increases the chance that monoaromatic chemicals become degraded.

Geobacter species were recently observed to synthesize flagella and were chemotactic towards Fe(II) when grown on insoluble Fe(III)-oxide (Childers et al., 2002). Other iron-reducing species like *Shewanella* and *Geothrix* are non-motile under these conditions, but instead synthesize electron-shuttling compounds to reduce Fe(III)-oxides. Dominance of *Geobacter* species over *Shewanella* and *Geothrix* species has been observed in this plume (Chapter 4), as well as in other sedimentary environments. This suggests that accessing iron oxides in these environments by chemotaxis and attachment may be a better adaptive strategy for reductive dissolution of Fe-oxide than by synthesizing electron shuttles (Childers et al., 2002). From another perspective, the fact that leachate DOC consists partly of humic acids (Christensen et al., 1998), which act as natural electron shuttles (Lovley et al., 1998), makes the capability of synthesizing electron shuttling compounds probably not a competitive advantage in landfill leachate plumes.

Firm conclusions could already be drawn on microbiological processes and future developments by interpreting the spatial distribution of abiotic properties in the aquifer. Yet, knowledge on the microbial communities present increased insight in microbial processes and strengthened hydrogeochemical interpretations. Community-level physiological profiling (CLPP) and culture-independent profiling of the community structure were performed, and presence of microbial species was established. The hypothesis was tested and found accepted, that microbial community structure and functional diversity are linked with environmental factors such as redox conditions, and inflow of landfill leachate.

7.2 Natural attenuation potential for the Banisveld landfill leachate plume

Degradation coupled to Fe(III) reduction taking place inside the plume is essential for natural attenuation of the Banisveld landfill leachate plume, since NA at the plume fringe was not significant. Escaped methane from the plume consumed oxidants in pristine groundwater, while dilution by diffusive and dispersive mixing was limited. Whether the Heiloop stream physically restrains the plume by drainage, or that the plume migrates further downstream underneath this water course towards the nature reserve is not clear. However, excavation of the upper soil layer seems to have triggered the ammonium-rich plume to rise towards the

surface, and may cause unwanted nutrient enrichment. Therefore, it is urgent to assess whether upward leachate flow continues.

Occurrence of degradation of BTEX and naphthalene in the leachate plume could not be ascertained because sorption and spatial or temporal source heterogeneity could produce the decreasing concentration profiles as well (Chapter 2). Laboratory cosms (results not published) were also not able to show potential degradation of aromatic hydrocarbons at this field site, but the inability of laboratory cosms to reflect the field situation has been generally observed (Röling and Van Verseveld, 2002). Recently, biodegradation of aromatic hydrocarbons was unambiguously proven at an industrial location using compound-specific isotope analysis (CSIA) of hydrogen and carbon isotopes of benzene and ethylbenzene (Mancini et al., 2002). Unfortunately, this technique is not (yet) suitable to verify BTEX degradation in landfill leachate plumes, since the detection limit of CSIA is still too high ($\delta^{13}C \approx 300$ μg/l; $\delta^{2}H \approx 4500$ μg/l). However, enhanced degradation of substrates containing an aromatic nucleus by microbial communities in the plume, as determined in Eco-Biolog plates (Chapter 3), suggests that there could be potential for degradation of mono-aromatic hydrocarbons. Furthermore, presence of *Geobacter* spp. increases the chance that mono-aromatic hydrocarbons become degraded in this plume, because this species is the only known iron-reducing and mono-aromatic hydrocarbon-degrading bacterium.

However, even if degradation were to occur, degradation potential for these contaminants probably worsens in the future when the limited pool of iron-oxide depletes near the landfill. This could happen after a few decades, assuming the concentration and reactivity of DOC leaving the landfill remains comparable. An extensive methanogenic zone will then form expanding in downstream direction following the iron-oxide front, and would probably lead to a downstream extension of the zone with high concentrations of aromatic hydrocarbons.

One could argue whether ammonium is not a more problematic leachate constituent than organic pollutants for both quality of drinking water and ecology (Erskine, 2000). Ammonium is transported non-conservatively due to cation-exchange (e.g., Ceazan et al., 1989). However, the potential for ammonium oxidation at the plume fringe is limited because of the cation-exchange induced retardation, and the likelihood that a considerable part of available oxygen and/or nitrate has been used for methane-oxidation. This enables ammonium to be transported across considerable distances.

7.3 Development of the redox sequence and associated degradation potential in landfill leachate plumes

The ability to predict the development of redox processes and associated degradability of organic contaminants in time and space is essential for addressing the sustainability of NA. The concept of the redox sequence developing in organic pollution plumes has been depicted in many research papers (e.g., Christensen et al., 2000a; Christensen et al., 2001; Lovley, 2001). However, the position of a sulfate-

reducing zone downstream of the methanogenic zone in the literature is wrong. After depletion of reactive iron-oxide, sulfate reduction follows and finally methanogenesis. However, this does not imply that this is also the spatial order towards the source zone. Sulfate, present upstream or in the source, reduces first, and after depletion, methanogenesis will follow downstream of the sulfate-front, and upstream from a downstream propagating iron reduction zone. This correct order has been depicted in Figure 1.1 (Chapter 1). However, conditions in leachate plumes (e.g., low sulfate and high DIC concentration) result in small differences in Gibbs free energy and may cause sulfate reduction and methanogenesis to occur simultaneously.

The contribution of aerobic and nitrate-reducing zones to NA of a plume increases with the O_2 and NO_3^- concentrations in pristine groundwater and the extent of mixing with the leachate plume. Research at the present site shows that the transversal mixing zone is very narrow, which is also observed at other locations (e.g., Brun et al., 2002; Mayer et al., 2001), and oxygen and nitrate concentrations can be zero or low, limiting the importance of NA at the plume fringe. Furthermore, secondary redox processes at the fringe considerably limit degradation potential for mono-aromatic chemicals within the plume. In landfill leachate several reduced species such as DOC, Fe(II), NH_4^+, but especially CH_4 will compete with mono-aromatic chemicals for available oxidants at the plume fringe. However, presence of reduced species could enhance degradation potential for halogenated hydrocarbons in leachate plumes. Absence of significant NA at the plume fringe results in extensive lateral migration of pollution.

Iron reduction prevails inside landfill leachate plumes and an extensive redox zone is formed with reasonable degradation potential for aromatic hydrocarbons. Chapter 5 discusses that iron reduction kinetics in landfill leachate plumes is probably controlled by content and type of iron-oxide, reactivity and concentration of DOC, and availability of phosphorous as nutrient for iron-reducing microorganisms. A positive effect of iron-oxide content on the degradation rate of DOC and aromatic hydrocarbons at iron-reducing conditions was found in a comparison with three other well described landfill leachate plumes (Vejen and Grindsted in Denmark, Norman in the U.S.A.).

Absence or depletion of reactive iron-oxides in aquifer sediments has been observed at a few sites (Chapelle et al., 2000; Cozzarelli et al., 2000; Heron et al., 1994b), and although degradation of aromatic hydrocarbons has been observed to occur under sulfate-reducing and methanogenic conditions, degradation rates are often lower (Lovley, 2000; Lovley and Anderson, 2000). Degradation of DOC did not happen in a landfill leachate plume where only hematite was present and reactive iron-oxides were apparently lacking (Cozzarelli et al., 2000). Decreased efficiency of natural attenuation of benzene was observed after iron-oxides and sulfate where depleted in an aquifer and methanogenesis became active (Chapelle et al., 2000). Cozzarelli et al. (2001) observed that after a period when hydrocarbon concentrations under iron-reducing conditions decreased, a period followed that hydrocarbons were migrating again as microbial degradation shifted to methanogenesis as a consequence of iron oxide depletion.

Iron reduction was also the dominant degradation process at the present site. But low iron-oxide concentrations are prone to depletion in a couple of decades, which will shift redox conditions to sulfate reduction and methanogenesis having less potential for degradation of BTEX and naphthalene. Sulfate concentration in landfill leachate is generally too low to maintain a degradation potential equal to iron reduction. Sulfate concentration in leachate was so low at the present site, that a future sulfate-reducing zone present downstream of the landfill border will be insignificant. This causes methanogenesis to directly succeed iron reduction in the plume. Eventually, an extensive methanogenic zone will form in a specific area of the plume: downstream of, or having overlap with, a restricted sulfate-reducing zone surrounding the landfill. This methanogenic zone expands in downstream direction following the iron oxide depletion front.

In order to improve our ability to predict the development of redox conditions at contaminated sites, more insight is needed on physical mixing processes due to dispersion and molecular diffusion, competing secondary reactions, reactivity of iron oxide and DOC, degradation potential at sulfate-reducing and methanogenic conditions as substitutes for iron-reducing conditions, and the source function of landfills.

7.4 Availability of Fe(III)-oxide for iron reduction in leachate plumes

During reductive-dissolution of Fe(III)-oxide minerals, several secondary Fe(II)-containing minerals may form (Zachara et al., 2002): siderite ($FeCO_3$), magnetite ($Fe(III)_2Fe(II)O_4$), vivianite ($Fe_3(PO_4)_28H_2O$), and green rust (mixed Fe(II)-Fe(III) mineral of variable composition). Presence of phosphate (absent in Banisveld landfill leachate plume) triggers vivianite formation, while green rusts are metastable to magnetite and siderite (Zachara et al., 2002). Magnetite is a mixed Fe(II)-Fe(III) mineral, and has been observed to accumulate as an end-product of Fe(III)-oxide reduction, because of its stability to further microbial iron reduction (Lovley et al., 1986). For the sustainability of NA it is important to address whether or not magnetite formation as a result of iron reduction happens, because then part of Fe(III) will be sequestered in a form which could be microbially unavailable (Fredrickson et al., 1998). For instance, two-thirds of the Fe(III) capacity will end up as inaccessible for iron reduction if magnetite is the only mineral formed during reductive dissolution of other Fe(III)oxyhydroxides.

The groundwater composition determines whether siderite or magnetite forms as secondary mineral during reduction of Fe(III)-oxides (Fredrickson et al., 1998; Zachara et al., 2002). Siderite and little or none magnetite forms if bicarbonate concentrations are high (promoting siderite precipitation), and pH is around or below neutral, while pe is low causing undersaturation for magnetite (Zachara et al., 2002). Otherwise, magnetite will be the stable end product. Magnetite is probably not an intermediate in siderite formation; rather high bicarbonate concentrations (18-40 mmol/l) promote siderite formation and could inhibit magnetite formation

(Zachara et al., 2002). Furthermore, Dong et al. (2000) recently discovered that magnetite is bio-reducible if conditions are favorable for siderite formation. Microscopic evidence showed that then reductive-dissolution of magnetite and precipitation of siderite happens.

Field evidence on formation of magnetite during iron reduction in organic carbon pollution plumes is limited. Scanning electron microscopy (SEM) showed that primarily ferroan calcite and little magnetite precipitated in the Bemidji hydrocarbon plume having a high DIC concentration (Baedecker et al., 1992). Good methods to quantify siderite and magnetite do not exist. However, absence of magnetite can be established using a 5M HCl extraction, as this method extracted 78 % of the magnetite from a pure magnetite sample (Heron et al., 1994b). Consequently, formation of magnetite seems not important in the Vejen landfill leachate plume, because Fe(III) extracted with a 5M HCl extraction decreased and not increased towards the landfill (Heron et al., 1994b). The Banisveld landfill leachate plume is more supersaturated for siderite than for magnetite, indicating that siderite is the more stable Fe(II)-mineral in the plume. In contrast, geochemical transport modelling of a petroleum hydrocarbon plume, which was undersaturated for siderite due to a low DIC concentration, showed that magnetite formation during goethite reduction explained observations best, and consequently a significant part of Fe(III) was sequestered in a non-reducible form (Prommer et al., 1999).

However, even in the case that solely siderite and no magnetite forms, part of Fe(III) may end up as inaccessible, when precipitation of siderite coats the iron-oxide and thereby blocks access to surface sites (Liu et al., 2001b). Still, the extent to which iron-oxide minerals become coated by precipitation of secondary Fe(II)-minerals has yet to be established. Liu et al. (2001b) showed in a lab experiment on iron reduction that a significant fraction of formed siderite was not associated with goethite as surface precipitate. In conclusion, the Fe(III)-reducing capacity of an aquifer will probably be nearly fully available for NA of a landfill leachate plume because leachate composition (high DIC) promotes siderite instead of magnetite formation. In contrast, magnetite formation due to low DIC concentrations may limit the availability of Fe(III) in hydrocarbon plumes (e.g., Prommer et al., 1999).

7.5 Molecular microbial ecology research: perspectives for MNA

A typical geochemist attitude on addressing subsurface microbiological processes is that deducing them from spatial hydrogeochemical patterns will suffice, while a typical conviction is that kinetics of microbial processes can be formulated using solely abiotic factors. No necessity is felt for obtaining microbial information. Hydrogeochemical data indeed reflect the result of microbial processes, but still form factually indirect evidence for microbial metabolism. Measurements of microbial properties providing a direct proof of occurrence of microbial degradation would strongly increase public confidence in NA, and would be superior to methods constituting ”lines of evidence”. Effectiveness of degradation processes

varies among sites or even within an aquifer (Lovley, 2001). Presence of specific microorganisms will determine occurrence of benzene degradation at iron-reducing conditions, while environmental variables are not predictive (Rooney-Varga et al., 1999). This example illustrates that kinetics of degradation cannot be described in a mechanistic way using solely abiotic factors, and thorough knowledge on subsurface microbial communities is needed in order to predict potential for degradation in detail.

This thesis shows that establishing the occurrence and sustainability of degradation of organic pollutants at an individual site is a complicated, time-, and resource-consuming task. Biological and hydrogeochemical properties should be identified that are discriminating for predicting the degradability of specific organic contaminants at individual sites. This would lower the overall cost of dealing with the problem of groundwater pollution. The obvious approach would be to archive world-wide information regarding presence and activity of microbial communities related to environmental variables (redox conditions, concentration electron-acceptors, availability nutrients and substrate, etc), and extent of degradation (Röling and Van Verseveld, 2002).

Considerable progress is currently being made in the field of molecular microbial ecology on obtaining information from microbial communities in the environment. Overviews of existing and promising molecular methods, their applications and pitfalls have been discussed (Madsen, 2000; Newman and Banfield, 2002; Röling and Van Verseveld, 2002). In this thesis information on subsurface microbiology was obtained by physiological and phylogenetic profiling methods and the species composition of the microbial communities present in groundwater was determined. Artificial neural networks (ANNs) could be used to find, for example, bands in fingerprints of the microbial community structure or presence of specific species that indicate potential for contaminant degradation (Röling and Van Verseveld, 2002).

However, presence of microorganisms is not necessarily synonymous with metabolic activity. On the contrary, information on gene expression is directly compatible with metabolic potential/activity. It is possible to determine which genes are involved in degradation processes, as anaerobic microorganisms involved in some important bioremediation processes are closely related to existing pure cultures that are able to perform these processes in the laboratory and whose genomes are available (Lovley, 2001). Currently, the entire genome for the two most important iron-reducing microorganisms *Geobacter* and *Shewanella* is being sequenced, which will lead to new insight into the genes involved in metal reduction, and is of importance for development of bioremediation strategies (Nealson and Cox, 2002). Probes can be developed which target functional genes encoding for any metabolic activity like degradation and respiration to evaluate potential for occurrence of biochemical processes, whereas detection of mRNA transcribed from functional genes relates to metabolic activity (Newman and Banfield, 2002).

As stated by Bakermans and Madsen (2002), one of the longstanding goals in environmental microbiology is to simultaneously ascertain the identity, activity, and biogeochemical impact of individual microorganisms in-situ. They made progress towards this goal by developing a fluorescent in situ hybridization with tyramide

signal amplification (FISH-TSA) method, and applied it to the detection of naphthalene dioxygenase mRNA transcripts from bacteria in groundwater samples from a coal tar waste-contaminated site. A further step would be to predict in-situ biochemical reaction rates from signal intensity, if calibration is possible in pure culture studies. This method bypasses incubation- and/or sampling-induced alteration in metabolic activity of microbial communities present in environmental samples. Beller et al. (2002) recently quantified hydrocarbon-degrading bacteria using a real-time PCR method targeting a catabolic gene associated with anaerobic toluene and xylene degradation.

DNA microarray technology simultaneously monitors gene expression for many messenger RNAs (mRNAs) in a sample, but application is at present limited to the study of simple systems (Newman and Banfield, 2002; Röling and Van Verseveld, 2002). Newman and Banfield (2002) presented a view on "genome-enabled ecosystem modelling" aiming at identifying the networks that govern simple biogeochemical systems and how they change over time. In this approach the environmental biogeochemistry, the microbial community, the species composition, and the metabolic activity measured using microarrays, should be determined in an iterative cycle.

An associated development in microbiology is the comeback of the research field of recombinant microbes for cleaning-up pollution (Zwillich, 2000). The likelihood for success is expected to be much higher than three decades ago, since microbes are used which thrive naturally at contaminated sites instead of lab organisms and environmental conditions are taken more into account. However, strict regulations have limited the use of recombinant microbes in the field to only one – a *Pseudomonas* species that fluoresces when it contacts naphthalene.

Degradation potential for various groundwater contaminants (e.g., BTEX, trichloroethylene, NO_3^-) can be assessed to some extent using solely abiotic parameters. However, the properties of microbial communities (e.g., presence of species and activity of genes) may be decisive for evaluating degradation potential under less benign conditions and for less common contaminants. Smets et al. (2002) put forward another issue related to NA sustainability: evolution could change microbial community physiology over the time period needed for MNA. This change can be positive, resulting in new or better metabolic activities (Van der Meer et al., 1998), or negative when degradation pathways for specific contaminants cease to exist. Increased knowledge on genes encoding biochemical degradation pathways should enable a simultaneous screening of the degradation potential for various contaminants.

7.6 Directions for future research to natural attenuation of landfill leachate

Scientific research on NA needs to address in particular aspects associated with sustainability in order to implement cost-effective and successful MNA. Degradability of poorly understood organic contaminants like the fuel oxygenate MTBE

and heterogeneity of the subsurface are other research issues put forward (Bekins et al., 2001). A continued development of 2D or 3D geochemical transport models including simulation of isotope geochemistry is essential to consider NA sustainability, assess uncertainty, and to guide new data needs. Studies to the research themes indicated below should be performed to improve weak aspects of current models.

First, knowledge on the leachate source flux is limited. Data collection and model formulation on change in leachate composition and leachate DOC reactivity in time would improve evaluation of NA sustainability at landfill sites. Second, detailed field studies to natural attenuation at the fringe of plumes should increase the understanding of physical mixing, and indicate the potential and kinetics of secondary redox processes induced by mixing. Third, improvement in understanding iron reduction kinetics in aquifers is essential as this process controls degradation inside organic pollution plumes to a large extent. Therefore, further biogeochemical research is needed to determine the reactivity of iron oxides and organic carbon (leachate DOC, sedimentary organic carbon, etc), and for obtaining essential information on microbial communities involved. Laboratory and field studies in combination with the application of metabolic and ecological control analysis (e.g., Röling and Van Verseveld, 2002) to these ecological systems will improve the prediction of iron reduction kinetics. The control of the following factors should be determined: content and reactivity of iron oxide, concentration and reactivity of organic carbon, availability of nutrients and microbial abundance, replicative potential and community structure. Finally, the kinetics and associated degradation potential of sulfate reduction and methanogenesis for aquifers depleted with iron-oxide needs more consideration.

A continuing development of measurement techniques would improve our understanding and would reduce the uncertainty on NA performance. Application of novel molecular microbial ecology techniques holds much promise (see Section 7.5). Decreasing the detection limit of component-specific isotope analysis (CSIA) down to 1 μg/l makes application possible for assessing the occurrence of degradation for a wide variety of organic compounds in landfill leachate plumes. Development of a technique to quantify low siderite contents would make it possible to use precipitated siderite as a cumulative process variable for iron reduction, since formation of other Fe(II)-minerals like magnetite seems of less importance in landfill leachate plumes (see Section 7.4). Currently, no good method exists for measurement of siderite (Christensen et al., 2000a). However, thermal gravimetric analysis (TGA) holds promise for quantification of siderite at low contents (Hartog et al., 2002).

Groundwater dating is of importance for determining the advective velocity of landfill leachate plumes. Unfortunately, many tools are not applicable to date the age of landfill leachate. Potential degassing of ^{3}He and SF_6 in plumes makes $^{3}H/^{3}He$ and SF_6 dating impossible, while age dating using chlorofluorocarbons is unreliable because these compounds are susceptible to decay under the anaerobic conditions in plumes. This leaves ^{85}Kr as the most expensive but only alternative dating tool (Jonker et al., 2002). However, direct measurement of ^{85}Kr atoms with a laser-based mass spectrometric technique (resonance-ionization mass spectrome-

try; RIMS), rather than counting the decay of the ^{85}Kr atoms, reduces the required sample size from the $\approx$ 200+ liters required by the best low-level decay-counting methods to 10 liters, or less (pers. comm. N. Thonnard). Thonnard and coworkers from the University of Tennessee currently develop this technique, which would make ^{85}Kr a much more attractive and affordable groundwater dating tool.

Finally, single-well, "push-pull" tests have proven valuable to obtain rate constants on in-situ microbial metabolic activities in aquifers (Istok et al., 1997). The method is based on a pulse-type of injection ("push") of a test solution into an aquifer via the screen of a monitoring well, followed, after an incubation period, by the extraction ("pull") of the test-solution/groundwater mixture from the well. The test solution contains a conservative tracer (e.g., Br^-) and one or more reactive solutes to investigate specific microbial activities. Rates are computed from breakthrough curves of solutes measured in extracted groundwater. Push-pull tests have been used to determine rates of oxygen-consumption, denitrification, and sulfate reduction (Istok et al., 1997), carbon source degradation (Kleikemper et al., 2002), enzymatic reactions (β-glucosidase activity; Istok et al., 2001), and toluene/xylene degradation (Reusser et al., 2002). Injection of hydrogen gas and measuring its consumption appeared a useful test to assess subsurface metabolic activity, and is the only push-pull test performed so far in a landfill leachate plume (Smith et al., 2002).

Application of isotope techniques increased the capabilities of push-pull tests. Denitrification was better determined using isotope-labeling of nitrate and quantification of the mass of denitrification gasses (Addy et al., 2002). Measurement of δ^{34}S-SO_4^{2-} aided in determining sulfate reduction rates (Kleikemper et al., 2002). Isotope-labeling of substrate in combination with measurement of ^{13}C incorporation in dissolved inorganic carbon and phospholipid-derived fatty acids (PLFA) enabled determination of the type of microorganisms active (Pombo et al., 2002). Finally, conservative rates on toluene and xylene degradation were obtained via addition of deuterium-labeled surrogates and measurement of the formed deuterated metabolites (Reusser et al., 2002). The push-pull test seems a promising technique in NA research on landfill leachate plumes. Potential applications could be: evaluation of BTEX degradation, obtaining rates on sulfate- and nitrate reduction, evaluation of sulfate or nitrate addition on stimulation of degradation in plumes, and demonstration of methane oxidation in pristine groundwater at the fringe.

7.7 Current needs in MNA as remediation strategy for landfill leachate plumes

In this final section recommendations are given on the technical aspects of MNA of landfill leachate plumes. Furthermore, some deficiencies are noticed in the Dutch environmental policy and its consequences for landfill leachate pollution will be discussed.

The practical issue of design of long-term monitoring networks to verify that NA is working as expected, is still unsolved (Bekins et al., 2001). Application of monitored natural attenuation (MNA) can be accepted as a remediation option

in the Netherlands, if calculations show that a stationary plume will be reached within a time frame of 30 years (Doorstart-A5, 2001). Reactive transport modelling is therefore of utmost importance for implementation of MNA. These models predict the development in plume hydrochemistry in time and space, including the time frame within a stable end-situation is reached. Consequently, these models should also guide in deciding which variables should be measured, at what locations and when, to verify the model predictions. The budget available for monitoring can in this way be better allocated, which would lead to more cost-effective MNA. The most diagnostic monitoring locations are those where significant concentration changes in hydrochemical variables are predicted. These locations are typically present somewhat downstream of reaction fronts. Diagnostic locations and overall associated variables would be:

- Front of the plume: measurement of conservative leachate indicators (e.g., Cl^-, Br^-) to verify continuing spreading of leachate.
- Potassium and ammonium fronts, which keep migrating in time in the plume core.
- Individual fronts of contaminants, which need to be remediated.
- Degradation curve of dissolved organic carbon (DOC), which reflects the continuation of DOC degradation and governing redox processes.
- Iron-oxide depletion front, where the transition from iron reduction to sulfate reduction/methanogenesis could be monitored using hydrogen-gas analysis, redox-species (Fe(II), SO_4^{2-}, CH_4), and isotope techniques ($\delta^{34}S$ of SO_4^{2-}, and δ^2H and $\delta^{13}C$ of CH_4). Concentrations of organic contaminants should be measured, when the redox condition changes, to verify whether degradation potential has been deteriorated.

Landfill leachate contains a range of solutes often present in concentrations above the EU norm for drinking water (Table 7.1). Spreading landfill leachate deteriorates the quality of groundwater as a source for drinking water (e.g., organic pollutants), and threatens nearby nature areas (e.g., NH_4^+, salts). Remarkably, intervention values for organic pollutants are considerably higher than the EU norms for drinking water (Table 7.1). The intervention value is the concentration norm for a contaminant at which groundwater is considered polluted, additional research to the urgency of the pollution should be performed, and the perpetrator is held responsible, if pollution occurred after 1975, according to the Dutch Act on Soil Conservation. Furthermore, no corporation can be held responsible for pollution of groundwater with ammonium, as intervention values have not been formulated for macro parameters. However, ammonium is usually the leachate component with greatest impact on both the ecology and quality of drinking water (Erskine, 2000).

The current Dutch policy results in the unsatisfactorily situation that spreading of landfill leachate is in reality legitimate, since intervention values are generally not exceeded or are not existing (Table 7.1), although economic activities (drinking

water winning) and environmental health could be impaired. However, in the case economic activities are at stake, this situation will be in conflict with the principle of "functie-gericht saneren" (land-use function oriented remediation), which is in practice operative since a few years in the Netherlands (Griffioen, 2002). Griffioen (2002) argues that drinking water norms should apply for that part of the subsurface that is within the withdrawal area of groundwater abstractions. The environmental problem of aquifer pollution with landfill leachate needs to be taken more seriously into consideration. Einarson and Mackay (2001) argued that the quality of water abstracted can still fulfill drinking water norms in case of groundwater pollution, if blending of plumes with clean groundwater simultaneously captured and extracted by wells happens. For that reason, however, some level of pollution should not be allowed locally in aquifers, since dilution, as sole NA mechanism, is not accepted in the Netherlands.

Table 7.1: Leachate compositions observed and quality criteria

Parameter	Drinking[a] water norm	Target[b] value	Intervention[b] value	DK[c]	USA[d]	UK[e]	NL[f]	Banisveld landfill
Hardness (mmol/l)	2.5			≈9		≈14	≈8	≈14
Na^+ (mg/l)	150			210		700	306	183
K^+ (mg/l)	12			140		780	255	235
Fe^{2+} (mg/l)	0.2			76		540	12	45+
Mn^{2+} (mg/l)	0.05			3.5		27		0.5
NH_4^+ (mg/l)	0.2			110		800	64	360
P (mg/l)				1.5				2.2
Cl^- (mg/l)	150	100		360		2000	378	260
SO_4^{2-} (mg/l)	150			150		70	8	<3
BTEX (μg/l)							29	
Benzene (μg/l)	1	0.2	30	22	123			5–33
Ethylbenzene (μg/l)	1	4	150	38	110			0–53
Toluene (μg/l)	1	7	1000	210	417			0.2–0.7
Xylene (μg/l)	1	0.2	70	30	461			1–120
Naphthalene (μg/l)	0.1	0.01	70	34				0–31

[a] *Waterleidingbesluit, 2001.*
[b] *Interventiewaarden, 2000.*
[c] *Kjeldsen and Christophersen, 2001. Denmark, average of 43 landfills.*
[d] *Krug and Ham, 1997. Wisconsin, USA, average of 13 landfills.*
[e] *Erskine, 2000. UK.*
[f] *IPO, 2002. The Netherlands, average of 80 landfills*

REFERENCES

Abrams, R.H., Loague, K., 2000a. A compartmentalized solute transport model for redox zones in contaminated aquifers 1. Theory and development. Water Resour. Res., 36(8): 2001-2013.

Abrams, R.H., Loague, K., 2000b. A compartmentalized solute transport model for redox zones in contaminated aquifers 2. Field-scale simulations. Water Resour. Res., 36(8): 2015-2029.

Acton, D.W., Barker, J.F., 1992. In situ biodegradation potential of aromatic hydrocarbons in anaerobic aquifers. J. Contam. Hydrol., 9: 325-352.

Addy, K., Kellogg, D.Q., Gold, A.J., Groffman, P.M., Ferendo, G., Sawyer, C., 2002. In situ push-pull method to determine ground water denitrification in riparian zones. J. Environ. Qual., 31(3): 1017-1024.

Albrechtsen, H.-J., Bjerg, P.L., Ludvigsen, L., Rügge, K., Christensen, T.H., 1999. An anaerobic field injection experiment in a landfill leachate plume, Grindsted, Denmark 2. Deduction of anaerobic (methanogenic, sulfate-, and Fe(III)-reducing) redox conditions. Water Resour. Res., 35(4): 1247-1256.

Albrechtsen, H.-J., Heron, G., Christensen, T.H., 1995. Limiting factors for microbial Fe(III)-reduction in a landfill leachate polluted aquifer (Vejen, Denmark). FEMS Microb. Ecol., 16: 233-248.

Albrechtsen, H.-J., Smith, P.M., Nielsen, P., Christensen, T.H., 1996. Significance of biomass support particles in laboratory studies on microbial degradation of organic chemicals in aquifers. Water Res., 30(12): 2977-2984.

Albrechtsen, H.-J., Winding, A., 1992. Microbial biomass and activity in subsurface sediment from Vejen, Denmark. Microb. Ecol., 23: 303-317.

Altschul, S.F., Gish, W., Miller, W., Myers, E.W., Lipman, D.J., 1990. Basic local alignment search tool. J. Mol. Biol., 215: 403-410.

Amann, R.I., Ludwig, W., Schleifer, K.H., 1995. Phylogenetic identification and in situ detection of individual microbial cells without cultivation. Microbiol. Rev., 59: 143-169.

Amann, R.I., Stromley, J., Devereux, R., Key, R., Stahl, D.A., 1992. Molecular and microscopic identification of sulfate-reducing bacteria in multispecies biofilms. Appl. Environ. Microbiol., 58(2): 614-623.

Amirbahman, A., Schonenberger, R., Johnson, C.A., Sigg, L., 1998. Aqueous- and solid-phase biogeochemistry of a calcareous aquifer system downgradient from a municipal solid waste landfill (Winterthur, Switzerland). Environ. Sci. Technol., 32(13): 1933-1940.

Andrews, J.N., 1992. Mechanisms for noble gas dissolution by groundwaters. Isotopes of noble gases as tracers in environmental studies. IAEA, Vienna, pp. 87-110.

Appelo, C.A.J., Postma, D., 1993. Geochemistry, groundwater and pollution. A.A. Balkema, Rotterdam, 536 pp.

Appelo, C.A.J., Verweij, E., Schäfer, H., 1998. A hydrogeochemical transport model for an oxidation experiment with pyrite/calcite/exchangers/organic matter containing sand. Appl. Geochem., 13(2): 257-268.

Appelo, C.A.J., Willemsen, A., 1987. Geochemical calculations and observations on salt water intrusions, 1. A combined geochemical/mixing cell model. J. Hydrol., 94: 313-330.

Appelo, C.A.J., Willemsen, A., Beekman, H.E., Griffioen, J., 1990. Geochemical calculations and observations on salt water intrusions. II. Validation of a geochemical model with laboratory experiments. J. Hydrol., 120: 225-250.

Baedecker, M.J., Back, W., 1979. Hydrogeological processes and chemical reactions at a landfill. Ground Water, 17: 429-437.

Baedecker, M.J., Cozzarelli, I.M., Eganhouse, R.P., Siegel, D.I., Bennett, P.C., 1993. Crude oil in a shallow sand and gravel aquifer-III. Biogeochemical reactions and mass balance modeling in anoxic groundwater. Appl. Geochem., 8(6): 569-586.

Baedecker, M.J., Cozzarelli, I.M., Evans, J.R., Hearn, P.P., 1992. Authigenic mineral formation in aquifers rich in organic material. *In*: Y.K. Kharaka, A.S. Maest (Eds.), Water-Rock Interaction. A. A. Balkema, Rotterdam, pp. 257-261.

Bakermans, C., Madsen, E.L., 2002. Detection in coal tar waste-contaminated groundwater of mRNA transcripts related to naphthalene dioxygenase by fluorescent in situ hybridization with tyramide signal amplification. J. Microbiol. Methods, 50(1): 75-84.

Beller, H.R., Kane, S.R., Legler, T.C., Alvarez, P.J.J., 2002. A real-time polymerase chain reaction method for monitoring anaerobic, hydrocarbon-degrading bacteria based on a catabolic gene. Environ. Sci. Technol., 36(18): 3977-3984.

Barlaz, M.A., Schaefer, D.M., Ham, R.K., 1989. Bacterial population development and chemical characteristics of refuse decomposition in a simulated sanitary landfill. Appl. Environ. Microbiol., 55: 55-65.

Bekins, B., Rittmann, B.E., MacDonald, J.A., 2001. Natural attenuation strategy for groundwater cleanup focuses on demonstrating cause and effect. EOS, 82(5): 53.

Bennett, P.C., Hiebert, F.K., Rogers, J.R., 2000. Microbial control of mineral-groundwater equilibria: Macroscale to microscale. Hydrogeol. J., 8(1): 47-62.

Bergamaschi, P., 1997. Seasonal variations of stable hydrogen and carbon isotope ratios in methane from a Chinese rice paddy. J. Geophys. Res.-Atmos., 102(D21): 25383-25393.

BEVER/UPR, 2000. Eindrapport UitvoeringsPRogramma BEleidsVERnieuwing Bodemsanering (BEVER/UPR). Samenvattende eindrapportage. Den Haag. 35 pp.

Bjerg, P.L., Ammentorp, H.C., Christensen, T.H., 1993. Model simulations of a field experiment on cation exchange- affected multicomponent solute transport in a sandy aquifer. J. Contam. Hydrol., 12(4): 291-311.

Bjerg, P.L., Jakobsen, R., Bay, H., Rasmussen, M., Albrechtsen, H.-J., Christensen, T.H., 1997. Effects of sampling well construction on H2 measurements made for characterization of redox conditions in a contaminated aquifer. Environ. Sci. Technol., 31(10): 3029-3031.

Bjerg, P.L., Rügge, K., Pedersen, J., Christensen, T.H., 1995. Distribution of redox-sensitive groundwater quality parameters downgradient of a landfill (Grindsted, Denmark). Environ. Sci. Technol., 29(5): 1387-1394.

Blicher-Mathiesen, G., McCarty, G.W., Nielsen, L.P., 1998. Denitrification and degassing in groundwater estimated from dissolved dinitrogen and argon. J. Hydrol., 208(1-2): 16-24.

Bosatta, E., Ågren, G.I., 1995. The power and reactive continuum models as particular cases of the Q-theory of organic-matter dynamics. Geochim. Cosmochim. Acta, 59(18): 3833-3835.

Brockman, F.J., Li, S.W., Fredrickson, J.K., Ringelberg, D.B., Kieft, T.L., Spadoni, C.M., White, D.C., McKinley, J.P., 1998. Post-sampling changes in microbial community composition and activity in a subsurface paleosol. Microbial. Ecol., 36(2): 152-164.

Bruggenwert, M.G.M., Kamphorst, A., 1982. Survey of experimental information on cation exchange in soil systems. *In*: G.H. Bolt (Ed.), Soil Chemistry B. Physico-chemical models. Elsevier, Amsterdam, pp. 141-204.

Brun, A., Engesgaard, P., 2002. Modelling of transport and biogeochemical processes in pollution plumes: literature review and model development. J. Hydrol., 256(3-4): 211-227.

Brun, A., Engesgaard, P., Christensen, T.H., Rosbjerg, D., 2002. Modelling of transport and biogeochemical processes in pollution plumes: Vejen landfill, Denmark. J. Hydrol., 256(3-4): 228-247.

Caccavo, F., Coates, J.D., Rossellomora, R.A., Ludwig, W., Schleifer, K.H., Lovley, D.R., Mcinerney, M.J., 1996. *Geovibrio ferrireducens*, a phylogenetically distinct dissimilatory Fe(III)-reducing bacterium. Arch. Microbiol., 165(6): 370-376.

Ceazan, M.L., Thurman, E.M., Smith, R.L., 1989. Retardation of ammonium and potassium transport through a contaminated sand and gravel aquifer: the role of cation exchange. Environ. Sci. Technol., 23(11): 1402-1408.

Chanton, J.P., Martens, C.S., 1985. The effects of heat and stannous chloride addition on the active destillation of acid volatile sulfide from pyrite-rich marine sediment samples. Biogeochemistry, 1: 375-383.

Chapelle, F.H., Bradley, P.M., Landmeyer, J.E., 2000. Evolution of redox processes and the natural attenuation of petroleum hydrocarbons in ground-water systems, GSA Annual Meeting, Reno, Nevada, USA, p. A-127.

Chapelle, F.H., McMahon, P.B., 1991. Geochemistry of dissolved inorganic carbon in a coastal plain aquifer. 1. Sulfate from confining beds as an oxidant in microbial CO_2 production. J. Hydrol., 127: 85-108.

Chapelle, F.H., Vroblesky, D.A., Woodward, J.C., Lovley, D.R., 1997. Practical considerations for measuring hydrogen concentrations in groundwater. Environ. Sci. Technol., 31: 2873-2877.

Childers, S.E., Ciufo, S., Lovley, D.R., 2002. Geobacter metallireducens accesses insoluble Fe(III) oxide by chemotaxis. Nature, 416(6882): 767-769.

Cho, J.-C., Kim, S.-J., 2000. Increase in bacterial community diversity in subsurface aquifers receiving livestock waste water input. Appl. Environ. Microbiol., 66: 956-965.

Christensen, J.B., Jensen, D.L., Grøn, C., Filip, Z., Christensen, T.H., 1998. Characterisation of the dissolved organic carbon in landfill leachate polluted groundwater. Water Res., 32(1): 125-135.

Christensen, T.H., Bjerg, P.L., Banwart, S.A., Jakobsen, R., Heron, G., Albrechtsen, H.-J., 2000a. Characterization of redox conditions in groundwater contaminant plumes. J. Contam. Hydrol., 45(3-4): 165-241.

Christensen, T.H., Bjerg, P.L., Kjeldsen, P., 2000b. Natural attenuation: A feasible approach to remediation of ground water pollution at landfills? Ground Water Monit. Remediat., 20(1): 69-77.

Christensen, T.H., Kjeldsen, P., Albrechtsen, H.-J., Heron, G., Nielsen, P.H., Bjerg, P.L., Holm, P.E., 1994. Attenuation of landfill leachate pollutants in aquifers. Crit. Rev. Environ. Sci. Technol., 24(2): 119-202.

Christensen, T.H., Kjeldsen, P., Bjerg, P.L., Jensen, D.L., Christensen, J.B., Baun, A., Albrechtsen, H.-J., Heron, C., 2001. Biogeochemistry of landfill leachate plumes. Appl. Geochem., 16(7-8): 659-718.

Chung, J.B., Zasoski, R.J., 1994. Ammonium-potassium and ammonium-calcium exchange equilibria in bulk and rhizosphere soil. Soil Sci. Soc. Am. J., 58(5): 1368-1375.

Cirpka, O.A., Frind, E.O., Helmig, R., 1999. Numerical simulation of biodegradation controlled by transverse mixing. J. Contam. Hydrol., 40(2): 159-182.

Clement, T.P., Sun, Y., Hooker, B.S., Petersen, J.N., 1998. Modeling multispecies reactive transport in ground water. Ground Water Monit. Remediat., 18(2): 79-92.

Coates, J.D., Ellis, D.J., BluntHarris, E.L., Gaw, C.V., Roden, E.E., Lovley, D.R., 1998. Recovery of humic-reducing bacteria from a diversity of environments. Appl. Environ. Microbiol., 64(4): 1504-1509.

Coates, J.D., Ellis, D.J., Gaw, C.V., Lovley, D.R., 1999. *Geothrix fermentans* gen. nov., sp nov., a novel Fe(III)-reducing bacterium from a hydrocarbon-contaminated aquifer. Int. J. Syst. Bact., 49: 1615-1622.

Coates, J.D., Phillips, E.J.P., Lonergan, D.J., Jenter, H., Lovley, D.R., 1996. Isolation of *Geobacter* species from diverse sedimentary environments. Appl. Environ. Microbiol., 62(5): 1531-1536.

Costa, C., Dijkema, C., Friedrich, M., Garcia-Encina, P., Fernandez-Polanco, F., Stams, A.J.M., 2000. Denitrification with methane as electron donor in oxygen- limited bioreactors. Appl. Microbiol. Biotechnol., 53(6): 754-762.

Cozzarelli, I.M., Bekins, B.A., Baedecker, M.J., Aiken, G.R., Eganhouse, R.P., Tuccillo, M.E., 2001. Progression of natural attenuation processes at a crude-oil spill site: 1. Geochemical evolution of the plume. J. Contam. Hydrol., 53(3-4): 369-385.

Cozzarelli, I.M., Suflita, J.M., Ulrich, G.A., Harris, S.H., Scholl, M.A., Schlottmann, J.L., Christenson, S., 2000. Geochemical and microbiological methods for evaluating anaerobic processes in an aquifer contaminated by landfill leachate. Environ. Sci. Technol., 34(18): 4025-4033.

Crump, B.C., Armbrust, E.V., Baross, J.A., 1999. Phylogenetic analysis of particle-attached and free-living bacterial communities in the Columbia river, its estuary, and the adjacent coastal ocean. Appl. Environ. Microbiol., 65(7): 3192-3204.

Cummings, D.E., Caccavo, F., Spring, S., Rosenzweig, R.F., 1999. *Ferribacterium limneticum*, gen. nov., sp. nov., an Fe(III)-reducing microorganism isolated from mining-impacted freshwater lake sediments. Arch. Microbiol., 171(3): 183-188.

Dean, S.M., Lendvay, J.M., Barcelona, M.J., Adriaens, P., Katopodes, N.D., 1999. Installing multilevel sampling arrays to monitor ground water and contaminant discharge to a surface water body. Ground Water Monit. Remediat., 19(4): 90-96.

Delin, G.N., Landon, M.K., 1996. Multiport well design for sampling of ground water at closely spaced vertical intervals. Ground Water, 34(6): 1098-1104.

Devlin, J.F., 1990. Field evidence for the effect of acetate on leachate alkalinity. Ground Water, 28(6): 863-867.

Dobler, R., Saner, M., Bachofen, R., 2000. Population changes of soil microbial communities induced by hydrocarbon and heavy metal contamination. Biorem. J., 4(1): 41-56.

Dong, H.L., Fredrickson, J.K., Kennedy, D.W., Zachara, J.M., Kukkadapu, R.K., Onstott, T.C., 2000. Mineral transformation associated with the microbial reduction of magnetite. Chemical Geology, 169(3-4): 299-318.

Doorstart-A5, 2001. Eindrapport project doorstart-A5. Afwegingsproces voor de aanpak van mobiele verontreinigingen in de ondergrond. Procesbeschrijving en landelijke saneringsladder. 32 pp.

Eganhouse, R.P., Cozzarelli, I.M., Scholl, M.A., Matthews, L.L., 2001. Natural attenuation of volatile organic compounds (VOCs) in the leachate plume of a municipal landfill: Using alkylbenzenes as process probes. Ground Water, 39(2): 192-202.

Einarson, M.D., Mackay, D.M., 2001. Predicting impacts of groundwater contamination. Environ. Sci. Technol., 35(3): 66A-73A.

EPA, 1999. Use of Monitored Natural Attenuation at Superfund, RCRA Corrective Action, and Underground Storage Tank Sites.

Erskine, A.D., 2000. Transport of ammonium in aquifers: retardation and degradation. Q. J. Eng. Geol. Hydrogeol., 33: 161-170.

Essaid, H.I., Bekins, B.A., Godsy, E.M., Warren, E., Baedecker, M.J., Cozzarelli, I.M., 1995. Simulation of aerobic and anaerobic biodegradation processes at a crude oil spill site. Water Resour. Res., 31(12): 3309-3327.

Faure, G., 1986. Principles of isotope geology. John Wiley and Sons, New York.

Felske, A., Wolterink, A., Van Lis, R., Akkermans, A.D.L., 1998. Phylogeny of the main bacterial 16S rRNA sequences in Drentse A grassland soils (The Netherlands). Appl. Environ. Microbiol., 64(3): 871-879.

Fetter, C.W., 1993. Contaminant hydrology. Prentice-Hall, 458 pp.

Fossing, H., Jørgensen, B.B., 1989. Measurement of bacterial sulfate reduction in sediments: Evaluation of a single-step chromium reduction method. Biogeochemistry, 8: 205-222.

Fredrickson, J.K., Zachara, J.M., Kennedy, D.W., Dong, H.L., Onstott, T.C., Hinman, N.W., Li, S.M., 1998. Biogenic iron mineralization accompanying the dissimilatory reduction of hydrous ferric oxide by a groundwater bacterium. Geochim. Cosmochim. Acta, 62(19-20): 3239-3257.

Frind, E.O., Hokkanen, G.E., 1987. Simulation of the Borden plume using the alternating direction Galerkin technique. Water Resour. Res., 23(5): 918-930.

Fukui, M., Suwa, Y., Urushigawa, Y., 1996. High survival efficiency and ribosomal RNA decaying pattern of Desulfobacter latus, a highly specific acetate-utilizing organism, during starvation. FEMS Microbiol. Ecol., 19(1): 17-25.

Gamo, M., Shoji, T., 1999. A method of profiling microbial communities based on a most-probable-number assay that uses BIOLOG plates and multiple sole carbon sources. Appl. Environ. Microbiol., 65(10): 4419-4424.

Garland, J.L., 1997. Analysis and interpretation of community-level physiological profiles in microbial ecology. FEMS Microbiol. Ecol., 24(4): 289-300.

Garland, J.L., Mills, A.L., 1991. Classification and characterization of heterotrophic microbial communities on the basis of patterns of community-level sole-carbon-source utilization. Appl. Environ. Microbiol., 57(8): 2351-2359.

Gelhar, L.W., 1986. Stochastic subsurface hydrology from theory to applications. Water Resour. Res., 22(9): 135S-145S.

Graf-Pannatier, E., Griffioen, J., Gerritse, J., 1999. Oxidation capacity of sediments in relation to biodegradation of toluene. In: B.C. Alleman, A. Leeson (Eds.), In situ and On-site Bioremediation Symp. Battelle Press, Columbus, Richland, San Diego, pp. 189-194.

Greenberg, J., Tomson, M., 1992. Precipitation and dissolution kinetics and equilibria of aqueous ferrous carbonate vs temperature. Appl. Geochem., 7(2): 185-190.

Griffioen, J., 1992. Cation-exchange and carbonate chemistry in aquifers following groundwater flow. PhD Thesis, Vrije Universiteit, Amsterdam, 182 pp.

Griffioen, J., 1999. Comment on 'Kinetic modelling of microbially-driven redox chemistry of subsurface environments: Coupling transport, microbial metabolism and geochemistry' by K.S. Hunter, Y. Wang and P. van Cappellen. J. Hydrol., 226(1-2): 121-124.

Griffioen, J., 2002. Drinkwaternormen, grondwater en Wet Bodembescherming: brug of kloof? H_2O(6): 17-19.

Griffioen, J., Broers, H.P., 1993. Characterization of sediment reactivity: the feasibility of sequential extraction techniques. Report OS-93-65A, TNO Institute of Applied Geoscience, Delft, the Netherlands.

Grossman, E.L., Cifuentes, L.A., Cozzarelli, I.M., 2002. Anaerobic methane oxidation in a landfill-leachate plume. Environ. Sci. Technol., 36(11): 2436-2442.

Haack, S.K., Garchow, H., Klug, M.J., Forney, L.J., 1995. Analysis of factors affecting the accuracy, reproducibility, and interpretation of microbial community carbon source utilization patterns. Appl. Environ. Microbiol., 61(4): 1458-1468.

Haas, J.R., Shock, E.L., 1999. Halocarbons in the environment: Estimates of thermodynamic properties for aqueous chloroethylene species and their stabilities in natural settings. Geochim. Cosmochim. Acta, 63(19-20): 3429-3441.

Hackley, K.C., Liu, C.L., Coleman, D.D., 1996. Environmental isotope characteristics of landfill leachates and gases. Ground Water, 34(5): 827-836.

Haldeman, D.L., Penny, S.A., Ringelberg, D., White, D.C., Garen, R.E., Ghiorse, W.C., 1995. Microbial growth and resuscitation alter community structure after perturbation. FEMS Microbiol. Ecol., 17(1): 27-37.

Hanert, H.H., 1991. The genus *Gallionella*. *In*: A. Balows, H.G. Truper, M. Dworkin, W. Harder, K.-H. Schleifer (Eds.), The prokaryotes. Springer-Verlag, New York, N.Y., pp. 4082-4088.

Hanson, R.S., Hanson, T.E., 1996. Methanotrophic bacteria. Microbiol. Rev., 60(2): 439-471.

Hartog, N., Griffioen, J., Van der Weijden, C.H., 2002. Distribution and reactivity of O-2-reducing components in sediments from a layered aquifer. Environ. Sci. Technol., 36(11): 2338-2344.

Heath, J.S., 1999. Introduction: Guidance on natural attenuation in soils and groundwater. J. Soil Contam., 8(1): 3-7.

Heider, J., Spormann, A.M., Beller, H.R., Widdel, F., 1998. Anaerobic bacterial metabolism of hydrocarbons. FEMS Microbiol. Rev., 22(5): 459-473.

Hemond, H.F., 1990. Acid neutralizing capacity, alkalinity, and acid-base status of natural-waters containing organic-acids. Environ. Sci. Technol., 24(10): 1486-1489.

Heron, G., 1994. Redox buffering in landfill leachate contaminated aquifers. Ph.D. Thesis, Institute of Environmental Science & Engineering, Technical University of Denmark, Lyngby.

Heron, G., Bjerg, P.L., Gravesen, P., Ludvigsen, L., Christensen, T.H., 1998. Geology and sediment geochemistry of a landfill leachate contaminated aquifer (Grindsted, Denmark). J. Contam. Hydrol., 29(4): 301-317.

Heron, G., Christensen, T.H., 1995. Impact of sediment-bound iron on redox buffering in a landfill leachate polluted aquifer (Vejen, Denmark). Environ. Sci. Technol., 29: 187-192.

Heron, G., Christensen, T.H., Tjell, J.C., 1994a. Oxidation capacity of aquifer sediments. Environ. Sci. Technol., 28(1): 153-158.

Heron, G., Crouzet, C., Bourg, A.C.M., Christensen, T.H., 1994b. Speciation of Fe(II) and Fe(III) in contaminated aquifer sediments using chemical extraction techniques. Environ. Sci. Technol., 28(9): 1698-1705.

Hoehler, T.M., Alperin, M.J., Albert, D.B., Martens, C.S., 1994. Field and laboratory studies of methane oxidation in an anoxic marine sediment: Evidence for a methanogen-sulfate reducer consortium. Global Biogeochem. Cycles, 8(4): 451-463.

Hoehler, T.M., Alperin, M.J., Albert, D.B., Martens, C.S., 1998. Thermodynamic control on hydrogen concentrations in anoxic sediments. Geochim. Cosmochim. Acta, 62(10): 1745-1756.

Hofer, M., Aeschbach-Hertig, W., Beyerle, U., Haderlein, S.B., Hoehn, E., Hofstetter, T.B., Johnson, A., Kipfer, R., Ulrich, A., Imboden, D.M., 1997. Tracers as essential tools for the investigation of physical and chemical processes in groundwater systems. Chimia, 51: 941-946.

Holm, P.E., Nielsen, P.H., Albrechtsen, H.-J., Christensen, T.H., 1992. Importance of unattached bacteria and bacteria attached to sediment in determining potentials for degradation of xenobiotic organic contaminants in an aerobic aquifer. Appl. Environ. Microbiol., 58(9): 3020-3026.

Horita, J., Zhang, C.L., 2001. Oak Ridge National Laboratory, USA. Personal communication.

Hornibrook, E.R.C., Longstaffe, F.J., Fyfe, W.S., 2000. Evolution of stable carbon isotope compositions for methane and carbon dioxide in freshwater wetlands and other anaerobic environments. Geochim. Cosmochim. Acta, 64(6): 1013-1027.

Howard, P.J.A., 1997. Analysis of data from BIOLOG plates: comments on the method of Garland and Mills. Soil. Biol. Biochem., 29(11-12): 1755-1757.

Hunter, K.S., Van Cappellen, P., 2000. Reply to 'Comment on kinetic modeling of microbially-driven redox chemistry of subsurface environments: coupling transport, microbial metabolism and geochemistry' by J. Griffioen. J. Hydrol., 227(1-4): 292-294.

Hunter, K.S., Wang, Y., Van Cappellen, P., 1998. Kinetic modeling of microbially-driven redox chemistry of subsurface environments: coupling transport, microbial metabolism and geochemistry. J. Hydrol., 209: 56-80.

Inskeep, W.P., Bloom, P.R., 1985. An evaluation of rate equations for calcite precipitation kinetics at pCO_2 less than 0.01 atm and pH greater than 8. Geochim. Cosmochim. Acta, 49: 2165-2180.

Inskeep, W.P., Bloom, P.R., 1986. Kinetics of calcite precipitation in the presence of water-soluble organic ligands. Soil Sci. Soc. Am. J., 50: 1167-1172.

Interventiewaarden, 2000. Circulaire streefwaarden en interventiewaarden bodemsanering, 4 februari 2000, nr. DBO, 1999226863. DG Milieubeheer Directie Bodem.

IPO, 2002. Natural attenuation en voormalige stortplaatsen. DUIV-kerngroep NAVOS. IPO-publicatienummer 141.

Islam, J., Singhal, N., O'Sullivan, M., 2001. Modeling biogeochemical processes in leachate-contaminated soils: A review. Transp. Porous Media, 43(3): 407-440.

Istok, J.D., Field, J.A., Schroth, M.H., 2001. In situ determination of subsurface microbial enzyme kinetics. Ground Water, 39(3): 348-355.

Istok, J.D., Humphrey, M.D., Schroth, M.H., Hyman, M.R., Oreilly, K.T., 1997. Single-well, "push-pull" test for in situ determination of microbial activities. Ground Water, 35(4): 619-631.

Jakobsen, R., Albrechtsen, H.-J., Rasmussen, M., Bay, H., Bjerg, P.L., Christensen, T.H., 1998. H_2 concentrations in a landfill leachate plume (Grindsted, Denmark): in situ energetics of terminal electron acceptor processes. Environ. Sci. Technol., 32(14): 2142-2148.

Jensen, D.L., Boddum, J.K., Tjell, J.C., Christensen, T.H., 2002. The solubility of rhodochrosite ($MnCO_3$) and siderite ($FeCO_3$) in anaerobic aquatic environments. Appl. Geochem., 17(4): 503-511.

Jetten, M.S.M., Strous, M., van de Pas-Schoonen, K.T., Schalk, J., van Dongen, U., van de Graaf, A.A., Logemann, S., Muyzer, G., van Loosdrecht, M.C.M., Kuenen, J.G., 1998. The anaerobic oxidation of ammonium. FEMS Microbiol. Rev., 22(5): 421-437.

Jones, I., Lerner, D.N., Baines, O.P., 1999. Multiport sock samplers: A low-cost technology for effective multilevel ground water sampling. Ground Water Monit. Remediat., 19(1): 134-142.

Jonker, H., van Breukelen, B.M., Groen, J., Volkering, F., 2002. Isotopen analyse bij onderzoek naar bodem- en grondwaterverontreinigingen. SV-206, SKB, Gouda, the Netherlands.

Kazmierczak, T.F., Tomson, M.B., Nancollas, G.H., 1982. Crystal growth of calcium carbonate. A controlled composition kinetic study. J. Phys. Chem., 86: 103-107.

Keating, E.H., Bahr, J.M., 1998. Reactive transport modeling of redox geochemistry: Approaches to chemical disequilibrium and reaction rate estimation at a site in northern Wisconsin. Water Resour. Res., 34(12): 3573-3584.

Kehew, A.E., Passero, R.N., 1990. pH and redox buffering mechanisms in a glacial drift aquifer contaminated by landfill leachate. Ground Water, 28: 728-737.

Kemp, P.F., 1995. Can we estimate bacterial growth rates from ribosomal RNA content? *In*: I. Joint (Ed.), Molecular ecology of aquatic microbes. Springer-Verlag, Berlin, Germany, pp. 279-302.

Kilb, B., Kuhlmann, B., Eschweiler, B., Preuss, G., Ziemann, E., Schottler, U., 1998. Community structures of different groundwater habitats investigated using methods of molecular biology. Acta Hydrochim. Hydrobiol., 26(6): 349-354.

Kjeldsen, P., Christophersen, M., 2001. Composition of leachate from old landfills in Denmark. Waste Manage. Res., 19(3): 249-256.

Kleikemper, J., Schroth, M.H., Sigler, W.V., Schmucki, M., Bernasconi, S.M., Zeyer, J., 2002. Activity and diversity of sulfate-reducing bacteria in a petroleum hydrocarbon-contaminated aquifer. Appl. Environ. Microbiol., 68(4): 1516-1523.

Koch, D., Grupe, M., 1993. Heavy-metal sorption of a new developed porous borosilicate glass suction cup. Z. Pflanzen. Bodenk., 156(1): 95-96.

Konert, M., Vandenberghe, J., 1997. Comparison of laser grain size analysis with pipette and sieve analysis: a solution for the underestimation of the clay fraction. Sedimentology, 44: 523-535.

Krouse, H.R., Mayer, B., 2000. Sulphur and oxygen isotopes in sulphate. *In*: P. Cook, A.L. Herczeg (Eds.), Environmental tracers in subsurface hydrology. Kluwer Academic Publishers, Boston, pp. 195-231.

Krug, M.N., Ham, R.K., 1997. Analysis of long-term leachate characteristics. In: T.H. Christensen, R. Cossu, R. Stegmann (Eds.), Proceedings Sardinia 97, Sixth International Landfill Symposium. CISA, Cagliari, Italy, S. Margherita di Pula, Cagliari, Italy, pp. 117-131.

Krumholz, L.R., Caldwell, M.E., Suflita, J.M., 1996. Biodegradation of 'BTEX' hydrocarbons under anaerobic conditions. *In*: R.L. Crawford, D.L. Crawford (Eds.), Bioremediation: Principles and Applications. Cambridge University Press, UK, pp. 61-99.

Liu, C.G., Zachara, J.M., Gorby, Y.A., Szecsody, J.E., Brown, C.F., 2001a. Microbial reduction of Fe(III) and sorption/precipitation of Fe(II) on Shewanella putrefaciens strain CN32. Environ. Sci. Technol., 35(7): 1385-1393.

Liu, C.X., Kota, S., Zachara, J.M., Fredrickson, J.K., Brinkman, C.K., 2001b. Kinetic analysis of the bacterial reduction of goethite. Environ. Sci. Technol., 35(12): 2482-2490.

Lloyd-Jones, G., Lau, P.C.K., 1998. A molecular view of microbial diversity in a dynamic landfill in Quebec. FEMS Microbiol. Lett., 162(2): 219-226.

Lonergan, D.J., Jenter, H.L., Coates, J.D., Phillips, E.J.P., Schmidt, T.M., Lovley, D.R., 1996. Phylogenetic analysis of dissimilatory Fe(III)-reducing bacteria. J. Bacteriol., 178(8): 2402-2408.

Lovley, D.R., 1995. Bioremediation of organic and metal contaminants with dissimilatory metal reduction. J. Ind. Microbiol., 14(2): 85-93.

Lovley, D.R., 1997a. Microbial Fe(III) reduction in subsurface environments. FEMS Microbiol. Rev., 20: 305-313.

Lovley, D.R., 1997b. Potential for anaerobic bioremediation of BTEX in petroleum-contaminated aquifers. J. Ind. Microbiol. Biotechnol., 18(2-3): 75-81.

Lovley, D.R., 2000. Anaerobic benzene degradation. Biodegradation, 11(2-3): 107-116.

Lovley, D.R., 2001. Bioremediation - Anaerobes to the rescue. Science, 293(5534): 1444-1446.

Lovley, D.R., Anderson, R.T., 2000. Influence of dissimilatory metal reduction on fate of organic and metal contaminants in the subsurface. Hydrogeol. J., 8(1): 77-88.

Lovley, D.R., Baedecker, M.J., Lonergan, D.J., Cozzarelli, I.M., Philips, E.J.P., Siegel, D.I., 1989. Oxidation of aromatic contaminants coupled to microbial iron reduction. Nature, 339: 297-300.

Lovley, D.R., Fraga, J.L., Blunt-Harris, E.L., Hayes, L.A., Phillips, E.J.P., Coates, J.D., 1998. Humic substances as a mediator for microbially catalyzed metal reduction. Acta Hydrochim. Hydrobiol., 26(3): 152-157.

Lovley, D.R., Goodwin, S., 1988. Hydrogen concentrations as an indicator of the predominant terminal electron-accepting reaction in aquatic sediments. Geochim. Cosmochim. Acta, 52: 2993-3003.

Lovley, D.R., Phillips, E.J.P., 1986. Availability of ferric iron for microbial reduction in bottom sediments of the freshwater tidal Potomac river. Appl. Environ. Microbiol., 52(4): 751-757.

Ludvigsen, L., Albrechtsen, H.J., Heron, G., Bjerg, P.L., Christensen, T.H., 1998. Anaerobic microbial redox processes in a landfill leachate contaminated aquifer (Grindsted, Denmark). J. Contam. Hydrol., 33(3-4): 273-291.

Ludvigsen, L., Albrechtsen, H.J., Holst, H., Christensen, T.H., 1997. Correlating phospholipid fatty acids (PLFA) in a landfill leachate polluted aquifer with biogeochemical factors by multivariate statistical methods. FEMS Microbiol. Rev., 20(3-4): 447-460.

Ludvigsen, L., Albrechtsen, H.J., Ringelberg, D.B., Ekelund, F., Christensen, T.H., 1999. Distribution and composition of microbial populations in landfill leachate contaminated aquifer (Grindsted, Denmark). Microb. Ecol., 37(3): 197-207.

Lyngkilde, J., Christensen, T.H., 1992a. Fate of organic contaminants in the redox zones of a landfill leachate pollution plume (Vejen, Denmark). J. Contam. Hydrol., 10: 291-307.

Lyngkilde, J., Christensen, T.H., 1992b. Redox zones of a landfill leachate pollution plume (Vejen, Denmark). J. Contam. Hydrol., 10: 273-289.

MacDonald, J.A., 2000. Evaluating natural attenuation for groundwater cleanup. Environ. Sci. Technol., 34(15): 346A-353A.

Madsen, E.L., 2000. Nucleic-acid characterization of the identity and activity of subsurface microorganisms. Hydrogeol. J., 8(1): 112-125.

Mancini, S.A., Lacrampe-Couloume, G., Jonker, H., Van Breukelen, B.M., Groen, J., Volkering, F., Lollar, B.S., 2002. Hydrogen isotopic enrichment: An indicator of biodegradation at a petroleum hydrocarbon contaminated field site. Environ. Sci. Technol., 36(11): 2464-2470.

Matson, J.V., Schuhmann, R.J., 1999. Natural attenuation as a remedy not as an excuse. Journal of Soil Contamination, 8(1): 29-33.

Matsunaga, T., Karametaxas, G., Vongunten, H.R., Lichtner, P.C., 1993. Redox chemistry of iron and manganese minerals in river- recharged aquifers - a model interpretation of a column experiment. Geochim. Cosmochim. Acta, 57(8): 1691-1704.

Mayer, K.U., Benner, S.G., Frind, E.O., Thornton, S.F., Lerner, D.N., 2001. Reactive transport modeling of processes controlling the distribution and natural attenuation of phenolic compounds in a deep sandstone aquifer. J. Contam. Hydrol., 53(3-4): 341-368.

McCarty, P.L., 1971. Energetics and bacterial growth. *In*: S.D. Faust, J.V. Hunter (Eds.), Organic compounds in aquatic environments. Marcel Dekker, New York, pp. 495-531.

McNeill, J.D., 1980. Electromagnetic terrain conductivity measurement at low induction numbers. Technical Note TN-6, Geonics Limited, Mississauga, Ontario, Canada.

Mook, W.G., 2000. Environmental isotopes in the hydrological cycle. Principles and applications. Volume I. Introduction: Theory, Methods, Review. UNESCO/IAEA, 280 pp.

Murphy, E.M., Ginn, T.R., 2000. Modeling microbial processes in porous media. Hydrogeol. J., 8(1): 142-158.

Murphy, E.M., Schramke, J.A., 1998. Estimation of microbial respiration rates in groundwater by geochemical modeling constrained with stable isotopes. Geochim. Cosmochim. Acta, 62(21-22): 3395-3406.

Muyzer, G., Dewaal, E.C., Uitterlinden, A.G., 1993. Profiling of complex microbial populations by denaturing gradient gel electrophoresis analysis of polymerase chain reaction-amplified genes coding for 16S rRNA. Appl. Environ. Microbiol., 59(3): 695-700.

Nancollas, G.H., 1979. The growth of crystals in solution. Adv. Colloid Interface Sci., 10: 215-252.

Nauhaus, K., Boetius, A., Kruger, M., Widdel, F., 2002. In vitro demonstration of anaerobic oxidation of methane coupled to sulphate reduction in sediment from a marine gas hydrate area. Environ. Microbiol., 4(5): 296-305.

Nealson, K.H., Cox, B.L., 2002. Microbial metal-ion reduction and Mars: extraterrestrial expectations? Curr. Opin. Microbiol., 5(3): 296-300.

Newman, D.K., Banfield, J.F., 2002. Geomicrobiology: How molecular-scale interactions underpin biogeochemical systems. Science, 296(5570): 1071-1077.

Nicholson, R.V., Cherry, J.A., Reardon, E.J., 1983. Migration of contaminants in groundwater at a landfill: a case study, 6. Hydrogeochemistry. J. Hydrol., 63: 131-176.

Nobes, D.C., Armstrong, M.J., Close, M.E., 2000. Delineation of a landfill leachate plume and flow channels in coastal sands near Christchurch, New Zealand, using a shallow electromagnetic survey method. Hydrogeol. J., 8(3): 328-336.

Novarino, G., Warren, A., Butler, H., Lambourne, G., Boxshall, A., Bateman, J., Kinner, N.E., Harvey, R.W., Mosse, R.A., Teltsch, B., 1997. Protistan communities in aquifers: a review. FEMS Microbiol. Rev., 20(3-4): 261-275.

NRC, 2000. Natural attenuation for groundwater remediation. National Academy Press, Washington, DC.

Odermatt, J.R., 1999. Remediation by natural attenuation? Ground Water Monit. Remediat., 19(3): 58-60.

O'Steen, B., 1999. EPA Region 4 perspective on the OSWER monitored natural attenuation policy. J. Soil Contam., 8(1): 17-22.

Øvreås, L., Forney, L., Daae, F.L., Torsvik, V., 1997. Distribution of bacterioplankton in meromictic Lake Saelenvannet, as determined by denaturing gradient gel electrophoresis of PCR-amplified gene fragments coding for 16S rRNA. Appl. Environ. Microbiol., 63(9): 3367-3373.

Parkhurst, D.L., Appelo, C.A.J., 1999. User's guide to PHREEQC (Version 2): a computer program for speciation, batch-reaction, one-dimensional transport, and inverse geochemical calculations. Water-Resources Investigations Report 99-4259, U.S. Geol. Survey.

Phillips, C.J., Harris, D., Dollhopf, S.L., Gross, K.L., Prosser, J.I., Paul, E.A., 2000. Effects of agronomic treatments on structure and function of ammonia-oxidizing communities. Appl. Environ. Microbiol., 66(12): 5410-5418.

Pickens, J.F., Cherry, J.A., Grisak, G.E., Merritt, W.F., Risto, B.A., 1978. A multilevel device for groundwater sampling and piezometric monitoring. Ground Water, 16(5): 322-327.

Pitkin, S.E., Cherry, J.A., Ingleton, R.A., Broholm, M., 1999. Field demonstrations using the Waterloo ground water profiler. Ground Water Monit. Remediat., 19(2): 122-131.

Plummer, L.N., Prestemon, E.C., Parkhurst, D.L., 1994. An interactive code (NETPATH) for modeling NET geochemical reactions along a flow PATH-Version 2.0. Water-Resources Investigations Report 94-4169, U.S. Geol. Survey.

Plummer, L.N., Wigley, T.M.L., Parkhurst, D.L., 1978. The kinetics of calcite dissolution in CO_2 water systems at 5 °C to 60 °C and 0.0 to 1.0 atm CO_2. Am. J. Sci., 278: 179-216.

Pombo, S.A., Pelz, O., Schroth, M.H., Zeyer, J., 2002. Field-scale ^{13}C-labeling of phospholipid fatty acids (PLFA) and dissolved inorganic carbon: tracing acetate assimilation and mineralization in a petroleum hydrocarbon-contaminated aquifer. FEMS Microb. Ecol., 41: 259-267.

Postma, D., Boesen, C., Kristiansen, H., Larsen, F., 1991. Nitrate reduction in an unconfined sandy aquifer - water chemistry, reduction processes, and geochemical modeling. Water Resour. Res., 27(8): 2027-2045.

Postma, D., Jakobsen, R., 1996. Redox zonation: Equilibrium constraints on the Fe(III)/SO_4-reduction interface. Geochim. Cosmochim. Acta, 60(17): 3169-3175.

Prommer, H., Davis, G.B., Barry, D.A., 1999. Geochemical changes during biodegradation of petroleum hydrocarbons: field investigations and biogeochemical modelling. Org. Geochem., 30(6): 423-435.

Puls, R.W., Paul, C.J., 1997. Multi-layer sampling in conventional monitoring wells for improved estimation of vertical contaminant distributions and mass. J. Contam. Hydrol., 25(1-2): 85-111.

Radajewski, S., Ineson, P., Parekh, N.R., Murrell, J.C., 2000. Stable-isotope probing as a tool in microbial ecology. Nature, 403: 646-649.

Rademaker, J.L.W., Louws, F.J., Rossbach, U., Vinuesa, P., de Bruijn, F.J., 1999. Computer-assisted pattern analysis of molecular fingerprints and database construction. *In*: A.D.L. Akkermans, J.D. van Elsas, F.J. de Bruijn (Eds.), Molecular microbial ecology manual. Kluwer Academic Publishers, Dordrecht, the Netherlands, pp. 7.1.3/1-7.1.3/33.

Renner, R., 2000. Natural attenuation's popularity outpaces scientific support, NRC finds. Environ. Sci. Technol., 34(9): 203A-204A.

Reusser, D.E., Istok, J.D., Beller, H.R., Field, J.A., 2002. In situ transformation of deuterated toluene and xylene to benzylsuccinic acid analogues in BTEX-contaminated aquifers. Environ. Sci. Technol., 36(19): 4127-4134.

Revesz, K., Coplen, T.B., Baedecker, M.J., Glynn, P.D., Hult, M., 1995. Methane production and consumption monitored by stable H and C isotope ratios at a crude oil spill site, Bemidji, Minnesota. Appl. Geochem., 10(5): 505-516.

Rittmann, B.E., van Briesen, J.M., 1996. Microbiological processes in reactive modeling. *In*: P.C. Lichtner, C.I. Steefel, E.H. Oelkers (Eds.), Reactive transport in porous media. Reviews in mineralogy. Mineral. Soc. Am. Rev. Mineral., Washington, pp. 311-334.

Roden, E.E., Urrutia, M.M., 1999. Ferrous iron removal promotes microbial reduction of crystalline iron(III) oxides. Environ. Sci. Technol., 33(11): 1847-1853.

Roden, E.E., Zachara, J.M., 1996. Microbial reduction of crystalline iron(III) oxides: Influence of oxide surface area and potential for cell growth. Environ. Sci. Technol., 30(5): 1618-1628.

Röling, W.F.M., Van Breukelen, B.M., Braster, M., Goeltom, M.T., Groen, J., Van Verseveld, H.W., 2000a. Analysis of microbial communities in a landfill leachate polluted aquifer using a new method for anaerobic physiological profiling and 16S rDNA based fingerprinting. Microb. Ecol., 40(3): 177-188.

Röling, W.F.M., Van Breukelen, B.M., Braster, M., Lin, B., Van Verseveld, H.W., 2001. Relationships between microbial community structure and hydrochemistry in a landfill leachate-polluted aquifer. Appl. Environ. Microbiol., 67(10): 4619-4629.

Röling, W.F.M., Van Breukelen, B.M., Braster, M., Van Verseveld, H.W., 2000b. Linking microbial community structure to pollution: Biolog-substrate utilization in and near a landfill leachate plume. Water Sci. Technol., 41(12): 47-53.

Röling, W.F.M., Van Verseveld, H.W., 2002. Natural attenuation: What does the subsurface have in store? Biodegradation, 13(1): 53-64.

Romanek, C.S., Grossman, E.L., Morse, J.W., 1992. Carbon isotopic fractionation in synthetic aragonite and calcite - effects of temperature and precipitation rate. Geochim. Cosmochim. Acta, 56(1): 419-430.

Ronen, D., Berkowitz, B., Magaritz, M., 1989. The development and influence of gas-bubbles in phreatic aquifers under natural flow conditions. Transp. Porous Media, 4(3): 295-306.

Rooney-Varga, J.N., Anderson, R.T., Fraga, J.L., Ringelberg, D., Lovley, D.R., 1999. Microbial communities associated with anaerobic benzene degradation in a petroleum-contaminated aquifer. Appl. Environ. Microbiol., 65(7): 3056-3063.

Rügge, K., Bjerg, P.L., Christensen, T.H., 1995. Distribution of organic compounds from municipal solid waste in the groundwater downgradient of a landfill (Grindsted, Vejen). Environ. Sci. Technol., 29(5): 1395-1400.

Schaal, K.P., 1991. The genera *Actinomyces, Arcanobacterium*, and *Rothia*. *In*: A. Balows, H.G. Truper, M. Dworkin, W. Harder, K.-H. Schleifer (Eds.), The prokaryotes. Springer-Verlag, New York, N.Y., pp. 850-905.

Schäfer, D., Schäfer, W., Kinzelbach, W., 1998. Simulation of reactive processes related to biodegradation in aquifers - 2. Model application to a column study on organic carbon degradation. J. Contam. Hydrol., 31(1-2): 187-209.

Schink, B., 1997. Energetics of syntrophic cooperation in methanogenic degradation. Microbiol. Molecular Biol. Rev., 61(2): 262-280.

Schirmer, M., Durrant, G.C., Molson, J.W., Frind, E.O., 2001. Influence of transient flow on contaminant biodegradation. Ground Water, 39(2): 276-282.

Schmidt, I., Sliekers, O., Schmid, M., Cirpus, I., Strous, M., Bock, E., Kuenen, J.G., Jetten, M.S.M., 2002. Aerobic and anaerobic ammonia oxidizing bacteria competitors or natural partners? FEMS Microbiol. Ecol., 39(3): 175-181.

Schulz, S., Conrad, R., 1996. Influence of temperature on pathways to methane production in the permanently cold profundal sediment of lake Constance. FEMS Microbiol. Ecol., 20(1): 1-14.

Sinke, A.J.C., Heimovaara, T.J., Tonnaer, H., Ter Meer, J., 2001. Beslissingsondersteunend systeem voor de beoordeling van natuurlijke afbraak als saneringsvariant. Versie 2.0. NOBIS 98-1-21. 42 pp.

Smets, B.F., Siciliano, S.D., Verstraete, W., 2002. Natural attenuation: extant microbial activity forever and ever? Environ. Microbiol., 4(6): 315-317.

Smith, R.L., Harris, S.H., Suflita, J., 2002. Comparison of hydrogen consumption kinetics in two contaminated aquifers (Cape Cod, MA and Norman, OK) using single well injection tests. In: H.-J. Albrechtsen, J. Aamand (Eds.), International Symposium on Subsurface Microbiology, Copenhagen, Denmark, p. 20.

Smith, R.L., Howes, B.L., Garabedian, S.P., 1991. Insitu measurement of methane oxidation in groundwater by using natural-gradient tracer tests. Appl. Environ. Microbiol., 57(7): 1997-2004.

Snoeyenbos-West, O.L., Nevin, K.P., Anderson, R.T., Lovley, D.R., 2000. Enrichment of *Geobacter* species in response to stimulation of Fe(III) reduction in sandy aquifer sediments. Microbial. Ecol., 39(2): 153-167.

Sorensen, K.B., Finster, K., Ramsing, N.B., 2001. Thermodynamic and kinetic requirements in anaerobic methane oxidizing consortia exclude hydrogen, acetate, and methanol as possible electron shuttles. Microb. Ecol., 42(1): 1-10.

Stouthamer, A.H., Bulthuis, B.A., Van Verseveld, H.W., 1990. Energetics of growth at low growth rates and its relevance for the maintenance concept. *In:* Microbial growth dynamics, SGM Special Publications 28, pp. 85-102.

Straub, K.L., Benz, M., Schink, B., 2001. Iron metabolism in anoxic environments at near neutral pH. FEMS Microbiol. Ecol., 34(3): 181-186.

Strebel, O., Böttcher, J., Fritz, P., 1990. Use of isotope fractionation of sulfate-sulfur and sulfate-oxygen to assess bacterial desulfurication in a sandy aquifer. J. Hydrol., 121(1-4): 155-172.

Stumm, W., Morgan, J.J., 1996. Aquatic chemistry: chemical equilibria and rates in natural waters. John Wiley & Sons, Inc.

Suflita, J.M., Gerba, C.P., Ham, R.K., Palmisano, A.C., Rathje, W.L., Robinson, J.A., 1992. The worlds largest landfill - a multidisciplinary investigation. Environ. Sci. Technol., 26(8): 1486-1495.

Swett, G.H., Rapaport, D., 1998. Natural attenuation: Is the fit right? Chem. Eng. Prog., 94(6): 37-43.

Thamdrup, B., Dalsgaard, T., 2002. Production of N-2 through anaerobic ammonium oxidation coupled to nitrate reduction in marine sediments. Appl. Environ. Microbiol., 68(3): 1312-1318.

Thomas, G.W., 1982. Exchangeable cations. *In*: R.H. Miller, D.R. Keeny (Eds.), Methods of soil analysis, Part 2. Chemical and microbiological properties. ASA-SSSA, Madison, USA, pp. 159-165.

Thonnard, N., 2000. University of Tennessee, USA. Personal communication.

Tipping, E., Hurley, M.A., 1992. A unifying model of cation binding by humic substances. Geochim. Cosmochim. Acta, 56(10): 3627-3641.

Tweede Kamer der Staten-Generaal, 1997. Vergaderjaar 1996-1997, 25411, nr 1.

UNEP, 1999. Global Environmental Outlook 2000, Nairobi, Kenya.

Urbach, E., Vergin, K.L., Giovannoni, S.J., 1999. Immunochemical detection and isolation of DNA from metabolically active bacteria. Appl. Environ. Microbiol., 65(3): 1207-1213.

Valentine, D.L., Reeburgh, W.S., 2000. New perspectives on anaerobic methane oxidation. Environ. Microbiol., 2(5): 477-484.

Van Breukelen, B.M., Appelo, C.A.J., Olsthoorn, T.N., 1998. Hydrogeochemical transport modeling of 24 years of Rhine water infiltration in the dunes of the Amsterdam water supply. J. Hydrol., 209(1-4): 281-296.

Van Breukelen, B.M., Griffioen, J. Biogeochemical processes at the fringe of a landfill leachate pollution plume: Potential for dissolved organic carbon, CH_4, NH_4^+, Fe(II), and Mn(II) oxidation. submitted to J. Contam. Hydrol.

Van Breukelen, B.M., Griffioen, J., Röling, W.F.M., Van Verseveld, H.W. Reactive transport modelling of biogeochemical processes and carbon isotope geochemistry inside a landfill leachate plume. submitted to J. Contam. Hydrol.

Van Breukelen, B.M., Röling, W.F.M., Groen, J., Griffioen, J., Van Verseveld, H.W. Biogeochemistry and isotope geochemistry of a landfill leachate plume. J. Contam. Hydrol. (in press)

Van Cappellen, P., Wang, Y., 1995. Metal cycling in surface sediments: modeling the interplay of transport and reaction. *In*: H.E. Allen (Ed.), Metal contaminated aquatic sediments. Ann Arbor Press, Chelsea, Michigan, pp. 21-64.

Van der Lee, J., De Windt, L., 2001. Present state and future directions of modeling of geochemistry in hydrogeological systems. J. Contam. Hydrol., 47(2-4): 265-282.

Van der Meer, J.R., Werlen, C., Nishino, S.F., Spain, J.C., 1998. Evolution of a pathway for chlorobenzene metabolism leads to natural attenuation in contaminated groundwater. Appl. Environ. Microbiol., 64(11): 4185-4193.

Van Kasteren, J., 1999. Hergebruik van stortplaatsen? ROM Magazine(3): 4-6.

Van Verseveld, H.W., Van Breukelen, B.M., Röling, W.F.M., Braster, M., Soeteman, A.A., Groen, J., 1999. In situ bioremediation at old Dutch landfills: plume delineation, intrinsic degradation capacity and determination of microbial community structure. In: C.D. Johnston (Ed.), Contaminated site remediation: challenges posed by urban and industrial contaminanants. Centre for Groundwater Studies, CSIRO, Wembley, W.A., Australia, pp. 415-424.

Vilomet, J.D., Angeletti, B., Moustier, S., Ambrosi, J.P., Wiesner, M., Bottero, J.Y., Chatelet-Snidaro, L., 2001. Application of strontium isotopes for tracing landfill leachate plumes in groundwater. Environ. Sci. Technol., 35(23): 4675-4679.

Von Wintzingerode, F., Gobel, U.B., Stackebrandt, E., 1997. Determination of microbial diversity in environmental samples: pitfalls of PCR-based rRNA analysis. FEMS Microbiol. Rev., 21(3): 213-229.

Vukovic, M., Soro, A., 1992. Determination of hydraulic conductivity of porous media from grain-size composition. Water Resources Publications, Littleton, Colorado, USA, 82 pp.

Wajon, J.E., Ho, G.-E., Murphy, P.J., 1985. Rate of precipitation of ferrous iron and formation of mixed iron-calcium carbonates by naturally occurring carbonate materials. Water Res., 19(7): 831-837.

Waterleidingbesluit, 2001. Staatsblad van het Koninkrijk der Nederlanden, nr. 31.

Wenzel, W.W., Sletten, R.S., Brandstetter, A., Wieshammer, G., Stingeder, G., 1997. Adsorption of trace metals by tension lysimeters: Nylon membrane vs. porous ceramic cup. J. Environ. Qual., 26(5): 1430-1434.

Wessel-Bothe, S., Patzold, S., Klein, C., Behre, G., Welp, G., 2000. Sorption of pesticides and DOC on glass and ceramic suction cups. J. Plant Nutr. Soil Sci.-Z. Pflanzenernahr. Bodenkd., 163(1): 53-56.

Whitman, W.B., Coleman, D.C., Wiebe, W.J., 1998. Prokaryotes: The unseen majority. Proc. Natl. Acad. Sci. USA, 95(12): 6578-6583.

Wiedemeier, T.H., Wilson, J.T., Kampbell, D.H., Miller, R.N., Hansen, J.E., 1995. Technical protocol for implementing intrinsic remediation with long-term monitoring for natural attenuation of fuel contamination dissolved in groundwater, U.S. Air Force Center for Environmental Excellence, Technology Transfer Division, Brooks Air Force Base, San Antonio, Texas.

Williams, G.M., 1999. Natural attenuation of leachate - letting nature take its course (Reprinted from Trans. Instn Min. Metall., vol 108, 1999). Tran. Inst. Min. Metall. Sect. B-App. Earth Sci., 108: B33-B37.

Woldt, W.E., Hagemeister, M.E., Jones, D.D., 1998. Characterization of an unregulated landfill using surface-based geophysics and geostatistics. Ground Water, 36(6): 966-974.

Yager, R.M., Fountain, J.C., 2001. Effect of natural gas exsolution on specific storage in a confined aquifer undergoing water level decline. Ground Water, 39(4): 517-525.

Zachara, J.M., Kukkadapu, R.K., Fredrickson, J.K., Gorby, Y.A., Smith, S.C., 2002. Biomineralization of poorly crystalline Fe(III) oxides by dissimilatory metal reducing bacteria (DMRB). Geomicrobiol. J., 19(2): 179-207.

Zak, J.C., Willig, M.R., Moorhead, D.L., Wildman, H.G., 1994. Functional diversity of microbial communities - a quantitative approach. Soil Biol. Biochem., 26(9): 1101-1108.

Zhang, C.L., Horita, J., Cole, D.R., Zhou, J.Z., Lovley, D.R., Phelps, T.J., 2001. Temperature-dependent oxygen and carbon isotope fractionations of biogenic siderite. Geochim. Cosmochim. Acta, 65(14): 2257-2271.

Zhou, J.Z., Fries, M.R., Cheesanford, J.C., Tiedje, J.M., 1995. Phylogenetic analyses of a new group of denitrifiers capable of anaerobic growth on toluene and description of *Azoarcus tolulyticus* sp nov. Int. J. Syst. Bact., 45(3): 500-506.

Zwillich, T., 2000. Hazardous waste cleanup - A tentative comeback for bioremediation. Science, 289(5488): 2266-2267.

SAMENVATTING

Natural attenuation van vuilstort perkolaat: een gecombineerde biogeochemische proces analyse en microbiële ecologie benadering

Sanering van verontreinigde locaties met conventionele technieken zoals het afgraven van grond in combinatie met reiniging of gecontroleerde opslag, oppompen van grondwater en zuivering, of het isoleren van vervuiling, zijn duur en vaak weinig effectief. De gehele saneringsoperatie loopt daardoor aanzienlijke vertraging op. Dit belemmert landinrichtingsplannen en heeft verdere verspreiding van vervuiling naar het grondwater tot gevolg. Onderzoek heeft aangetoond dat vele soorten organische verontreinigingen onder specifieke omstandigheden biologisch afbreekbaar zijn. De afbreekbaarheid is sterk gerelateerd aan de redox condities (aeroob, denitrificerend, ijzer-/mangaan-reducerend, sulfaat-reducerend of methanogeen). Afbraak door micro-organismen in combinatie met processen zoals verdunning en sorptie aan bodemdeeltjes leidt tot een afname van concentratie in de stromingsrichting van het grondwater. Dit verschijnsel wordt "natural attenuation"(letterlijk: natuurlijke afneming) genoemd. Natural attenuation (NA) kan na verloop van tijd tot een evenwichtssituatie leiden waardoor verdere verspreiding niet plaatsvindt. Indien NA voldoende sterk is en een ontstane evenwichtssituatie toelaatbaar is, kan dit een aanzienlijke reductie in saneringskosten opleveren (geschat op enkele miljarden € voor de 3800 voormalige vuilstorten in Nederland). De kennis over NA is echter nog te beperkt om met enige zekerheid de ontwikkeling van een pluim van grondwaterverontreiniging te kunnen voorspellen. Het in de gaten houden van een pluim door middel van monitoring blijft dan ook noodzakelijk.

Dit proefschrift heeft als doel om de kennis over NA van vuilstort perkolaat pluimen te vergroten. Hiertoe is een combinatie van biogeochemische proces analyse en microbieel ecologisch onderzoek uitgevoerd bij de voormalige Banisveld vuilstort, nabij Boxtel in Noord-Brabant, in de periode 1998-2002. Vuilstort perkolaat water ontstaat doordat stoffen uit de stort oplossen in infiltrerend regenwater. Het lekken van perkolaat water uit de stort leidt tot de vorming van een perkolaat pluim in het grondwater. Perkolaat water bevat hoge concentraties organisch koolstof (TOC), inorganisch koolstof, ammonium en methaan ten gevolge van biologische afbraak van organisch materiaal in de stort, alsmede zouten en mogelijk een cocktail van organische microverontreinigingen (voornamelijk benzeen, tolueen, ethylbenzeen, xyleen (BTEX) en naftaleen). Een verbeterde kennis over

de (duurzaamheid van) biogeochemische (afbraak) processen, de snelheidsbepalende factoren, en de betrokken micro-organismen is nodig om de ontwikkeling van perkolaat pluimen te kunnen voorspellen en om te kunnen beoordelen of NA een geschikte saneringsoptie kan zijn voor nazorg van voormalige vuilstortplaatsen.

In hoofdstuk 2 worden de biogeochemische processen onderzocht die resulteerden in een stroomafwaartse verbetering in samenstelling van de vuilstort perkolaat pluim. De geofysische technieken EM-34 en geleidbaarheid sonderingen werden toegepast om de pluim te kunnen uitkarteren en monstername te optimaliseren. Diverse metingen zijn verricht (waterstof-gas concentraties en de concentraties en stabiele isotopen van oxidanten en reductanten) om de redox condities in de pluim te kunnen bepalen. Afbraak van TOC bleek gekoppeld te zijn aan microbiële reductie van ijzer-oxiden. Dit wordt weerspiegeld in de dominantie van ijzer-reducerende micro-organismen van de familie *Geobacteraceae* in de pluim (hoofdstuk 4). Stabiele isotopen analyse bevestigde dat methanogenese niet optreedt in de pluim, maar dat methaan afkomstig is uit de stort.

De microbiële ecologie van de aquifer is met verschillende technieken onderzocht: microbiële gemeenschaps analyse op basis van fysiologische respons in ECO-Biolog platen (in vervolg CLPP genoemd, ofwel Community Level Physiological Profiling) in hoofdstuk 3 en PCR-DGGE (Polymerase Ketting Reactie - Denaturing Gradiënt Gel Electroforese; DNA profielen) gericht op 16S ribosomale RNA genen, om de diversiteit van de microbiële gemeenschappen zichtbaar te maken in hoofdstuk 4. Van een drietal locaties is de base volgorde van gekloneerd 16S rDNA bepaald (sequencing) om te kunnen vaststellen welke micro-organismen in het grondwater aanwezig waren. Zowel CLPP als PCR-DGGE profielen van *Bacteria* en *Archaea* waren duidelijk verschillend binnen en buiten de pluim. De metabolische potentie gemeten met CLPP was hoger in de pluim dan in onvervuild grondwater. De gemeenschapsstructuur in de pluim bleek in stroomafwaartse richting enigszins te veranderen, hoewel de variatie groot was. De verhoogde metabolische potentie gemeten met CLPP bleef echter gelijk. De met sediment geassocieerde gemeenschapsstructuur was verschillend van die in grondwater en minder beïnvloed door het perkolaat. Schoon en onvervuild grondwater worden door verschillende *Bacteria* klassen gedomineerd. Metabole eigenschappen zijn in overeenstemming met redox condities: potentieel denitrificerende bacteriën in schoon nitraat bevattend grondwater stroomopwaarts van de stort, ijzer-reducerende bacteriën van de *Geobacteraceae* familie in de pluim van vervuiling.

In hoofdstuk 2, 5 en 6 worden modellen - gemaakt met de PHREEQC code - toegepast om het biogeochemische reactie netwerk te kunnen ontrafelen en te kwantificeren. Een eenvoudig invers geochemisch model, gekalibreerd op de perkolaat samenstelling aan de bron en het front van de pluim, bevestigde de dominantie van ijzer-reductie (hoofdstuk 2). In hoofdstuk 5 wordt een complexer reactief transport model gebruikt om de hydrogeochemische veranderingen in de stromingsrichting te simuleren. Verscheidende secondaire geochemische processen blijken zich af te spelen: kinetische neerslag van calciet en sideriet, cation-uitwisseling, proton-buffering en ontgassing van methaan. Neerslag van sideriet maskeert het optreden van ijzer-reductie. De Fe(II) concentratie is daardoor weinig diagnostisch voor ijzer reductie. Model parameters werden geoptimaliseerd door mid-

del van kalibratie met het niet-lineaire optimalisatie programma PEST. De snelheid van sideriet en calciet precipitatie was laag en dit is vermoedelijk een gevolg van afwezigheid van deze mineralen in de onvervuilde aquifer, inhibitie door fulvozuren in perkolaat en de lage temperatuur van grondwater. Modelleren van de koolstof-13 isotopen geochemie kon het reactienetwerk onafhankelijk bevestigen. Het expliciet modelleren van populatie groei van ijzer-reducerende microorganismen blijkt in dit geval niet nodig te zijn; het kan de betrouwbaarheid van model voorspellingen verminderen.

NA processen op de pluimrand werden onderzocht in hoofdstuk 6. Voorheen is nauwelijks onderzoek verricht naar de potentie en affiniteit van reductanten in perkolaat zoals Fe(II), Mn(II), ammonium en methaan, om oxidanten aanwezig in schoon water op de pluimrand te consumeren, waardoor afbraak van organische verontreinigingen belemmerd wordt. Deze kennis is essentieel voor het modelleren en voorspellen van NA. De oxidant nitraat was aanwezig in het onvervuilde grondwater boven de pluim aan het begin van het onderzoek in 1998. De pluim bleek enkele meters gestegen te zijn in de periode 1998-2001, mogelijk als indirect gevolg van afgravingen ten behoeve van natuurontwikkeling in het gebied. Oxidatie van de reductanten Fe(II), Mn(II) en ammonium werd uitgesloten doordat sorptie resulteerde in een ruimtelijke scheiding met mogelijke oxidanten buiten de pluim. Niet-sorberend TOC lijkt wel af te breken. Anaërobe oxidatie van methaan - ontgast uit de stijgende pluim (tengevolge van een afname van hydrostatische druk) en heropgelost in onvervuild water daarboven - lijkt het nitraat nog aanwezig in 1998 te hebben verbruikt. Consumptie van oxidanten door vervluchtigd methaan uit de pluim en een beperkte menging met schoon water resulteren in een lage NA op de pluimrand.

Afbraak van specifieke mono-aromatische koolwaterstoffen (BTEX) en naftaleen kon niet onomstotelijk worden vastgesteld op deze locatie. Dit lijkt wel aannemelijk: *Geobacter* species zijn aanwezig - de enige bekende ijzer-reducerende bacteriën die mono-aromatische koolwaterstoffen kunnen afbreken - en CLPP toonde aan dat substraten met een aromatische ring beter werden omgezet in de pluim. Ontwikkelingen in de moleculaire microbiologie zullen leiden tot methoden om direct de metabolische activiteit van micro-organismen te kunnen bepalen. Afbraak van TOC bleek gekoppeld te zijn aan reductie van ijzer oxide in de pluim. Dit redox proces wordt in het algemeen in pluimen van organische verontreiniging waargenomen. De afbreekbaarheid van BTEX blijkt op andere locaties aanzienlijk af te nemen indien ijzer oxide opraakt en redox condities sulfaat-reducerend en/of methanogeen worden. De snelheid van ijzer-reductie lijkt ook af te nemen met het gehalte aan beschikbaar ijzer-oxide in een vergelijking met andere studies. Het wordt aanbevolen om verder onderzoek uit te voeren naar de volgende aspecten om de ontwikkeling van vuilstort perkolaat pluimen beter te kunnen voorspellen: hydrodynamische- en redox processen op pluimranden, kinetiek van ijzer-reductie, de afbreekbaarheid van BTEX onder methanogene en sulfaat-reducerende condities, en de nalevering van vuilstorten.

DANKWOORD

Waar is het allemaal begonnen? Zes jaar geleden werd ik gevraagd om na mijn afstuderen in de Milieuwetenschappen aan de faculteit Aardwetenschappen van de Vrije Universiteit voor een jaar onderzoek te doen in het NOBIS (Nederlands Onderzoeksprogramma Biotechnologische In-situ Sanering) project ïn-situ bioremediatie van oude vuilstortplaatsen"(NOBIS 96-3-04). Dit project sprak me erg aan omdat hydrogeochemisch en microbiologisch onderzoek geïntegreerd werden uitgevoerd en omdat het project een samenwerking betrof van specialisten met een verschillende achtergrond afkomstig van de afdelingen Hydrologie en Moleculaire Cel Fysiologie van de Vrije Universiteit en adviesbureau IWACO (tegenwoordig Royal Haskoning). De Coupépolder vuilstort bij Alphen aan de Rijn was helaas geen ideale onderzoekslocatie omdat een duidelijke pluim van grondwater verontreiniging niet aanwezig was. Wel konden microbiologische technieken ontwikkeld worden in deze periode. Het project werd met een jaar verlengd en het onderzoek verplaatste zich vanaf 1998 naar de Banisveld vuilstort nabij Boxtel. Deze locatie bleek gelukkig wel geschikt als onderzoekslocatie vanwege de duidelijke en ondiepe pluim van grondwaterverontreiniging. Hier is dan ook al het onderzoek uitgevoerd waarop dit proefschrift berust. Het bestuur van de Faculteit der Aardwetenschappen heeft mij in de gelegenheid gesteld om met een drie jarige verlenging het onderzoek te kunnen continueren tot een promotie. Daarnaast heb ik in de jaren 2000-2001 ook onderzoek uitgevoerd in het SKB (Stichting Kennisontwikkeling Kennistransfer Bodem) project "Toepassingen van isotopen analyse bij onderzoek naar bodemverontreinigingen"(SV-206). Een deel van dit onderzoek is terug te vinden in dit proefschrift. Behalve NOBIS/SKB en de Vrije Universiteit hebben de provincies Noord-Brabant, Utrecht, Zuid-Holland en Zeeland financieel bijgedragen. Tenslotte ben ik het bestuur van de Faculteit der Aard- en Levenswetenschappen dankbaar voor de verlenging van mijn contract en de aanstelling tot universitair docent sinds Maart 2003.

Ik heb tijdens mijn onderzoek hulp gehad van vele personen. Deze wil ik hier graag bedanken. In de eerste plaats mijn begeleiders en Henk van Verseveld en Jasper Griffioen. Jasper heeft het geochemische gedeelte van het onderzoek met veel interesse begeleid en heeft mij goed geholpen met de artikelen waarop hoofdstukken 2, 5 en 6 zijn gebaseerd. Ook Koos Groen wil ik bedanken voor het management van de NOBIS en SKB projecten, de hulp bij het opstellen van onderzoeksplannen en voor alle logistieke zaken die bij een groot veldonderzoek spelen, en niet op de laatste plaats, zijn enthousiasme.

Met Wilfred Röling heb ik uitstekend kunnen samenwerken. Ik heb veel geleerd. Hoofdstukken 3 en 4 zijn gebaseerd op artikelen waar hij hoofdauteur van is, en waar ik, Henk van Verseveld, Martin Braster en Lin Bin co-auteur van zijn. Ik verwacht in de toekomst nog veel van ons gezamenlijk onderzoek! Rik Jonker was voor ruim een jaar een andere goede collega. Hij was er tijdens meerdere veldwerken. Zijn praktisch oplossend vermogen nam bij mij veel zorgen weg tijdens de veldcampagnes waarbij veel mis kon gaan.

Alle studenten die mij geholpen hebben tijdens veldwerk ben ik heel dankbaar voor hun inzet en het plezier dat we beleefd hebben: Arjen Naafs, Bertus Beaumont, Akke Soeteman, Elien Neep, Xander Kaspers, Rik Jonker, Paulo Simoes, Filipe Dias en Esther Bloem.

Natuurmonumenten en in het bijzonder de Heer Klein, boswachter van het Campina natuurgebied, en zijn medewerkers wil ik bedanken voor alle logistieke steun die ze mij geboden hebben tijdens het veldwerk. Zonder hun hulp had ik temidden van distels en zwermen muggen de grondwaterbemonstering moeten uitvoeren. Veldwerk spullen heb ik in hun boerderij kunnen opslaan. Ook bedankt voor hulp met de trekker!

Het geochemisch modelleren neemt een centrale plaats in mijn proefschrift. Dit heb ik geleerd van Toni Appelo tijdens mijn afstudeerstage bij Gemeentewaterleidingen. Hij heeft me geleerd om de processen te *zien* in hydrochemische gegevens.

Niels Hartog (Universiteit Utrecht), Timo Heimovaara (Royal Haskoning), Frank Volkering (Tauw), Jeroen ter Meer, Marien Harkes, Alette Langenhof, Huub Reijnaarts (TNO-MEP) en Axel Suckow (GGA, Duitsland) wil ik bedanken voor de goede samenwerking die ik heb ervaren in deelprojecten.

De volgende personen hebben mij geholpen met laboratorium-analyses, veldwerk en/of het maken van instrumenten: Hetty Schäfer, Pieter Vroon, Martin Konert, Bert Kers en Harro Meijer (CIO, Groningen), Richard Elgood en Bob Drimmie (University of Waterloo, Canada), Rik Zoomer, Johan de Lange, Jan Vink, Hans Bakker en Harry Visch. Niek van Harlingen en Michel Groen: bedankt voor jullie hulp en ideeën voor het ontwikkelen van grondwater bemonsteringstechnieken.

Verder ben ik de leden van de leescommissie, prof. dr. H.V. Westerhoff, dr. I. Head, dr. J. Gerritse, dr. P.J. Stuyfzand en prof. dr. ir. A. Leijnse erkentelijk voor het beoordelen en becommentariëren van het proefschrift.

Op de VU en ook daarbuiten heb ik met veel lotgenoten een leuke tijd beleefd: Ben Gouweleeuw, Peter van Rossum, Remco van de Bos, Albert van Dijk, Richard de Jeu, Patrick Boogaart, Florian Maurer, Remke van Dam, Govert van Nugteren, Mark Bokhorst, Miriam Vriend en Ana Maria Garavito. Dit geldt ook voor Henk Kooi, Kay Beets en alle andere van de donderdorst. Met Vincent Post, Victor Bense, Elmer van de Berg en Rik Jonker heb ik onvergetelijke momenten beleefd. Ik zal deze gaan missen.

Tenslotte wil ik mijn familie, vrienden en Friederike bedanken voor de steun die jullie me hebben gegeven, en het plezier dat ik met jullie heb beleefd naast het promotieonderzoek.

Boris van Breukelen, April 2003